2010

Transcriptional regulation of proapoptotic kinase PKCÎ´ expression in dopaminergic neurons: relevance to gene-gene and gene-environment interactions in neurodegeneration

Huajun Jin
Iowa State University

Transcriptional regulation of proapoptotic kinase PKCδ expression in dopaminergic neurons: relevance to gene-gene and gene-environment interactions in neurodegeneration

by

Huajun Jin

A dissertation submitted to the graduate faculty

in partial fulfillment of the requirements for the degree of

DOCTOR OF PHILOSOPHY

Major: Molecular, Cellular, and Developmental Biology

Program of Study Committee:

Anumantha G Kanthasamy, Major Professor
Drena Dobbs
Michael Shogren-Knaak
Arthi Kanthasamy
Qijing Zhang

Iowa State University

Ames, Iowa

2010

TABLE OF CONTENTS

ABSTRACT

We investigated the mechanisms of transcriptional regulation of the PKCδ gene. By deletion analysis of the ~1.4 kb (-1448 to +1, relative to transcription start site) 5'-flanking sequence of the mouse PKCδ gene, we have identified a basal promoter region, nucleotide -148 to +1, required for sufficient PKCδ transcription in NIE115, MN9D, and N2a cells. We further identified two NFκB binding sites (κB 1, κB 2) as well as a NERF1a site within the basal promoter as key regulatory elements in the mouse PKCδ TATA-less promoter. Subsequent functional studies using site-directed mutation analysis revealed that κB 1, but not κB 2, is necessary for PKCδ basal expression in both NIE115 and MN9D cells. To further facilitate analysis of the regulation of the PKCδ promoter, we cloned a ~2 kb (-1694 to +289) 5'-promoter segment of the mouse PKCδ gene including the putative PKCδ promoter (1694 bp) as well as the GC-rich sequences of the first, non-coding exon (289 bp). Deletion analysis of this region indicated the non-coding exon1 GC-rich region that contains multiple Sp sites, including four GC boxes and one CACCC box, greatly enhances the basal PKCδ promoter activity and directs the highest levels of transcription in NIE115 and MN9D cells. In addition, an upstream regulatory region containing adjacent repressive and anti-repressive elements with opposing regulatory activities was identified within the region -712 to -560. Detailed mutagenesis revealed that each Sp site made a positive contribution to PKCδ promoter expression. Overexpression of Sp family proteins markedly stimulated PKCδ promoter activity without any synergistic transactivating effect in NIE115 cells. Furthermore, experiments in SL2 fly cells identified the long-isoform Sp3 as the essential activator of PKCδ transcription. Importantly, both PKCδ promoter activity and endogenous PKCδ mRNA in NIE115 cells and primary striatal cultures were inhibited by the Sp protein

inhibitor, mithramycin-A. The results from chromatin immunoprecipitation and gel shift assays further confirmed the functional binding of Sp proteins to the PKCδ promoter. Additionally, we demonstrated that overexpression of p300 or CBP increases the PKCδ promoter activity. This stimulatory effect requires intact Sp binding sites and is independent of p300 HAT activity. We also investigated the possible involvement of epigenetic mechanisms, such as DNA methylation and histone acetylation, in regulation of the PKCδ gene. Using bioinformatics method, we found a putative CpG island (+39 to +400) that overlaps with mouse PKCδ promoter. By methylation-specific PCR, we found that the PKCδ promoter is partially methylated in NIE115, MN9D, and N2a cells. Furthermore, administration of DNA methylation inhibitor 5-Aza-deoxycytidine induced hypomethylation of the PKCδ promoter and increased expression of PKCδ mRNA in NIE115 cells, further suggesting that DNA methylation is involved in mouse PKCδ gene expression in these cells. To examine the role of histone acetylation in PKCδ gene expression, we also explored the effects of various histone deacetylase (HDAC) inhibitors both *in vitro* and *in vivo*. Treatment with sodium butyrate (NaBu) significantly enhanced the PKCδ protein and mRNA levels in primary striatal and nigral neurons and in NIE115 and MN9D cells. Other HDAC inhibitors, valproic acid (VPA), scriptaid, trichostatin A (TSA), and apicidin, all mimicked the action of NaBu to induce PKCδ. Furthermore, NaBu treatment in the C57 black mouse model caused a time-dependent induction of PKCδ gene expression in the substantial nigra and striatum regions. NaBu-induced PKCδ expression correlated with hyperacetylation of the H4 histone associated with PKCδ promoter, clearly suggesting that acetylation-dependent chromatin remodeling may play a role in PKCδ upregulation. To further explore the molecular basis of histone acetylation-dependent PKCδ upregulation, PKCδ promoter analysis was performed

using reporter gene assays. NaBu and other tested HDAC inhibitors all dramatically increased the PKCδ promoter activity in a dose-dependent manner. By using deletion analyses, the minimal fragment of the PKCδ promoter in response to NaBu was mapped to an 81 bp non-coding exon 1 region (+209 to +289). The site-directed mutagenesis studies revealed that multiple GC sites within this region are major elements conferring the responsiveness to NaBu-induced promoter activity. In addition, transcriptional activities of Sp1 and Sp3 were significantly induced by NaBu. Importantly, the ectopic expression of Sp1, Sp3, or Sp4 significantly enhanced NaBu-mediated transactivation of PKCδ promoter, whereas the ectopic expression of dominant negative mutant of Sp1 or Sp3 did not cause this effect. Moreover, the Sp protein inhibitors mithramycin-A and tolfenamic acid dose-dependently blocked NaBu-induced PKCδ promoter activity. In addition, transcriptional activity of Sp1 and Sp3 was significantly induced by NaBu in a one-hybrid system. By utilizing the same assay, we found that the B domain and the glutamine-rich segment of the A domain of Sp1 and Sp3 (amino acids Sp1 146-494; Sp3 81-499) was essential for the NaBu-induced transactivation of the PKCδ promoter. Transient overexpression of p300 or CBP potentiated NaBu-induced transactivation potential of Sp1 or Sp3, whereas transient overexpression of HDACs attenuated this effect, suggesting that p300/CBP and HDACs may act as co-activators or co-repressors in response to NaBu exposure. Next, we evidenced a novel association between α-synuclein, a protein associated with the pathogenesis of Parkinson's diseases (PD), and PKCδ, in which α-synuclein negatively modulates the p300- and NFκB-dependent transactivation to down-regulate proapoptotic kinase PKCδ expression and thereby protects against apoptosis in dopaminergic neuronal cells. Stable-expression human wild-type α-synuclein at physiological levels in

dopaminergic neuronal cells resulted in an isoform-dependent transcriptional suppression of PKCδ expression without changes in the stability of mRNA and protein or DNA methylation. The reduction in PKCδ transcription was mediated, in part, through the suppression of constitutive NFκB activity targeted at two proximal PKCδ-promoter κB sites. This occurred independently of NFκB/IκBα nuclear translocation, but was associated with decreased NFκB-p65 acetylation. Also, αsyn reduced p300 levels and its histone acetyl-transferase (HAT) activity, thereby contributing to diminished PKCδ transactivation. Importantly, reduced PKCδ and p300 expression also were observed within nigral dopaminergic neurons in αsyn transgenic mice. Finally, we examined whether environmental neurotoxicant exposure alters PKCδ expression. Manganese exposure potently induced PKCδ levels in primary striatal neurons and NIE115 cells. The use of primary neurons from mice lacking PKCδ subsequently demonstrated that the level of PKCδ plays a critical role in manganese-induced neurodegeneration. Experiments on manganese-exposed mice also confirmed the action of manganese in upregulation of PKCδ. Using NIE115 cells, we further elucidated the mechanisms underlying the manganese-induced up-regulation of PKCδ. We identified that NFκB is essential for the manganese-mediated expression of PKCδ in NIE115 cells. Taken together, our studies show that 1) PKCδ promoter contains multiple positive and negative *cis*-acting elements, and both Sp family proteins and NFκB function as essential *trans*-acting factors to regulate PKCδ transcription, 2) epigenetic mechanisms including DNA methylation and histone acetylation appear to have a direct role in PKCδ expression, 3) PKCδ expression can be induced by parkinsonian environmental toxin, manganese, or negatively regulated by the PD-related gene, α-synuclein.

CHAPTER I: GENERAL INTRODUCTION

Dissertation Organization

This dissertation is organized in six chapters and some chapters are written in a journal paper format. The first chapter, General Introduction, includes an introduction describing the objectives of my research subjects and a literature review, which provides background information related to the present investigation. The references cited in this chapter are listed at the end of the dissertation. In the following four chapters (II-V) are four research papers, entitled "Transcriptional regulation of protein kinase Cδ, a pro-apoptotic kinase: implications of oxidative damage in dopaminergic neurodegeneration," "Histone acetylation upregulates PKCδ *via* Sp-dependent transcription in dopaminergic neurons: relevance to epigenetic mechanisms of neurodegeneration in Parkinson's Disease," "Alpha-synuclein negatively regulates PKCδ expression to suppress apoptosis in dopaminergic neurons by reducing p300 HAT activity," and "Increased expression of pro-apoptotic kinase PKCδ following exposure to manganese: implications for gene-environment interactions in neurodegeneration." These papers will be submitted for publication in the *Journal of Biological Chemistry*, the *Journal of Biological Chemistry*, the *Journal of Neuroscience*, and *Environmental Health Perspectives*, respectively. The list of references cited is placed at the end of each chapter. Chapter VI, General Conclusion, summarzies and discusses the entire dissertation. In this part, the future perspectives also are presented.

Introduction

Parkinson's disease (PD) is the most frequently occurring movement disorder in the United States. It results from the progressive degeneration of the dopaminergic neurons in the substantia nigra pars compacta (SNc) and the associated dopamine deficiency in the striatum. Although the relative contribution of genetic and environmental risk factors in PD has not been fully elucidated, there is ample evidence from the last three decades suggesting that oxidative stress, mitochondrial dysfunction, protein aggregation and impairment of ubiquitin-proteasome system (UPS), and apoptosis may contribute to PD pathogenesis (Dawson and Dawson, 2003). In particular, a key role for kinase signaling in the PD neurodegenerative process is increasingly being recognized. Mutations in the mitochondrial kinase PTEN-induced kinase 1 (PINK1) (Valente et al., 2004b) and the leucine-rich repeat kinase 2 (LRRK2) (Paisan-Ruiz et al., 2004; Zimprich et al., 2004) have been reported to be associated with familial forms of PD. Alterations in kinase activity of PINK1 or LRRK2 are thought to account for, at least in part, the pathogenic effects of their PD-linked mutations (Cookson et al., 2007); suggesting that aberrant protein phosphorylation may represent a molecular mechanism underlying PD. In addition, data obtained in neurotoxin, environmental and genetic models of PD have suggested an important role for a number of redox-sensitive kinase signaling pathways in the pathogenesis of PD (Harper and Wilkie, 2003; Kanthasamy et al., 2003a; Peng and Andersen, 2003; Inglis et al., 2009). Our laboratory previously reported that the kinase, protein kinase Cδ (PKCδ), functions as an oxidative stress-sensitive kinase, and that its persistent activation by caspase-3-mediated proteolytic cleavage has a promotional role in multiple models of PD-associated

dopaminergic neurodegeneration (Anantharam et al., 2002; Kaul et al., 2003; Kitazawa et al., 2003; Kaul et al., 2005b; Latchoumycandane et al., 2005). Follow-up analysis demonstrated that blocking of the PKCδ signaling pathway by administration of pharmacological inhibitors of PKCδ or expression of a dominant negative PKCδ kinase or depletion of PKCδ *via* siRNA-mediated knockdown has been shown to effectively prevent neurotoxin-induced dopaminergic neurodegeneration *in vivo* and *in vitro* (Yang et al., 2004; Kanthasamy et al., 2006; Zhang et al., 2007a), suggesting that PKCδ is a promising candidate for therapeutic intervention in PD. Although both the molecular bases of PKCδ activation and its roles in neurodegeneration have been the subject of intense investigation, little is known about the regulation of PKCδ expression. Thus, the primary objective of this dissertation is to systematically investigate the cellular and molecular mechanisms underlying the transcriptional regulation of PKCδ in neuronal cells. We also are interested in the effect of epigenetic modifications of the PKCδ promoter on its transcriptional regulation and the subsequent impact of alterations in PKCδ expression on the functional role of PKCδ in parkinsonian neurodegeneration. A better understanding of the regulation of PKCδ expression might help to identify ways to control PKCδ activity and alleviate PKCδ pro-apoptotic function in PD. Meanwhile, further studies on the potential crosstalk between PKCδ expression and genetic risk factors as well as environmental risk factors involved in PD pathology, particularly the α-synuclein and manganese, also have been extended in the dissertation. Taken together, these studies will provide useful insights for understanding the pathogenesis of PD and may be beneficial for novel drug targets selection and therapeutic intervention.

Literature Review

This section provides background information related to the studies described in the dissertation: (1) Parkinson's disease; (2) Etiology of Parkinson's disease; (3) Pathogenesis of Parkinson's disease; (4) Protein kinase C delta.

1.1 Parkinson's disease

Parkinson's disease (PD) was first described in medical literature by James Parkinson in 1817 (Pearn and Gardner-Thorpe, 2001). This disease is estimated to affect 100 to 150 per 100,000 individuals, making it the second most common neurodegenerative disease after Alzheimer's disease (AD) (Jankovic, 1988; Tanner, 1992b).

1.1.1 Epidemiology

Accurate measurements of the incidence of PD are relatively difficult due to the rarity of the autopsy data and the variability in diagnostic criteria and case ascertainment methods in studies (Nussbaum and Polymeropoulos, 1997). The most consistent risk factor for developing PD is increasing age, with approximately 1% of the population above the age of 65 being affected, rising to 4-5% of the population over 85 years (Van Den Eeden et al., 2003; Farrer, 2006). The mean age of onset of PD is approximately 62 years, although up to 10% of PD cases occur before the age of 40 (Rajput, 2001). Apart from age, epidemiological studies also have shown that the prevalence of PD varies by gender and race/ethnicity (Van Den Eeden et al., 2003). PD occurs more frequently in men than in woman (Twelves et al., 2003;

Wooten et al., 2004; Taylor et al., 2007). The reasons for the gender differences are not clear, but there are several lines of evidence suggesting that they are at least in part under the influence of genetic factors (Burn, 2007; Taylor et al., 2007). PD also may be more common in people of European ancestry living in Europe and North America, however, the evidence is far from clear (Van Den Eeden et al., 2003).

1.1.2 Clinical phenotype

The onset of symptoms in PD is insidious, and the clinical course is steadily progressive (Farrer, 2006). Its main clinical phenotype is parkinsonism, a neurological syndrome characterized by severe motor symptoms including resting tremor, rigidity, bradykinesia, and postural instability caused by striatal dopamine deficiency or direct striatal damage. PD is the most common form of parkinsonism, making up approximately 80% of total cases (Farrer, 2006). In addition to the motor deficits, patients with PD often exhibit a number of non-motor symptoms as well, such as autonomic dysfunction, cognitive and neurobehavioral disorders, and sensory and sleep abnormalities (Jankovic, 2008). Constipation, daytime sleepiness, and an impaired sense of smell can be early signs of PD (Abbott et al., 2005; Abbott et al., 2007; Haehner et al., 2007). Based on the predominance of the various cardinal symptoms, age of onset, and progression rate, PD has been classified into either a tremor-predominant form that displays a slow rate of progression and is often observed in younger people, or a postural instability and gait disorder (PIGD) subtype that is more apt to develop in older people (>70 years old) and is characterized by rigidity, bradykinesia, and gait disturbance (Obeso et al., 2010).

1.1.3 Neuropathological phenotype

The pathological hallmark of PD is the progressive and selective loss of dopaminergic neurons (Figure 1) within the substantia nigra pars compacta (SNc), leading to the marked depletions of dopamine, its metabolites including homovanillic acid (HVA) and 3,4-dihydroxyphenylacetate (DOPAC), its biosynthetic enzyme tyrosine hydroxylase (TH), and the dopamine transporter in the striatum, as well as in the SNc. Such depletions are believed to underlie many of the clinical manifestations of PD (Crossman, 1989; Dunnett and Bjorklund, 1999; Zhang et al., 2000a). The dopaminergic neuronin the SNc, sometimes referred to as the A9 cell group that forms the nigrostriatal dopaminergic pathway, contain cytoplasmic neuromelanin, a pigment that gives these nuclei a macroscopical black appearance (Forno, 1996). The cell bodies of these neurons are located in the SNc, while their axons run along the medial forebrain bundle and project primarily to the putamen in the dorsal striatum. At the onset of symptoms, approximately 60% of the SNc dopaminergic neurons correlated with depigmentation (Figure 1) in SNc and about 80% of the putamen dopamine have been lost (Kirik et al., 1998). Another important pathological feature for PD is the formation of round eosinophilic inclusion bodies that contain aggregates of many different proteins and lipids in the cytoplasm of neurons (Lewy bodies [LB]) and thread-like proteinaceous deposits within

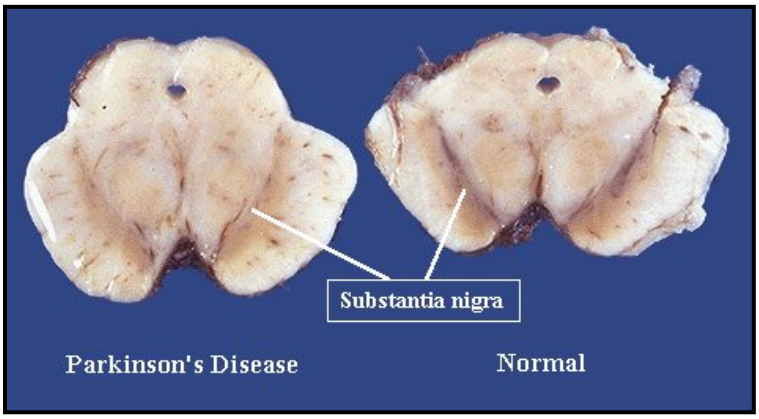

Figure 1: Neuronal loss associated with depigmentation in SNc of PD patients. This figure is obtained from: http://www.gwc.maricopa.edu/class/bio201/parkn/parkn1.jpg.

neurites (Lewy neurites [LN]) in the surviving dopaminergic neurons (Figure 2) (Werner et al., 2008). The mechanism underlying the LB or LN formation, as well as their pathogenic relevance to PD, however, is still controversial. In addition to the dopaminergic neurons in SNc, neurodegeneration and LB formation also are observed in noradrenergic neurons of the locus coeruleus and dorsal vagal nucleus, serotonergic neurons in the dorsal raphe, and cholinergic neurons within the nucleus basalis of Meynert and dorsal motor nucleus of vagus nerve, as well as in the cerebral cortex, olfactory bulb, and autonomic nervous system (Jellinger, 1990; Quinn, 1995; Hatano et al., 2009). Impairment of these neurochemical systems significantly contributes to some of the non-motor symptoms of PD (Deumens et al., 2002). For example, loss of cholinergic neurons in the nucleus basalis of Meynert is found to relate to cognitive impairment, similar to that found in AD (Whitehouse et al., 1983). Furthermore, the damages to the dorsal motor nucleus of the vagus nerve were thought to lead to constipation, while the changes of the coeruleus and raphe nuclei may underlie the symptoms of depression and sleep disturbances. The pathophysiologic progression of PD is thought to begin in the regions of the dorsal motor nucleus of the vagus and the olfactory bulb, progressing rostrally along the brain stem to affect the locus coeruleus and raphe nuclei, and then extending to the substantia nigra and ultimately involving the cortex as the disease advances (Braak et al.,

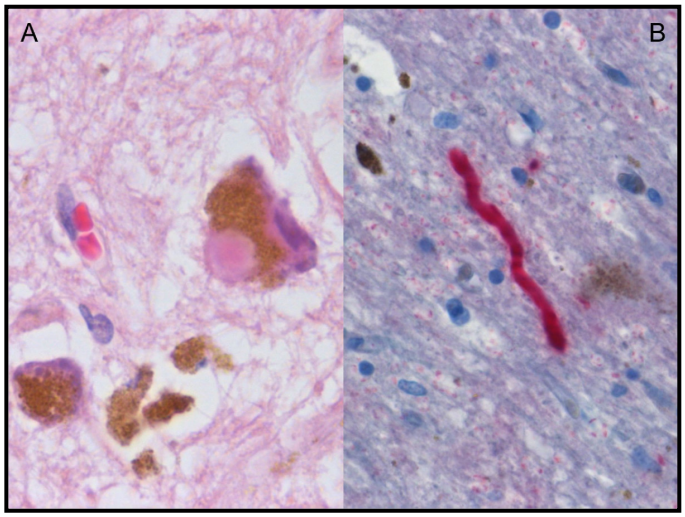

Figure 2: Lewy bodies (A) stained with haematoxylin/eosin and α-synuclein-positive Lewy neurites (B) in SNc of PD brains. This figure is adapted from (Werner et al., 2008).

2003; Bonuccelli and Del Dotto, 2006). However, this proposal has been controversial and remains to be proven (Burke et al., 2008; Lees, 2009).

1.1.4 Pharmacological treatment

Unfortunately, there is no cure for PD. All current treatments for PD are symptomatic; none slow or prevent neuronal death progression in the dopaminergic system (Obeso et al., 2010; Olanow, 2004a). Current standard treatment therapy is based on levodopa, one of the intermediate molecules in the genesis of dopamine (Clarke, 2004). Although the dopamine replacement therapy with levodopa is initially effective for most patients to improve PD symptoms, long-term manipulation of levodopa can lead to disabling side effects such as wearing-off, dyskinesias, and dystonia. Moreover, the clinical efficacy often declines as the disease advances (Lewitt, 2008). There also is a concern that levodopa may be toxic *in vivo* and may therefore induce further damage to the remaining nigrostriatal neurons in levodopa-treated patients with PD (Davie, 2008). Besides alleviating motor symptoms, new PD treatment strategies should be designed to slow and ultimately halt disease progression or to reduce the growing prevalence of non-motor disease symptoms (Obeso et al., 2010).

1.2 Disease etiology

Despite decades of research, the specific etiology of PD remains to be fully understood. There is a general agreement that PD has a complex and multifactorial etiology involving different genetic, cellular and environmental factors that may independently or concomitantly contribute for the development of PD (Obeso et al., 2010). The majority (approximately 90-95%) of PD cases are sporadic, while monogenic forms of PD only

account for 5-10% of all cases, suggesting that nongenetic factors are more important risk factors.

1.2.1 Environmental risk factors

Epidemiological studies indicated that a variety of environmental factors including exposure to pesticides, herbicides, trace metals, industrial chemicals, wood pulp mills, farming, well-water consumption, rural residence, and head trauma may confer an increased risk of PD (Olanow and Tatton, 1999; Davie, 2008). Furthermore, a number of additional endogenous toxins have been associated with the development of PD, including dopamine and its metabolites, tetrahydroisoquinolines, and beta-carbolines (Olanow and Tatton, 1999; Dauer and Przedborski, 2003). Normal metabolism of dopamine generates harmful reactive oxygen species (ROS) such as hydrogen peroxide, superoxide radical, and hydroxyl radical (Stokes et al., 1999). A second mechanism responsible for cytotoxic potential of dopamine involves oxidation of the neurotransmitter that produces a reactive dopamine quinone molecule (Smythies and Galzigna, 1998). The resulting reactive quinones have been demonstrated to covalently modify and damage cellular maromolecules (Stokes et al., 1999). In addition to these factors that increase PD risk, potentially protective factors such as cigarette smoking, alcohol and caffeine intake, and hormone replacement have been noted (Benedetti et al., 2000; Allam et al., 2004; Currie et al., 2004; Popat et al., 2005), although it is not clear how these agents influence disease risk. The only consistent environmental factor associated with the development of the disease is cigarette smoking; the prevalence decreases by approximately 60% in smokers with a dose-response relationship between cigarette consumption and PD incidence (Hernan et al., 2002).

1.2.1.1 MPTP

Although environmental risk factors for PD have gained considerable attention during the 20th century, definitive proof of the implicatiom of any specific agent as a cause of PD is still missing (Hardy, 2006). The most compelling evidence emerged with discovery of the synthetic heroin analog, 1,2,3,6-methyl-phenyl-tetrahydropyridine (MPTP) in 1982 when several drug users in California developed subacute onset of severe parkinsonism (Langston et al., 1983). It is now well established that MPTP induces, in humans, nonhuman primates, and mice, irreversible and severe motor abnormalities replicating all of the clinical features of PD, including tremor, rigidity, bradykinesia, and postural instability. Neuropathological data in both primates and mice indicate that MPTP primarily damages the nigrostriatal dopaminergic pathway in a pattern similar to that seen in PD patients, including a preferential loss of dopaminergic neurons in the SNc and a significant reduction in striatal dopamine content (Beal, 2001). As in PD, the toxin also induces additional neurodegeneration in the locus coeruleus (Varastet et al., 1994). Moreover, reminiscent of PD in humans, an excellent response to levodopa and dopamine receptor agonists and the development of motor complications after long-term manipulation of levodopa were observed in MPTP-treated primates (Dauer and Przedborski, 2003). Therefore, MPTP administration has been extensively used as a toxicant-induced PD model for studying the disease. However, this toxin model normally lacks significant LB formation for reasons that remain unclear (Forno et al., 1993), suggesting that LB formation may be not required to evoke nigral cell death.

1.2.1.2 Paraquat and rotenone

After MPTP, several widely used pesticides, particularly paraquat and rotenone, have been extensively examined for their possible involvement in PD because of their toxicological and structural similarities to MPTP and its toxic metabolite, MPP^+ (Bove et al., 2005; Brown et al., 2006). The toxicologic evidence in laboratory animals suggests that with certain routes of administration, both paraquat and rotenone can lead to a Parkinson-like syndrome, selective SNc dopaminergic neuron degeneration, and α-synuclein-positive cellular inclusions that resemble LB microscopically (Brooks et al., 1999; Betarbet et al., 2000; McCormack et al., 2002). Moreover, epidemiological studies have suggested exposure to paraquat or rotenone may confer an increased risk for PD (Liou et al., 1997; Brown et al., 2006; Hancock et al., 2008). Despite remaining uncertainties and data gaps, the overall evidence supports the conclusion that pesticide exposures can cause PD or parkinsonism in some people.

1.2.1.3 Metals

Exposure to metals, such as lead, manganese, iron, copper, and others, has also been investigated as a risk factor for PD based on some occupational studies (Tanner, 1992a; Rybicki et al., 1993; Gorell et al., 1999; Tanner et al., 1999). Among these heavy metals, manganese is of special concern due to its long-known toxicity and ability to produce a severe and degenerative neurologic condition that resembles PD, known as manganism or manganese-induced parkinsonism (Huang et al., 1989; Mergler et al., 1994). This disease, characterized by excessive manganese deposition in basal gangalia of the central nervous system, begins with a variety of psychiatric disturbances (Roth, 2006), such as emotional

liability, mania, compulsive or violent behavior, hallucinations, and loss of appetite, while motor symptoms including bradykinesia, rigidity, and dystonia are manifested at the latter stages of the disorder (Liu et al., 2006b). Although symptoms of manganism are similar to those associated with PD, they are distinct in both clinical presentation and pathology (Calne et al., 1994; Erikson and Aschner, 2003; Jankovic, 2005). Clinically, there is usually a relative absence of resting tremor, more frequent dystonia, severe gait disturbance with difficulty in backward walking, and a poor response to levodopa in patients with manganese-induced parkinsonism, while resting tremor, asymmetry, and a good response to levodopa are normally present in PD (Lu et al., 1994; Pal et al., 1999; Erikson and Aschner, 2003; Olanow, 2004b). Unlike PD, which is associated with preferential dopaminergic neurodegeneration in the SNc and the presence of LB inclusions in surviving neurons, pathologically manganese primarily causes neuronal loss in the globus pallidus and striatum with no formation of LBs (Yamada et al., 1986; Olanow, 2004b; Aschner et al., 2009b). Moreover, the damages to other regions specifically affected in PD, including the locus coeruleus, the nucleus basalis of Meynert, and the dorsal motor nucleus of vagus nerve, are not observed in manganese-intoxicated patients (Olanow, 2004b; Jankovic, 2005). In humans, manganese toxicity primarily has been observed in occupational settings, such as manganese mines and the manufacturing facilities producing dry batteries, steel, aluminum, welding metals, and organochemical fungicides (Keen et al., 2000). In addition, manganese neurotoxicity has been reported in individuals receiving total parenteral nutrition (Bertinet et al., 2000) and in patients with chronic liver failure (Hauser et al., 1994; Krieger et al., 1995). Other sources of excessive manganese exposure include well water rich in manganese (Wasserman et al., 2006), soy-based infant formulas (Lonnerdal, 1994; Krachler and

Rossipal, 2000), as well as atmospheric manganese resulting from the addition of methylcyclopentadienyl manganese tricarbonyl (MMT) to gasoline (Finkelstein and Jerrett, 2007; Walsh, 2007; Santamaria, 2008; Aschner et al., 2009b). To date, pathogenic mechanisms underlying manganism are not fully understood but possibly involve increased oxidative stress and excitotoxicity (Brouillet et al., 1993; Chen and Liao, 2002), attenuation of astrocytic glutamate uptake (Hazell and Norenberg, 1997; Erikson and Aschner, 2003), and upregulation of binding sites for peripheral benzodiazepine receptor ligands (Hazell et al., 1999). Chelation therapy with ethylene-diamine-tetraacetic acid (ETA) has been used as the primary treatment for manganese intoxication (Discalzi et al., 2000; Herrero Hernandez et al., 2006), but in some cases neurological symptoms progressed even after many years of cessation of chronic exposure (Rosenstock et al., 1971; Cook et al., 1974; Calne et al., 1994).

1.2.2 Genetic risk factors

Over the past decade, the role of genetic factors in PD has been the subject of intense investigation. Although purely genetic forms of PD appear to be rare, accounting for only 5-10% of the overall PD population, understanding the genetic variations impacting dopamine neurons will accelerate the identification of the underlying disease mechanisms and provide the rational for developing new therapeutic approaches to slow or halt the disease progression. To date, more than 15 loci (PARK 1-15) and 15 causative genes (Table 1) have been mapped and found to be linked to familial forms of PD (see update at PD Gene: http://www.pdgeen.org) (Gasser, 2007; Klein and Schlossmacher, 2007; Hatano et al., 2009). Polymorphisms of these genes are being further examined in idiopathic PD patients. Among them, PARK1 and PARK4/*SNCA*, PARK5/*ubiquitin carboxyl-terminal esterase L1*

(*UCHL1*), PARK8/*leucine-rich repeat kinase 2* (*LRRK2*), and another currently unknown gene PARK3 are shown to cause dominantly inherited parkinsonism (Klein and Schlossmacher, 2006; Gasser, 2007; Hatano et al., 2009); Four genes, PARK2/*parkin*, PARK6/*PTEN-induced putative kinase 1* (*PINK1*), PARK7/*DJ-1*, and recently, PARK9/*ATPase type 13A2* (*ATP13A2*) are shown to cause recessively inherited parkinsonism (Ramirez et al., 2006; Gasser, 2007; Hatano et al., 2009).

Table 1: Summary of PD-associated genes

Locus	Chromosome	Gene	Inheritance and phenotype
PARK1	4q21-q23	*SNCA*	Dominant, DLB features
PARK2	6q25.2-q27	*Parkin*	Recessive, EO, no LB
PARK3	2p13	Unknown	Dominant, Classic PD
PARK4	4q21	*SNCA* (triplication)	Dominant, EO with DLB features
PARK5	4p13	*UCH-L1*	Classic PD
PARK6	1p36.2	*PINK1*	Recessive, EO, slow progression with LB
PARK7	1p36	*DJ1*	Recessive, EO, slow progression
PARK8	12q12	*LRRK2*	Dominant, Classic PD
PARK9	1p36	*ATP13A2*	Recessive, Atypical-Kufor-Rakeb syndrome
PARK10	1p32	Unknown	Classic PD
PARK11	2p37.1	*GIGYF2*	Dominant, Classic PD
PARK12	Xq21-q25	Unknown	Classic PD
PARK13	2p13.1	*HTRA2/OMI*	Classic PD
PARK14	22q13.1	*PLAG26*	Recessive
PARK15	22q12-q13	*FBXO7*	Recessive
-	17q21.1	*MAPT*	
-	1q21	*GBA*	Parkinsonism with LB
-	5q23.1-q23.3	*Synphilin-1*	Classic PD
-	2q22-q23	*NR4A2/Nurr1*	Classic PD

EO: early onset, DLB: Dementia with Lewy bodies, LB: Lewy bodies. Classic PD refers to the late-onset clinical idiopathic PD phenotype.

1.2.2.1 α-Synuclein

The *SNCA* gene coding for the protein alpha-synuclein (α-synuclein) was the first gene implicated in the familial forms of PD when a missense mutation A53T within the gene

was isolated from a large Italian-Greek family with autosomal dominant PD with a relatively earlier age at onset (50 years) and rapid disease progression (Polymeropoulos et al., 1996; Polymeropoulos et al., 1997). Subsequent studies identified two further point mutations (A30P and E46K) in the *SNCA* gene in a German and Spanish family, respectively (Kruger et al., 1998; Zarranz et al., 2004). All these families had clinical and pathological features similar to those observed in sporadic PD and responded to levodopa medication, although some atypical phenotypes also have been observed. For example, cognitive decline and severe central hypoventilation have been noted in several A53T-assoacited patients (Polymeropoulos et al., 1997; Spira et al., 2001), and interestingly, the patients with the E46K mutation exhibited some clinical features typical of dementia with Lewy bodies (DLB) in addition to parkinsonism (Zarranz et al., 2004). These mutations are exceedingly rare and have not been found in sporadic PD. Apart from these missense substitutions, genomic rearrangements including duplication and triplication of the wild-type *SNCA* gene were also reported to cause autosomal-dominantly inherited PD in several families (Singleton et al., 2003; Chartier-Harlin et al., 2004; Ibanez et al., 2004; Nishioka et al., 2006; Ahn et al., 2008). In contrast to the families with the gene triplications, who were affected in their thirties and often presented with a severe phenotypes, such as rapid progression, early dementia, and reduced lifespan, the clinical phenotype in patients with *SNCA* duplications resembles more closely those of sporadic PD patients (Chartier-Harlin et al., 2004; Fuchs et al., 2007). Interestingly, a Rep1 microsatellite polymorphism located on the *SNCA* gene promoter (Maraganore et al., 2006) and several single nucleotide polymorphisms (SNPs) at the 5’ and 3’ regions have been associated with higher risk for sporadic PD(Mueller et al., 2005; Mizuta et al., 2006; Winkler et al., 2007; Pankratz et al., 2009). Although the cases of

familial PD associated with α-synuclein mutations are extremely rare (Lee and Trojanowski, 2006), a significant role for α-synuclein in the pathogenesis of PD is highlighted by the identification of α-synuclein as the major component of the LBs in both sporadic and familial PD (Spillantini et al., 1997; Spillantini et al., 1998; Takeda et al., 1998; Bayer et al., 1999). Additionally, α-synuclein-positive inclusions also are prominent in a range of other neurodegenerative diseases, classified as synucleinopathies, including diffuse Lewy body dementia (DLBD), Lewy body variant of Alzheimer disease (LBVAD), and multiple system atrophy (MSA) (Spillantini et al., 1998; Takeda et al., 1998; Wakabayashi et al., 1998; Bayer et al., 1999). Ultrastructurally, LBs are composed of fine filaments that are mainly made of fibrillar α-synuclein, an aggregated form of the protein (Schulz-Schaeffer, 2010; Dickson, 2002), suggesting that abnormalities of α-synuclein accumulation might be crucial in the pathophysiology of PD. It should be pointed out however, that whether LBs are neurotoxic or cytoprotective remains debatable (Maries et al., 2003; Jellinger, 2009; Power and Blumbergs, 2009). In spite of the potentially deleterious effects, LB formation might be part of a normal cellular process to protect neuron by sequestering misfolded or incompletely degraded proteins from the cell (Mouradian, 2002; Tanaka et al., 2004; Power and Blumbergs, 2009).

As a 140 amino acid small protein, α-synuclein is abundantly expressed as a cytosolic and lipid-binding phosphoprotein throughout the vertebrate brain (Vekrellis et al., 2004). This protein belongs to the synuclein protein family additionally including β-synuclein and γ-synuclein (George, 2002). All synucleins have a six or seven 11-residue imperfectly conserved repeats distributed throughout most of the N-terminal region and a variable C-terminal hydrophilic tail (George, 2002). Structurally, α-synuclein is usually subdivided into three distinct domains (Figure 3): (1) the N-terminal amphipathic domain (residues 1-65)

including seven copies of 11-residue imperfect repeat with a hexameric core motif (KTKEGV), (2) the central hydrophobic domain (residues 66-95) that is known as the non-amyloid-β component (NAC) domain, and (3) the acidic C-terminal glutamate-rich domain (residues 96-140) (Recchia et al., 2004; Beyer, 2006). The highly conserved N-terminal repeat domain is thought to confer the lipid-binding properties for direct membrane interaction (Maroteaux and Scheller, 1991; Jensen et al., 1998; Jo et al., 2000; Fortin et al., 2004; Kubo et al., 2005). This domain shares a natively unfolded structure in solution, but under certain conditions it can shift to an α-helical conformation (Clayton and George, 1998; Kahle et al., 2002). Several studies indicate that association with lipids stabilizes α-synuclein in an α-helical structure (Jo et al., 2000; Perrin et al., 2000; Eliezer et al., 2001; Chandra et al., 2003; Jao et al., 2004) accompanied by extensive aggregation and fibril formation (Giasson et al., 1999; Conway et al., 2000a; Serpell et al., 2000; Lee et al., 2002a; Barghorn et al., 2004), suggesting that the membrane-associated conformation of α-synuclein may contribute to Lewy body pathology in neurodegenerative diseases. The NAC domain is highly amyloidogenic and appears to be essential for α-synuclein aggregation, which confers to the protein the ability to undergo a conformational change from random coil to β-sheet structure (Giasson et al., 2001; Recchia et al., 2004), resulting in fibril formation that are similar to

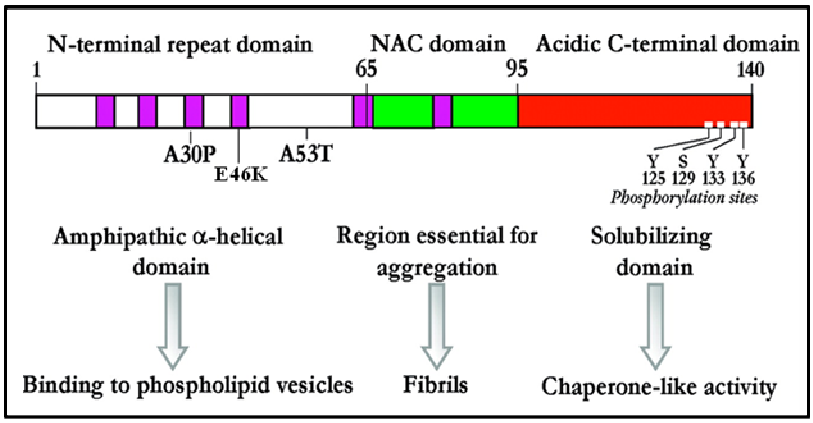

Figure 3: Protein domains of huamn α-synuclein. This figue is adapted and modified from (Recchia et al., 2004).

that formed from other amyloidogenic proteins (Giasson et al., 2001; el-Agnaf and Irvine, 2002). The role of NAC domain in α-synuclein aggregation also was supported by the observation that the highly homologous β-synuclein, which lacks 11 central hydrophobic residues, fails to aggregate (Biere et al., 2000). The C-terminal acidic tail has no distinct structural propensity but has a strong negative charge (George, 2002) that is believed to positively regulate solubility of α-synuclein (Recchia et al., 2004). Both *in vitro* and *in vivo* studies have suggested an inhibitory role for this region on aggregation of α-synuclein (Crowther et al., 1998; Serpell et al., 2000; Murray et al., 2003; Periquet et al., 2007).

Little is known about the physiological functions of α-synuclein. However, given the predominant synaptic location of α-synuclein, it may have a role in synaptic plasticity. In support of this idea, an avian homologue of α-synuclein, synelfin is transiently expressed during early stages of song learning in zebra finch (George et al., 1995). α-Synuclein can bind to acidic phospholipid vesicles (Davidson et al., 1998) and can also function as a potent inhibitor of phospholipase D by physical interaction (Jenco et al., 1998), suggesting a putative role for α-synuclein in regulation of synaptic vesicle recycling. Indeed, depletion of α-synuclein in cultured hippocampal neurons or mice exhibited a significant reduction in the distal pool of synaptic vesicles (Murphy et al., 2000; Cabin et al., 2002). Furthermore, significantly enhanced dopamine release at nigrostriatal terminals in response to paired electrical stimuli was observed in α-synuclein knockout mice, suggesting that α-synuclein might be an important regulatory component for dopaminergic neurotransmission (Abeliovich et al., 2000). Additionally, Ostrerova and colleagues observed that α-synuclein shares a 40% homology with a chaperone protein 14-3-3, suggesting that α-synuclein may function as a chaperone protein (Ostrerova et al., 1999). Furthermore, they also have shown

that α-synuclein is able to bind to and inhibit the activity of protein kinase C (PKC) (Ostrerova et al., 1999). PKC plays a central role in the signal transduction pathways that control various cellular processes, and therefore α-synuclein may also be involved in signal transduction. Finally, in addition to neurotoxicity, there is accumulating evidence suggesting that native α-synuclein plays a beneficial role in the prevention of neurodegeneration *in vitro* and *in vivo* (da Costa et al., 2000; Alves Da Costa et al., 2002; Seo et al., 2002; Jensen et al., 2003; Manning-Bog et al., 2003; Albani et al., 2004; Sidhu et al., 2004; Chandra et al., 2005; Leng and Chuang, 2006; Monti et al., 2007). It has been shown, for example, that overexpression of either wild-type human α-synuclein or its A53T mutant form in mice completely protected against paraquat-induced neurodegeneration (Manning-Bog et al., 2003). Another *in vivo* work by Chandra and colleagues revealed that α-synuclein can cooperate with the synaptic co-chaperone, cysteine-string protein-α (CSPα), to protect against injury at nerve terminals (Chandra et al., 2005). However, the precise mechanisms involved in α-synuclein neuroprotective action remains to be fully defined.

Although the process of α-synuclein fibrillization appears to be the key pathogenic event in PD, the mechanism underlying α-synuclein aggregation is still poorly understood. Current hypothesis for α-synuclein fibrillogenesis is that natively or disordered α-synuclein monomers become soluble oligomers, also referred to as protofibrils, which form stable amyloid-like fibrils and eventually aggregate into LB inclusions (Maries et al., 2003). Supporting this view is the observation that *in vitro* wild-type α-synuclein itself can self-aggregate in solution to form amyloid-like fibrils (Recchia et al., 2004; Moore et al., 2005) and that the oligomeric species of α-synuclein have been observed in human brain (Sharon et al., 2003). However, it is still not clear which species is responsible for the

neurotoxicity (Taymans and Cookson, 2010; Cookson, 2005). Some investigators believe that the oligomers but not the fibrils are toxic based on the *in vitro* finding that both A53T and A30P mutants promote oligomers formation, but only the A53T mutant promotes the formation of fibrils (Conway et al., 1998; Conway et al., 2000b). However, transgenic overexpression of the protofibrillogenic A30P mutant α-synuclein failed to display neurodegeneration (Lee et al., 2002b), suggesting that oligomers may not be the primary toxic species. Several mechanisms underlying abnormal α-synuclein accumulation have been proposed, including mitochondrial dysfunction, oxidative damage, failure of the ubiquitin-proteasome system, and posttranslational modifications (Moore et al., 2005).

1.2.2.2 LRRK2

The PARK8 locus encompassing *LRRK2* gene was initially mapped in a large Japanese family with late-onset autosomal dominant PD (Funayama et al., 2002). Subsequently, two groups concurrently identified mutations within the *LRRK2* gene as the causative gene for PARK8-linked familial PD (Paisan-Ruiz et al., 2004; Zimprich et al., 2004). Since then, six point mutations with definite pathogenicity (R1441C, R1441G, Y1699C, G2019S, I1122V and I2020T) and numerous putative pathogenic mutations have been identified in *LRRK2* gene; both in familial and sporadic cases of PD (Cookson, 2005; Funayama et al., 2005; Gilks et al., 2005; Nichols et al., 2005; Mata et al., 2006a; Tomiyama et al., 2006; Lu and Tan, 2008; Hatano et al., 2009; Haugarvoll and Wszolek, 2009). *LRRK2* mutations are the most frequently known cause of autosomal dominant form of familial PD (Klein and Schlossmacher, 2007; Mizuno et al., 2008). The known *LRRK2* variants are estimated to account for approximately 2% of sporadic and 10% of familial PD cases (Berg

et al., 2005; Di Fonzo et al., 2005; Mata et al., 2006b). In particular, the *LRRK2* G2019S mutation is the best studied and most frequent substitution in the Caucasian population, accounting for approximately 0.5-2.0% of apparently sporadic and 5-6% of familial PD cases (Di Fonzo et al., 2005; Farrer et al., 2005; Gilks et al., 2005; Kachergus et al., 2005; Nichols et al., 2005; Tomiyama et al., 2006). However, the G2019S mutation frequency appears to vary with ethnicity (Tan et al., 2005; Lesage et al., 2006), with an extremely high frequency (30-40%) of familial and sporadic PD patients from North Africa (Lesage et al., 2006) and 10-30% of Ashkenazi Jews (Ozelius et al., 2006), but very rare found in Asia, south Africa and some European countries (Tan et al., 2005; Xiromerisiou et al., 2007; Okubadejo et al., 2008). Additionally, two polymorphic mutations R1628P and G2385R have been found to confer susceptibility to PD in Asian populations (Funayama et al., 2007; Ross et al., 2008). The penetrance of G2019S-associated disease appears to be age-dependent (Kachergus et al., 2005), but variations are reported in subsequent reports (Lesage et al., 2005; Clark et al., 2006b; Goldwurm et al., 2007). The clinical and neurochemical phenotype of patients with *LRRK2* mutations usually resembles sporadic PD, with neuronal degeneration accompanied by LB and good a response to levodopa. However, the disease pathologies can be quite variable, even within the same family (Tan and Skipper, 2007). These include motor neuron features, pure nigral degeneration without LB, neuronal loss with nuclear ubiquitin inclusions, neurofibrillary tangles, widespread LBs consistent with DLBD, and even progressive supranuclear palsy (PSP)-like tau pathology (Funayama et al., 2002; Zimprich et al., 2004; Gilks et al., 2005; Khan et al., 2005; Giasson et al., 2006; Giordana et al., 2007; Hasegawa et al., 2009; Hatano et al., 2009; Santpere and Ferrer, 2009).

The *LRRK2* gene encodes a large (2,527 amino acids) protein, also known as dardarin, which belongs to the ROCO protein family and contains multiple domains (Figure 4) consisting of an N-terminal leucine-rich repeat (LRR) region, a GTPase ROC/COR domain, a mitogen-activated protein kinase kinase kinase (MAPKKK) and C-terminal WD40 repeat

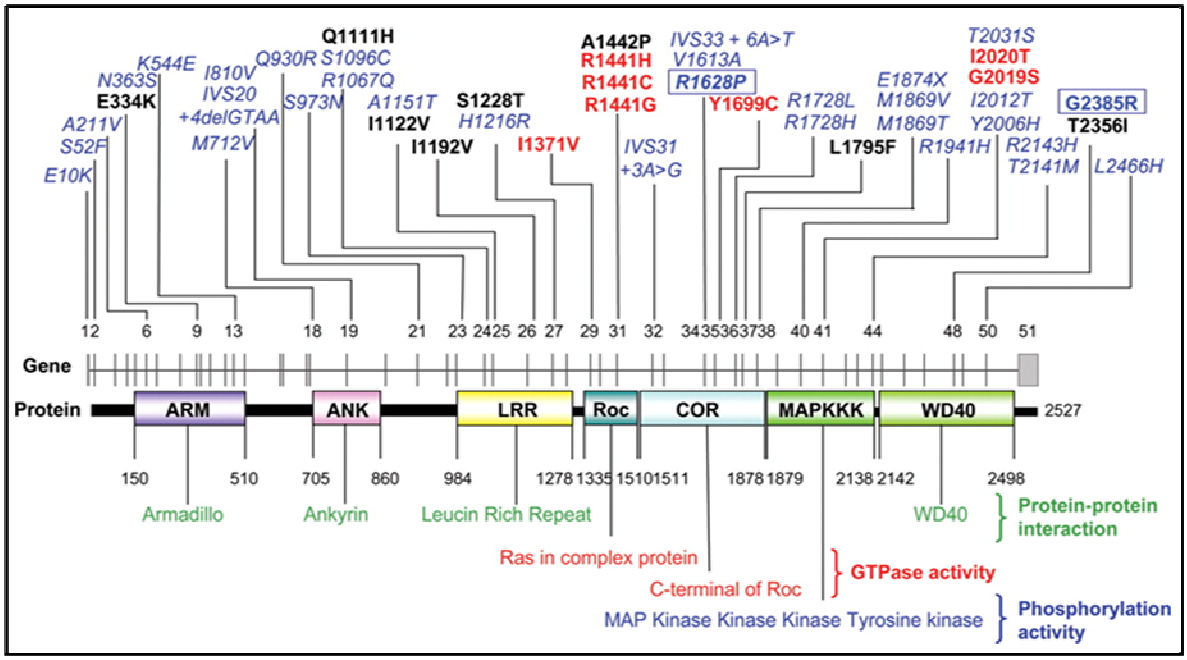

Figure 4: LRRK2 domain architecture and genetic variation in the *LRRK2* gene. ARM: Armadillo, ANK: Ankyrin repeat, LRR: leucine rich repeat, Roc: Ras of complex proteins: GTPase, COR: C-terminal of Roc, MAPKKK: mitogen activated kinase kinase kinase. Figure is adapted from (Lesage and Brice, 2009).

domains (Taymans and Cookson, 2010; Mata et al., 2006a; Lesage and Brice, 2009). All the six known pathogenic mutations are located within the catalytic center of the protein, i.e., within the region consisting of GTPase ROC/COR and kinase domains. LRRK2 is abundantly expressed in most brain regions and other tissues (Paisan-Ruiz et al., 2004; Zimprich et al., 2004), implicating a broad range of cellular functions. The normal function of LRRK2 protein remains unknown, but it may play a role in intracellular signaling according to the presence of both GTPase and kinase domains (Taymans and Cookson, 2010; Gandhi et al., 2009). In addition, given the fact that best known LRRK2-interacting proteins

are involved in cytoskeleton and trafficking (Dachsel et al., 2007; Jaleel et al., 2007; Gandhi et al., 2008), it is reasonable to speculate that LRKK2 plays a role in membrane trafficking and axon guidance through the association with lipid rafts (Hatano et al., 2007).

To date, the pathogenic role of LRRK2 is largely unknown, but several in vitro studies indicate that it may be associated with an increased kinase activity (Gloeckner et al., 2006; Greggio et al., 2006), suggesting that kinase inhibition may be a promising therapy for PD. In addition, recent evidence on the basis of cell culture experiments suggest that the extrinsic apoptosis involving the Fas-associated protein with death domain (FADD)/caspase-8 signaling pathway may contribute to the toxic effect of LRRK2 mutations (Iaccarino et al., 2007; Ho et al., 2009), however, it remains to be seen if this is relevant in vivo.

1.2.2.3 UCHL1

A heterozygous I93M mutation in the *UCHL1* gene was identified in a small German family with autosomal dominant PD (Leroy et al., 1998b). Affected family members display clinical signs similar to those of sporadic PD (Leroy et al., 1998a). As yet no additional pathogenic mutations in *UCHL1* have been reported. Thus, it remains contentious whether this gene is causative for inherited PD.

UCHL1 is a highly abundant and neuron-specific protein, constituting 1-2% of the soluble brain protein, and is also a component of LB in brains of sporadic PD (Wilkinson et al., 1989; Lowe et al., 1990). This protein belongs to the ubiquitin C-terminal hydrolase family of deubiquitinating enzyme that is responsible for hydrolysis of polyubiquitin chain to free monomeric ubiquitin (Larsen et al., 1996; Larsen et al., 1998). In addition to a

deubiquitinating function, UCHL1 might also function as a dimerization-dependent ubiquitin protein ligase (Liu et al., 2002). The mechanism by which the UCHL1 mutant causes PD remains unclear, but the I93M pathogenic mutation exhibits markedly reduced ubiquitin hydrolase activity *in vitro* (Leroy et al., 1998b; Liu et al., 2002), suggesting that the impaired polyubiquitin hydrolysis leading to a reduction in free ubiquitin monomers and accumulation of potentially deleterious proteins, might contribute to PD pathogenesis.

1.2.2.4 Parkin

Mutations in the *parkin* gene were originally identified in Japanese families with autosomal recessive juvenile-onset parkinsonism (AR-JP) (Ishikawa and Tsuji, 1996; Kitada et al., 1998). Subsequent studies have identified a wide variety of *parkin* mutations in PD cases, including point mutations, exonic rearrangements, deletions and duplications (Lucking et al., 2001; Tan and Skipper, 2007). To date, more than 100 different *parkin* mutations have since been identified (Tan and Skipper, 2007). *Parkin* mutations are the most commonly known cause of autosomal recessive early-onset PD (Mizuno et al., 2008; Hatano et al., 2009), accounting for about 50% of the familial and 20% of the sporadic early-onset PD cases (Lucking et al., 2000). In general, *parkin*-proven disease has typical signs of PD but with an earlier age of diseases onset (typically before 40 years), dystonia at onset, a slower diseases progression, and a dramatic response to levodpa manipulation (Lohmann et al., 2003). However, several mutations in *parkin* may lead to a clinical presentation indistinguishable from typical late-onset idiopathic PD (Abbas et al., 1999; Klein et al., 2000; Foroud et al., 2003; Oliveira et al., 2003; Hatano et al., 2009). The pathological features of *parkin*-associated parkinsonism include typical loss of nigral neurons and moderate loss of

neurons in the locus coeruleus region (Mori et al., 1998). However, LB are usually absent (Mizuno et al., 2001b; Mizuno et al., 2001a; Mata et al., 2004). Nevertheless, for the sporadic forms of PD, parkin has been identified as a component of LB.

Parkin is a 465-amino acid protein and primarily expressed in the central nervous system, which has a modular structure (Figure 5) consisting of an ubiquitin-like (UBL) domain at the N terminus, a RING-box domain at the C terminus, and a central linker region (von Coelln et al., 2004). The presence of UBL and RING-box domains implicates a role for parkin in the ubiquitin proteasome system (UPS). Indeed, parkin has been found to function as an E3 ubiquitin protein ligase (Shimura et al., 2000; Zhang et al., 2000b) that ubiquitinates unnecessary, damaged or misfolded proteins, and eventually triggers their degradation by the 26S proteasomes protein complexes (Glickman and Ciechanover, 2002). To date, a number of putative targets for parkin's E3 ligase activity have been identified, including a rare *O*-glycosylated α-synuclein (Shimura et al., 2001), CDCrel-1 (Zhang et al., 2000b), CDCrel-2 (Choi et al., 2003), the parkin-associated endothelin like receptor (Pael-R) (Imai et al., 2001), synphilin-1 (Chung et al., 2001b), cyclin E (Staropoli et al., 2003), programmed cell death 2 (Fukae et al., 2009), the p38 subunit of the aminoacyl-tRNA synthetase complex (Corti et al., 2003), α/β tubulin (Ren et al., 2003), and synaptotagmin XI (Huynh et al., 2003), as well as parkin itself (Shimura et al., 2000;

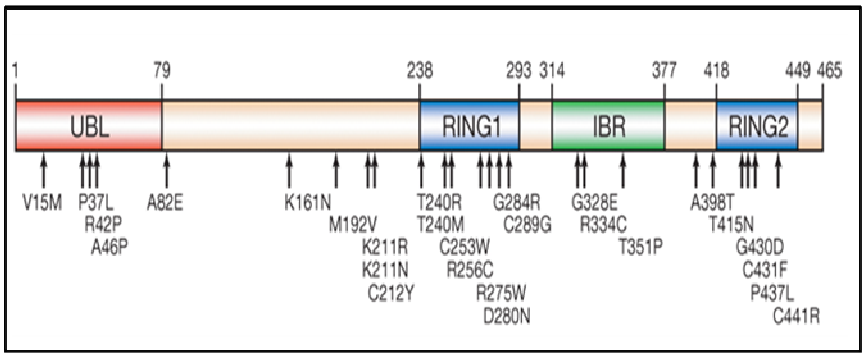

Figure 5: Functional domains of parkin protein and pathogenic mutations in the *parkin* gene. This figure is adapted from (Moore et al., 2005).

Zhang et al., 2000b). Interestingly, some of these substrates are synaptic proteins, suggesting a role of parkin in synaptic function (Fallon et al., 2002). Additionally, a role for parkin in maintaining mitochondrial function and preventing oxidative stress has been demonstrated in *parkin*-deficient mice and drosophila models (Greene et al., 2003; Palacino et al., 2004; Hatano et al., 2009). Consistent with this view, a neuroprotective function of parkin is well established on the basis of both *in vivo* and *in vitro* experiments (Moore et al., 2005; Casarejos et al., 2006; Vercammen et al., 2006; Schiesling et al., 2008). Although the precise mechanisms remain unclear, it appears that deleterious accumulation of toxic substrates as a consequence of parkin E3 ligase function loss, may at least partly explain the pathogenesis in parkin-associated parkinsonism (Moore et al., 2005). In support of this hypothesis, some parkin's substrates have been shown to be neurotoxic when overexpressed (Imai et al., 2001; Corti et al., 2003; Dong et al., 2003; Yang et al., 2003). In addition, parkin dysfunction has also been implicated in the pathogenesis of sporadic PD based on the fact that functions of parkin can be altered by a wide array of oxidative stressors, including rotenone, MPP^+, paraquat, nitric oxide and iron, as well as dopamine (Chung et al., 2004; Yao et al., 2004; Wang et al., 2005a).

1.2.2.5 PINK1

PINK1 mutations were initially identified in a large Italian family with an autosomal recessive form of PD (Valente et al., 2001). Since then, more than 50 pathogenic *PINK1* mutations have been identified (Hatano et al., 2009). These mutations include point mutations, as well as insertions and deletions that result in frameshift and truncation of the protein (Atsumi et al., 2006; Exner et al., 2007). Mutations in *PINK1* gene were estimated to

account for 1-8% of familial or early onset PD (Klein and Schlossmacher, 2007), and as such, *PINK1* mutations are the second most commonly known cause of autosomal recessive PD, after parkin mutations (Hatano et al., 2004a; Valente et al., 2004b). The clinical phenotype of *PINK1*-associated PD resembles sporadic PD with rare atypical features such as dystonia at onset and dementia similar to those with parkin mutations (Hatano et al., 2004b; Valente et al., 2004b; Valente et al., 2004a; Steinlechner et al., 2007). It is not clear whether LB are present in this PINK1-linked disease, since no neuropathological examination of homozygous pathogenic mutation has been reported (Hardy et al., 2009).

PINK1 gene encodes a ubiquitously expressed 581-amino acid protein that contains an N-terminal mitochondrial targeting motif, a catalytic serine/threonine kinase domain and a C-terminal autoregulatory domain (Valente et al., 2004b; Silvestri et al., 2005). Numerous studies, both *in vitro* and *in vivo*, have demonstrated that PINK1 is a mitochondrial kinase, suggesting a role for it in mitochondrial dynamics (Silvestri et al., 2005; Gandhi et al., 2006; Haque et al., 2008). Indeed, *PINK1* knockout models in drosophila exhibited mitochondrial abnormality and increased oxidative stress similar to those seen with *parkin*-deficient drosophila (Clark et al., 2006a). More interestingly, the mitochondrial dysfunction in *PINK1*-deficient drosophila can be rescued with parkin, indicating that PINK1 acts upstream of parkin in a common pathway that maintains the normal function of mitochondria (Clark et al., 2006a; Park et al., 2006; Poole et al., 2008). As for parkin, PINK1 also is reported to be neuroprotective, implicating its role in sporadic PD (Schiesling et al., 2008). As most pathogenic mutations are in the serine/threonine kinase domain, disruption of the PINK1 kinase activity is believed to the most probable mechanism responsible for PINK1-associated

parkinsonism (Abou-Sleiman et al., 2006). Clearly, further analysis is required to elucidate the precise role of PINK1 in nigral neuronal loss in PINK1-linked PD.

1.2.2.6 DJ-1

Mutations in *DJ-1* were first identified in one Dutch family with autosomal recessive early-onset PD (van Duijn et al., 2001). Additional mutations including missense, exonic deletions, and splice site alterations were further identified (Bonifati et al., 2003; Bonifati et al., 2004; Hering et al., 2004). The *DJ-1* mutations are extremely rare, accounting for less than 1% of early-onset PD cases (Clark et al., 2004; Lockhart et al., 2004). In general, patients with *DJ-1* mutations exhibit a clinical presentation similar to that of *parkin* or *PINK1* mutations-associated parkinsonism (Hatano et al., 2009). Like *PINK1* mutations, a neuropathological investigation has not yet been reported, and for this reason it is not clear whether the LB phenotype is present in this disorder (Hardy et al., 2009). Although DJ-1 is not an essential component of LBs, it appears to be consistently colocalized with neuronal tau-positive inclusions and glial cytoplasmic inclusions (Neumann et al., 2004), providing a link between DJ-1 and distinct neurodegenerative diseases.

The *DJ-1* gene encodes a highly conserved 189-amino acid protein that can form a dimer and belongs to the DJ-1/ThiJ/Pfp1 superfamily. Expression of DJ-1 protein is ubiquitous in most mammalian tissues. In the human brain, it predominately localizes into astrocytes, with little localization in neurons (Bandopadhyay et al., 2004). In cells, it is mainly distributed in the cytoplasm, with smaller amounts associated with mitochondria (Zhang et al., 2005). The normal functions of DJ-1 remain elusive although many lines of evidence suggest that DJ-1 can serve as a redox-sensitive chaperone or an anti-oxidant that is

involved in mitochondria protection against oxidative stress (Hatano et al., 2009). Furthermore, DJ-1 can also function as a direct scavenger of ROS (Taira et al., 2004). Consistent with these findings, DJ-1 confers neuroprotection against a range of oxidative stress (Aleyasin et al., 2010; Moore et al., 2005). However, the precise mechanism underlying the neuroprotective action of DJ-1 awaits further clarification (Aleyasin et al., 2010). In addition, several studies suggest that it may possess a chaperone-like activity and proteolytic activity (Lee et al., 2003; Olzmann et al., 2004). Importantly, DJ-1 may play an important role in the sporadic forms of PD, since analysis of the sporadic PD brain revealed oxidative damage to DJ-1, as well as a dramatic increase in the DJ-1 protein levels (Choi et al., 2006a; Waragai et al., 2006). The mechanism of DJ-1 function loss in DJ-1-associated parkinsonism is not clear. So far, the L166P mutant is the best studied DJ-1 mutation, which destabilizes the DJ-1 proteins through the impairment in their ability to self-interact, and eventually enhances their proteasome-dependent degradation (Macedo et al., 2003; Miller et al., 2003; Moore et al., 2003).

1.2.2.7 ATP13A2

ATP13A2 mutations were first identified in a Jordanian family with autosomal recessive early onset parkinsonism known as Kufor Rakeb disease (Ramirez et al., 2006). As yet no pathological examinations have been reported. This gene encodes a lysosomal type 5 P-type ATPase and is presumed to be located in the lysosome (Lesage and Brice, 2009). How the loss-of-function mutations to ATP13A2 cause PD pathogenesis remains elusive, but the interference with localization of this protein into lysosome leading to lysosomal dysfunction appears to be involved (Hatano et al., 2009).

1.3 Disease pathogenesis

In spite of decades of intense research, the precise pathogenesis of PD remains unknown. However, several pathogenic mechanisms underlying development of the disease, including oxidative and nitrosative stress, mitochondrial dysfunction, impairment of

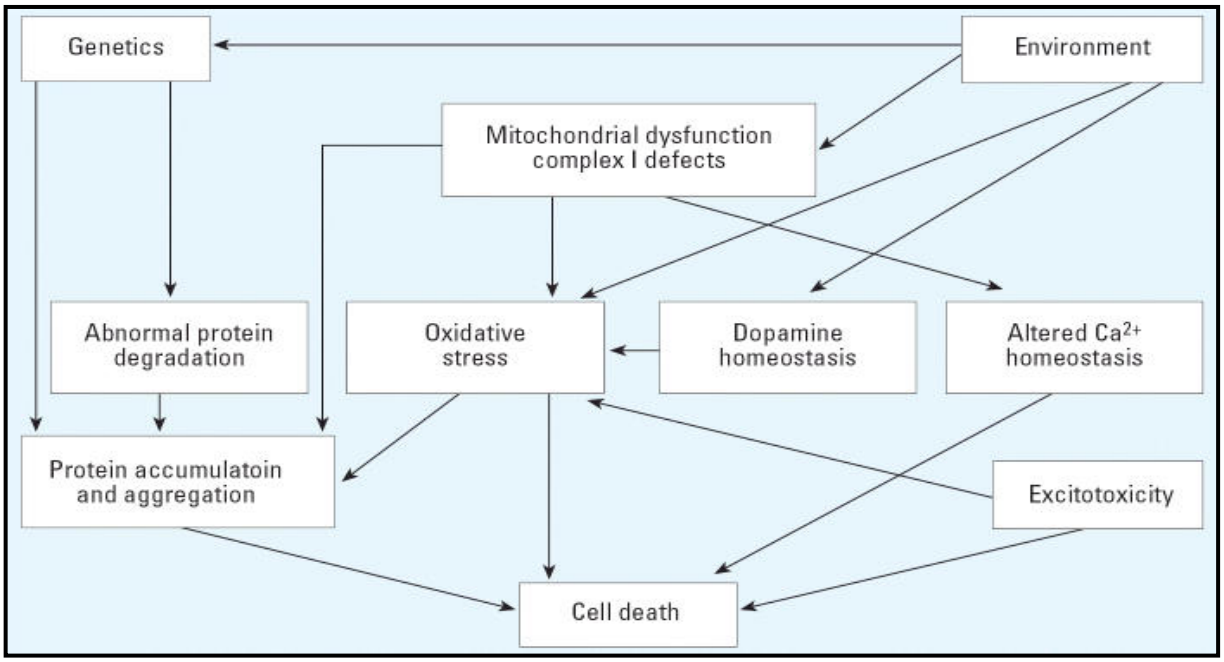

Figure 6: Potential mechanisms involved in the development of PD. Adapted from Brown et al. (2006).

ubiquitin-proteasome system, apoptosis, inflammation and excitotoxicity, have been proposed (Mattson, 2000; Chung et al., 2001a; Vila and Przedborski, 2003; Abou-Sleiman et al., 2006; Olanow, 2007; Tansey et al., 2007; Burke, 2008). Currently, the culprit of dopamine neuron loss in PD is likely to be a combination of multiple interlinking pathways (Figure 6), called the "multiple hit hypothesis," rather than a unifying mechanism (Obeso et al., 2010; Sulzer, 2007).

1.3.1 Oxidative stress and mitochondrial dysfunction

Oxidative stress has long been implicated in the process of neurodegeneration in PD pathogenesis. Oxidative stress, arising from excessive production of ROS and/or defective ROS removal, can potentially damage cellular lipids, proteins, and DNA. Postmortem studies have consistently observed high levels of oxidation of lipids, proteins, and nucleic acids in the SNc of sporadic PD brains (Dexter et al., 1989b; Yoritaka et al., 1996; Alam et al., 1997; Floor and Wetzel, 1998; Jenner, 2003; Tsang and Chung, 2009). Also, significant alterations of the antioxidant defense system, in particular reduced glutathione, are found in the SNc of PD patients (Sian et al., 1994). Mitochondrial respiratory chain is the major source of ROS, in particular the hydrogen peroxide and superoxide anions (Migliore and Coppede, 2009). In the presence of ferrous iron, these ROS can be converted to even more potent ROS, such as the hydroxyl radical and hydroxyl anion (Chinta and Andersen, 2008; Winterbourn, 2008). Not surprisingly, the level of iron is significantly increased in the SNc of PD brains (Sofic et al., 1988; Dexter et al., 1989a; Riederer et al., 1989; Jenner and Olanow, 1996). Apart from being the main source of increased oxidative stress in PD brains, mitochondrial function itself also can be affected by oxidative stress (Cardoso et al., 1999; Cadenas and Davies, 2000; Cecarini et al., 2007), which further takes part in the accumulation of ROS and mitochondrial damage in a vicious cycle. In this context, the feedforward mechanism appears to be a common mechanism underlying neuronal cell death in neurodegenerative diseases. In addition to mitochondria, auto-oxidation of dopamine, a reaction known to generate superoxide and hydrogen peroxide, as well as reactive dopamine quinones, specifically contributes to the cellular ROS in dopaminergic neurons (LaVoie and Hastings, 1999; Hastings, 2009). This dopamine-dependent oxidative stress is suggested to partially explain

the selective vulnerability of dopaminergic neurons in PD. Another important contributor of oxidative stress is nitric oxide (NO), which is generated by nitric oxide synthase (NOS) (Jenner, 2003). Reaction of ROS with NO produces highly toxic reactive nitrogen species (RNS), such as the peroxynitrite and nitro-tyrosyl radicals (Zhang et al., 2000a). Besides damaging cellular proteins, lipids, and DNA, oxidative stress also can activate a variety of effector pathways including ERK, JNK, PI3K/Akt, NF-κB, p53, PKC, caspases and Bcl-2 family members, as well as inflammation, contributing to the downstream processes that lead ultimately to cell survival or cell death (Finkel and Holbrook, 2000; Hartmann et al., 2000; Hartmann et al., 2001a; Hartmann et al., 2001b; Beal, 2003; Kanthasamy et al., 2003a; Perier et al., 2005; Loh et al., 2006; Mattson, 2006; Perier et al., 2007).

Over the last several decades, mitochondrial dysfunction is a widely accepted pathogenic pathway contributing to PD pathogenesis. There is considerable evidence for mitochondrial dysfunction in the brains of PD patients. Impairment of complex I activity of the mitochondrial electron transport chain has been detected in the SNc, skeletal muscle, lymphocytes, and platelets of patients with PD (Mizuno et al., 1989; Parker et al., 1989; Schapira et al., 1989; Yoshino et al., 1992; Barroso et al., 1993; Mann et al., 1994; Haas et al., 1995; Penn et al., 1995; Blandini et al., 1998). Increased oxidation of complex I subunits and reduced rates of electron transfer through complex I, as well as misassembly of complex I, were also demonstrated in PD brains (Keeney et al., 2006). It is noteworthy that a significant reduction in complex I activity was recently reported in purified mitochondria isolated from PD frontal cortex (Keeney et al., 2006; Parker et al., 2008; Navarro and Boveris, 2009), which may contribute to impaired cognition in PD. Moreover, increased mtDNA deletions were detected in nigral neurons in PD brains (Bender et al., 2006). Although no pathogenic

mutations in mtDNA have as yet been reported, a specific polymorphism in the gene encoding NADH dehydrogenase 3 (ND3) of complex I was shown to lead to a significant decrease in the risk of PD (van der Walt et al., 2003).

Further evidence for involvement of mitochondrial dysfunction and oxidative stress in PD comes from epidemicological studies using the environmental toxin MPTP that results in an acute and irreversible parkinsonism in human and non-human primates (Langston et al., 1983). MPTP (Figure 7) is a lipophilic molecule that can easily cross the blood-brain barrier and be metabolized to 1-methyl-4-phenyl-2,3-dihydropyridinium (MPDP) in a reaction catalyzed by the monoamine oxidase B (MAOB) in glial cells. This unstable metabolite is further metabolized to the pyridinium ion (MPP^+, 1-methyl-4-phenylpyridiniu m iron), the active toxic compound (Langston et al., 1984; Markey et al., 1984). MPP^+ then is selectively taken up by the dopamine neurons *via* the dopamine transporter (DAT), where it is concentrated in mitochondaria, causes the complex I defect and in turn produces ROS, activating microglia and leading ultimately to cell death (Javitch et al., 1985; Nicklas et al., 1985; Ramsay et al., 1986; Przedborski et al.,

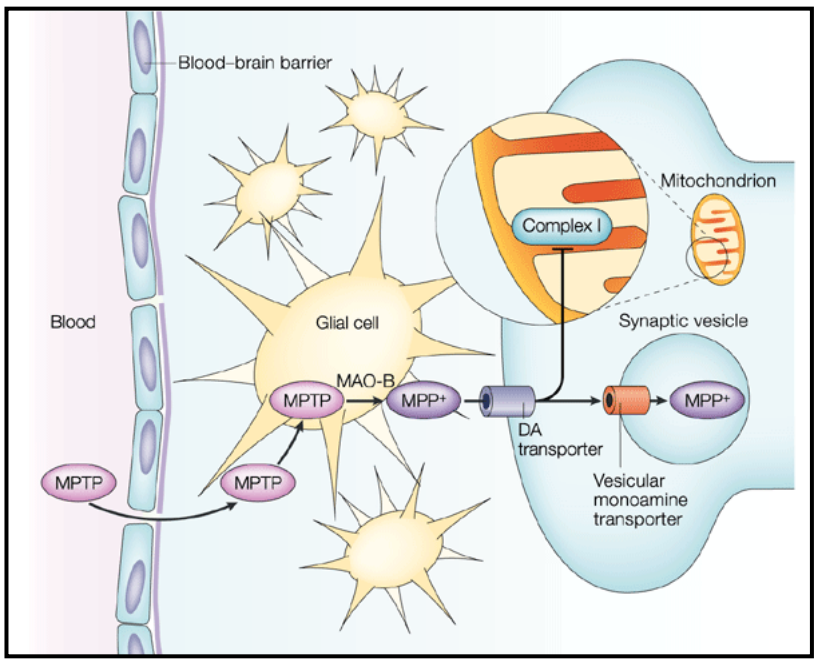

Figure 7: The MPTP metabolism. Adapted from Vila and Przedborski (2003).

2001; Kotake and Ohta, 2003; Schober, 2004; McGeer and McGeer, 2008). MPP^+ can also be taken up by the dopaminergic synaptic vesicles *via* vesicular monoamine transporter 2 (VMAT2) (Del Zompo et al., 1991, 1992; Peter et al., 1994). This uptake may cause the cytoplasmic distribution of dopamine, leading to increased dopamine-dependent oxidative stress (Lotharius and Brundin, 2002). A number of downstream apoptotic events that are responsible for MPTP-mediated degeneration of SNc neurons have been revealed. These include NFκB-dependent transactivation of iNOS (Carbone et al., 2009), up-regulation of JNK (Saporito et al., 1999) and Bax (Vila et al., 2001), release of cytochrome c and activation of caspase-3 and caspase-9 (Viswanath et al., 2001). In addition to MPTP, a variety of pesticides with related properties, such as rotenone, paraquat, dieldrin, and maneb, also have been extensively investigated. It appears that all of these toxins exhibit a common feature, i.e., inhibition of mitochondrial respiratory chain and production of oxidative stress (Brown et al., 2006; Migliore and Coppede, 2009). Consistent with this view, antioxidants can be used to ameliorate their toxicity (Suntres, 2002; Uversky, 2004). It is noteworthy that, unlike MPTP and paraquat, rotenone is uniformly distributed throughout the brain, but it still results in selective loss of SNc neurons (Bove et al., 2005; Miller et al., 2009).

The identification of PD-linked genes in the last decade has further supported the relevance of mitochondrial oxidative stress and dysfunction in PD pathogenesis. Indeed, these genes, including *α-synuclein*, *parkin*, *DJ-1*, *PINK1*, *LRRK2*, and *HrtA2*, either directly or indirectly link their pathogenic roles with mitochondrial dysfunction and subsequent oxidative stress. Post-translational modifications of α-synuclein, such as nitration and oxidation, increase α-synuclein propensity to aggregate (Giasson et al., 2000; Yamin et al., 2003; Hodara et al., 2004; Glaser et al., 2005; Uversky et al., 2005; Lee and Trojanowski,

2006). Moreover, nitrated and oxidized forms of α-synuclein have been found commonly in Lewy bodies (Giasson et al., 2000; Ischiropoulos and Beckman, 2003; Navarro and Boveris, 2009), implicating that oxidative stress may play a role in the formation of LB inclusions. Recently, the nitrated form of α-synuclein has been shown to be more toxic to dopaminergic neurons *in vitro* and *in vivo*, suggesting that oxidation/nitration of α-synuclein might be relevant to PD pathogenesis (Yu et al., 2010). In addition, several *in vitro* studies have shown that auto-oxidation of dopamine can modulate the aggregation of α-synuclein possibly through the formation of the α-synuclein-dopamine quinone adducts that retain an unfolded conformation and thus inhibit fibril formation (Conway et al., 2001; Li et al., 2005; Norris et al., 2005; Leong et al., 2009). There is also evidence to suggest that α-synuclein has a neuroprotective function protecting neurons against oxidative stress through distinct pathways (Hashimoto et al., 2002; Quilty et al., 2006). Accumulating evidence also suggests a close connection between α-synuclein and mitochondria. In neurotoxin-treated cellular and animal models, complex I defects consistently causes selective dopaminergic degeneration with associated α-synuclein-positive inclusions (Forno et al., 1988; Betarbet et al., 2000; Manning-Bog et al., 2002). In addition, *in vitro* and *in vivo* overexpression of wildtype or mutant α-synuclein can lead to a variety of mitochondrial alterations, such as decreased mitochondrial membrane potential, oxidation of mitochondrial proteins, exacerbation of effects of mitochondrial toxins, and ultrastructural abnormalities, suggesting that α-synuclein might play a role in mitochondrial function (Hsu et al., 2000; Tabrizi et al., 2000; Song et al., 2004; Poon et al., 2005; Stichel et al., 2007; Parihar et al., 2009). Interestingly, although debated, it has been proposed that α-synuclein can be localized into mitochondria (Li et al., 2007; Nakamura et al., 2008; Shavali et al., 2008; Zhang et al., 2008). Recently, Devi and

colleagues located a cryptic mitochondrial targeting signal to the N-terminal 32-amino acid region of α-synuclein, and they also reported that mitochondrial accumulation of α-synuclein resulted in mitochondrial dysfunction and increased ROS generation (Devi et al., 2008). They concluded that the accumulation of α-synuclein in mitochondria might be relevant to PD pathogenesis since an enhanced level of α-synuclein was found in SNc and striatum of PD brains compared to healthy control brains. The mitochondrial localization of α-synuclein might be dependent on intracellular pH, and under some pathological conditions, such as pH changes during oxidative stress, mitochondrial accumulation of α-synuclein might be significantly enhanced (Cole et al., 2008). Further studies are needed to elucidate the precise functions of α-synuclein in the regulation of mitochondria functions.

Additionally, other genes linked to familial PD have been implicated in the mitochondrial function and stress response. *S*-nitrosylated form of parkin is detected in LBs of PD brains (Chung et al., 2004), further implying a role of oxidative/nitrative stress in LB formation. The *S*-nitrosylation of parkin can negatively regulate its E3 ligase activity, which may contribute to the accumulation of misfolded proteins (Chung et al., 2004; Yao et al., 2004). Parkin could also be covalently modified by dopamine, resulting in the loss of its activity (LaVoie et al., 2005). Although largely present in the cytosol, parkin can be found within mitochondria or associated with the outer mitochondrial membrane under certain conditions (Shimura et al., 1999; Darios et al., 2003; Kuroda et al., 2006). Multiple lines of studies have suggested that parkin plays a key role in maintaining mitochondrial integrity and function. Mitochondrial abnormalities have been noted in both parkin-knockout and parkin-mutant transgenic mice and files, as well as in leukocytes from PD patients with parkin pathogenic mutations (Greene et al., 2003; Muftuoglu et al., 2004; Palacino et al.,

2004; Stichel et al., 2007; Wang et al., 2007; Mortiboys et al., 2008). Furthermore, Riparbelli et al. reported that in files functional parkin is required for proper mitochondrial organization and morphology throughout spermatid development (Riparbelli and Callaini, 2007). Deficiency in PINK1, a mitochondrial kinase, also leads to mitochondrial abnormalities in files (Clark et al., 2006a). Interestingly, PINK1 and parkin appear to act in a common pathway in PD pathogenesis because overexpression of parkin can rescue PINK1-null linked damage (Clark et al., 2006a; Park et al., 2006). Moreover, the mitochondrial abnormalities due to the loss function of parkin or PINK1 can be rescued by knockdown of mitofusin, optic atrophy 1, or overexpression of dynamin-related protein 1 (Deng et al., 2008). These proteins are associated with mitochondrial fusion and fission, thus lending more support to the hypothesis that parkin and PINK1 are important for mitochondrial function. Finally, DJ-1 can function as an anti-oxidant, and interestingly, oxidative stress due to complex I inhibition can enhance the mitochondrial localization of DJ-1 (Canet-Aviles et al., 2004), which indicates that DJ-1 may also play a role in mitochondrial function. However, it appears that DJ-1 does not function within the PINK1/parkin pathway, since overexpression of DJ-1 could not rescue the mitochondrial abnormalities in parkin- or PINK1-deficient flies (Yang et al., 2006; Exner et al., 2007). It is noteworthy that parkin, PINK1, and DJ-1 all seems to play an important role in cell protection against a wide spectrum of stressors, including mitochondrial dysfunction and proteasome inhibition, etc. (Canet-Aviles et al., 2004; Taira et al., 2004; Valente et al., 2004b; Kim et al., 2005; Menzies et al., 2005; Petit et al., 2005; Moore, 2006; Paterna et al., 2007; Winklhofer, 2007; Haque et al., 2008; Wood-Kaczmar et al., 2008).

1.3.2 Impairment of the ubiquitin-proteasome system

Emerging evidence suggests a key role for the ubiquitin-proteasome system (UPS) in the molecular pathogenesis of PD. In fact, the presence of insoluble ubiquitin-positive proteinaceous aggregates or inclusion bodies is a common pathological feature in human neurodegenerative disorders (Kopito, 2000; Goldberg, 2003; Ross and Poirier, 2004). The UPS plays a pivotal role in degrading mutant, damaged, or misfolded intracellular proteins that could otherwise form potentially deleterious aggregates (Goldberg, 2003; Cook and Petrucelli, 2009). Ubiquitination is accomplished by posttranslational covalent conjugation of ubiquitin polypeptide to a lysine residue in specific target proteins through an ATP-dependent enzymatic pathway (Hershko and Ciechanover, 1998). Protein ubiquitination is catalyzed by a series of enzymatic steps involving an E1 activating enzyme, an E2 conjugating enzyme, and an E3 ligase that typically confers specificity to the ubiquitin machinery (Lydeard and Harper, 2010). The polyubiquitinated proteins are then targeted to the 26S proteasome for degradation. The 26S proteasome consists of a 20S catalytic core particle and a 19S regulatory particle (Hershko and Ciechanover, 1998; Pickart and Cohen, 2004; Mukhopadhyay and Riezman, 2007). Polyubiquitin chains released from target proteins are subsequently disassembled into monomeric ubiquitin through a reaction catalyzed by deubiquitinating enzymes (Wilkinson, 1997). Therefore, defects in either ubiquitination or the 26S proteasome may lead to the accumulation and aggregation of toxic proteins eventually resulting in neurodegeneration as seen in PD.

The first indication of protein misfolding in the pathogenesis of PD is the presence of intracytoplasmic proteinaceous inclusions together with the accumulation of oxidatively damaged, denatured, mutated, or misfolded proteins known as LB in the SNc of most PD

brains, although the relevance of LB formation to nigral neuronal death is still uncertain (Pollanen et al., 1993; Forno, 1996). LB are composed of a variety of free and ubiquitinated proteins, including ubiquitin, α-synuclein, parkin, proteasome subunits, UCHL1, torsin-A, synphilin-1, chaperons and neurofilaments (Lowe et al., 1990; Forno, 1996; Ii et al., 1997; Spillantini et al., 1998; Shimura et al., 1999; Shashidharan et al., 2000; Wakabayashi et al., 2000; Shimura et al., 2001; Auluck et al., 2002). In particular, the accumulation of ubiquitinated proteins in LB indicates an overwhelming of the UPS or loss of function in proteasomal protein degradation in the PD pathogenesis. Consistently with this hypothesis, postmortem studies have detected both structural and functional impairments of the UPS in the SNc of PD brains (McNaught and Jenner, 2001; McNaught et al., 2002; McNaught et al., 2003). Moreover, systemic administration of proteasome inhibitors into rats can lead to the selective loss of SNc dopamine neurons, as well as the formation of LB-like inclusions and recapitulate many key features of sporadic PD (McNaught et al., 2004; Miwa et al., 2005; McNaught and Olanow, 2006). However, whether UPS dysfunction in PD is a primary cause or a secondary effect remains a matter of debate. As the ubiquitin/proteasome pathway is ATP-dependent, impairment of UPS might be a consequence of the inhibition of complex I activity and/or oxidative damage. In addition, the role of proteasome inhibition in the PD pathogenesis is still controversial. Several in vivo studies using proteasome inhibitors failed to show loss of nigral neurons (Bove et al., 2006; Kordower et al., 2006), and strikingly, there is also data demonstrating that proteasome inhibition can provide a neuroprotective effect against a variety of insults both in vivo and in vitro (Phillips et al., 2000; van Leyen et al., 2005; Yamamoto et al., 2007; Maher, 2008; Oshikawa et al., 2009).

The most compelling evidence linking UPS with the degeneration of nigrostriatal dopamine neurons in PD is the identification that mutations in *parkin* gene represent one of the most commonly known genetic causes of early-onset PD (Kitada et al., 1998). Parkin is a member of the E3 ubiquitin ligase family, and several substrates of parkin have been identified (Poole et al., 2008). It is currently thought that pathogenic parkin gene mutations cause loss of ubiquitination activity, leading to the abnormal accumulation of toxic proteins and neurodegeneration (Lesage and Brice, 2009). In addition, a missense mutation (I93M) in the *UCHL1* gene has been identified in a few rare familial PD cases (Leroy et al., 1998b), although the relevance of the I93M mutation in PD is still contentious. UCHL1 belongs to a family of deubiquitinating enzymes and the I93M mutant displays reduced ubiquitin hydrolase activity, suggesting that a defect in polyubiquitin hydrolysis might also lead to impaired clearance of abnormal proteins and consequent neurodegeneration (Leroy et al., 1998b; Liu et al., 2002).

1.3.3 Apoptosis

Apoptosis has been widely implicated in dopaminergic neuron death of PD although there is still debate on it (Mattson, 2000; Vila and Przedborski, 2003). Initially, efforts focused on apoptotic cells in postmortem brains of PD patients in an attempt to identify morphological and biochemical markers of apoptosis (Mochizuki et al., 1996). TdT-mediated dUTP digoxigenin nick end labeling (TUNEL), which is considered to be the most sensitive method for detect fragmentated DNA in situ, was the main approach used for these studies, and it was demonstrated that increased numbers of TUNEL-positive dopaminergic neurons exist in the postmortem brains of PD patients. Further studies also showed the activation of

different initiator and effector caspases, including caspase-8, -9 and -3 in the brains of PD patients (Hartmann et al., 2000; Hartmann et al., 2001b; Viswanath et al., 2001), although other studies failed to find such activation (Banati et al., 1998; Jellinger, 2000). The controversy of these results makes the involvement of apoptosis in PD still debatable. It has to be considered that postmortem brain samples of PD patient are usually at the last stage of disease, when most dopaminergic neurons are already lost and apoptotic changes may not be detected at all (Vila and Przedborski, 2003). To bypass this problem, many *in vitro* cell and *in vivo* animal models of PD have been developed. Among these models, the MPTP mouse model has been extensively used in all aspects of studies of PD (Przedborski and Vila, 2003). In this mouse model, damage of complex I of mitochondria respiratory chain in substantial nigral dopaminergic neurons was observed, which also existed in the postmortem brain samples of PD patients (Gluck et al., 1994). Together with elevated ROS generation and perturbation of calcium homeostasis after MPTP administration (Jackson-Lewis et al., 1995), mitochonadial respiratory chain damage was thought to be the early events triggering the intrinsic apoptotic pathway in dopaminergic neuron death. Substantial evidence also has demonstrated all major events of an apoptotic intrinsic pathway, including cytochrome C release, caspase-3 activation and further cell death after MPTP administration. In addition to the clear evidence of a role for apoptosis in neurotoxin models, and somewhat controversial evidence from human postmortem studies, there is abundant evidence that some of the genetic causes of PD, including α-synuclein (Manning-Bog et al., 2003; Sidhu et al., 2004; Chandra et al., 2005; Machida et al., 2005; Leng and Chuang, 2006), parkin (Darios et al., 2003; Jiang et al., 2004; Machida et al., 2005), PINK1 (Petit et al., 2005; Plun-Favreau et al., 2007), and DJ-1 (Canet-Aviles et al., 2004; Junn et al., 2005; Xu et al., 2005), are directly

and primarily involved in the regulation of apoptotic pathways. Taken together, apoptotic death was strongly implicated in dopaminergic neuron and then the pathogenesis of PD. However, the selective death of nigral dopaminergic neurons in PD suggests that specific factors in signal pathways or regulatory mechanisms of apoptotic death, other than general intrinsic apoptotic pathways, may exist and contribute to the selective apoptotic death of dopaminergic neuron.

1.4 Protein Kinase C delta

1.4.1 Protein Kinase C delta activation and its role in PD

The protein kinase C (PKC) family is one of the major serine/threonine protein kinase families fulfilling the protein phosphorylation, and thus mediating different cellular processes, including proliferation, differentiation, survival and apoptosis (Gschwendt, 1999). PKC was first identified in 1977 by Nishizuka and co-workers as a nucleotide-independent and calcium-dependent serine kinase (Inoue et al., 1977). This family is composed of at least 11 isoforms that are further divided into three groups based on their structure and mode of stimulation. The conventional PKCs (α, βI, βII, γ) are activated by the binding of diacylglyerol (DAG) in a calcium-dependent manner, whereas the novel PKCs (δ, ε, η, θ) require DAG, but not calcium, for their activity. The atypical PKCs (ζ, ι, λ) do not respond to either DAG or calcium for activation (Churchill et al., 2008). All PKC isoforms are composed of an N-terminal regulatory domain and a C-terminal catalytic domain that are separated by a flexible-hinge V3 region (Newton, 1995a). The regulatory domain contains two conserved regions, C1 and C2, as well as a pseudo-substrate region that mimics a substrate and interacts with the substrate-binding cavity in the catalytic domain, keeping the

protein inactive within the cytosol (Soderling, 1990; Liu and Heckman, 1998). For the conventional PKCs, binding of calcium and DAG to the C2 domain and the zinc finger-rich region of the C1 domain, respectively, leads to the release of the autoinhibition and subsequent activation of the enzyme (Newton and Johnson, 1998; Newton, 2003). The lack of the amino acids essential for a functional calcium-binding site in C2 domain confers calcium independence to novel PKCs. The catalytic domain is composed of the conserved C3 and C4 regions, which function as the catalytic ATP binding site and kinase catalytic site, respectively (Newton, 1995b). The flexible-hinge V3 region has been identified as a target for caspase-dependent cleavage (Steinberg, 2008). PKCδ (see Figure 8 for its domain structure), a member of the novel PKC subfamily, was first discovered by Gschwendt et al. (Gschwendt et al., 1986). Consistent with other PKC isoforms, PKCδ consists of a regulatory domain (N-terminus) and a catalytic domain (C-terminus). The PKCδ regulatory domain, lacking an authentic C2 region, only has a C2-like region, thus explaining its inability to be activated by calcium. Also, a pseudo-substrate sequence is located between the C2-like and C1 region, which is proposed to keep the enzyme in an inactive conformation.

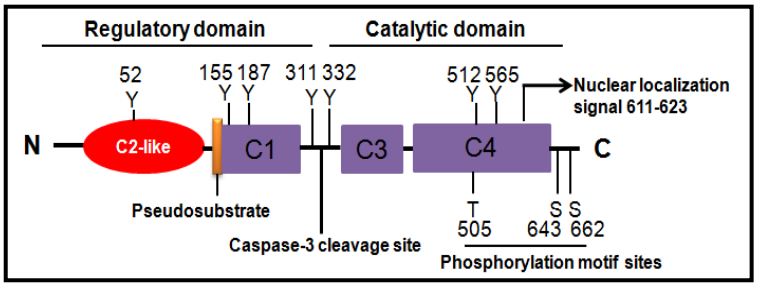

Figure 8: Domain structure of PKCδ.

Like other conventional and novel PKC isoforms, PKCδ is primarily activated by a lipid-mediated mechanism involving its translocation from cytosol to membrane. In addition, two other pathways of PKCδ activation have been elucidated: phosphorylation and proteolytic activation (Kikkawa et al., 2002a; Brodie and Blumberg, 2003). It has been

reported that phosphorylation of Thr-505, Ser-643, and Ser-662 in activation loop can increase PKCδ kinase activity (Toker, 1998). In contrast to the phosphorylation of Thr/Ser sites, tyrosine phosphorylation at tyrosine residues Tyr-52, Tyr-155, Tyr-187, Tyr-311, Tyr-332, and Tyr-565 has also been implicated to modulating PKCδ activity (Gschwendt, 1999). A range of stimulus has been reported to induce the tyrosine phosphorylation of PKCδ (Kikkawa et al., 2002a). For example, treatment with the known oxidative stress-inducing agent hydrogen peroxide (H_2O_2) was reported to cause Tyr-311 and Tyr-332 phosphorylation of PKCδ (Konishi et al., 2001). We have found that under certain stimuli (H_2O_2), the phosphorylation of Tyr-311on PKCδ is particularly important for the proteolytic activation of PKCδ in dopaminergic neurons (Kaul et al., 2005b). Because multiple tyrosine residues on PKCδ can be phosphoylated by upstream kinase, the effect of tyrosine phosphorylation may vary depending on both the position of phosphoylated-tyrosine and the specific cellular context. Another activation mechanism of PKCδ, proteolytic activation, was discovered recently. This caspase-3-mediated cleavage of PKCδ yields 41-kDa catalytically active and 38-kDa regulatory fragments. The proteolytic activation of PKCδ has been implicated in apoptosis in many cell types (D'Costa and Denning, 2005; Ryer et al., 2005; Choi et al., 2006b). Our recent studies have characterized a critical role for the caspase-3-dependent proteolytic activation of PKCδ in oxidative stress-induced dopaminergic cell death in cell culture models of PD. In rat mesencephalic dopaminergic neuronal N27 cell models, exposure to dopaminergic neurotoxins, such as inorganic manganese (Latchoumycandane et al., 2005), an organic manganese containing the gasoline additive, MMT (Anantharam et al., 2002), the agriculture chemical dieldrin (Kitazawa et al., 2003), MPP^+ (Kaul et al., 2003; Yang et al., 2004), the proteasome inhibitor MG-132 (Sun et al., 2008), or the oxidative

stress-inducing agent H_2O_2 (Kaul et al., 2005b), induced a dose-dependent and time-dependent increase in the proteolytic activation of PKCδ. Furthermore, using pharmacological inhibitors (PKCδ-specific inhibitor rottlerin, and caspase-3 inhibitors z-DEVD-fmk, or z-DIPD-fmk) and genetic tools (PKCδ siRNA or PKCδ cleavage-resistant mutant), we have demonstrated that the caspase-3-dependent proteolytic activation of PKCδ plays an important role in neurotoxin-induced apoptotic death (Yang et al., 2004; Kanthasamy et al., 2006; Sun et al., 2008). We also found that the active PKCδ form is not translocated to the cell membrane, suggesting that the lipid-mediated activation mechanism is not involved in this process (Kaul et al., 2003; Yang et al., 2004). Native or cleaved PKCδ was also shown to move to the mitochondria or nucleus in apoptotic cells (Reyland et al., 1999; Brodie and Blumberg, 2003), where it may phosphotylate its substrate or interact with other proteins. In the nucleus, it was reported that PKCδ can induce phosphorylation of lamin B (Cross et al., 2000). Several other proteins have also been identified to interact with PKCδ, including DNA-dependent protein kinase (DNA-PK), (Bharti et al., 1998), and p73 (Ren et al., 2002), etc. Additionally, a positive feedback amplification loop between PKCδ and caspases-3 has been discovered by our laboratory (Kaul et al., 2003). We found that the proteolytic activation of PKCδ regulates upstream caspase-3 activity, thus suggesting that PKCδ may function as both the mediator and signal amplifier within the neurotoxin-induced apoptotic pathway.

1.4.2 Genomic organization of PKCδ genes

The genomic structure of PKCδ related genes was shown for human PRKCD (http://www.ncbi.nlm.nih.gov/sites/entrez?db=gene&cmd=retrieve&dopt=full_report&list_ui

ds=5580), mouse Prkcd (http://www.ncbi.nlm.nih.gov/sites/entrez?db=gene&cmd=retrieve&dopt=full_report&list_uids=18753), and rat Pkcd (http://www.ncbi.nlm.nih.gov/sites/entrez?db=gene&cmd=retrieve&dopt=full_report&list_uids=170538). The genomic location of PKCδ gene is on chromosomes 3, 14, and 19 of human, mouse and rat, respectively (Kikkawa et al., 2002b). The PKCδ of rat, mouse, and human markedly resembled each other in genomic organization (Suh et al., 2003). The rat PKCδ gene comprises 19 exons and 18 introns, and spans approximately 29 kb (Figure 9),

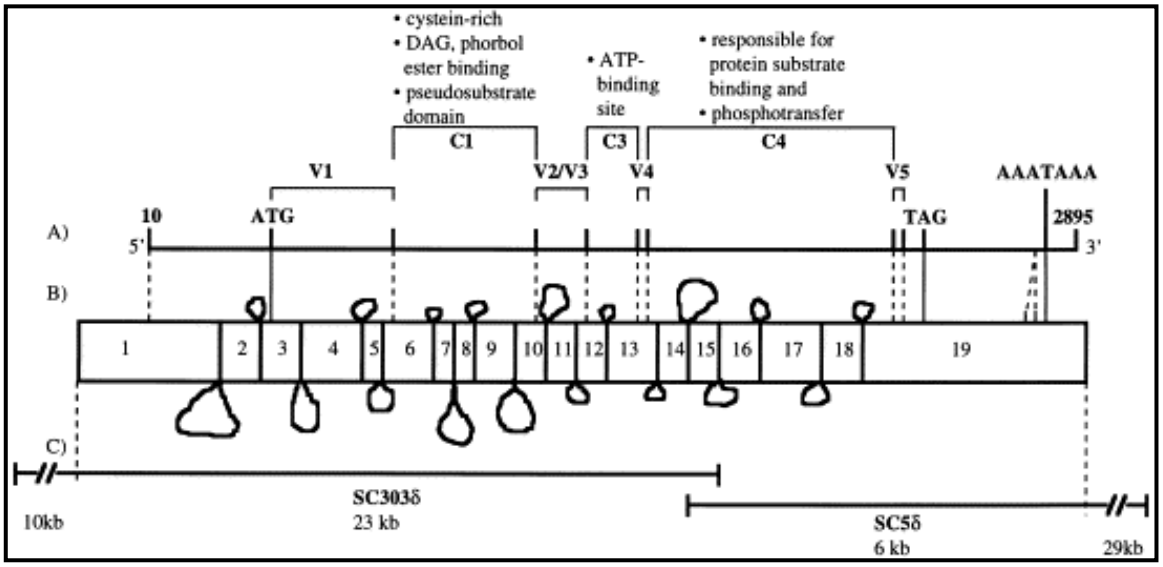

Figure 9: Genomic structure of rat PKCδ (adapted from Kurkinen et al. 2000).

whereas the murine and human PKCδ genes are both composed of 18 exons and 17 introns that span approximately 23 kb and 32 kb, respectively (Figure 10) (Kurkinen et al., 2000; Suh et al., 2003). The translation start codon of the murine and human PKCδ is located at the second exon, whereas rat PKCδ contains an extra exon in the 5'UTR and places the translation start codon at the third exon. Among these three mammalian PKCδ genes, the ORF size of the corresponding exons are highly conserved while the size of introns are

significantly conserved, indicating that they are evolutionarily conserved (Suh et al., 2003). The considerably long 5' untranslated region (UTR), as long as 675 bp in rat, is rarely found among the PKC family. Moreover, a huge gap, nearly 17 kb in human and 12 kb in rat and

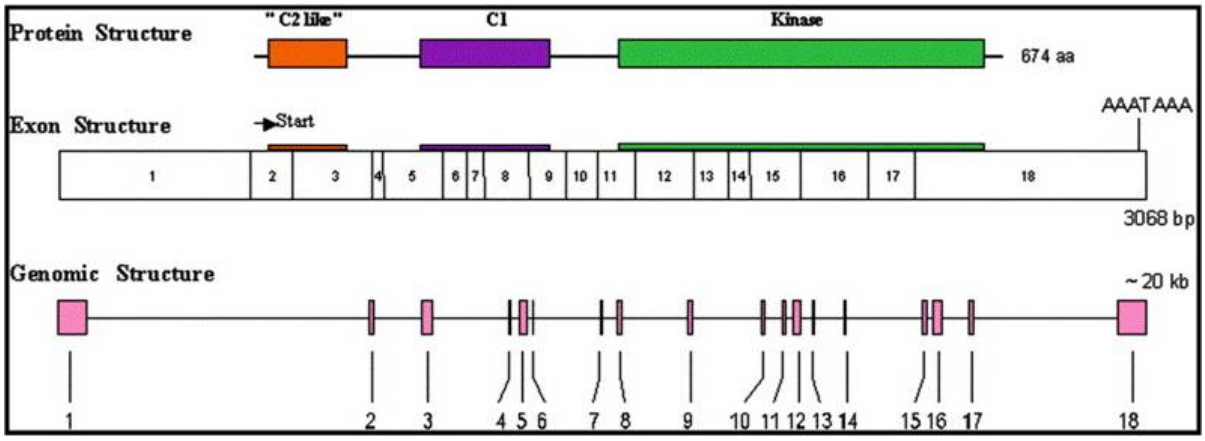

Figure 10: Genomic structure of murine PKCδ (adapted from Suh et al. 2003).

mouse, is found between the transcription start and translation start sites, suggesting a complexity may be involved in gene splicing. In contrast, there is great difference in genomic structure between nematodes and the three mammalian species. The exon/intron junctions mainly follow the GT/AG-rule among these four species.

1.4.3 PKCδ expression and gene regulation

PKCδ is expressed in most tissues, including brain, spleen, ovary, lung and uterus, as well as many cell types (Leibersperger et al., 1991). In rodent, northern blot shows that PKCδ has a high expression in the brain, spleen, epidermis, uterus, placenta and kidney (Ono et al., 1988). In the CNS, a survey of expression of PKC isoforms in the brain by immunostaining of different isoforms of PKC reveals that PKCδ was highly expressed in the thalamus and septal nuclei, hippocampal CA1 pyramidal cell layer (Naik et al., 2000); In

parallel, another study of expression of PKC isoforms in the brain by both immunostaining and *in situ* hybridization reveals that PKCδ expresses highly in some purkinje neurons in the cerebellum (Barmack et al., 2000). Both studies also indicate that PKCδ mainly localizes in the cytosol of cell body (Barmack et al., 2000; Naik et al., 2000). Recently, we reported that PKCδ is highly expressed in mouse nigral tissues and co-localizes with the tyrosine hydroxylase (TH) by double immunostaining method (Zhang et al., 2007c).

It has been reported that PKCδ expression could be regulated in a number of cell models through either a gnomic or non-genomic mechanism by diverse extracellular stimuli, including insulin, etoposide, estrogens, vitamin D3, mechanical forces, or bryostatin 1 (Berry et al., 1996; Shanmugam et al., 1999; Peters et al., 2000; Geng et al., 2001; Shin et al., 2004; Choi et al., 2006b; Horovitz-Fried et al., 2006). Despite extensive investigations on the molecular mechanisms of activation of PKCδ, little information is available on the mechanisms that control PKCδ expression at the transcriptional level. It has been reported that NFκB played an important role in the UV-induced and TNF-α-mediated mouse PKCδ expression in mouse keratinocytes, and mouse fibroblasts, respectively (Suh et al., 2003; Liu et al., 2006a). In human prostate cancer cells, androgen receptor can bind to a functional androgen-responsive element in response to androgen stimulation in the human PKCδ expression (Gavrielides et al., 2006). In human Saos-2 cells, p53 family proteins (p63, and p73) can recognize three-p53 binding sites in human PKCδ promoter to induce PKCδ expression (Ponassi et al., 2006; Horovitz-Fried et al., 2007). Furthermore, Sp-1 transcriptional factor is involved in the insulin-induced increase in PKCδ expression via an upstream Sp site in the PKCδ promoter (~1500 bp upstream of transcription start site) in

mouse L6 cells (Horovitz-Fried et al., 2007). However, the regulatory mechanisms in neuronal cells are largely unknown so far.

CHAPER II: TRANSCRIPTIONAL REGULATION OF PROTEIN KINASE Cδ, A PRO-APOPTOTIC KINASE: IMPLICATIONS FOR OXIDATIVE DAMAGE IN DOPAMINERGIC NEURODEGENERATION

A paper submitted to *Journal of Biological Chemistry*

Huajun Jin, Arthi Kanthasamy, Vellareddy Anantharam, Ajay Rana, and Anumantha Kanthasamy

Abstract

We previously demonstrated that protein kinase Cδ (PKCδ) is an oxidative stress sensitive kinase that plays a causal role in apoptotic cell death in neuronal cells. While PKCδ activation has been extensively studied, relatively little is known about the molecular mechanisms controlling PKCδ expression. To characterize the regulation of PKCδ expression, we cloned a ~2k-bp 5'-promoter segment of the mouse PKCδ gene. Deletion analysis indicated that the non-coding exon 1 region contained multiple Sp sites, including four GC boxes and one CACCC box, which directed the highest levels of transcription in neuronal cells. In addition, an upstream regulatory region containing adjacent repressive and anti-repressive elements with opposing regulatory activities was identified within the region -712 to -560. Detailed mutagenesis revealed that each Sp site made a positive contribution to PKCδ promoter expression. Overexpression of Sp family proteins markedly stimulated PKCδ promoter activity without any synergistic transactivating effect. Furthermore, experiments in

Sp-deficient SL2 cells indicated long-isoform Sp3 as the essential activator of PKCδ transcription. Importantly, both PKCδ promoter activity and endogenous PKCδ expression in NIE115 cells and primary striatal cultures were inhibited by mithramycin A. The results from chromatin immunoprecipitation and gel shift assays further confirmed the functional binding of Sp proteins to PKCδ promoter. Additionally, we demonstrated that overexpression of p300 or CBP increases the PKCδ promoter activity. This stimulatory effect requires intact Sp binding sites and is independent of p300 HAT activity. These findings may have implications for development of new therapeutic strategies against oxidative damage.

Introduction

PKC represents a large family of at least 12 serine/threonine kinases that particpate in a wide variety of cellular events, including proliferation, cell cycle progression, differentiation, and apoptosis (Dempsey et al., 2000). Based on their structure and substrate requirements, PKC isoforms are divided into three groups: conventional PKCs (α, βI, βII, and γ), novel PKCs (δ, ε, η, and θ), and atypical PKCs (ζ and ι/λ). As a novel PKC, PKCδ has been recognized as a key pro-apoptotic effector in various cell types (Brodie and Blumberg, 2003). The role of PKCδ in nervous system function is beginning to emerge, and recent studies show that PKCδ plays a role in regulation of receptor and channel activity, differentiation, migration, and apoptosis (Saito, 1995). In addition to lipid-mediated activation and phosphorylation activation, a new pathway of PKCδ activation, proteolytic cleavage, was discovered recently. Previously, we showed that PKCδ is an oxidative stress-sensitive kinase, and that persistent activation of PKCδ by caspase-3-mediated

proteolytic cleavage is a key mediator in oxidative stress-induced dopaminergic neurodegeneration (Anantharam et al., 2002; Kaul et al., 2003; Kitazawa et al., 2003; Kaul et al., 2005; Latchoumycandane et al., 2005). Alternatively, pharmacological inhibiton of PKCδ and depletion of PKCδ by siRNA are each sufficient to prevent dopaminergic neurodegeneration in cell culture and animal models of Parkinson's disease (Yang et al., 2004; Kanthasamy et al., 2006; Zhang et al., 2007a). We also showed that PKCδ negatively regulates tyrosine hydroxylase (TH) activity and dopamine synthesis by enhancing protein phosphatase 2A activity in dopaminergic neurons (Zhang et al., 2007b). An elevated striatal dopamine level was observed in PKCδ knockout mice as compared to wild type mice, further demonstrating a key role of the kinase in the nigrostriatal dopaminergic function (Zhang et al., 2007b). In addition, increased PKCδ activity, caused by aberrant expression of PKCδ, has been implicated in disease conditions, such as ischemia/hypoxia (Hlavackova et al., 2010; Li et al., 2010; Miettinen et al., 1996) and cancer (Reno et al., 2008). Therefore, an understanding of the molecular mechanisms that control the amount and activity of PKCδ is of physiological and pathophysiological interest.

PKCδ is ubiquitously expressed although the expression pattern is varied and complex (Ono et al., 1988; Leibersperger et al., 1991; Barmack et al., 2000; Naik et al., 2000). Evidence suggests that diverse stimuli can induce PKCδ expression (Berry et al., 1996; Shanmugam et al., 1999; Peters et al., 2000b, a; Shin et al., 2004; Choi et al., 2006; Horovitz-Fried et al., 2006), but the detailed mechanisms responsible for transcriptional regulation of PKCδ, especially in neuronal cells, have never been explored. The PKCδ promoter is surprisingly complex and does not contain a TATA box. The considerably long 5' untranslated region, as

long as 675 bp in rat, is rarely found among the PKC family (Kurkinen et al., 2000; Suh et al., 2003). Moreover, a huge distance, nearly 17 kb in human and 12 kb in rat and mouse, is revealed between the transcription start and translation start sites (Kurkinen et al., 2000; Suh et al., 2003). To our knowledge, only a few studies have documented the functional elements in the PKCδ promoter, or the characteristics of the factors involved in the control of PKCδ transcription (Gavrielides et al., 2006; Liu et al., 2006; Ponassi et al., 2006; Horovitz-Fried et al., 2007). In this study we analyzed the mouse PKCδ promoter to identify the transcriptional mechanisms underlying neuronal PKCδ expression. By combining cell biological, molecular and biochemical approaches, we cloned ~2 kb of mouse PKCδ promoter, characterized multiple DNA regulatory elements that positively or negatively regulate PKCδ gene expression, and identified members of the Sp protein family of transcription factors as fundamentally critical determinants of basal PKCδ gene transactivation.

Experimental Procedures

Reagents

Mithramycin A (MA) and hydrogen peroxide (H2O2) were purchased from Sigma-Aldrich (St. Louis, MO). Antibodies against PKCδ, Sp1, Sp3, and Sp4 were purchased from Santa Cruz Biotechnology (Santa Cruz, CA). Lipofectamine 2000 reagent and all cell culture reagents were obtained from Invitrogen (Carlsbad, CA).

Cloning of the 5'-flanking region of PKCδ gene and Plasmids construction

The 2.0-kb (-1694/+289) mouse PKCδ promoter sequence was amplified by fusion PCR from mouse genomic DNA prepared from the MN9D cells. Briefly, the -1694/-1193 and -1217/+289 fragments of the mouse PKCδ promoter first were amplified using mouse genomic DNA as a template and the primer sets P-1694F/P-1193R1 and P-1217F/P+289R (for all primers see Table S1), respectively. The two gel-purified PCR products then were mixed and used as a template to amplify the -1694/+289 fragment with the primer set P-1694F/P+289R. The conditions used in this second PCR were 95°C for 2 min; 25 cycles of 95°C for 45 sec, 57.5°C for 30 sec, and 68°C for 2 min; and 68°C for 5 min. The resultant 2.0-kb PKCδ promoter fragment was inserted into XhoI/HindIII sites of pGL3-Basic luciferase vector (Promega, Madison, WI) and designated as pGL3-1694/+289. Using pGL3-1694/+289 as a template, a series of truncated PKCδ promoter reporter constructs were constructed by PCR with appropriate primers and cloned into pGL3-Basic vectors, similar to the preparation of pGL3-1694/+289. To generate the reporter plasmid pGL3-Promoter-660/-561, fragment -660/-561 was PCR-amplified and inserted into the upstream of the SV40 promoter in pGL3-Promoter vector (Promega). For construction of pGL3-660/-561 plus +2/+289, primer pairs P-660F/P-561+2R and P-561+2F/P+289R were used for application of fragments -660/-561 and +2/+289, respectively. The fusion fragment -660/-561 plus +2/+289 was then amplified by the fusion PCR technique as described above using the primers P-660F/P+289R, followed by cloning into pGL3-Basic vector. To generate plasmids pGL3-147/+2 plus +2/+289 or pGL3-147/+2 plus +289/+2, fragment +2/+289 was PCR-amplified using a primer pair P+2F/P+289R that included a flanking XhoI site at both ends, digested with XhoI, and cloned in either orientation into the pGL3-147/+2 reporter

construct at the distant SalI site downstream of the luciferase gene. All reporter constructs were verified by DNA sequencing.

The expression plasmid bearing the cDNA of GFP-PKCδ was a kind gift from Dr. Mary Reyland at the University of Colorado Health Sciences Center (Denver, CO), and the pEGFP-C1 control vector was purchased from Clontech Laboratories (Mountain View, CA). The constructs for mammalian expression of pN3-Sp1, pN3-Sp4, and pN3-Sp3 FL encoding both long and short isoforms of Sp3 (Sapetschnig et al., 2004), and the Drosophila actin promoter-driven expression vectors for Sp1 (pPac-Sp1), the short isoforms of Sp3 (pPac-Sp3), the long isoforms of Sp3 (pPac-USp3), the full length of Sp3 (pPac-Sp3 FL, which is equivalent to the mammalian vector pN3-Sp3FL), Sp4 (pPac-Sp4), and β-galactosidase (p97b) (Lopez-Soto et al., 2006), as well as the "empty" control vectors pN3 and pPac0, were generously provided by Dr. G. Suske (Philipps-Universität Marburg, Germany). The plasmid pPac-Sp2 (Saur et al., 2002) was a kind gift from Dr. Dieter Saur (Technische Universität München, Germany). The p300 wild-type expression plasmid pCI-p300 and its histone acetyltransferase (HAT) deletion mutant, pCI-p300ΔHAT, were kindly provided by Dr. Joan Boyes (Institute of Cancer Research, United Kingdom) and generated as described previously (Boyes et al., 1998). The empty vector pCIneo was a gift from Dr. Christian Seiser (University of Vienna, Austria). The expression plasmid pcDNA-CBP (Yang et al., 1996) was a gift from Dr. Xiang-Jiao Yang (McGill University, Canada). To generate the luciferase-reporter plasmids, Sp1-Luc and mSp1-Luc (Sowa et al., 1999), which contains three consensus Sp1 binding sites underlined from SV40 promoter and three mutant Sp1 binding sites, respectively, the oligonucleotides with the sequences (Sp1-Luc:5'-ATATATCTCGAGCGCGTGGGCGGAACTGGGCGGAGTTAGGGGCGGG

AAAGCTTATATAT-3'; mSp1-Luc:5'-ATATATCTCGAGCGCGTGTTTTGAACTGTTTT GAGTTAGGTTTTGGAAAGCTTATATAT-3') were synthesized, annealed, and subcloned into the pGL3-Basic luciferase vector. To build the eukaryotic expression plasmid pcDNA-Sp2, Sp2 cDNA was cut out with XhoI from the pPac-Sp2 construct and inserted into the XhoI site of the pcDNA3.1 vector (Invitrogen).

Site-directed mutagenesis

Point mutations of potential transcription elements (GC and CACCC motifs) were introduced into the proximal PKCδ promoter reporter plasmid pGL3-147/+289, pGL3-147/+209, or pGL3+165/+289 by using the GeneTailor Site-Directed Mutagenesis System (Invitrogen) with overlapping PCR primers indicated in Table S1, according to the manufacturer's instructions. To generate double mutants, plasmids carrying a single mutation were used as a template to further introduce the second mutation. For triple mutants, plasmids carrying double mutations were utilized. The mutated sequences of all mutants were confirmed by DNA sequencing.

Primary mouse striatal neuronal culture and treatment

Plates (6-well) were coated overnight with 0.1 mg/ml poly-D-lysine. Striatal tissue was dissected from gestational 16- to 18-day-old murine embryos and kept in ice-cold Ca^{2+}-free Hanks's balanced salt solution. Cells then were dissociated in Hank's balanced salt solution containing trypsin-0.25% EDTA for 30 min at 37 °C. After enzyme inhibition with 10% heat-inactivated fetal bovine serum (FBS) in Dulbecco's Modified Eagle's Medium, the cells were suspended in Neurobasal medium supplemented with 2% Neurobasal supplement

(B27), 500 μM L-glutamine, 100 units penicillin, and 100 units streptomycin, plated at 2 × 10^6 cells in 2 ml/well and incubated in a humidified CO_2 incubator (5% CO_2 and 37 °C). Half of the culture medium was replaced every 2 days, and experiments were conducted using cultures between 6 and 7 days old. After exposure to doses of mithramycin A ranging from 0.5 to 5 μM for 24 h, the primary striatal cultures were subjected to quantitative real-time RT-PCR or immunocytochemical analysis.

Cell lines, Transient transfections, and Reporter gene assays

The mouse dopaminergic MN9D cell line was a generous gift from Dr. Syed Ali (National Center for Toxicological Research/FDA, Jefferson, AR). The mouse neuroblastoma NIE115 cell line was a kind gift from Dr. Debomoy Lahiri (Indiana University School of Medicine, Indianapolis, IN). The Drosophila SL2 cell line was purchased from ATCC (Manassas, VA). NIE115 and MN9D cells were cultured in Dulbecco's Modified Eagle's Medium supplemented with 10% FBS, 2 mM L-glutamine, 50 units penicillin, and 50 units streptomycin (37 °C/5% CO2). For H2O2 treatment studies, before addition of H2O2 (final concentration 0.5-2.0 mM), MN9D cells were switched to serum-free Dulbecco's Modified Eagle's Medium. Drosophila SL2 cells were maintained at 23°C without CO2 in Schneider's Drosophila medium containing 10% FBS.

Transient transfections of NIE115 and MN9D cells were performed using Lipofectamine 2000 reagent according to the manufacturers' instructions. Cells were plated at 0.3 × 106 cells/well in six-well plates 1 day before transfection. Each transfection was performed with 4 μg of reporter constructs along with 0.5 μg of pcDNA3.1-βgal (Invitrogen) used to monitor transfection efficiencies. Cells were harvested at 24 h post-transfection, lysed

in 200 µl of Reporter Lysis Buffer (Promega), and assayed for luciferase activity. For cotransfection assays, various amounts of expression plasmids as indicated in figures were added to the reporter plasmids. The total amount of DNA was adjusted by adding an empty vector. In some experiments, mithramycin A (0-5 µM) was added 4 h after DNA transfection, and luciferase activity was measured 24 h later. For transfection of SL2 cells, one day before transfection, cells were plated onto six-well plates at a density of 2.1 × 106 cells/well. Cells were transfected using the Calcium Phosphate Transfection kit (Invitrogen), as described previously (Suske, 2000). Each well received 4 µg of reporter construct, 4 µg of β-galactosidase expression plasmid p97b for normalization of transfection efficiencies, and varying amounts (0-4 µg) of the fly Sp expression plasmids. DNA amounts of expression plasmids were compensated with the empty plasmid pPac0. After 24 h of transfection, the medium was changed, and 24 h later the cells were harvested, lysed by freeze-thawing in 200 µl of 0.25 M Tris-HCl (pH 7.8), and assayed for luciferase activity.

Luciferase activity was measured on a Synergy 2 Multi-Mode Microplate Reader (BioTek, Winooski, VT) using the Luciferase Assay system (Promega), and β-galactosidase activity was detected using the β-Galactosidase Enzyme Assay system (Promega). The ratio of luciferase activity to β-galactosidase activity was used as a measure of normalized luciferase activity.

Quantitative real-time RT-PCR

Total RNA was isolated from fresh cell pellets using the Absolutely RNA Miniprep kit (Stratagene, La Jolla, CA). First strand cDNA was synthesized using an AffinityScript QPCR cDNA Synthesis kit (Stratagene). Real-time PCR was performed in an Mx3000P

QPCR system (Stratagene) using the Brilliant SYBR Green QPCR Master Mix kit (Stratagene), with cDNAs corresponding to 150 ng of total RNA, 12.5 μl of 2 × master mix, 0.375 μl of reference dye, and 0.2 μM of each primer in a 25-μl final reaction volume. All reactions were performed in triplicate. Sequences for PKCδ primers are shown in Table S1. β-actin was used as internal standard with the primer set purchased from Qiagen (QuantiTect Primers, catalog number QT01136772). The PCR cycling conditions contained an initial denaturation at 95 °C for 10 min, followed by 40 cycles of denaturation at 95 °C for 30 sec, annealing at 60 °C for 30 sec, and extension at 72°C for 30 sec. Fluorescence was detected during the annealing step of each cycle. Dissociation curves were run to verify the singularity of the PCR product. The data were analyzed using the comparative threshold cycle (Ct) method (Livak and Schmittgen, 2001).

Methylation specific PCR (MSP)

For MSP experiments, genomic DNA was isolated using the DNeasy blood & tissue kit as mentioned earlier. Bisulfite modification was subsequently carried out on 500 ng of genomic DNA by the MethylDetector bisulfite modification kit (Active Motif, Carlsbad, CA) according to the manufacturer's instructions. Two pairs of primers were designed to amplify specifically methylated or unmethylated PKCδ sequence using MethPrimer software (Li and Dahiya, 2002). The cycling condition was: 94 °C for 3 min, after which 35 cycles of 94 °C for 30 sec, 54 °C for 30 sec, 68 °C for 30 sec, and finally 72 °C for 5 min. PCR products were loaded onto 2% agarose gels for analysis.

Immunoblotting

Cell lysates were prepared as previously described (Zhang et al., 2007c). Immunoblotting was performed as previously described (Kanthasamy et al., 2006). Briefly, the samples containing equal amounts of protein were fractionated through a 7.5% SDS-PAGE and transferred onto a nitrocellulose membrane (Bio-Rad Laboratories, Hercules, CA). Membranes were blotted with the appropriate primary antibody and developed with either IRDye 800 anti-rabbit or Alexa Fluor 680 anti-mouse secondary antibodies. The immunoblot imaging was performed with an Odyssey Infrared Imaging system (Li-cor, Lincoln, NE).

Immunostaining and microscopy

Immunostaining of PKCδ was performed in primary striatal neurons. Cells grown on coverslips pre-coated with poly-D-lysine were washed with PBS and fixed in 4% paraformaldehyde for 30 min. After washing, the cells were permeabilized with 0.2% Triton X-100 in PBS, washed with PBS, and blocked with blocking agent (5% bovine serum albumin, 5% goat serum in PBS). Cells then were incubated with the antibody against PKCδ (1:1000, Santa Cruz) overnight. Fluorescently conjugated secondary antibody (Alexa 568-conjugated anti-rabbit antibody red, 1:1500) was used to visualize the protein. Nuclei were counterstained with Hoechst 33342 for 3 min at a final concentration of 10µg/ml. Finally, images were viewed using an oil-immersion 60 × Plan Apo lens with a 1.45 numerical aperture on a Nikon inverted fluorescence microscope (model TE2000, Nikon, Tokyo, Japan). Images were captured with a SPOT color digital camera (Diagnostic Instruments, Sterling Heights, MI) and processed using Metamorph 5.07 image analysis

software (Molecular Devices). For quantitative analysis of immunofluorescence, we measured average pixel intensities from the region of interest (ROI) using the Metamorph 5.07 image analysis software.

Nuclear extracts preparation and EMSA

NIE115 nuclear extract was prepared as previously described (Tavares et al., 1999). For EMSAs, the IRye^{TM} 700-labeled complementary single-stranded oligonucleotides corresponding to sequences +205 to +236 of the mouse PKCδ promoter were synthesized (Li-cor), annealed and used as labeled probe. The unlabeled competitor oligos were obtained from Integrated DNA Technologies, Inc (Coralville, IA). The sequences of oligos used for EMSAs are illustrated in Table S2. In each reaction, 50 fmol labeled probes and 10 μg nuclear or cytoplasmic extracts were added. The resulting DNA-protein complexs were resolved on a 7% nondenaturing polyacrylamide gel and analyzed on the Odyssey imaging system (Li-cor). In competition experiments, before the addition of the labeled probe, nuclear extracts were pre-incubated for 30 min at room temperature with a 100-fold molar excess of unlabeled competitor oligos.

Chromatin immunoprecipitation (ChIP)

ChIP assays were conducted with chromatin isolated from NIE115 cells using the ChIP-IT Express Enzymatic kit from Active Motif according to the manufacturer's instructions with slight modifications. Briefly, after cross-linking, the nuclei were prepared and applied to enzymatic digestion to generate chromatin fragments between 200 to 1500 bp. The sheared chromatin was collected by centrifuge, and a 10-μl aliquot was removed to serve

as a positive input sample. Aliquots of 70-µl sheared chromatin were immunoprecipitated with 3 µg indicated antibody and protein-G magnetic beads. Equal aliquots of each chromatin sample were saved for no-antibody controls. The immunoprecipitated DNA was analyzed by PCR using PKCδ-specific primer set P+2F/P+289R indicated in Table S1 to amplify a region (+2 to +289) within PKCδ promoter. Conditions of linear amplification were determined empirically for these primers. PCR conditions are as follows: 94°C 3 min; 94°C 30 sec, 59°C 30 sec, and 68°C 30 sec for 35 cycles. PCR products were resolved by electrophoresis in a 1.2% agarose gel and visualized after ethidium bromide staining.

DNA fragmentation assays

DNA fragmentation assay was performed using a Cell Death Detection ELSA plus kit as previously described (Anantharam et al., 2002). Briefly, after treatment with various doses of H_2O_2 for 20 h, cells were collected and lysed in 450 µl of lysis buffer supplied with the kit for 30 min at room temperature, and spun down at 2300 × *g* for 10 min to collect the supernatant. The supernatant then was used to measure DNA fragmentation as per the manufacturer's protocol. Measurements were made at 405 and 490 nm using a SpectraMax 190 spectrophotometer (Molecular Devices).

Bioinformatics

The search for phylogenetic sequence conservation among rat, human, and murine PKCδ promoter was conducted with the program DiAlign TF (Morgenstern et al., 1996) (Genomatix Software). This program identifies common transcription factor binding-site (TFBS) matches located in aligned regions though a combination of alignment of input

sequences using the program DiAlign with recognition of potential TFBS by MatInspector software (Cartharius et al., 2005) (Genomatix Software).

Statistical analysis

Unless otherwise stated, all data were determined from three independent experiments, each done in triplicate, and expressed as average values ± SEM. All statistical analyses were performed using the GraphPad Prism 4.0 software (GraphPad Software, San Diego, CA). One-way analysis of variance (ANOVA test) followed by the Tukey multiple comparison test were used for statistical comparisons, and differences were considered significant if *P*-values less than 0.05 were obtained.

Results

Identification of DNA elements involved in transcriptional regulation of mouse PKCδ gene

The mouse PKCδ gene, located on mouse chromosome 14, comprises 18 exons that span ~20 kb (Fig. 1A). The PKCδ promoter lacks a TATA box and contains GC-rich sequences in the proximal promoter region. Further, examination of the PKCδ promoter did not reveal the classic initiator element (Inr) or the downstream promoter element (DPE), which are located at various distances downstream of the transcription start site (TSS) and are utilized by most TATA-less promoters to initiate transcription, suggesting that there might be other promoter motifs involved in the regulation of PKCδ gene transcription. To

facilitate analysis of the regulation of the PKCδ promoter, an approximately 2k-bp fragment containing the putative PKCδ promoter (1694 bp), as well as partial sequences of the first, non-coding exon (289 bp), was amplified by the fusion PCR technique from MN9D cells. This sequence has been deposited in the GenBank data bank under accession number GU182370. The resulting -1694/+289 region of the PKCδ promoter was placed upstream of the pGL3-Basic vector, designated as pGL3-1694/+289, and it was transiently transfected into NIE115 and MN9D cells along with the pcDNA3.1-βgal plasmid to monitor transfection efficiency. Luciferase activity of this construct increased nearly 30-fold as compared with the pGL3-Basic control, suggesting that this 2-kb sequence possesses functional promoter activity in both cells (Fig. 1B-C). To further delineate the location of functional elements that govern the PKCδ promoter activity, we introduced a series of truncated promoter fragments in the pGL3-1694/+289 construct by PCR and cloned into the pGL3-Basic vector. Both NIE115 and MN9D cells displayed similar profiles of reporter activity upon transfection with these reporter constructs. Two constructs pGL3-147/+289 and pGL3+2/+289, which contain sequences with high GC content in the proximal first exon, each exhibited a maximal luciferase activity that averaged ~260% of the activity of the pGL3-1694/+289 construct in both cells. Furthermore, lack of the sequence from +2 to +289 led to near background reporter activity in six truncated promoter constructs (pGL3-1694/-148, pGL3-1694/-659, pGL3-1694/-1193, pGL3-1192/-659, pGL3-1192/-148, and pGL3-660/-148). Thus, these data suggest the particular importance of the GC-rich sequences in the region between +2 to +289 for sustaining PKCδ gene transcription in neuronal cells. It should be noted that a vector, pGL3-147/+2, containing the -147/+2 fragment in which the basal promoter region was placed to drive luciferase expression, demonstrated modest transcriptional activity

(average activity in both cells, ~45% of that produced by the construct pGL3-1694/+289). Addition of the 5' fragment of -660 to -147 into the pGL3-147/+289 construct result in a complete loss of activity in construct pGL3-660/+289, indicating the presence of a strong repressive element that negatively regulates transcription activity within the -660 to -147 region. Further addition of the 5' sequence from -1192 to -660 into the pGL3-660/+289 construct partially blocked this repressive effect, indicating that the region (between -1192 and -660) contained either an enhancer element or an anti-repressor element that overcame the repression. Construct pGL3-1192/-660, however, displayed no luciferase activity in either cell line, thus, within this region (-1192 to -660 bp) an anti-repressive element existed, but not an enhancer element. The region between -1694 to -1193 may contain a weak inhibitory cis-element, as deletion of this ~500 bp from the construct pGL3-1694/+289 resulted in a slight increase in the promoter activity. Taken together, these results demonstrate that the PKCδ promoter contains multiple positive and negative regulatory elements in NIE115 and MN9D cells. The GC-rich region located between bp +2 and +289 contains a sequence of nucleotides necessary for transcription of the mouse PKCδ gene, and the sequence between -660 to -147 and -1192 to -660 contains a strong negative regulatory element (NREI) and an anti-repressive element with opposing activities controlling PKCδ gene expression. The region of -1694 to -1193 also contains a weak negative regulatory element (NREII).

Next, the identified negative regulatory element and anti-repressive element within the region between -1192 and -148 were investigated in more detail. First, to define the borders of these regulatory elements more precisely, series of detailed 5' deletions were constructed in this region and tested for their relative transcriptional activity utilizing the -147/+289 fragment as the baseline. As shown in Fig. 2A-B, in either MN9D or NIE115

cells, the anti-inhibitory effect of the anti-repressive element was retained, even after deletion of the sequence between nucleotides -1192 and -712. However, the anti-inhibitory effect was completely abolished when the sequence between -712 to -660 was deleted, suggesting that the anti-repressive element resides between the nucleotides -712 and -660. Further deletion of the region between -660 and -560 restored almost full promoter activity; however, all six of the 5'-deltion constructs from -560 to -197 exhibited comparable transcriptional activities to that of the -147/+289 fragment. This suggests that the NREI is limited to the region between -660 and -560.

Two functional types of NRE have been defined: promoter-specific NRE and the so-called silencer elements that are able to repress promoter activity in an orientation- and position-independent fashion, as well as in the context of both native and heterologous promoter (Brand et al., 1985). To further characterize the functional properties of the NREI in the PKCδ promoter, a chimeric fragment corresponding to the transcriptionally inhibited sequence from -660 to -561 was subcloned immediately 5' of the PKCδ proximal promoter construct pGL3-147/+289 to obtain pGL3-660/-561 plus -147/+289. As shown in Fig. 2C, the repressive activity of this region was significantly attenuated, and indeed, the luciferase activity in MN9D cells was actually increased, suggesting that the inhibitory activity of this repressive element is dependent upon its physical location in the PKCδ promoter. Furthermore, when the same fragment was placed 5' upstream of the heterologous SV40 early promoter (pGL3-Promoter-660/-561, Fig. 2D), no repressive activity was observed in either NIE115 or MN9D cells. Taken together, these data demonstrate that the NREI in the PKCδ promoter is functioning mechanistically as a promoter-specific repressive element, but not as a classic transcriptional silencer element.

Five Sp sites act as crucial cis-elements regulating the PKCδ promoter

We further concentrated our studies on the sequences with high GC content between +2 and +289 since experiments described earlier suggested the critical role of this proximal 288 bp region in the regulation of mouse PKCδ transcription. A comparison of this region with the corresponding regions of the rat and human PKCδ genes using a DiAlign TF program (Cartharius et al., 2005) revealed that this region is conserved between all three species; the identities are 89%, 60%, and 61% between rat and mouse, human and mouse, and human and rat, respectively (Fig. 3A). Further, the regions of all species are GC-rich and contain >66% GC content. Subsequent analysis with the program MatInspector (Cartharius et al., 2005) revealed the presence of a number of potentially important transcription factor-binding sites that are phylogenetically conserved among all species (identities are more than 95%), including four consecutive GC boxes (consensus GGGGCGGGG) designated GC(1) to GC(4) within ~250 bp downstream of the TSS. In addition, a CACCC box (also called GT box) that matches consensus CCACCCC was found at position +35 bp downstream of the TSS (Fig. 3A). GC boxes, GT/CACCC box and related GC-rich motifs, which are frequently designated Sp sites, often act as the binding sites for Sp transcription factors to regulate the basal and induced transcription of the core promoter as well as operate as essential enhancer sequences (Suske, 1999; Black et al., 2001). The functional importance of different Sp binding sites for transactivation of the PKCδ promoter was investigated by site-directed mutagenesis of these binding sites within the context of the PKCδ reporter construct pGL3-147/+289. Transient transfections of NIE115 and MN9D cells were carried out with these mutant constructs and promoter activity was determined and expressed relative

to that of the wild-type construct. As shown in Fig. 3B-C, the mutation of the CACCC box at +35 slightly diminished promoter activity in NIE115 (~15%) and MN9D (~10%) cell lines as compared with the wild-type construct. Alteration of the most distal GC(4) site at +256 displayed ~12% and 30% reduction in promoter activity over the wild-type construct in NIE115 and MN9D cells, respectively, whereas the inhibition observed with the GC(3) mutant, located just upstream of GC(4), was more pronounced, (reduced by ~30% and 40% in NIE115 and MN9D cells, respectively). In contrast, mutation of either the proximal GC(2) box or GC(1) box caused major decrements in reporter activity (~50% and 55% elimination in NIE115 and MN9D cells, respectively), suggesting that GC(2) and GC(1) represent more important motifs in activating the PKCδ promoter in comparison to the GC(3), GC(4), and CACCC sites. To investigate the regulatory interplay of different Sp sites, we performed simultaneous mutations of different Sp sites, and more reductions in promoter activity were seen with this strategy, thus suggesting that a functional synergism between these Sp sites is critical for the PKCδ promoter activity. For example, double mutations ablating the CACCC box with the GC(3) box, or GC(2) box, or GC(1) box resulted in a reduction of promoter activity by ~60% in both cell lines. However, double mutations of GC(3) and GC(2) boxes, or GC(3) and GC(1) boxes, reduced the activity of the PKCδ promoter in NIE115 and MN9D cells by ~73% and 80%, respectively. A further reduction in promoter activity by ~95% occurred when both the GC(2) box and GC(1) box were mutated. Finally, triple mutations of CACCC, GC(2), and GC(1) sites, or triple mutations of GC(3), GC(2), and GC(1) sites entirely abolished the PKCδ promoter activity. Taken together, these functional data suggest that GC(1) and GC(2) sites, and less significantly, GC(3), GC(4), and CACCC sites, are critical *cis*-elements for constitutive expression of PKCδ in neuronal cells. In addition,

these Sp sites can cooperate in an additive manner to regulate the PKCδ promoter transactivation.

Given the great enhancing effect of the crucial GC-rich motif from +2 to +289 bp on the transcriptional activity of the PKCδ basal promoter region -147 to +2 (Fig. 1), we next investigated whether this GC-rich domain is sufficient to function as an enhancer element in NIE115 cells. To address this, the sequences around the region between +2 and +289 were subcloned in either orientation into the pGL3-147/+2 reporter construct, at the distant SalI site downstream of the luciferase stop codon (pGL3-147/+2 plus +2/+289 or pGL3-147/+2 plus +289/+2, Fig. 3D). Then the relative transcriptional strength of these constructs was measured in NIE115 cells. The results showed that, somewhat surprisingly, the GC-rich motif in either orientation and at some distance completely lost the ability to enhance transcription compared with the vector pGL3-147/+289 (Fig. 3D). These data demonstrate that the GC-rich fragment is distance- and orientation-dependent, and thus cannot operate as a classic enhancer element for PKCδ transcription in NIE115 cells.

PKCδ promoter expression is stimulated by Sp1, Sp2, Sp3 and Sp4 in NIE115 cells and MN9D cells

The Sp family members including Sp1, Sp2, Sp3 and Sp4 are the major transcription factors that bind to the GC box, GT/CACCC box, and other closely related GC-rich motifs. Sp1, Sp2, and Sp3 are ubiquitously expressed in mammalian cells, whereas Sp4 expression is restricted to brain tissue (Suske, 1999). All of them share the same target sequences with similar binding affinities. To assess the functional significance of those Sp family proteins for the activity of mouse PKCδ promoter, various amounts (from 4-8 μg) of expression

vectors for Sp1 (pN3-Sp1), Sp2 (pcDNA-Sp2), the full length of Sp3 (pN3-Sp3 FL encoding both long and short isoforms of Sp3), Sp4 (pN3-Sp4) and empty vectors (pN3 or pcDNA3.1) were individually cotransfected along with the PKCδ promoter construct pGL3-147/+289 into NIE115 and MN9D cells. Normalized luciferase activities were expressed as fold induction over cotransfections with empty vectors. As shown in Fig. 4A, all four Sp proteins exhibited a dose-dependent activation of PKCδ luciferase activity in NIE115 cells, with Sp3 being the most potent transactivator (1.4- to 2.3-fold, 1.2- to 1.6-fold, 1.4- to 3.1-fold, and 1.4- to 2.4-fold stimulation for Sp1, Sp2, Sp3 and Sp4, respectively). These results suggest that all Sp transcription factors can potently transactivate the PKCδ promoter in NIE115 cells. Likewise, overexpression of Sp3 in MN9D cells transactivated the PKCδ promoter in a dose-dependent manner from 1.5- to 2.5-fold. However, Sp1, Sp2 and Sp4 activated the PKCδ promoter much less efficiently than Sp3 in MN9D cells (maximal inductions of only 1.2-, 1.8-, and 1.2-fold with 8 µg of Sp1, Sp2 or Sp3 expression vector, respectively), suggesting that Sp3 is a strong activator of mouse PKCδ transcription in MN9D cells, whereas Sp1, Sp2 and Sp4 are weak. Overexpression of Sp1, Sp3, and Sp4 in transfected NIE115 (Fig. 4B, left panel) and MN9D (Fig. 4B, right panel) was verified by Western blot analysis. Note that Sp3 and Sp4 are endogenously expressed at appreciable levels in either cell line, but unexpectedly, the expression of endogenous Sp1 was not detected in both cells, which is discordant with the fact that Sp1 is a ubiquitous transcription factor.

Members of the Sp family share a high affinity to the same GC-rich binding sequences, and therefore they can act synergistically or antagonistically to activate transcription, depending on the nature of the cell and the promoter context. To investigate

whether synergism or competition exists between these Sp family members to modulate expression of the PKCδ promoter, cotransfections of NIE115 were performed with various combinations of these Sp transcription factors, together with the PKCδ reporter construct pGL3-147/+289. As shown in Fig. 4C, coexpression of 4 μg of pN3-Sp1 and pN3-Sp3 FL expression vectors stimulated PKCδ promoter transcription by 2.7-fold, which approximates the combined contributions from transfection of individual Sp3 (1.5-fold induction) and Sp1 (1.4-fold induction). These results indicate that the effects of Sp1 and Sp3 are additive to activate expression of the PKCδ promoter. Also, cotransfection of Sp4 with Sp1 or Sp3 (Fig. 4C), as well as cotransfection of Sp3 with Sp2 (Fig.S1), results in a similar additive induction of PKCδ promoter transcription. Thus, the Sp family members exert additive response rather than synergistic or competitive effects on the transcription of the PKCδ promoter in NIE115 cells.

To further clarify the contributions of the different Sp-regulatory elements, including the proximal CACCC box and four distal GC boxes, to the Sp-mediated increase in PKCδ promoter activity in NIE115 cells, we performed site-directed mutagenesis of these sites in the context of the pGL3-147/+209 and pGL3+165/+289 constructs. The former possesses the proximal CACCC site, whereas in the latter only the four GC boxes are present (Fig. 5A). The pGL3-147/+209 construct displayed much higher responsiveness to Sp1, Sp3, and Sp4 than did the pGL3+166/+289 construct in transfected NIE115 cells, although a similar level of Sp2-mediated activation was obtained for these two constructs (Fig. 5B-5C). As expected, mutation of the CACCC site in region -147/+209 (mCACCC) exhibited greatly reduced basal and Sp1-, Sp3-, or Sp4-mediated transcriptional activities relative to the wild-type

pGL3-147/+209 construct. Moreover, complete loss of Sp2-mediated activation was observed with the same mutant (Fig. 5B). These results indicate that the proximal CACCC element is able to respond to Sp1-, Sp2-, Sp3-, and Sp4-mediated activation of PKCδ promoter. In addition, because the CACCC mutation did not completely abolish the responsiveness to Sp1, Sp3, and Sp4 overexpression, there may be additional GC boxes present in pGL3-147/+209. In the +165/+289 region, similar to previous experiments, triple mutants mGC123, mGC124, mGC134, or mGC134, in which only site GC(4), GC(3), GC(2), or GC(1) is still active, respectively, all resulted in a strong negative effect on basal promoter activity. Somewhat surprisingly, these mutants did not decrease the inducibility of wild-type pGL3+165/+289 by Sp1, Sp3, or Sp4. However, this was not the case of Sp2-mediated activation where these triple mutants abolished all Sp2-mediated transactivation potential. On the other hand, the Sp2 expression vector activated the single mutants mGC(1), mGC(2), mGC(3), or mGC(4) to a similar extent as the wild-type pGL3+165/+289 promoter construct (Fig. 5D). These results indicate that each of the four distal GC boxes is sufficient to mediate response to Sp1, Sp3 or Sp4 overexpression, whereas cooperative interactions among the different GC sites are required to mediate the transactivation effect of Sp2 on the PKCδ promoter.

Functional analysis of the mouse PKCδ promoter in Drosophila SL2 cells

To further address the transcriptional functions displayed by members of the Sp families of transcription factors in regulation of mouse PKCδ gene transcription, *Drosophila* SL2 cells, which are deficient in endogenous Sp-related proteins (Suske, 2000), were utilized. The SL2 cells are devoid of many ubiquitous mammalian transcription factor

activities (Courey and Tjian, 1988; Noti, 1997) and thus, their transcriptional properties can be investigated in the absence of interference by endogenous factors. Varying amounts of expression vectors (1- 4µg) under the control of insect actin promoter for Sp1 (pPac-Sp1), Sp2 (pPac-Sp2), Sp4 (pPac-Sp4), the long (pPac-USp3) and short isoforms of Sp3 (pPac-Sp3), the full length of Sp3 (pPac-Sp3FL encoding long and short isoforms of Sp3 like the mammalian expression vector pN3-Sp3 FL in Fig. 4) and empty pPac0 vector together with the PKCδ promoter construct pGL3-147/+289 were individually transfected into SL2 cells. The β-galactosidase insect expression vector p97b was included to monitor transfection efficiency. Normalized luciferase activities were compared with those obtained with empty vector pPac0. As shown in Fig. 6A, addition of either pPac-Sp1 or pPac-Sp4 slightly increased PKCδ promoter activity in a dose-dependent manner. The optimal stimulation (2.3-fold) was saturated at 2 µg of pPac-Sp1 or pPac-Sp4. Interestingly, a dual effect was seen when different isoforms of Sp3 were transfected into SL2 cells. Increasing amounts of the short isoform of Sp3 plasmid (pPac-Sp3) had no effect on transactivation of PKCδ promoter. In contrast, cotransfection of pGL3-147/+289 with the long isoform of Sp3 plasmid (pPac-USp3) induced a maximal 136.2-fold increase in luciferase activity. In addition, the pGL3-147/+289 promoter activity was also activated in a dose-dependent manner by expression with either pPac-Sp2 or pPac-Sp3FL, reaching maximal 6.9- and 5.0-fold stimulation with 4 µg of pPac-Sp2 or pPac-Sp3FL, respectively. These results indicate that the long isoform of Sp3, but not the short isoform of Sp3, is a potent activator of the PKCδ promoter in *Drosophila* SL2 cells, and that Sp1, Sp2 and Sp4 exert weak positive effects on the transactivation of the PKCδ promoter.

Because overexpression of Sp1, Sp2, or Sp4 only modestly increased PKCδ promoter activity in SL2 cells, we next investigated the interplay between them with the long isoform of Sp3 in PKCδ gene regulation. As shown in Fig. 6B, cotransfections of varying amounts of pPac-Sp1 (1-2 µg) with a fixed amount of the pPac-USp3 (0.1 µg) had no effect on promoter activation of pGL3-147/+289. Likewise, there was no significant stimulation of luciferase activity when 1 µg of pPac-Sp4 was cotransfected with 0.1 µg of pPac-USp3, whereas, similar to the mammalian expression system, an additive transactivation was seen after cotransfection of 2 µg of pPac-Sp4 with pPac-USp3. In contrast, combining pPac-USp3 with either 1 µg (6.4-fold induction) or 2 µg (17.0-fold induction) of pPac-Sp2 resulted in a synergistic transactivation of PKCδ promoter activity. This is different from the data in mammalian cells (Fig. S1), indicating that two different mechanisms may be operative in insect and mammalian cells.

Mithramycin A inhibits PKCδ gene expression

To further confirm the role of Sp transcription factors on PKCδ expression, we examined the inhibition of the exogenous PKCδ promoter activity by mithramycin A, which is known to bind to the GC-rich motif and inhibit Sp transcription factor binding (Ray et al., 1989; Blume et al., 1991). The transiently transfected NIE115 cells were treated with increasing doses of mithramycin A, and the effects of mithramycin A on PKCδ promoter activity were analyzed by luciferase assays. The mithramycin A concentrations used were not toxic to NIE115 cells. As shown in Fig. 7, addition of mithramycin A to transfected cells led to a dose-dependent decrease in promoter activity for both reporter construct pGL3-147/+289

(Fig.7A) and full length pGL3-1694/+289 (Fig.7B). At the highest dose of mithramycin A (5 µM), the transcriptional activity of pGL3-147/+289 and pGL3-1694/+289 was dropped by 60% and 80%, respectively. In addition, we also performed a real-time RT-PCR assay to investigate the effects of mithramycin A on the endogenous PKCδ expression in NIE115 cells (Fig. 7C). Dose studies indicated that incubation with the highest dose of mithramycin A (5 µM) for 24 h resulted in a modest but significant reduction in PKCδ mRNA expression by ~30%. Furthermore, the inhibition of PKCδ endogenous expression by mithramycin A was confirmed in additional experiments in primary striatal cell culture. As shown in Fig. 7D, similar to the trend seen in the NIE115 cells, the highest dose of mithramycin A (5 µM) induced a ~30% decrease in PKCδ mRNA. Immunocytochemical analysis of PKCδ immunoreactivity of striatal neurons substantiated the inhibitory effect of mithramycin A on PKCδ gene expression (Fig. 7E, left panel). Quantification of the PKCδ fluorescent intensity with Metamorph Image analysis software revealed a ~35% ($p<0.01$) reduction in PKCδ immunoreactivity in 5 µM mithramycin A-treated neurons (Fig. 7E, right panel). Altogether, these results again established that PKCδ expression is Sp-factors dependent. In addition, because the repression of PKCδ transcripts at the endogenous level by mithramycin A (Fig. 7C) was far less pronounced than that of the exogenous promoter reporter activity (Fig.7A-B), regulation of the endogenous PKCδ may also be controlled by additional mechanisms that are not manifested in exogenous reporter plasmids during a transient luciferase assay.

Binding of Sp family of transcription factors to the PKCδ promoter in NIE115 cells

To directly address whether Sp family proteins are associated with the PKCδ promoter *in vivo*, we performed a chromatin immunoprecipitation assay. NIE115 cells were transfected with either the expression vectors for Sp proteins or the empty vector, and proteins were then formaldehyde cross-linked to chromatin. The immunoprecipitation was performed with antibody directed against Sp1, Sp3, or Sp4. The precipitated DNA was isolated and subjected to PCR analysis with the primer set P+2F/P+289R encompassing the promoter region +2 to +289. In the empty vector control samples, an expected 312-bp DNA fragment was amplified from DNA immunoprecipitated by Sp3 or Sp4 antibody, but not from Sp1 immunoprecipitation (Fig. 8A, lane 2, 3, and 4). This result correlates with the previous observation that Sp1 factor is present at extremely low or undetectable levels in NIE115 cells (Fig. 4B). Furthermore, significantly increased levels of amplification of the PKCδ promoter were observed in DNA immunoprecipitated by any of the Sp antibodies from Sp-enriched cells when compared with levels seen for empty vector transfected controls (Fig. 8A, lane 2 *vs* 7; lane 3 *vs* 10; and lane 4 *vs* 13). Together, the ChIP results provide evidence for direct *in vivo* association of Sp proteins with the PKCδ promoter in the chromatin of NIE115 cells.

For an additional experiment to further characterize the binding of Sp proteins to the PKCδ proximal promoter region, we performed gel shift assays using a double-stranded 32-bp IRye^{TM} 700-labeled oligonucleotide (+205/+236) (see Table S2 for all oligonucleotides used in EMSA experiments) containing the two proximal Sp binding sites GC(1) and GC(2) as probe. As shown in Fig. 8B (lane 2), a shift protein-DNA complex band was detected after incubating the probe with NIE115 nuclear extracts. This shifted band was

almost completely abolished either by addition of an excess of the unlabeled +205/+236 self-oligonucleotide or by a Sp1 consensus oligonucleotide, establishing the nucleic acid-protein binding specificity (Fig. 8B, lane 3 and 5). In contrast, when a 100-fold molar excess of unlabeled mutant +205/+236 self-oligonucleotide, in which the GC(1) and GC(2) motifs were double mutated (Fig 8B, lane 4) or unlabeled mutant Sp1 consensus oligonucleotide (Fig.8B, lane 6) was used, the formation of specific complex was only partially blocked. Moreover, the addition of excess of either an unlabelled PKCδ +218/+238 oligonucleotide or unlabelled PKCδ +201/+220 oligonucleotide corresponding to the single GC(2) or GC(1) motif, respectively, (Fig. 8B, lane 7 and 8), failed to completely abrogate the formation of the DNA-protein complex, suggesting that GC(1) and GC(2) boxes are both functional binding sites for the DNA-protein interaction of this complex. In addition, another shifted band without competition by excess of the unlabeled +205/+236 oligonucleotide was considered as nonspecific binding and marked as N.S. in Fig. 8B.

Coactivators p300/CBP stimulate PKCδ promoter activity through Sp binding sites in NIE115 cells

Because p300/CBP can function as co-activators of Sp transcription factors, we next analyzed whether they play a role in regulating mouse PKCδ gene expression by studying the effect of ectopic p300/CBP expression on promoter activation of pGL3-147/+289 construct in NIE115 cells. As shown in Fig. 9A-B, both p300 and CBP significantly enhance the PKCδ promoter activity. Interestingly, when a mutant p300 protein without intrinsic HAT activity was overexpressed, an even stronger up-regulation of PKCδ promoter activity was seen (Fig. 9A), suggesting that the HAT activity of p300 is not required for transactivating PKCδ

promoter. Moreover, to assess whether p300/CBP meditate their transcriptional activation through the Sp sites, two luciferase reporter constructs, Sp1-Luc and mSp1-Luc, which contain three consensus Sp1 binding sites and three mutant Sp1 sites, respectively, were utilized. As shown Fig. 9C-D, similar to the PKCδ promoter construct pGL3-147/+289, overexpression of p300/CBP significantly stimulated the wild-type Sp1-Luc activity, whereas the mutant mSp1-Luc completely lost the responsiveness to increased expression of p300/CBP, suggesting that the stimulatory effect of p300/CBP may be mediated through the Sp biding sites on PKCδ promoter.

Ectopic PKCδ expression increased vulnerability of dopaminergic neurons to oxidative stress-stimulated degeneration

Oxidative stress, arising due to excessive production of ROS and/or defective ROS removal has long been implicated in the pathogenesis of many neurodegenerative diseases, including PD (Jenner, 2003; Greenamyre and Hastings, 2004). Based on our observation that nigral dopaminergic neurons display high levels of PKCδ expression (12), and that proteolytic activation of this kinase plays a key role in meditating oxidative stress-dependent neurodegeneration (Kaul et al., 2005), we further assessed whether the extent of PKCδ expression correlates with H_2O_2-induced degeneration. To address this, we performed ectopic expression of PKCδ in MN9D dopaminergic neurons and investigated its effect on H_2O_2-induced apoptotic cell death. Fluorescence microscopic imaging of PKCδ-GFP-transfected cells revealed that ~60% of cells were expressing PKCδ-GFP proteins (Fig. 10, right panel), confirming the high efficiency of ectopic expression of PKCδ in MN9D cells. Quantification of H_2O_2-induced cell death in the EGFP-C1 control

vector-transfected cells by DNA fragmentation assay showed that H_2O_2 treatment dose-dependently induced neuronal degeneration, having a maximum (~300% of untreated cells) at dose 2 mM. In contrast, overexpression of PKCδ induced an increased level of H_2O_2-induced DNA fragmentation (Fig. 10, left panel). Together, these results suggest that the level of PKCδ gene expression may have important regulatory roles in oxidative stress-dependent neurodegeneration.

Discussion

The present study addresses the regulatory *cis*-acting elements and candidate regulatory factors involved in the transcription of the mouse PKCδ gene in neuronal cells. PKCδ has been widely identified as a pro-apoptotic effector of signals in various cell types (DeVries et al., 2002; Brodie and Blumberg, 2003; Kanthasamy et al., 2003). Recent evidence supports a prominent role for caspase-dependent PKCδ activation in oxidative stress-induced dopaminergic cell death in experimental models of PD because of a high expression of the kinase in nigrostriatal dopaminergic neurons (Anantharam et al., 2002; Kaul et al., 2003). Despite extensive investigations of the molecular mechanisms of activation of PKCδ, relatively little information is available on the mechanisms that control PKCδ expression at the transcriptional level (Gavrielides et al., 2006; Liu et al., 2006; Ponassi et al., 2006; Horovitz-Fried et al., 2007). Previous studies on the regulatory elements of the PKCδ gene are all based on analysis of the 5'-flanking sequences upstream of the TSS; however, no attempt was made to examine the importance of the GC-rich domains in the first exon. Emerging evidence indicates that the non-coding region in the exon downstream of

TSS has been recognized as a major regulatory region of various gene expressions (MacCarthy-Morrogh et al., 2000; Saur et al., 2002; Whetstine et al., 2002; Solovyev and Shahmuradov, 2003; Karban et al., 2004). Thus, we cloned and characterized the mouse PKCδ promoter including the first exon GC-rich sequences, in an effort to define mechanisms underlying the transcriptional regulation of PKCδ.

In this report, ~2.0-kb fragment of mouse genomic DNA encompassing the 5'-flanking region and the partial first exon of the PKCδ gene, was isolated and cloned into a luciferase reporter vector. The PKCδ promoter does not have a consensus TATA motif in the vicinity of the TSS (Suh et al., 2003). Our own sequence analysis found further upstream TATA-like elements at -1651, -1185, and -932 (data not shown). However, these TATA-like motifs appear to be non-functional, as no significant transcriptional activity was observed in the region between -1694 to -659 (Fig 1B, pGL3-1694/-659). Additionally, other known core promoter motifs, such as the CAAT box, Inr, and DPE, were not identified at consensus positions within the PKCδ promoter.

We showed that the 2.0-kb PKCδ promoter/luciferase construct displayed significant transcriptional activity (Fig. 1B, ~30 times higher than the promoterless pGL3-Basic vector) upon transfection into the PKCδ-expressing neuronal cell lines NIE115 and MN9D. Deletion analysis of this 2.0-kb region revealed multiple positive and negative elements, all of which contribute to the PKCδ expression. A strong negative element (NREI) present at -660 to -147 is capable of repressing the gene activity by 100%. Negative elements have also been implicated in the regulation of several other PKC family genes. For example, a silencer-like element at -1821 to -1702 was identified for the human PKCη promoter (Quan and Fisher,

1999). Furthermore, we characterized that this element is not in itself a true silencer but rather functions as a PKCδ-promoter-specific repressive element. Computational analysis of this region did not reveal significant sequence identity with any known silencer motif, however, it contains multiple TFBS (data not shown), such as an overlapping STAT1/Ets site (-656 to -639) and an adjacent NF-Y site (-637 to -627), as well as a downstream WHNF site (-596 to -591). Notably, STAT1, Ets and NF-Y are all known to serve a dual role in transcriptional regulation, as an activator or as a repressor (Mavrothalassitis and Ghysdael, 2000; Ramana et al., 2000). Whether these elements are involved in the repressing activity has yet to be determined. Studies are under way to dissect the exact location of this negative element and the proteins that bind to it. Additionally, located farther upstream of NREI is another negative regulatory element (NREII, between -1694 and -1193). This element, however, is relatively weak.

In deletion studies we also identified two novel positive regulatory elements within the 2.0-kb region of the PKCδ promoter. We previously identified a basal PKCδ promoter (-147 bp to the TSS) that displays ~6 times greater activity over the pGL3-Basic vector in NIE115 and MN9D cells (Fig.1B, pGL3-147/+2), and a NFκB and NERF1a sites are responsible for its activity (H. Jin et al., unpublished data). In the present study, we found that the downstream fragment in exon 1 from bp +2 to +289 was capable of dramatically enhancing the basal PKCδ promoter activity in both NIE115 and MN9D cells (Fig. 1B), suggesting that this region contains most of the positive *cis*-acting elements necessary for PKCδ expression. Notably, when the location of this 288-bp positive element was altered, its enhancing activity was entirely lost (Fig. 3D). This suggests that proper distance arrangement

of this element with respect to the basal PKCδ promoter is important. In addition the region between -147 and +289 appears to confer the greatest transcriptional activity in neurons, thus functioning as a PKCδ core promoter. Of particular interest was an additional positive regulatory element from bp -1192 to -660. This element, which resides directly adjacent to the NREI in the 52-bp region between -712 and -660, was able to significantly overcome the activity of NREI. Curiously, this region acts mechanistically as a novel anti-repressive element. To date, only a few anti-repressive elements have been reported for eukaryotic genes (Wu et al., 2004). At this time, we could not provide any further characterization of this interesting element or its binding protein. Future studies will address this issue. Taken together from all these studies, the transcription of PKCδ is tightly controlled by multiple elements acting in concert to ensure its differential expression pattern in a variety of biological processes.

Next, the major positive regulatory element immediately downstream of the PKCδ transcription start site (bp from +2 to +289) was analyzed in detail. *In silico* analysis identified four GC boxes in close proximity to each other at +208/+216, +225/+233, +239/+247, and +256/+264, as well as an upstream CACCC box (also called the GT box) at +35/+43 (Fig. 3A). The functional importance of these multiple Sp binding motifs was assessed by site-specific mutagenesis and transfection of the mutated constructs into NIE115 and MN9D cells (Fig. 3B). The results showed that all these motifs are functional in activating PKCδ transcription, and that the five Sp binding sites appear functionally different. The magnitude of activating effects is in the order GC(1) or GC(2) > GC(3) > GC(4) or CACCC. Furthermore, an essential role for the cooperative action of all these Sp sites for the

transactivation of PKCδ transcription was confirmed. In addition to the Sp binding sites, i*n silico* analysis also revealed the presence of multiple other TFBS within this +2/+289 segment (data not shown). Conceivably, these *cis* elements may also contribute to the regualtion of PKCδ expression.

The Sp family of transcription factors including Sp1, Sp2, Sp3 and Sp4 are all structurally similar and are the most well-characterized GC-rich-motif binding proteins. To elucidate the roles of Sp family members in transcriptional regulation of PKCδ, cotransfection studies using a reporter containing the PKCδ promoter -147/+289 along with Sp expression vectors were performed (Fig. 4A). These studies revealed a similar activation profile of Sp transcription factors in NIE115 and MN9D cells, although less pronounced transcriptional activation was observed in the latter. In both cell lines, Sp3 is the strongest transactivator, whereas overexpression of Sp1, Sp2, and Sp4 displayed much less activation of the PKCδ promoter. It should be noted that both NIE115 and MN9D cells expressed easily detectable levels of endogenous Sp3 and Sp4, but undetectable levels of endogenous Sp1(Fig. 4B), suggesting that Sp3 and Sp4 may be responsible for a major part of PKCδ promoter activity in these two neuronal cell lines. The contribution of the multiple Sp-binding sites found within the PKCδ promoter to the Sp-mediated promoter activity was further assessed using substitution mutant constructs. By using a smaller construct, namely pGL3-147/+209, which possesses the upstream CACCC motif but lacks the downstream four GC boxes, we found that the CACCC motif is required for complete Sp2-mediated promoter activity in this promoter context (-147 to +209). In contrast, this site is insufficient for complete Sp1, Sp3 and Sp4 transactivation (Fig. 5B). This suggests additional Sp-like binding sites within this region that are important for Sp transactivation of the PKCδ promoter. On the other hand,

cotransfection of Sp expression plasmids with pGL3+165/+289 triple mutant constructs confirmed that each of the four downstream GC boxes is sufficient for complete Sp1, Sp3 and Sp4 transactivation. However, cooperative action of different GC boxes is required for mediating Sp2 transactivation, since triple GC boxes mutation failed to mediate any Sp2 transactivation (Fig. 5C-D). This different mode of action between Sp2 and other Sp family members is not surprising, as they have different DNA binding specificity and affinities. For example, Sp1, Sp3 and Sp4 bind GC boxes with similar specificity and affinities, whereas Sp2 binds with much lower affinity (Hagen et al., 1992).

To precisely analyze the transcriptional roles of the Sp family of transcription factors in a Sp-deficient background, transfection assays were carried out in *Drosophila* SL2 cells (Fig. 6). We demonstrated a dual function of Sp3 in regulating PKCδ transcription: the long isoforms of Sp3 most potently activate the PKCδ promoter, whereas the short isoforms of Sp3 are transcriptionally inactive on their own, which may be due to the absence of the N-terminal transactivation A domain present in the long isoforms of Sp3 (Sapetschnig et al., 2004). These data together suggest that the Sp3 isoform expression may have a dramatic effect on PKCδ expression. Indeed, alteration of the Sp3 isoform ratio has been observed under certain conditions (Sapetschnig et al., 2004). In combination experiments (Fig. 6B), overexpression of Sp1 had no effect on the transcriptional activation by the long Sp3 isoform, although Sp4 was able to transactivate the promoter activation by the long Sp3 isoform in an additive manner, only when a higher amount of Sp4 expression vector was transfected. In contrast, obvious synergistic activation of PKCδ promoter transcription was observed when combining Sp2 with a long isoform of Sp3. However, this finding is not seen in mammalian cells, probably because there is already enough endogenous Sp2 and Sp3 in

these cells.

Several additional lines of evidence solidify the essential role of Sp family transcription factors in controlling PKCδ expression. First, by using the Sp inhibitor mithramycin A, we demonstrated that transcription of the PKCδ promoter is dependent on Sp activity (Fig. 7A-B). At the highest dose of 5 μM mithramycin A, more than an 80% decrease of full length PKCδ promoter activity was achieved in NIE115 cells. Second, the more importantly, mithramycin A also suppresses, albeit to a much lesser extent, the endogenous PKCδ expression in NIE115 cells and primary striatal neurons (Fig. 7C-E). This information also suggests that the endogenous PKCδ gene is under different layers of regulatory control in addition to the 5'-promoter in the context of an exogenous reporter plasmid. Epigenetic regulatory mechanisms, such as DNA methylation or histone modifications, might be involved in the regulation of PKCδ expression and could account for this complexity. The mouse PKCδ promoter is GC rich and contains a putative CpG island that is partly methylated in NIE115 and MN9D cells (data not shown). Furthermore, treatment of NIE115 cells by the methylation-specific inhibitor 5'-aza-2'-deoxycytidine (5-Aza-dC) significantly increased the endogenous PKCδ mRNA expression and attenuated its methylation status (Fig. S2). DNA methylation has been shown to interfere with the binding of Sp1 to DNA (Kudo, 1998). Experiments are in progress to elucidate whether CpG methylation of the PKCδ promoter could affect the function of Sp transcriptional factors in regulation of PKCδ expression. Third, chromatin immunoprecipitation assays confirmed that transcription factors Sp1, Sp3 and Sp4 bind to the PKCδ promoter for transcriptional activation in NIE115 cells, in the environment of chromatin *in vivo* (Fig. 8A). Finally, gel

mobility shift assays with nuclear extracts from NIE115 cells detected the formation of one specific complex with the PKCδ +205/+236 oligonucleotide, of which relevance to Sp factors was further confirmed by using specific competitors (Fig. 8B).

The Sp-factors regulate a variety of genes that are involved in the apoptotic cascade. This has been reported for the caspase-3 (Sudhakar et al., 2008), caspase-8 (Liedtke et al., 2003), FasL (Kavurma et al., 2001), and finally as shown in the present study for PKCδ. While the Sp1 factor functions as activator of transcription, the function of Sp3 is less clear. It is generally accepted that Sp3 is the only protein in the Sp subfamily that can either positively or negatively modulate the gene expression. The role of Sp3 as an activator or repressor remains elusive. Evidence suggests that its activity strongly depends on the structure and arrangement of Sp-recognition sites as well as the cell type-specific difference (Sapetschnig et al., 2004). Our results suggest that for the mouse PKCδ basal promoter, Sp3 acts as a strong activator. In addition, regulation of Sp1 and Sp3 activity is achieved by post-translational modifications. For examples, the post-translational modification to Sp1/Sp3 by acetylation stimulates their activity (Ammanamanchi et al., 2003; Hung et al., 2006), whereas sumoylation of Sp1/Sp3 causes their inactivation (Spengler and Brattain, 2006). Although our Sp1 or Sp3 acetylation immunoprecipitation and Western blot analysis failed to detect any endogenous acetylation of Sp1 or Sp3 in normal NIE115 cells (data not shown), we could not exclude the possibility that Sp1 or Sp3 is acetylated in response to specific stimuli, such as oxidative stress (Ryu et al., 2003). In addition to posttranslational modifications, regulation of the activities of Sp family members also includes protein-protein interactions. For examples, Sp1 and Sp3 bind directly to p300 and its homolog CBP (Suzuki et al., 2000; Walker et al., 2001). We previously demonstrated that rat PKCδ gene expression

is p300-dependent, and that p300 associates endogenously with the rat PKCδ gene. Nevertheless, the roles of p300/CBP in the facilitation of PKCδ gene expression are still poorly understood. In the present study, our evidence suggests that forced expression of p300 or CBP resulted in a dose-dependent activation of mouse PKCδ promoter (Fig. 9A-B) in the NIE115 cells. Furthermore, it appears that the GC boxes are crucial for the p300/CBP activation, as overexpression of CBP/p300 did not activate the Sp1-reporter containing mutations in the GC boxes (Fig. 9C-D). More interestingly, our results also indicate that p300 may activate PKCδ transcription by HAT-independent mechanisms (Fig. 9A), which may partly explain why we could not detect any endogenous acetylation of Sp1 or Sp3 in NIE115 cells.

In summary, we have functionally characterized for the first time the regulation of PKCδ gene promoter in neuronal cells. Our results clearly indicate that multiple positive and negative regulatory elements contribute to PKCδ promoter expression. In particular, we have identified the core promoter located between nucleotides -147 and +289, and demonstrated a functional role for five Sp sites within this region in the regulation of constitutive PKCδ expression. We have also shown that Sp1, Sp3, and Sp4 directly bind to the PKCδ promoter through the multiple Sp sites and positively regulate PKCδ expression. Furthermore, ectopic expression studies revealed that the expression level of the PKCδ gene correlates well with the sensitization of dopamine neurons to oxidative stress-induced neuronal cell death (Fig. 10). Taken together with our previous observation that PKCδ plays a critical role in the oxidative stress-induced dopaminergic degeneration in PD (Yang et al., 2004; Kaul et al., 2005), and that PKCδ inhibition has been explored in preclinical models of PD (Kanthasamy et al., 2006; Zhang et al., 2007a), these findings have important implications for the utility of

PKCδ as a target in developing novel drug therapies for PD.

Figure 1: Deletion analysis of PKCδ promoter activity in NIE115 and MN9D cells

A, The schematic diagram of mouse PKCδ gene structure on chromosome 14. Exons are marked by *boxes* and number below each box, and *black* and *red* regions indicate the coding and noncoding exons, respectively. *Arrow* indicates the position of the translation start codon (ATG). *B*, Schematic representation of PKCδ promoter deletion/luciferase reporter constructs. An extensive series of PKCδ promoter deletion derivatives was generated by PCR methods and inserted into the pGL3-Basic luciferase vector. The 5' and 3' positions of the constructs with respect to the transcription start site are depicted. *C*, Each construct as shown in *B* was transiently transfected into NIE115 (*black bar*) and MN9D (*blue bar*) cells. Cells were harvested 24 h after transfection and luciferase activities were determined. The plasmid pcDNA3.1-βgal was included in each transfection to normalize the promoter activity with transfection efficiency. The activity of full-length promoter construct (pGL3-1694/+289) was arbitrarily set to 100, and the relative luciferase activity of the other constructs was calculated accordingly. The results represent the mean ± SEM of three independent experiments performed in triplicate.

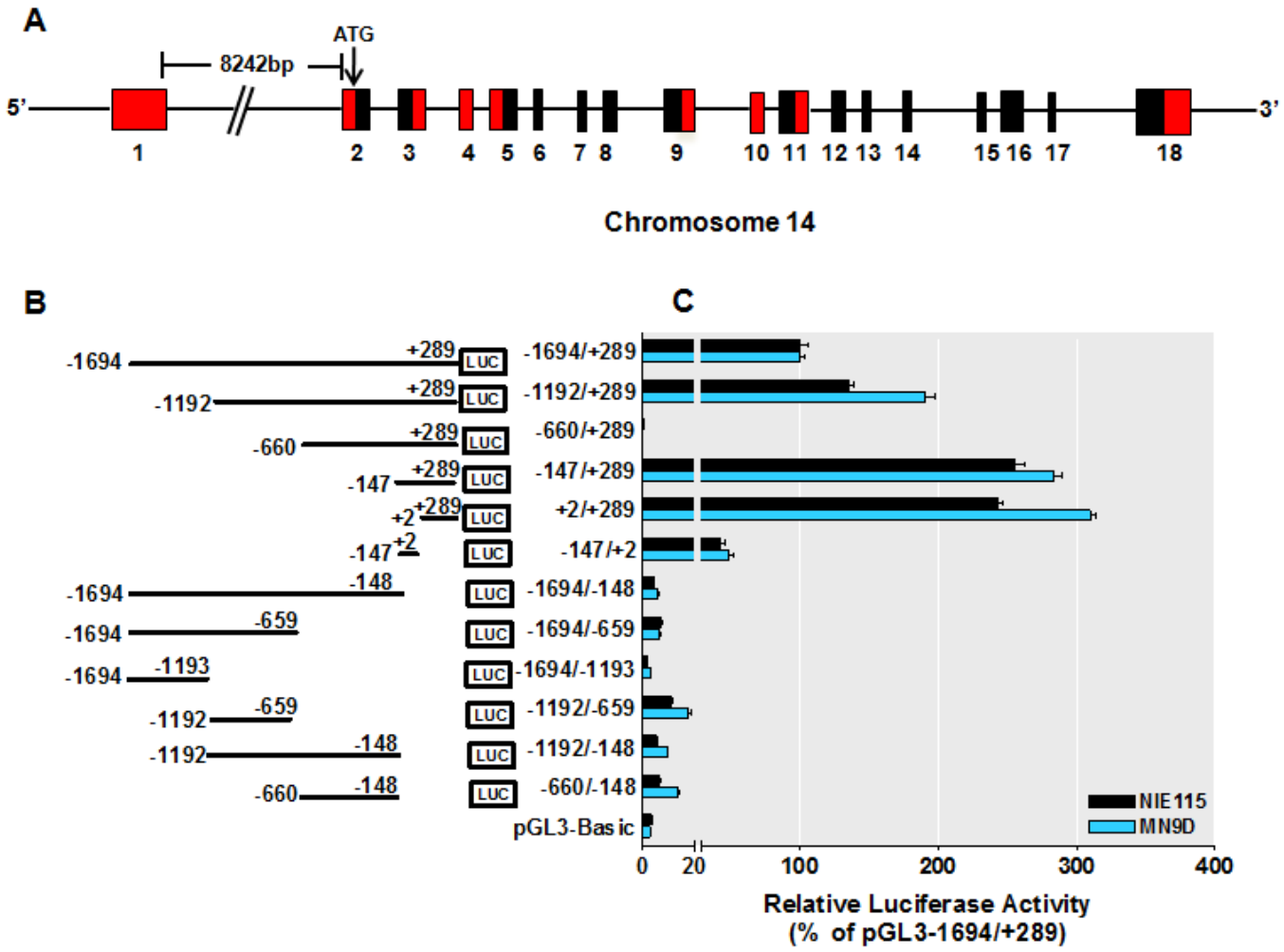

Figure 1

Figure 2: Mapping of the identified repressive and anti-repressive elements within the PKCδ promoter and evidence for the PKCδ promoter-specific repressive element

A, The schematic representation of PKCδ promoter 5' deletion constructs used for the fine mapping study. The 5' and 3' positions of the constructs with respect to the transcription start site are depicted. *B*, Each construct as depicted in *A* was transiently transfected into NIE115 (*black bar*) and MN9D (*blue bar*) cells. Cells were harvested 24 h after transfection for assaying luciferase activities. The plasmid pcDNA3.1-βgal was cotransfected into cells for data normalization. The activity of pGL3-147/+289 was arbitrarily set to 100, and the relative luciferase activity of the other constructs is presented. The results represent the mean ± SEM of three independent experiments performed in triplicate. *C*, The isolated repressive element of the PKCδ promoter does not function as a locus-independent DNA element. The sequences around the identified repressive element (-660 to –561 of the PKCδ promoter) were directly fused to the 5'-end of the region between -147 to +289 of the PKCδ promoter, and cloned into the pGL3-Basic luciferase vector to obtain pGL3-660/-561 plus -147/+289. NIE115 (*black bar*) and MN9D cells (*blue bar*) were transfected with pGL3-147/+289 or pGL3-660/-561 plus -147/+289 for 24 h, and luciferase activity was determined. Schematic diagram of these constructs are shown at the *right*. The activity of pGL3-147/+289 was set to 100, and the relative luciferase activity of pGL3-660/-561 plus -147/+289 is presented. The results represent the mean ± SEM of three independent experiments performed in triplicate. *D*, The isolated repressive element of the PKCδ promoter does not act on a heterologous promoter (SV40). The sequences of the putative PKCδ repressive element (-660 to –561 of the PKCδ promoter) were cloned upstream of the SV40 promoter in pGL3-Promoter vector

to obtain pGL3-Promoter-660/-561. NIE115 (*black bar*) and MN9D (*blue bar*) cells were transfected with pGL3-Promoter or pGL3-Promoter-660/-561 for 24 h, and luciferase activity was determined. Schematic diagram of these constructs are shown at the *right*. The activity of pGL3-Promoter was set to 100, and the relative luciferase activity of pGL3-Promoter-660/-561 is given. The results represent the mean ± SEM of three independent experiments performed in triplicate.

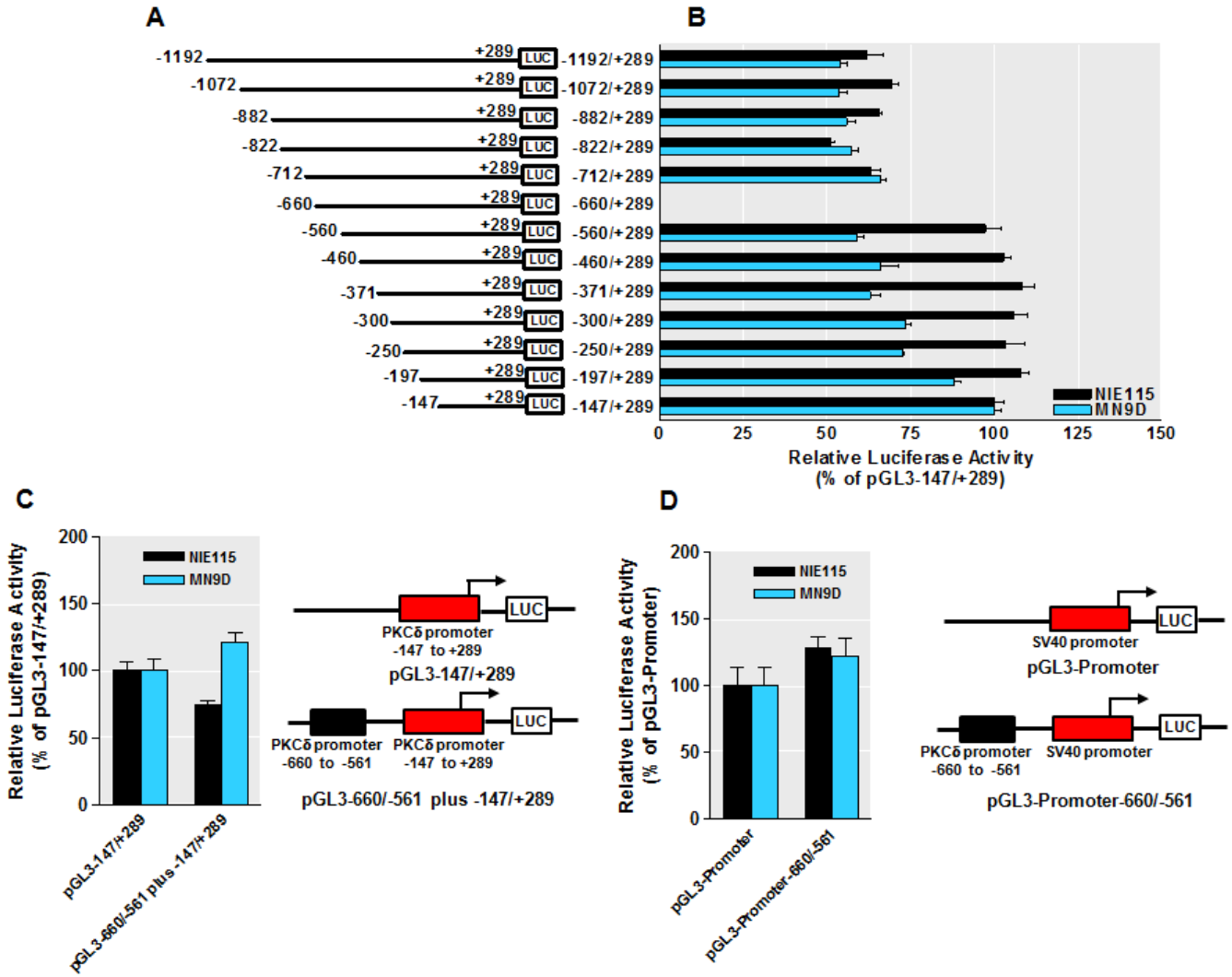

Figure 2

Figure 3: Functional analysis of the PKCδ proximal promoter

A, Sequence comparison of the mouse PKCδ promoter region between +2 to +289 with the corresponding regions of the rat and human PKCδ promoters. Sequences were aligned with the DiAlign TF program. Sequence differences are indicated and gaps introduced to maximize homology are marked by *dashes*. Phylogenetically conserved TFBS as well as the CACCC box present only in the mouse PKCδ promoter are indicated (*overlined*). *B*, Schematic representation of the wild-type or mutated PKCδ promoter reporter constructs containing targeted substitutions in the Sp binding sites. The potential Sp sites are indicated at the *top*. The mutated site is marked with ×, and the non-mutated Sp sites are indicated by either *circle* or *square*. *C*, The wild-type or mutated reporter constructs as shown in *B* were individually transfected into NIE115 (*black bar*) and MN9D (*blue bar*) cells, and luciferase activities were assayed after 24 h. To adjust for transfection efficiency, the plasmid pcDNA3.1-βgal was included in each transfection. The activity of wild-type construct (pGL3-147/+289) was arbitrarily set to 100, and promoter activity of the mutants is expressed as a percentage of the wild-type construct. The results represent the mean ± SEM of three independent experiments performed in triplicate. The sequences of wild-type and mutated Sp site are shown at the right side of the bar graph. The substituted nucleotides are shown in **bold**. *D*, Absence of enhancer elements in the GC-rich sequence (+2/+289) of the mouse PKCδ promoter in NIE115 cells. The PKCδ promoter GC-rich sequence (+2 to +289) was cloned in both orientations into the SalI site of the pGL3-147/+2 reporter constructs as described under *Experimental Procedures*. These constructs were individually transfected into NIE115 cells for 24 h, and luciferase activity was determined. Luciferase activity was

normalized with β-galactosidase. The right panel shows schematic diagram of the constructs. The activity of pGL3-147/+2 was set to 1, and the relative luciferase activity of all other constructs were calculated and expressed as fold of pGL3-147/+2. The results represent the mean ± SEM of three independent experiments performed in triplicate.

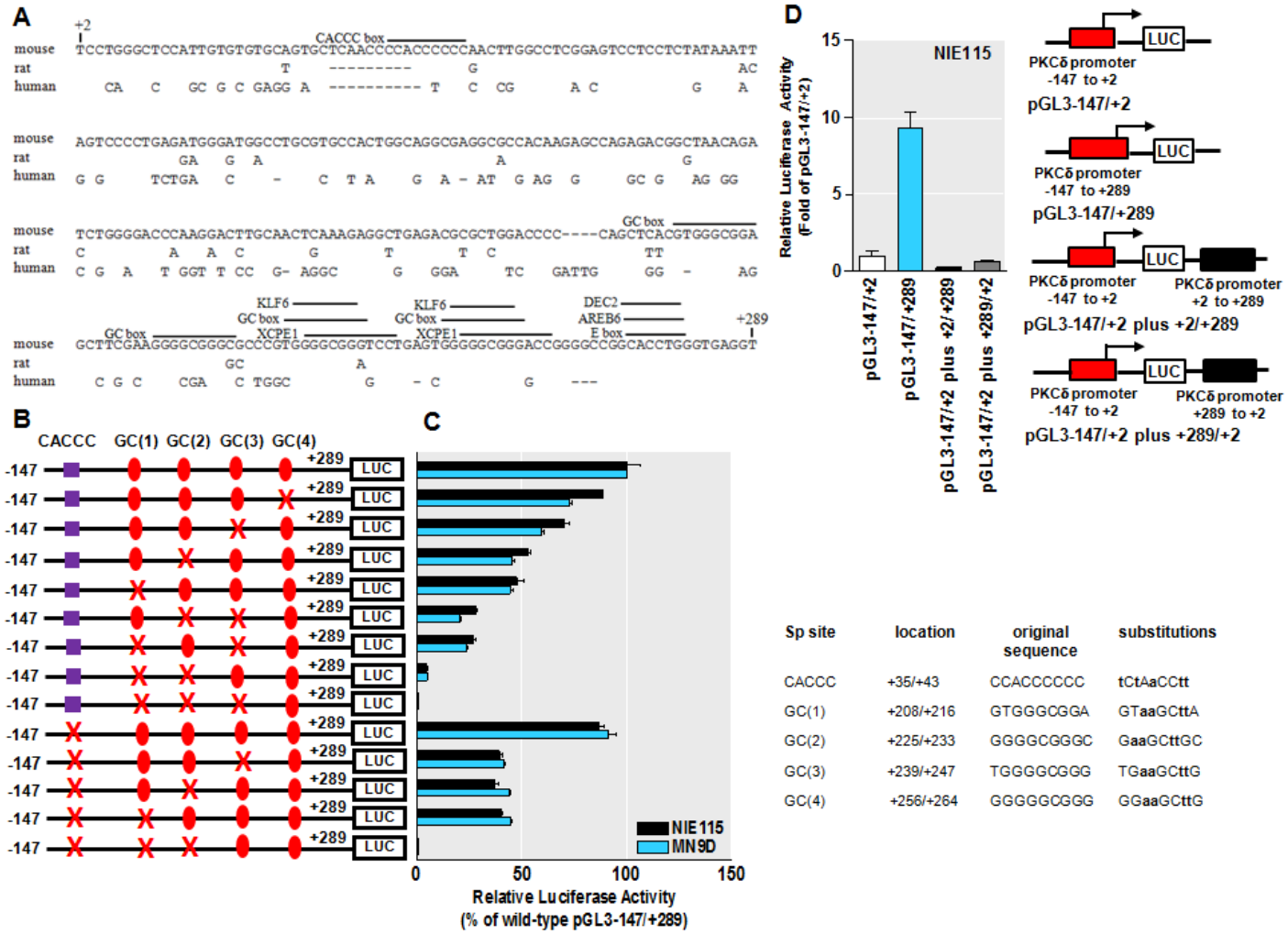

Sp site	location	original sequence	substitutions
CACCC	+35/+43	CCACCCCCC	tCtAaCCtt
GC(1)	+208/+216	GTGGGCGGA	GTaaGCttA
GC(2)	+225/+233	GGGGCGGGC	GaaGCttGC
GC(3)	+239/+247	TGGGGCGGG	TGaaGCttG
GC(4)	+256/+264	GGGGGCGGG	GGaaGCttG

Figure 3

Figure 4: PKCδ promoter activity is stimulated by Sp-family members of transcription factors in NIE115 and MN9D cells

A, Variable amounts (µg) of pN3-Sp1, pN3-Sp3 FL, pN3-Sp4, or pcDNA-Sp2 expression plasmid or empty vector (pN3 or pcDNA3.1), as indicated, were cotransfected with the PKCδ promoter reporter construct pGL3-147/+289 into NIE115 (*black bar*) and MN9D (*blue bar*) cells. Luciferase activity was measured after 24 h of transfection. The plasmid pcDNA3.1-βgal was included in each transfection for data normalization. Values are expressed as fold induction relative to that obtained from cells transfected with 8 µg of empty vector (*EV*) and represent the mean ± SEM of three independent experiments performed in triplicate. Variations in the amount of total DNA were compensated with the corresponding empty vector pN3 or pcDNA3.1. *B,* Overexpression of Sp factors in transfected NIE115 (*left panel*) and MN9D (*right panel*) cells was determined by immunoblotting analysis. The cells were transfected with Sp expression plasmids in the same manner as *A.* Whole cell lysates were prepared 24 h after transfection and immunoblotted for Sp1, Sp3, Sp4, or β-actin (loading control). Both short Sp3 (sSp3) and long Sp3 (lSp3) isoforms are shown. *C,* The expression plasmids pN3-Sp1, pN3-Sp3 FL, pN3-Sp4, and empty vector pN3 were cotransfected along with the PKCδ promoter reporter construct pGL3-147/+289 into NIE115 either alone or in the different combinations, as indicated (µg) below the bar graph. Luciferase activity was determined after 24 h of transfection. Data shown represent the mean ± SEM of three independent experiments performed in triplicate.

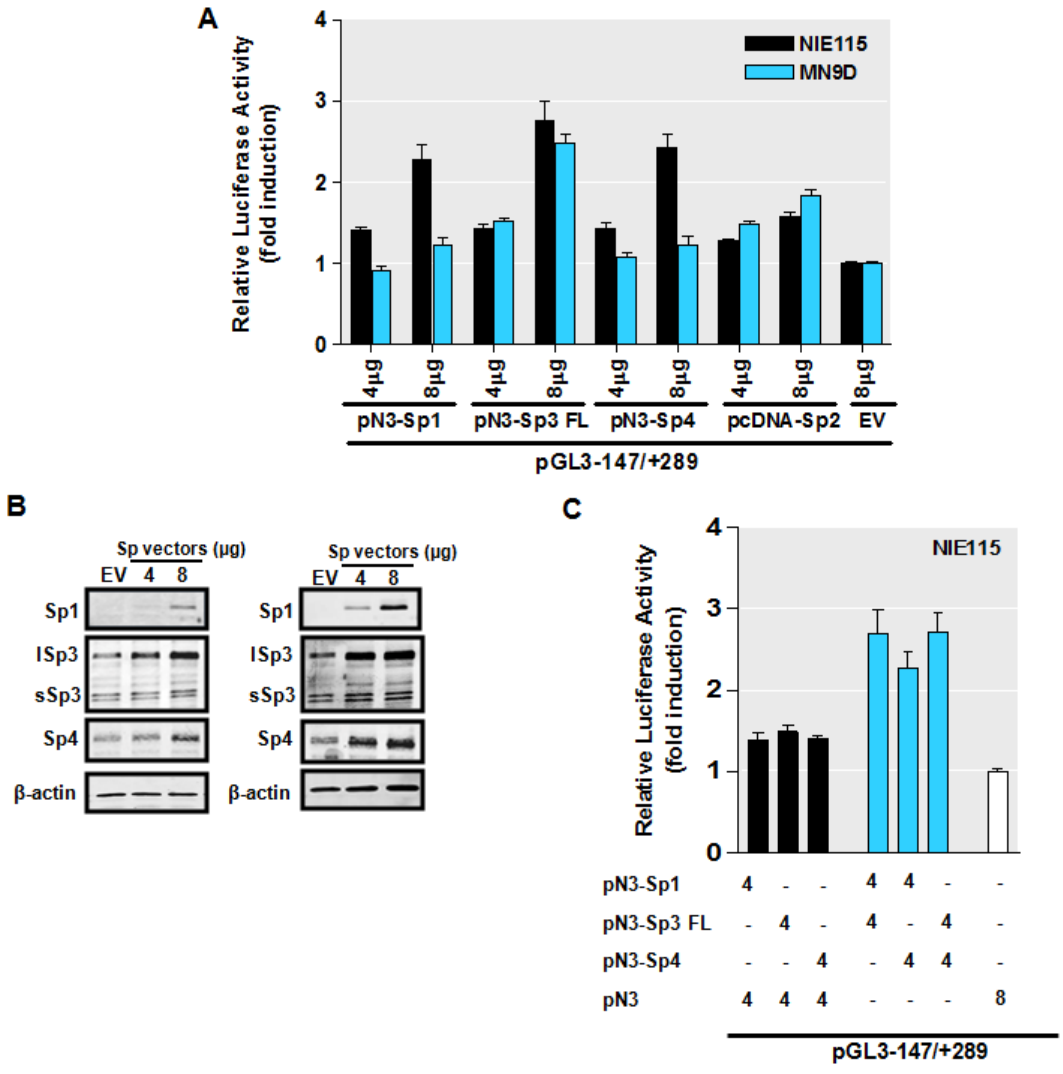

Figure 4

Figure 5: Effects of site-directed mutagenesis of Sp binding sites on PKCδ promoter activity transactivated by overexpression of Sp transcription factors in NIE115 cells

NIE115 cells were cotransfected with the indicated wild-type or mutated PKCδ reporter constructs and 8 μg of pN3-Sp1, pN3-Sp3 FL, pN3-Sp4, pcDNA-Sp2, or empty vector (EV) pN3 or pcDNA3.1. Luciferase activities were assayed after 24 h. The plasmid pcDNA3.1-βgal was included in each transfection to adjust for transfection efficiency. The activity that obtained following cotransfection of the wild-type construct (pGL3-147/+209 or pGL3+165/+289) with empty vector (*EV*) was arbitrarily set to 100, and all other data are expressed as a percentage thereof. The results represent the mean ±SEM of three independent experiments performed in triplicate. *A*, Schematic representation of the wild-type PKCδ promoter reporter constructs pGL3-147/+209 and pGL3+165/+289. The potential Sp sites are depicted by either *circle* or *square*. *B*, NIE115 cells were cotransfected with 4 μg either wild-type (pGL3-147/+209) or mCACCC mutated luciferase reporter constructs along with 8 μg of the expression plasmids pN3-Sp1, pN3-Sp3 FL, pN3-Sp4, pcDNA-Sp2, or empty vector (pN3 or pcDNA3.1). *C*, Wild-type (pGL3+165/+289) or triple mutated luciferase reporter constructs, as indicated, were cotransfected into NIE115 cells along with the expression plasmids for Sp-family members of transcription factors. *D*, Wild-type (pGL3+165/+289) or single mutated luciferase reporter constructs, as indicated, were cotransfected into NIE115 cells along with the pcDNA-Sp2 or empty pcDNA3.1 expression vector.

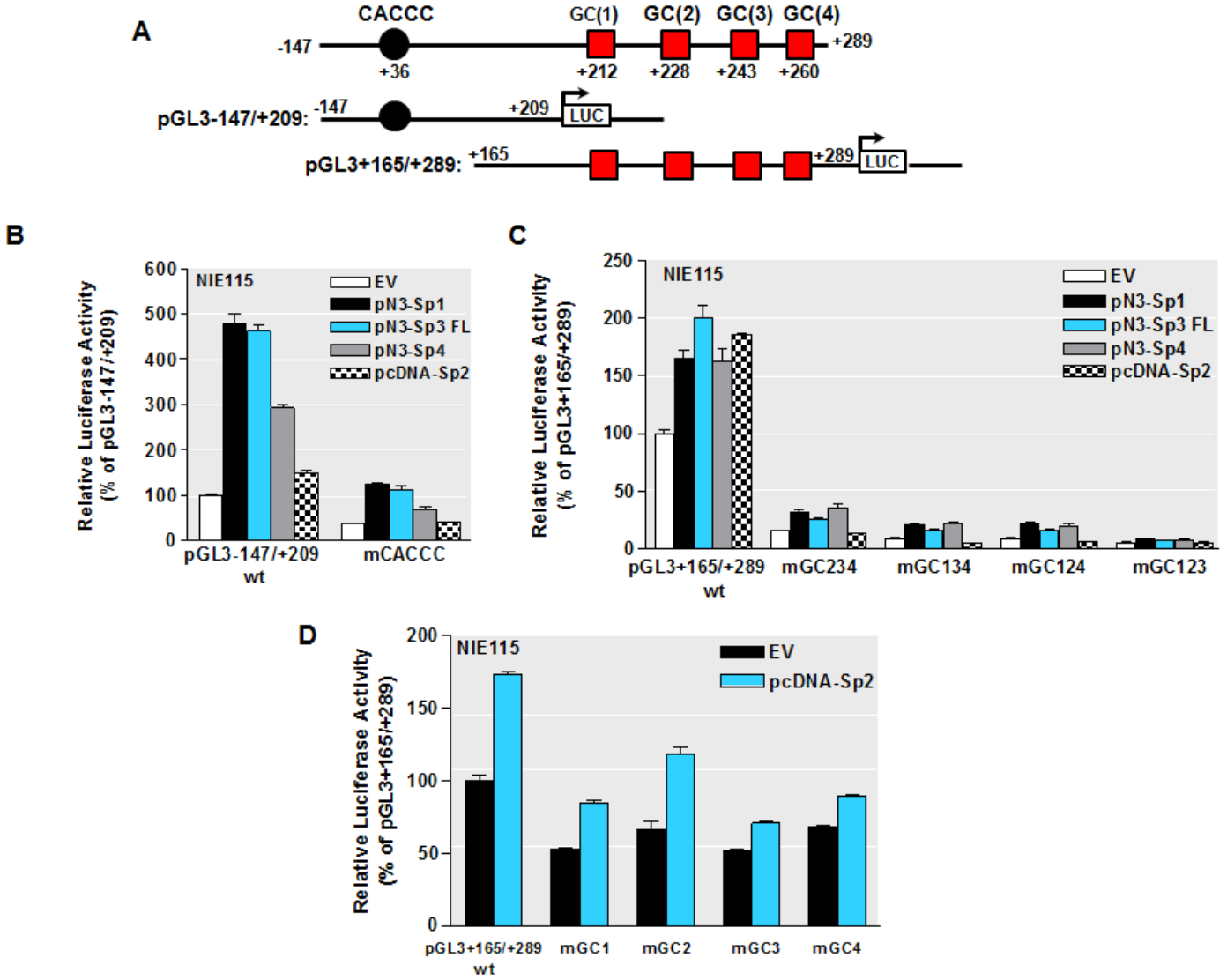

Figure 5

Figure 6: Effects of overexpression of Sp-family members of transcription factors on the PKCδ promoter activity in SL2 cells

A, The PKCδ promoter reporter construct pGL3-147/+289 (4 µg) was cotransfected with variable amounts (1-4µg) of *Drosophila* expression plasmids for Sp1 (pPac-Sp1), the short isoform of Sp3 (pPac-Sp3), the long isoform of Sp3 (pPac-USp3), the full length of Sp3 (pPac-Sp3FL), Sp4 (pN3-Sp4), or Sp2 (pPac-Sp2) in *Drosophila* SL2 cells. Luciferase activity was measured after 48 h of transfection. The *Drosophila* β-gal expression plasmid p97b was included in each transfection for data normalization. Values are expressed as fold induction relative to that obtained from cells transfected with 4 µg of empty vector (pPac0) and represent the mean ± SEM of three independent experiments performed in triplicate. Variations in the amount of total DNA were compensated with the corresponding empty vector pPac0. *B*, The *Drosophila* expression plasmids pPac-USp3, pPac-Sp1, pPac-Sp4, and pPac-Sp2 were cotransfected along with 4 µg of PKCδ promoter reporter construct pGL3-147/+289 into SL2 cells either alone or in the different combinations, as indicated (µg) below the bar graph. Variations in the amount of total DNA were compensated with the corresponding empty vector pPac0. Luciferase activity was determined after 48 h of transfection. Transfection efficiency was normalized by β-galactosidase activity. Values are expressed as fold induction relative to that obtained from cells transfected with pPac0 alone and represent the mean ± SEM of three independent experiments performed in triplicate.

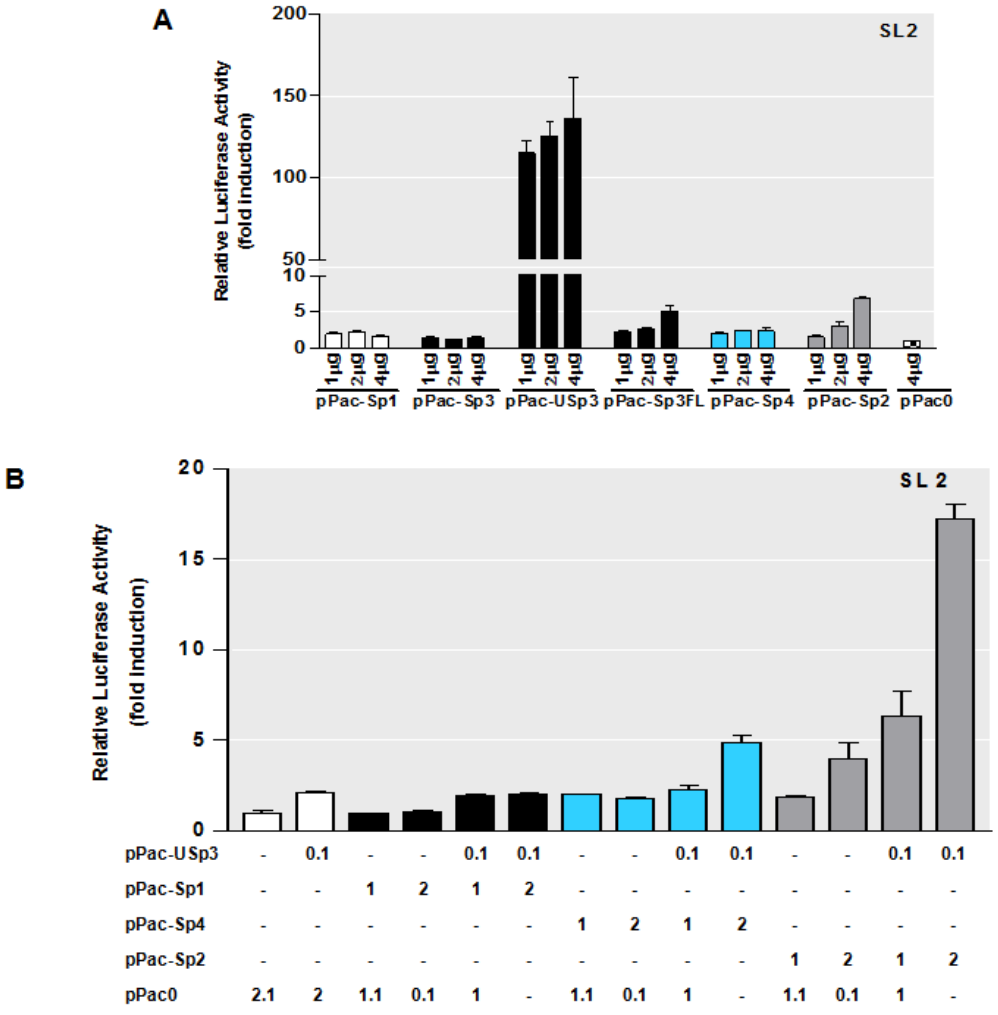

Figure 6

Figure 7: Mithramycin A (MA) inhibits expression of the PKCδ gene

A-B, PKCδ promoter activity is attenuated in NIE115 cells after treatment with mithramycin A. The PKCδ promoter reporter construct pGL3-1694/+289 (*A*) or pGL3-147/+289 (*B*) was transfected into NIE115 cells. After 4 h transfection, the cells were incubated with or without Sp-factor inhibitor mithramycin A at concentrations ranging from 0.05 to 5 μM for 24 h. Cells were then harvested and luciferase activities were determined. The plasmid pcDNA3.1-βgal was included in each transfection to correct the differences in transfection efficiencies. Values are expressed as a percentage of the activity of control and represent the mean ± SEM of three independent experiments performed in triplicate. (**, $p<0.01$; ***, $p<0.001$; between the control and mithramycin A-treated samples) *C-D*, Endogenous PKCδ mRNA levels are reduced by mithramycin A. NIE115 cells (*C*) or primary striatal neurons (*D*) were treated with different concentrations of mithramycin A for 24 h. Real-time RT PCR analysis of PKCδ mRNA level was performed. β-actin mRNA level was served as internal control. Values are expressed as a percentage of the activity of control and represent the mean ± SEM of three independent experiments performed in triplicate. (*, $p<0.05$; **, $p<0.01$ compared with the control and mithramycin A-treated samples) *E*, Left panel: Exposure of primary striatal neurons to 5 μM mithramycin A reduced PKCδ immunoreactivity. Primary striatal cultures were treated with or without 5 μM MA for 24 h. Cultures were immunostained for PKCδ (red), and the nuclei were counterstained by Hoechst 33342 (blue). Images were obtained using a Nikon TE2000 fluorescence microscope (magnification 60x). Scale bar, 10μm. Representative immunofluorescence images are shown. The insert shows a higher magnification of the cell body area. Right panel:

Immunofluorescence quantification of PKCδ fluorescence intensity. Fluorescence immunoreactivity of PKCδ was measured in each group using Metamorph software. Values expressed as percent of control group are mean ± SEM and representative for results obtained from three separate experiments in triplicate (**, $p<0.01$).

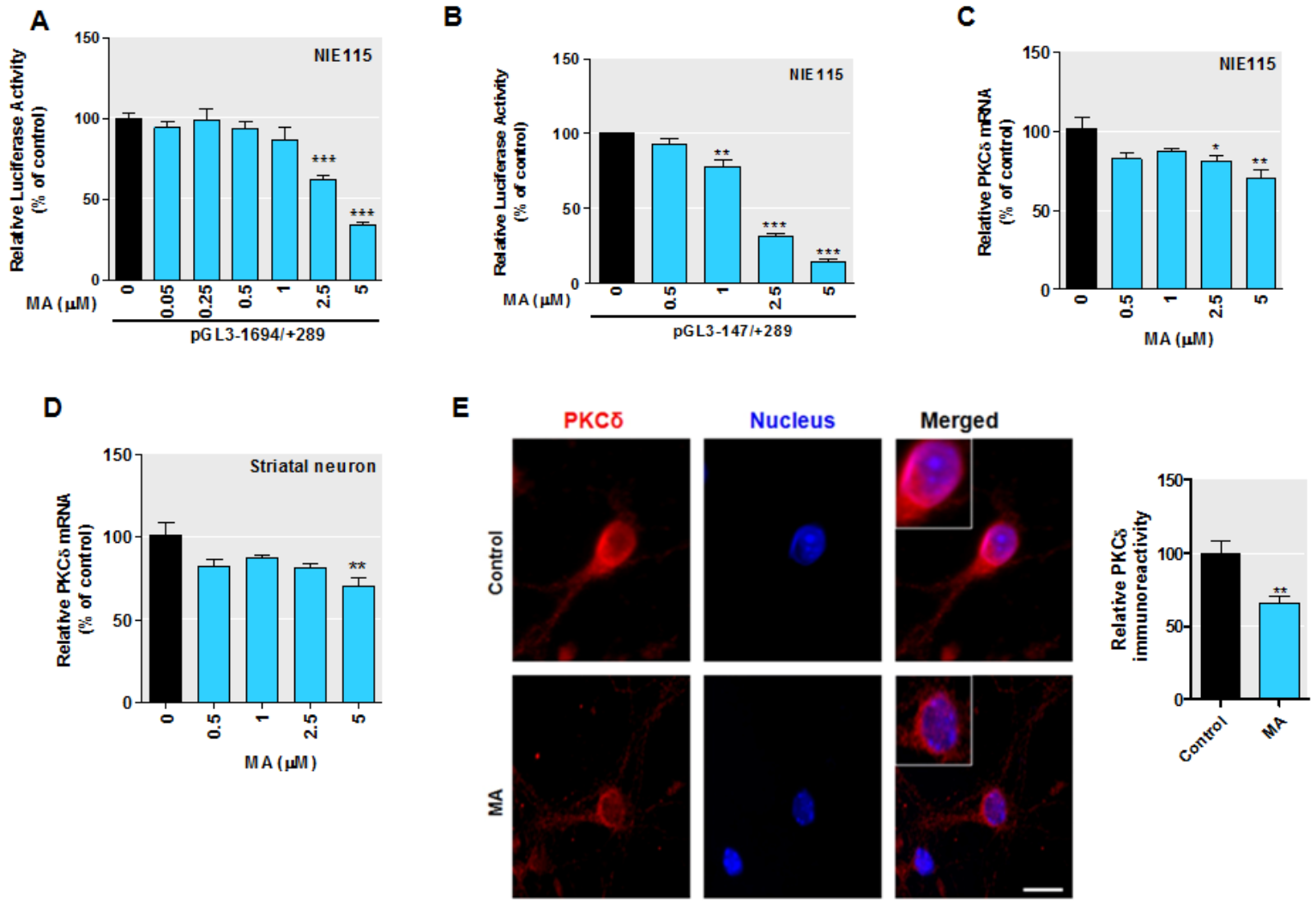

Figure 7

Figure 8: Binding of Sp-family of transcription factors to the PKCδ promoter in NIE115 cells

A, ChIP assays in NIE115 cells indicate a physical association of Sp1, Sp3, and Sp4 with the PKCδ promoter region. Cross-linked chromatin was isolated from NIE115 cells transfected with the expression plasmids for Sp1 (pN3-Sp1), Sp3 (pN3-Sp3 FL), Sp4 (pN3-Sp4), or the empty vector pN3, as indicated. Isolated chromatin was enzymaticlly digested and immunoprecipitated with anti-Sp1 (lane 2 and 7), anti-Sp3 (lane 3 and 10), anti-Sp4 (lane 4 and 13), or antibody-free control (lane 6, 9, 12, and 15). The subsequently purified DNA from immunoprecipitated samples and unimmunoprecipitated samples (labeled as *Input*, lane 5, 8, 11, and 14) was subjected to PCR amplification with primers specific for PKCδ promoter region that generates a 312-bp fragment. *B*, EMSA to test binding of nuclear proteins from NIE115 cells with the Sp site of the PKCδ promoter. EMSA was performed with an IRye700-labeled probe corresponding to the PKCδ promoter GC (1) and (2) motifs and 10 μg of nuclear extract from NIE115 cells. As indicated, various competitors (100-fold excess of unlabeled oligos, *lane* 3-8) were added to the mixture before adding probe. The sequences of the competitors are shown in Table S2. The specific and non-specific (labeled as N.S.) complexes are indicated by arrows.

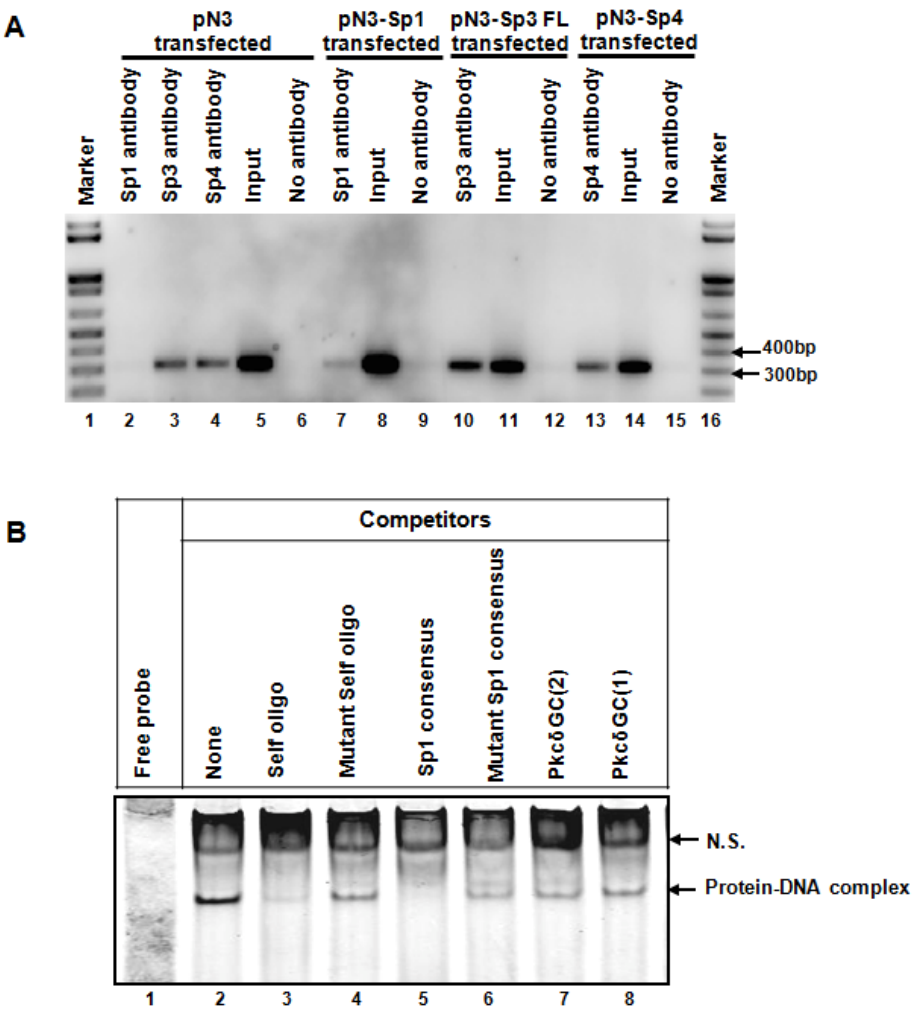

Figure 8

Figure 9: PKCδ promoter activity is stimulated by p300/CBP in NIE115 cells, and this effect is independent of p300 HAT activity and requires functional Sp sites

A-B, Variable amounts (µg) of expression plasmid for p300 (pCI-p300) and p300 mutant (pCI-p300ΔHAT) (*A*), or CBP (pcDNA-CBP) (*B*) were cotransfected with the PKCδ promoter reporter construct pGL3-147/+289 into NIE115 cells. Variations in the amount of total DNA were compensated with the corresponding empty vector (*EV*) pCIneo or pcDNA3.1. Luciferase activity was measured after 24 h of transfection. The plasmid pcDNA3.1-βgal was included in each transfection for data normalization. Values are expressed as fold induction relative to that obtained from cells transfected with 8 µg of empty vector and represent the mean ± SEM of three independent experiments performed in triplicate. (**, $p<0.01$; ***, $p<0.001$; as compared to the EV-transfected samples) *C-D*, luciferase reporter constructs Sp1-Luc or mSp1-Luc was cotransfected with variable amounts (µg) of expression plasmid pCI-p300 (*C*) or pcDNA-CBP (*D*) were into NIE115 cells. Luciferase activity was measured after 24 h of transfection. Values are expressed as percent of that obtained from cells cotransfected with 8 µg of EV and wild-type Sp1-Luc construct and represent the mean ± SEM of three independent experiments performed in triplicate.

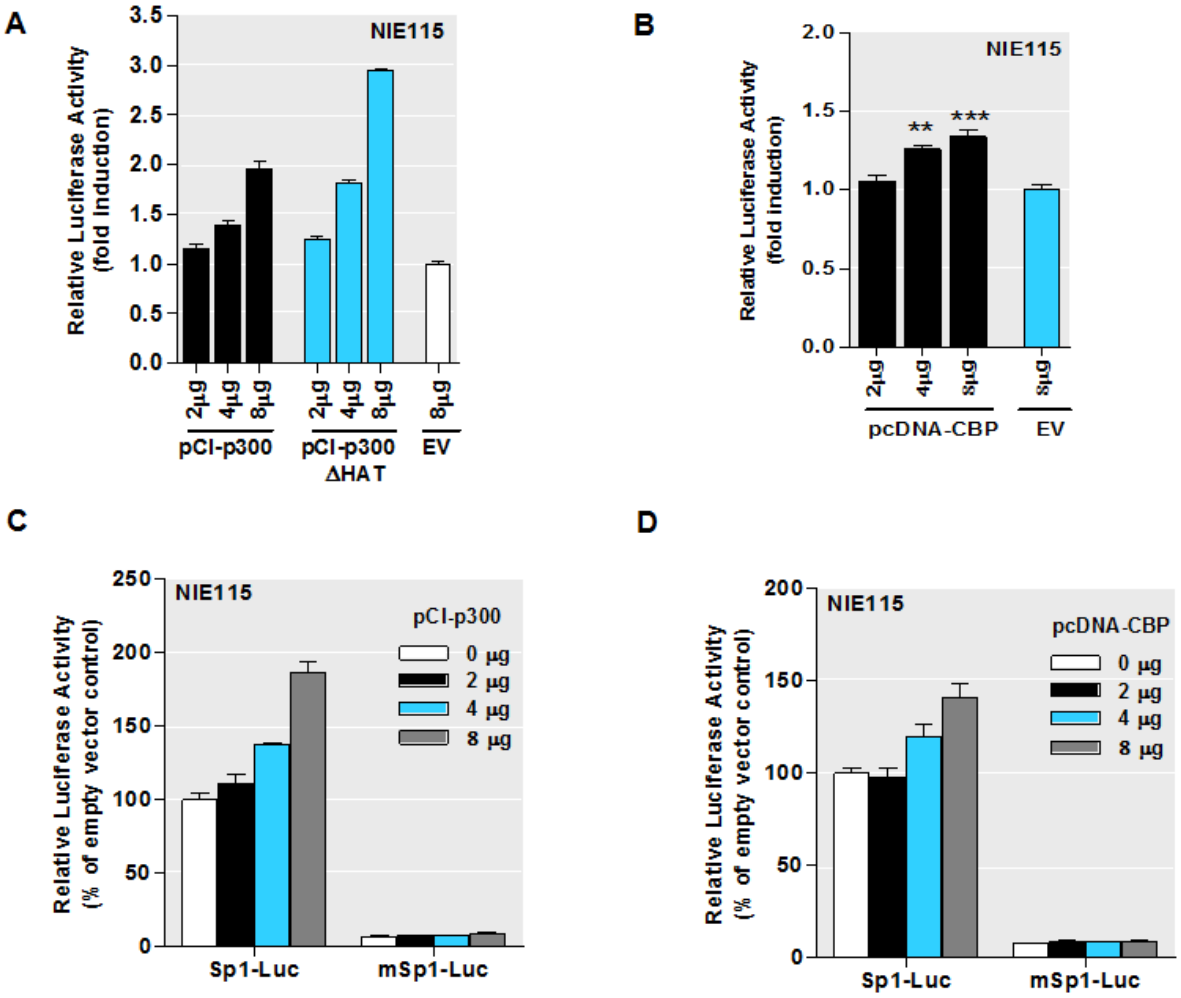

Figure 9

Figure 10: Overexpression of PKCδ sensitizes MN9D dopaminergic cells to oxidative stress-dependent neurodegeneration

MN9D cells were transfected with plasmid expressing PKCδ-GFP or control plasmid EGFP-C1 for 18 h. The cells were then switched to a serum-free medium and exposed to various doses of H_2O_2, ranging from 0.5 to 2.0 mM for 20 h. Cells were collected and assayed for DNA fragmentation (*left panel*). Data shown represent mean ± SEM from two independent experiments performed in quadruplicate (*, $p<0.05$; **, $p<0.01$; ***, $p<0.001$; compared with the control and H_2O_2-treated samples). The overexpression of PKCδ-GFP was confirmed by GFP fluorescence imaging (*right panel*). Images were obtained using a Nikon TE2000 fluorescence microscope (magnification 20x). Scale bar, 100μm.

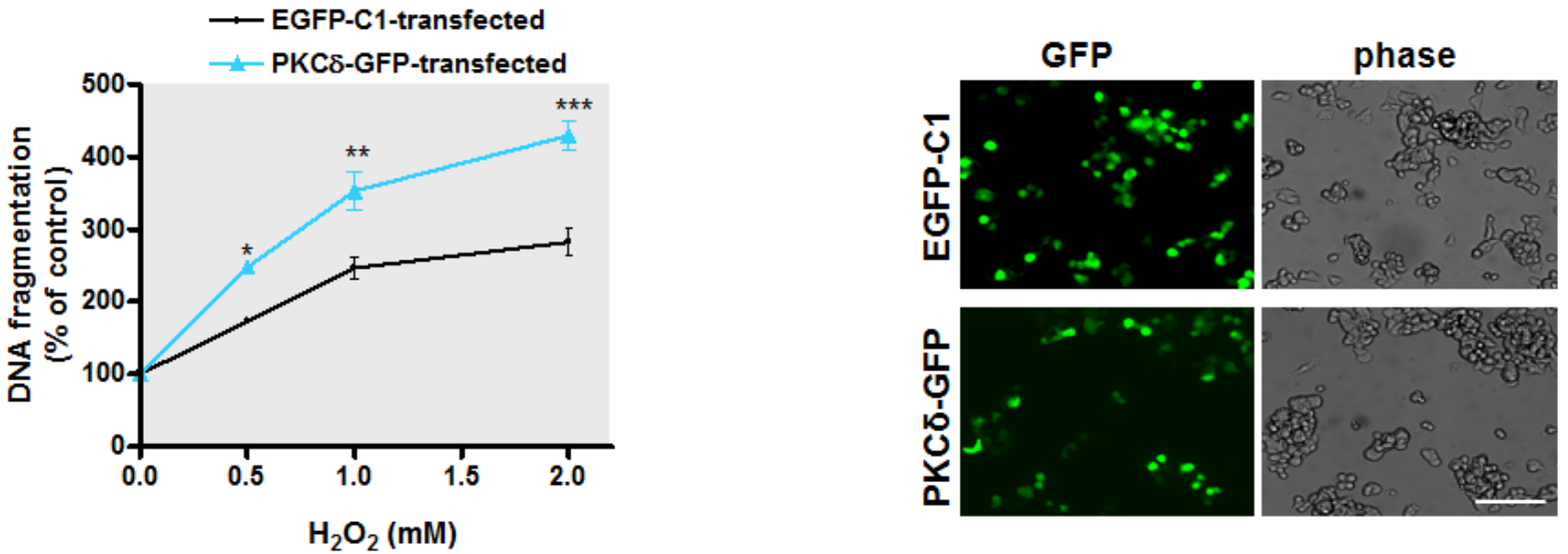

Figure 10

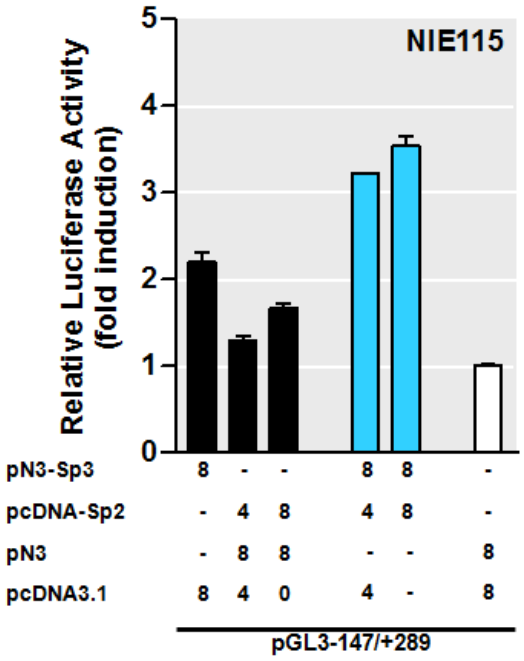

Figure S1: Additive activation of PKCδ promoter transcription by Sp2 and Sp3

The expression plasmids pN3-Sp3, pcDNA-Sp2, and empty vector pN3 or pcDNA3.1 were cotransfected along with the PKCδ promoter reporter construct pGL3-147/+289 into NIE115 either alone or in the different combinations, as indicated below the bar graph. Luciferase activity was determined after 24 h of transfection. Transfection efficiency was normalized by β-galactosidase activity. Data expressed as fold induction relative to that obtained from cells transfected with empty vector alone and represent the mean ± SEM of three independent experiments performed in triplicate.

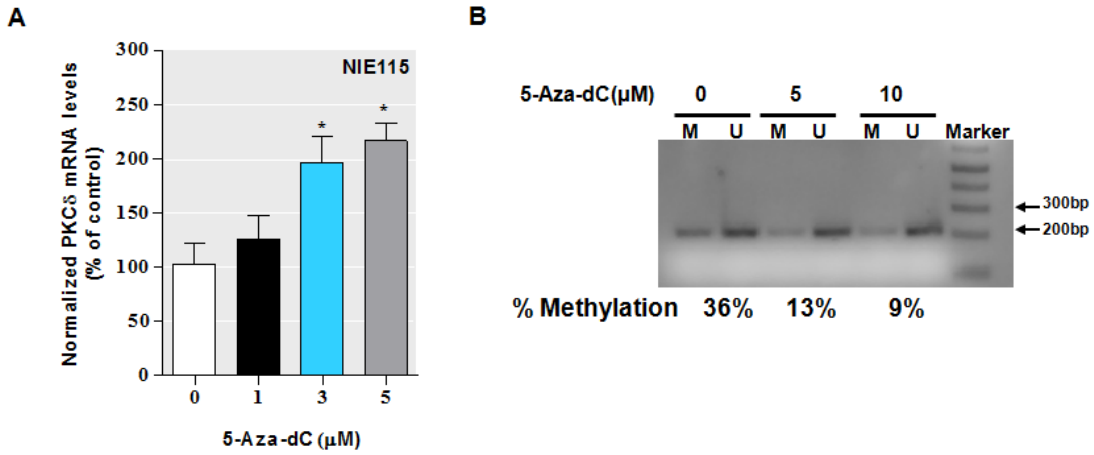

Figure S2: Treatment with methylation inhibitor 5'-aza-2'-deoxycytidine (5-Aza-dC) significantly increased endogenous PKCδ mRNA and attenuated PKCδ promoter methylation in NIE115 cells

NIE115 cells were treated with varying doses of 5-Aza-dC for 24 h, as indicated, and cells were than collected for real-time PCR analysis of PKCδ mRNA (*A*) or bisulfate-modification and subsequent MSP analysis (*B*) with primers for methylated (M) and unmethylated (U) DNA. PCR bands in (*B*) were analyzed using the one-dimensional image analysis software (Kodak Molecular Imaging System), and the relative methylation status was expressed as ratio of methylated versus unmethylated. (*, $p<0.05$; between the control and 5-Aza-dC-treated samples)

Table S1: List of primer sequences used in the study

Primer	Sequence (5'-3')
P-1694 F	GTCTATCTCGAGGATCTGACGCCCTCTTCTGGAGT
P-1193 R1	GTCCTGATAACTGTCCCCACCCCAT
P-1217 F	ATGGGGTGGGGACAGTTATCAGGAC
P+289 R	GTCTATAAGCTTACCTCACCCAGGTGCCGG
P-1192F	ATATATCTCGAGTGGGGACTTAAATACTAATT
P-1193R2	ATATATAAGCTTGTCCTGATAACTGTCCCCAC
P-660F1	ATATATCTCGAGTATCCTCCCAGGAAGAGTTCTCG
P-660F2	ATATATGGTACCTATCCTCCCAGGAAGAGTTCTCG
P-659R	ATATATAAGCTTTACAAGAGGGTTCTAATAGCC
P-147 F	ATATATCTCGAGTCTCGGGCAGGACTGGAACC
P-148R	ATATATAAGCTTGAAGGAGCTGGGAGGTCTCC
P+2 F	ATATATCTCGAGTCCTGGGCTCCATTGTGTGTG
P+2R	GTCTATAAGCTTAGGCACCGACGGGGCTTCC
P-1072F	ATATATCTCGAGCCCCAATGTACATTTAAAATAAGG
P-882F	ATATATCTCGAGGATCTCGTTAAGGATGGTTGTG
P-822F	ATATATCTCGAGTCGGAAGAGCAGTCGGGTGCTC
P-712F	ATATATCTCGAGAGGTAGTTTTCCAGAAGGAAC
P-560F	ATATATCTCGAGGAGCACTGGAGTATTATTCTGAG
P-460F	ATATATCTCGAGAGCCCAGGAAGTCATTTCTTTG
P-371F	ATATATCTCGAGATTTGGTGCTCAGACTTTGGGC
P-300F	ATATATCTCGAGTCTTATGAGCTTGACTGAGCAAGG
P-250F	ATATATCTCGAGAGACAGTGAGATGGGGGCAGA
P-197F	ATATATCTCGAGTGAGACAAACTGGCTAGAACCTC
P-561R1	ATATATGCTAGCAGGGGGAGAAAGCAGGAGAAT
P-561+2F	TGCTTTCTCCCCCTCCTGGGCTCCATTGTGTGTG
P-561+2R	CAATGGAGCCCAGGAGGGGGAGAAAGCAGGAGAA
P+209R	GTCTATAAGCTTACGTGAGCTGGGGGTCCAGC
P+165F	ATATATCTCGAGTTGCAACTCAAAGAGGCTGA
mGC(1) F	GGACCCCCAGCTCACGT**AA**GC**TT**AGCTTCGAAG
mGC(1) R	ACGTGAGCTGGGGGTCCAGCGCGTCTCAGC
mGC(2) F	TGGGCGGAGCTTCGAAG**AA**GC**TT**GCGCCCGTGG
mGC(2) R	CTTCGAAGCTCCGCCCACGTGAGCTGGGGG
mGC(3) F	AGGGGCGGGCGCCCGTG**AA**GC**TT**GTCCTGAGTG
mGC(3) R	CACGGGCGCCCGCCCCTTCGAAGCTCCGCC

F, Forward; R, Reverse; q, quantitative RT-PCR; m, mutant primers; ChIP, primers used for ChIP experiments; Methylated and unmethylated, primers used for MSP experiments.

Table S1 (continued)

Primer	Sequence (5'-3')	Amplicon
mGC(4) F	GGGCGGGTCCTGAGTGG**AA**GC**TT**GACCGGGGCC	
mGC(4) R	CCACTCAGGACCCGCCCCACGGGCGCCCGC	
mCACCC F	GTGTGCAGTGCTCAAC**T**C**T**AA**A**CC**TTT**AACTTGGCCT	
mCACCC R	GTTGAGCACTGCACACACAATGGAGCCCAG	
mGC(2,3) F	AGAAGCTTGCGCCCGTG**AA**GC**TT**GTCCTGAGTG	
mGC(2,3) R	CACGGGCGCAAGCTTCTTCGAAGCTCCGCC	
mGC(1,2,3) R	CACGGGCGCAAGCTTCTTCGAAGCTAAGCT	
PKCδ Fq	TCTGGGAGTGACATCCTAGACAACAACGGG	410
PKCδ Rq	CAGATGATCTCAGCTGCATAAAACGTAGCC	
ChIP F=P+2F	ATATATCTCGAGTCCTGGGCTCCATTGTGTGTG	312
ChIP R=P+289R	GTCTATAAGCTTACCTCACCCAGGTGCCGG	
Methylated F	TGTAATTTAAAGAGGTTGAGACGC	228
Methylated R	TAACCGTCTCTAACTCTTATAACGC	
Unmethylated F	TAGTTGGTTAGTGGGGAGTTTTG	228
Unmethylated R	TTAACCATCTCTAACTCTTATAACACC	

Sequence of primers for constructions mouse PKCδ promoter reporter plasmids, site-directed mutagenesis, real-time RT-PCR, and ChIP experiments. Boldface letters indicate mutated bases.

Table S2: Sense sequences of the oligonucleotides used in EMSAs

Probe/Competitor	Sense oligonucleotide (5'-3')
PkcδGC(1, 2)	CACGTGGGCGGAGCTTCGAAGGGGCGGGCGCC
PkcδGC(1, 2) mutant	CACGT**aa**TC**tt**AGCTTCGAAG**aa**TCT**tt**CGCC
Sp1 consensus	ATTCGATCGGGGCGGGGCGAGC
Sp1 consensus mutant	ATTCGATCG**aa**TC**ttt**GCGAGC
PkcδGC(1)	GCTCACGTGGGCGGAGCTTC
PkcδGC(2)	CTTCGAAGGGGCGGGCGCCCG

Nucleotide sequences of the consensus binding motif are underlined. Mutated base pairs in mutant oligos are highlighted in bold and in lowercase.

References

Ammanamanchi S, Freeman JW, Brattain MG (2003) Acetylated sp3 is a transcriptional activator. J Biol Chem 278:35775-35780.

Anantharam V, Kitazawa M, Wagner J, Kaul S, Kanthasamy AG (2002) Caspase-3-dependent proteolytic cleavage of protein kinase Cdelta is essential for oxidative stress-mediated dopaminergic cell death after exposure to methylcyclopentadienyl manganese tricarbonyl. J Neurosci 22:1738-1751.

Barmack NH, Qian Z, Yoshimura J (2000) Regional and cellular distribution of protein kinase C in cerebellar Purkinje cells. J Comp Neurol 427:235-254.

Berry DM, Antochi R, Bhatia M, Meckling-Gill KA (1996) 1,25-Dihydroxyvitamin D3 stimulates expression and translocation of protein kinase Calpha and Cdelta via a nongenomic mechanism and rapidly induces phosphorylation of a 33-kDa protein in acute promyelocytic NB4 cells. J Biol Chem 271:16090-16096.

Black AR, Black JD, Azizkhan-Clifford J (2001) Sp1 and kruppel-like factor family of transcription factors in cell growth regulation and cancer. J Cell Physiol 188:143-160.

Blume SW, Snyder RC, Ray R, Thomas S, Koller CA, Miller DM (1991) Mithramycin inhibits SP1 binding and selectively inhibits transcriptional activity of the dihydrofolate reductase gene in vitro and in vivo. J Clin Invest 88:1613-1621.

Boyes J, Byfield P, Nakatani Y, Ogryzko V (1998) Regulation of activity of the transcription factor GATA-1 by acetylation. Nature 396:594-598.

Brand AH, Breeden L, Abraham J, Sternglanz R, Nasmyth K (1985) Characterization of a "silencer" in yeast: a DNA sequence with properties opposite to those of a transcriptional enhancer. Cell 41:41-48.

Brodie C, Blumberg PM (2003) Regulation of cell apoptosis by protein kinase c delta. Apoptosis 8:19-27.

Cartharius K, Frech K, Grote K, Klocke B, Haltmeier M, Klingenhoff A, Frisch M, Bayerlein M, Werner T (2005) MatInspector and beyond: promoter analysis based on transcription factor binding sites. Bioinformatics 21:2933-2942.

Choi SH, Hyman T, Blumberg PM (2006) Differential effect of bryostatin 1 and phorbol 12-myristate 13-acetate on HOP-92 cell proliferation is mediated by down-regulation of protein kinase Cdelta. Cancer Res 66:7261-7269.

Courey AJ, Tjian R (1988) Analysis of Sp1 in vivo reveals multiple transcriptional domains, including a novel glutamine-rich activation motif. Cell 55:887-898.

Dempsey EC, Newton AC, Mochly-Rosen D, Fields AP, Reyland ME, Insel PA, Messing RO (2000) Protein kinase C isozymes and the regulation of diverse cell responses. Am J Physiol Lung Cell Mol Physiol 279:L429-438.

DeVries TA, Neville MC, Reyland ME (2002) Nuclear import of PKCdelta is required for apoptosis: identification of a novel nuclear import sequence. Embo J 21:6050-6060.

Gavrielides MV, Gonzalez-Guerrico AM, Riobo NA, Kazanietz MG (2006) Androgens regulate protein kinase Cdelta transcription and modulate its apoptotic function in prostate cancer cells. Cancer Res 66:11792-11801.

Greenamyre JT, Hastings TG (2004) Biomedicine. Parkinson's--divergent causes, convergent mechanisms. Science 304:1120-1122.

Hagen G, Muller S, Beato M, Suske G (1992) Cloning by recognition site screening of two novel GT box binding proteins: a family of Sp1 related genes. Nucleic Acids Res 20:5519-5525.

Hlavackova M, Kozichova K, Neckar J, Kolar F, Musters RJ, Novak F, Novakova O Up-regulation and redistribution of protein kinase C-delta in chronically hypoxic heart. Mol Cell Biochem.

Horovitz-Fried M, Jacob AI, Cooper DR, Sampson SR (2007) Activation of the nuclear transcription factor SP-1 by insulin rapidly increases the expression of protein kinase C delta in skeletal muscle. Cell Signal 19:556-562.

Horovitz-Fried M, Cooper DR, Patel NA, Cipok M, Brand C, Bak A, Inbar A, Jacob AI, Sampson SR (2006) Insulin rapidly upregulates protein kinase Cdelta gene expression in skeletal muscle. Cell Signal 18:183-193.

Hung JJ, Wang YT, Chang WC (2006) Sp1 deacetylation induced by phorbol ester recruits p300 to activate 12(S)-lipoxygenase gene transcription. Mol Cell Biol 26:1770-1785.

Jenner P (2003) Oxidative stress in Parkinson's disease. Ann Neurol 53 Suppl 3:S26-36; discussion S36-28.

Kanthasamy AG, Kitazawa M, Kanthasamy A, Anantharam V (2003) Role of proteolytic activation of protein kinase Cdelta in oxidative stress-induced apoptosis. Antioxid Redox Signal 5:609-620.

Kanthasamy AG, Anantharam V, Zhang D, Latchoumycandane C, Jin H, Kaul S, Kanthasamy A (2006) A novel peptide inhibitor targeted to caspase-3 cleavage site of a proapoptotic kinase protein kinase C delta (PKCdelta) protects against

dopaminergic neuronal degeneration in Parkinson's disease models. Free Radic Biol Med 41:1578-1589.

Karban AS, Okazaki T, Panhuysen CI, Gallegos T, Potter JJ, Bailey-Wilson JE, Silverberg MS, Duerr RH, Cho JH, Gregersen PK, Wu Y, Achkar JP, Dassopoulos T, Mezey E, Bayless TM, Nouvet FJ, Brant SR (2004) Functional annotation of a novel NFKB1 promoter polymorphism that increases risk for ulcerative colitis. Hum Mol Genet 13:35-45.

Kaul S, Kanthasamy A, Kitazawa M, Anantharam V, Kanthasamy AG (2003) Caspase-3 dependent proteolytic activation of protein kinase C delta mediates and regulates 1-methyl-4-phenylpyridinium (MPP+)-induced apoptotic cell death in dopaminergic cells: relevance to oxidative stress in dopaminergic degeneration. Eur J Neurosci 18:1387-1401.

Kaul S, Anantharam V, Yang Y, Choi CJ, Kanthasamy A, Kanthasamy AG (2005) Tyrosine phosphorylation regulates the proteolytic activation of protein kinase Cdelta in dopaminergic neuronal cells. J Biol Chem 280:28721-28730.

Kavurma MM, Santiago FS, Bonfoco E, Khachigian LM (2001) Sp1 phosphorylation regulates apoptosis via extracellular FasL-Fas engagement. J Biol Chem 276:4964-4971.

Kitazawa M, Anantharam V, Kanthasamy AG (2003) Dieldrin induces apoptosis by promoting caspase-3-dependent proteolytic cleavage of protein kinase Cdelta in dopaminergic cells: relevance to oxidative stress and dopaminergic degeneration. Neuroscience 119:945-964.

Kudo S (1998) Methyl-CpG-binding protein MeCP2 represses Sp1-activated transcription of the human leukosialin gene when the promoter is methylated. Mol Cell Biol 18:5492-5499.

Kurkinen KM, Keinanen RA, Karhu R, Koistinaho J (2000) Genomic structure and chromosomal localization of the rat protein kinase Cdelta-gene. Gene 242:115-123.

Latchoumycandane C, Anantharam V, Kitazawa M, Yang Y, Kanthasamy A, Kanthasamy AG (2005) Protein kinase Cdelta is a key downstream mediator of manganese-induced apoptosis in dopaminergic neuronal cells. J Pharmacol Exp Ther 313:46-55.

Leibersperger H, Gschwendt M, Gernold M, Marks F (1991) Immunological demonstration of a calcium-unresponsive protein kinase C of the delta-type in different species and murine tissues. Predominance in epidermis. J Biol Chem 266:14778-14784.

Li X, Ma C, Zhu D, Meng L, Guo L, Wang Y, Zhang L, Li Z, Li E Increased expression and altered subcellular distribution of PKC-delta and PKC-varepsilon in pulmonary arteries exposed to hypoxia and 15-HETE. Prostaglandins Other Lipid Mediat.

Liedtke C, Groger N, Manns MP, Trautwein C (2003) The human caspase-8 promoter sustains basal activity through SP1 and ETS-like transcription factors and can be up-regulated by a p53-dependent mechanism. J Biol Chem 278:27593-27604.

Liu J, Yang D, Minemoto Y, Leitges M, Rosner MR, Lin A (2006) NF-kappaB is required for UV-induced JNK activation via induction of PKCdelta. Mol Cell 21:467-480.

Livak KJ, Schmittgen TD (2001) Analysis of relative gene expression data using real-time quantitative PCR and the 2(-Delta Delta C(T)) Method. Methods 25:402-408.

Lopez-Soto A, Quinones-Lombrana A, Lopez-Arbesu R, Lopez-Larrea C, Gonzalez S (2006) Transcriptional regulation of ULBP1, a human ligand of the NKG2D receptor. J Biol Chem 281:30419-30430.

MacCarthy-Morrogh L, Wood L, Brimmell M, Johnson PW, Packham G (2000) Identification of a novel human BCL-X promoter and exon. Oncogene 19:5534-5538.

Mavrothalassitis G, Ghysdael J (2000) Proteins of the ETS family with transcriptional repressor activity. Oncogene 19:6524-6532.

Miettinen S, Roivainen R, Keinanen R, Hokfelt T, Koistinaho J (1996) Specific induction of protein kinase C delta subspecies after transient middle cerebral artery occlusion in the rat brain: inhibition by MK-801. J Neurosci 16:6236-6245.

Morgenstern B, Dress A, Werner T (1996) Multiple DNA and protein sequence alignment based on segment-to-segment comparison. Proc Natl Acad Sci U S A 93:12098-12103.

Naik MU, Benedikz E, Hernandez I, Libien J, Hrabe J, Valsamis M, Dow-Edwards D, Osman M, Sacktor TC (2000) Distribution of protein kinase Mzeta and the complete protein kinase C isoform family in brain. J Comp Neurol 426:243-258.

Noti JD (1997) Sp3 mediates transcriptional activation of the leukocyte integrin genes CD11C and CD11B and cooperates with c-Jun to activate CD11C. J Biol Chem 272:24038-24045.

Ono Y, Fujii T, Ogita K, Kikkawa U, Igarashi K, Nishizuka Y (1988) The structure, expression, and properties of additional members of the protein kinase C family. J Biol Chem 263:6927-6932.

Peters CA, Cutler RE, Maizels ET, Robertson MC, Shiu RP, Fields P, Hunzicker-Dunn M (2000a) Regulation of PKC delta expression by estrogen and rat placental lactogen-1 in luteinized rat ovarian granulosa cells. Mol Cell Endocrinol 162:181-191.

Peters CA, Cutler RE, Maizels ET, Robertson MC, Shiu RP, Fields P, Hunzicker-Dunn M (2000b) Regulation of PKC delta expression by estrogen and placental lactogen-1 in luteinized ovarian granulosa cells. Mol Cell Endocrinol 162:181-191.

Ponassi R, Terrinoni A, Chikh A, Rufini A, Lena AM, Sayan BS, Melino G, Candi E (2006) p63 and p73, members of the p53 gene family, transactivate PKCdelta. Biochem Pharmacol 72:1417-1422.

Quan T, Fisher GJ (1999) Cloning and characterization of the human protein kinase C-eta promoter. J Biol Chem 274:28566-28574.

Ramana CV, Chatterjee-Kishore M, Nguyen H, Stark GR (2000) Complex roles of Stat1 in regulating gene expression. Oncogene 19:2619-2627.

Ray R, Snyder RC, Thomas S, Koller CA, Miller DM (1989) Mithramycin blocks protein binding and function of the SV40 early promoter. J Clin Invest 83:2003-2007.

Reno EM, Haughian JM, Dimitrova IK, Jackson TA, Shroyer KR, Bradford AP (2008) Analysis of protein kinase C delta (PKC delta) expression in endometrial tumors. Hum Pathol 39:21-29.

Ryu H, Lee J, Olofsson BA, Mwidau A, Dedeoglu A, Escudero M, Flemington E, Azizkhan-Clifford J, Ferrante RJ, Ratan RR (2003) Histone deacetylase inhibitors prevent oxidative neuronal death independent of expanded polyglutamine repeats via an Sp1-dependent pathway. Proc Natl Acad Sci U S A 100:4281-4286.

Saito N (1995) [Differential involvement of PKC subspecies in neuronal function]. Nippon Yakurigaku Zasshi 105:127-136.

Sapetschnig A, Koch F, Rischitor G, Mennenga T, Suske G (2004) Complexity of translationally controlled transcription factor Sp3 isoform expression. J Biol Chem 279:42095-42105.

Saur D, Seidler B, Paehge H, Schusdziarra V, Allescher HD (2002) Complex regulation of human neuronal nitric-oxide synthase exon 1c gene transcription. Essential role of Sp and ZNF family members of transcription factors. J Biol Chem 277:25798-25814.

Shanmugam M, Krett NL, Maizels ET, Cutler RE, Jr., Peters CA, Smith LM, O'Brien ML, Park-Sarge OK, Rosen ST, Hunzicker-Dunn M (1999) Regulation of protein kinase C delta by estrogen in the MCF-7 human breast cancer cell line. Mol Cell Endocrinol 148:109-118.

Shin SY, Kim CG, Ko J, Min DS, Chang JS, Ohba M, Kuroki T, Choi YB, Kim YH, Na DS, Kim JW, Lee YH (2004) Transcriptional and post-transcriptional regulation of the PKC delta gene by etoposide in L1210 murine leukemia cells: implication of PKC delta autoregulation. J Mol Biol 340:681-693.

Solovyev VV, Shahmuradov IA (2003) PromH: Promoters identification using orthologous genomic sequences. Nucleic Acids Res 31:3540-3545.

Sowa Y, Orita T, Minamikawa-Hiranabe S, Mizuno T, Nomura H, Sakai T (1999) Sp3, but not Sp1, mediates the transcriptional activation of the p21/WAF1/Cip1 gene promoter by histone deacetylase inhibitor. Cancer Res 59:4266-4270.

Spengler ML, Brattain MG (2006) Sumoylation inhibits cleavage of Sp1 N-terminal negative regulatory domain and inhibits Sp1-dependent transcription. J Biol Chem 281:5567-5574.

Sudhakar C, Jain N, Swarup G (2008) Sp1-like sequences mediate human caspase-3 promoter activation by p73 and cisplatin. Febs J 275:2200-2213.

Suh KS, Tatunchak TT, Crutchley JM, Edwards LE, Marin KG, Yuspa SH (2003) Genomic structure and promoter analysis of PKC-delta. Genomics 82:57-67.

Suske G (1999) The Sp-family of transcription factors. Gene 238:291-300.

Suske G (2000) Transient transfection of Schneider cells in the study of transcription factors. Methods Mol Biol 130:175-187.

Suzuki T, Kimura A, Nagai R, Horikoshi M (2000) Regulation of interaction of the acetyltransferase region of p300 and the DNA-binding domain of Sp1 on and through DNA binding. Genes Cells 5:29-41.

Tavares D, Tully K, Dobner PR (1999) Sequences required for induction of neurotensin receptor gene expression during neuronal differentiation of N1E-115 neuroblastoma cells. J Biol Chem 274:30066-30079.

Walker GE, Wilson EM, Powell D, Oh Y (2001) Butyrate, a histone deacetylase inhibitor, activates the human IGF binding protein-3 promoter in breast cancer cells: molecular mechanism involves an Sp1/Sp3 multiprotein complex. Endocrinology 142:3817-3827.

Whetstine JR, Flatley RM, Matherly LH (2002) The human reduced folate carrier gene is ubiquitously and differentially expressed in normal human tissues: identification of

seven non-coding exons and characterization of a novel promoter. Biochem J 367:629-640.

Wu Y, Diab I, Zhang X, Izmailova ES, Zehner ZE (2004) Stat3 enhances vimentin gene expression by binding to the antisilencer element and interacting with the repressor protein, ZBP-89. Oncogene 23:168-178.

Yang XJ, Ogryzko VV, Nishikawa J, Howard BH, Nakatani Y (1996) A p300/CBP-associated factor that competes with the adenoviral oncoprotein E1A. Nature 382:319-324.

Yang Y, Kaul S, Zhang D, Anantharam V, Kanthasamy AG (2004) Suppression of caspase-3-dependent proteolytic activation of protein kinase C delta by small interfering RNA prevents MPP+-induced dopaminergic degeneration. Mol Cell Neurosci 25:406-421.

Zhang D, Anantharam V, Kanthasamy A, Kanthasamy AG (2007a) Neuroprotective effect of protein kinase C delta inhibitor rottlerin in cell culture and animal models of Parkinson's disease. J Pharmacol Exp Ther 322:913-922.

Zhang D, Kanthasamy A, Yang Y, Anantharam V, Kanthasamy A (2007b) Protein kinase Cdelta negatively regulates tyrosine hydroxylase activity and dopamine synthesis by enhancing protein phosphatase-2A activity in dopaminergic neurons. J Neurosci 27:5349-5362.

CHAPER III: HISTONE ACETYLATION UPREGULATES PKCδ VIA SP-DEPENDENT TRANSCRIPTION IN DOPAMINERGIC NEURONS: RELEVANCE TO EPIGENETIC MECHANISMS OF NEURODEGENERATION IN PARKINSON'S DISEASE

A paper submitted to *Journal of Biological Chemistry*

Huajun Jin, Arthi Kanthasamy, Anamitra Ghosh, Vellareddy Anantharam, and Anumantha Kanthasamy

Abstract

Protein Kinase Cδ (PKCδ) is an oxidative stress sensitive kinase that plays a causal role in apoptotic cell death in cell culture and animal models of Parkinson's disease (PD). We previously characterized multiple DNA regulatory elements that positively or negatively regulate PKCδ gene expression in neurons. We identified members of the Sp protein family of transcription factors as fundamentally critical determinants of basal PKCδ gene transactivation. However, the association between epigenetic regulation and PKCδ expression has not yet been studied thus far. Here, we report that treatment with sodium butyrate (NaBu), a specific histone deacetylase (HDAC) inhibitor, significantly enhanced the PKCδ protein and mRNA levels in primary striatal and nigral neurons and in NIE115 and MN9D cells. Other HDAC inhibitors, valproic acid (VPA), scriptaid, trichostatin A (TSA), and apicidin, all mimicked the action of NaBu to induce PKCδ. NaBu-induced PKCδ

expression correlated with hyperacetylation of H4 histone associated with PKCδ promoter, suggesting that acetylation-dependent chromatin remodeling may play a role in PKCδ upregulation. To further explore the molecular basis of histone acetylation-dependent PKCδ upregulation, PKCδ promoter analysis was performed using reporter gene assays. NaBu and other tested HDAC inhibitors all dramatically increased the PKCδ promoter activity in a dose-dependent manner. By using deletion analyses, the minimal fragment of the PKCδ promoter in response to NaBu was mapped to an 81 bp non-coding exon 1 region (+209 to +289). The site-directed mutagenesis studies revealed that multiple GC sites within this region are major elements conferring the responsiveness to NaBu-induced promoter activity. In addition, transcriptional activity of Sp1 and Sp3 was significantly induced by NaBu. Importantly, the ectopic expression of Sp1, Sp3, or Sp4 significantly enhanced NaBu-mediated transactivation of PKCδ promoter, whereas the ectopic expression of dominant negative mutant of Sp1 or Sp3 didn't cause this effect. Moreover, the Sp protein inhibitors mithramycin-A and tolfenamic acid dose-dependently blocked NaBu-induced PKCδ promoter activity. In addition, transcriptional activity of Sp1 and Sp3 was significantly induced by NaBu in a one-hybrid system. By utilizing the same assay, we found that the B domain and the glutamine-rich segment of the A domain of Sp1 and Sp3 (amino acids Sp1 146-494; Sp3 81-499) were essential for the NaBu-induced transactivation of the PKCδ promoter. Transient overexpression of p300 or CBP potentiated NaBu-induced transactivation potential of Sp1 or Sp3, whereas transient overexpression of HDACs attenuated this effect, suggesting that p300/CBP and HDACs may act as co-activators or co-repressors in response to NaBu exposure. Finally, NaBu treatment in the C57 black mouse model caused a time-dependent induction of PKCδ gene expression. Taken together, our

studies reveal that histone acetylation regulates the expression of a proapoptotic kinase PKCδ in the nigrostriatal dopaminergic system *via* the Sp-dependent epigenetic mechanism, which may play a role in the pathogenesis of PD.

Introduction

PKC represents a large family of at least 12 serine/theronine kinases that regulate various cellular events, including proliferation, cell cycle progression, differentiation, and apoptosis (Dempsey et al., 2000). Based on their structure and substrate requirements, 11 PKC isoforms are categorizeded into three subfamilies, namely conventional PKCs (α, βI, βII, and γ), novel PKCs (δ, ε, η, and θ), and atypical PKCs (ζ, ι, and λ). The novel PKC member, PKCδ has been recognized as a key pro-apoptotic effector in various cell types (Brodie and Blumberg, 2003; Kanthasamy et al., 2003b). The role of PKCδ in nervous system function is beginning to emerge, and our recent studies showed that PKCδ is an oxidative stress-sensitive kinase, and that persistent activation of PKCδ by caspase-3-mediated proteolytic cleavage is a key mediator in multiple models of PD-associated dopaminergic neurodegeneration (Anantharam et al., 2002; Kaul et al., 2003; Kitazawa et al., 2003; Kaul et al., 2005b; Latchoumycandane et al., 2005). Alternatively, pharmacological inhibiton of PKCδ or depletion of PKCδ by siRNA is sufficient to prevent neurotoxin-induced dopaminergic neurodegeneration *in vivo* and *in vitro* (Yang et al., 2004; Kanthasamy et al., 2006; Zhang et al., 2007a), indicating that PKCδ could represent a valid pharmacological target for development of a neuroprotective strategy against oxidative stress-induced dopaminergic degeneration in PD. Furthermore, PKCδ has been found to act

as a key mediator of apoptosis in neurons of PD patients (Clarke, 2007). In addition, improper PKCδ activity, caused by aberrant expression of PKCδ, has been implicated in disease conditions, such as ischemia/hypoxia (Miettinen et al., 1996), manganism (see Chapter V), and cancer (Reno et al., 2008). Therefore, an understanding of the molecular mechanisms that control the amount and activity of PKCδ is of physiological and pathophysiological interest.

Previously, we characterized the PKCδ promoter in detail (see Chapter II). The promoter does not contain a TATA box. There are multiple major regulatory elements within the mouse PKCδ promoter, such as a strong positive regulatory element located at non-coding exon1 (+1 to +288), a core promoter (-147 to +1), a negative regulatory element (-660 to -561), and an interesting anti-inhibitory regulatory element (-712 to -660). Moreover, several functional TFBS within the mouse PKCδ promoter have been revealed, including NFκB, NERF1a, and PU.1 sites residing in the core promoter, as well as five Sp binding sites within the non-coding exon 1 region. It remains unknown, however, whether epigenetic mechanisms contribute to the regulation of PKCδ gene expression.

Acetylation and deacetylation of both histone and non-histone proteins play a pivotal role in the epigenetic regulation of gene expression. Histone acetylation catalyzed by histone acetyltransferases (HATs) promotes a more relaxed chromatin structure, which allows various transcription factors access to the promoter of target genes. In contrast, deacetylation by histone deacetylase (HDACs) leads to chromatin condensation and consequent transcriptional repression (Yang and Seto, 2007). The HDAC inhibitors are classified into four groups: short-chain fatty acids, hydroxamic acids, cyclic tetrapeptides, and benzamides

(Dokmanovic et al., 2007). Among them, butyrate is thought to be the most effective HDAC inhibitor due to its ability to cross the blood-brain barrier (Saha and Pahan, 2006). Although many studies show neuroprotective effects of HDAC inhibitors (Chuang et al., 2009), growing evidence also suggests a pro-apoptotic role for it in neurons (Dietz and Casaccia, 2010; Salminen et al., 1998; Boutillier et al., 2003; Wang et al., 2009).

In this study, we demonstrate that HDAC inhibition markedly induces PKCδ gene expression in the striatum and substantia nigra of animals, in primary nigral and striatal neuronal cultures, and in NIE115 and MN9D cells. Our *in vitro* experiments reveal that butyrate induces hyperacetylation of histone H4 associated with PKCδ promoter in NIE115 cells. Furthermore, the minimal region of the PKCδ promoter mediating butyrate induction is mapped to an 81 bp region, and four functioning GC boxes within this region regulate the butyrate-stimulated activity. Moreover, we present evidence to indicate that butyrate increases the transactivating capacity of Sp proteins to activate the PKCδ promoter. Taken together, upregulation of the pro-apoptotic PKCδ by HDAC inhibitors may represent a novel molecular mechanism of their neurodegenerative effects.

Experimental Procedures

Reagents

Mithramycin A, NaBu, TSA, mouse β-actin antibody, and tolfenamic acid were purchased from Sigma-Aldrich (St. Louis, MO). VPA, scriptaid, and apicidin were obtained from ALEXIS Biochemicals (Plymouth Meeting, PA). The Bradford protein assay kit was purchased from Bio-Rad Laboratories (Hercules, CA). Lipofectamine 2000 reagent, Alexa

680-conjugated anti-mouse secondary antibody, and all cell culture reagents were obtained from Invitrogen a. Antibodies against PKCδ, Sp1, Sp3, Sp4, c-myc, and HA-tag were purchased from Santa Cruz Biotechnology (Santa Cruz, CA). The pan-acetyl Histone H4 antibody was obtained from Active Motif (Carlsbad, CA), and the rabbit polyclonal antibody for acetyl-lysine, mouse p300, and histone H3 antibodies were obtained from Milipore (Billerica, MA). IR-Dye800 conjugated anti-rabbit secondary antibody was obtained from Rockland Labs (Gilbertsville, PA).

Plasmids construction

The mouse PKCδ promoter reporter constructs used in this study have been extensively described (see Chapter II). To construct Sp1-luc consisting of three consensus Sp1 binding sites from the SV40 promoter and its mutant plasmid mSp1-luc, complementary oligonucleotides (for Sp1-luc: sense, 5'-ATATATCTCGAGCGCGTGGGCGGAACTGGGC GGAGTTAGGGGCGGGAAAGCTTATATAT-3', antisense, 5'-ATATATAAGCTTTCCC GCCCCTAACTCCGCCCAGTTCCGCCCACGCGCTCGAGATATAT-3'; for mSp1-luc: sense, 5'-ATATATCTCGAGCGCGTGTTTTGAACTGTTTTGAGTTAGGTTTTGGAAAG CTTATATAT-3', antisense, 5'-ATATATAAGCTTTCCAAAACCTAACTCAAAACAGT TCAAAACACGCGCTCGAGATATAT-3') were synthesized, annealed, and cloned into the XhoI and HindIII sites of pGL3-Basic.

The constructs for mammalian expression pN3-Sp1, pN3-Sp4, and pN3-Sp3 encoding both long and short isoforms of Sp3 (Sapetschnig et al., 2004), as well as the "empty" control vectors pN3 were generously provided by Dr. G. Suske (Philipps-Universität Marburg, Germany). To generate the expression vectors for dominant negative forms Sp1 (amino acid

603-785) and Sp3 (amino acid 540-781), pN3-DN-Sp1 and pN3-DN-Sp3, the appropriate cDNA fragments were PCR-generated from pN3-Sp1 and pN3-Sp3 with the following primer pairs, respectively. For pN3-DN-Sp1, forward, 5'-ATATATCTCGAGACCATG GCATGCACCTGCCCCTACT-3', reverse, 5'-ATATATAAGCTTTCAATGGTGATGGTG ATGATGGAAGCCATTGCCACTGAT-3'; for pN3-DN-Sp3, forward, 5'-ATATATCTCG AGACCATGGAGAATGCTGACAGTCCTG-3', reverse, 5'-ATATATAAGCTTTCAATG GTGATGGTGATGATGCTCCATTGTCTCATTTCC-3'. The PCR products were then subcloned into the pN3 vector. The p300 wild-type expression plasmid pCl-p300 and its histone acetyltransferase (HAT) deletion mutant, pCl-p300ΔHAT, were kindly provided by Dr. Joan Boyes (Institute of Cancer Research, London, United Kingdom) and generated as described previously (Boyes et al., 1998), and the empty vector pCIneo was a gift from Dr. Christian Seiser (University of Vienna, Austria). The expression plasmid pcDNA3-CBP was a gift from Dr. Xiang-Jiao Yang (Yang et al., 1996). The expression vectors for HDAC1 (pcDNA3-Myc-His-HDAC1), HDAC4 (pcDNA3-Myc-His-HDAC4), and the empty vector pcDNA3-Myc-His were generously provided by Dr. Tony Kouzarides (Miska et al., 1999). Dr. Saadi Khochbin kindly provided the expression vectors for HDAC5 (pcDNA3-HA-HDAC5) and HDAC7 (pcDNA3-HA-HDAC7) (Lemercier et al., 2002). The Gal4 fusion constructs pM-Sp1 and pM-Sp3, as well as the Gal4-dependent reporter construct pG5-luc containing five Gal4 DNA binding sites, were gifts from Dr. Toshiyuki Sakai (Sowa et al., 1999), and the empty vector pM was kindly provided by Dr. Bruce Paterson (National Cancer Institute). To construct the Gal4 DNA-binding domain fused Sp1 or Sp3 truncated mutants, Gal4-Sp1N (83-785), Gal4-Sp1AB (83-494), Gal4-Sp1ABS/T (83-351), Gal4-Sp1A (83-251), Gal4-Sp1AS/T (83-145), Gal4-Sp1AQ

(146-251), Gal4-Sp1B (252-494), Gal4-Sp1BQ (352-494), Gal4-DN-Sp1 (603-785), Gal4-Sp3N (1-612), Gal4-Sp3AB (1-499), Gal4-Sp3ABS/T (1-371), Gal4-Sp3A (1-251), Gal4-Sp3AQ (81-251), Gal4-Sp3 (1-80), Gal4-Sp3B (252-499), Gal4-Sp3BQ (372-499), and Gal4-DN-Sp3 (540-781), the appropriate cDNA fragments were PCR-generated from pN3-Sp1 and pN3-Sp3 and cloned into the pM vector. All construction sequences were confirmed by DNA sequencing.

Animal experiments

Six- to eight-week-old C57B1/6 male mice were housed in a temperature-controlled and 12:12 h light/dark room, and were allowed free access to food and water. NaBu was dissolved in sterile saline and administered to C57B1/6 mice by IP injection at a dose of 1.2 g/kg for 6-24 h. An equal volume of saline was given to control animals. Mice were then sacrificed and the brain areas of interest were immediately and carefully dissected out and stored at -80°C. Animal care procedures strictly followed the NIH Guide for the Care and Use of Laboratory Animals and were approved by the Iowa State University IACUC.

Mouse striatal and nigral neurons in primary culture and treatment

Plates (6-well for striatal neurons and 12-well for nigral neurons) were coated overnight with 0.1 mg/ml poly-D-lysine. Striatal or substantia nigral tissue was dissected from gestational 16- to 18-day-old mice embryos and kept in ice-cold Ca^{2+}-free Hank's balanced salt solution. Cells were then dissociated in Hank's balanced salt solution containing trypsin-0.25% EDTA for 30 min at 37 °C. After enzyme inhibition with 10% heat-inactivated fetal bovine serum in Dulbecco's modified Eagle's medium, the cells were

suspended in Neurobasal medium supplemented with 2% Neurobasal supplement (B27), 500 μM L-glutamine, 100 IU/ml penicillin, and 100 μg/ml streptomycin, plated at 2×10^6 cells in 2 ml/well and incubated in a humidified CO_2 incubator (5% CO_2 and 37 °C). Half of the culture medium was replaced every 2 days, and experiments were conducted using 6 and 7 days-old cultures. After exposure to various doses of HDAC inhibitors (NaBu, VPA, Scriptaid, TSA, or apicidin) for 24-48 h, the primary cultures were collected for Western blot or real-time RT-PCR analysis.

Cell lines, Transient transfections, and Reporter gene assays

Mouse neuroblastoma NIE115 and mouse dopaminergic MN9D cells were cultured in Dulbecco's modified Eagle's medium supplemented with 10% fetal bovine serum (FBS), 2 mM L-glutamine, 50 units penicillin, and 50 units streptomycin (37 °C/5% CO2).

Transient transfections of NIE115 and MN9D cells were performed using Lipofectamine 2000 reagent according to the manufacturers' instructions. Cells were plated at 0.3 × 106 cells/well in six-well plates one day before transfection. Each transfection was performed with 4 μg of reporter constructs. Cells were harvested at 24 h post-transfection, lysed in 200 μl of Reporter Lysis Buffer (Promega), and assayed for luciferase activity. For cotransfection assays, various amounts of expression plasmid as indicated in figure were added to the reporter plasmids. The total amount of DNA was adjusted by adding empty vector. In HDAC inhibitors treatment experiments, indicated doses of HDAC inhibitors were added 24 h after DNA transfection, and cells were collected at designated time points and assayed for luciferase activity.

Luciferase activity was measured on a Synergy 2 Multi-Mode Microplate Reader (BioTek, Winooski, VT) using the Luciferase Assay system (Promega). The ratio of luciferase activity to total amount of proteins was used as a measure of normalized luciferase activity.

Quantitative real-time RT-PCR

Total RNA was isolated from fresh cell pellets using the Absolutely RNA Miniprep kit (Stratagene, La Jolla, CA). First strand cDNA was synthesized using an AffinityScript QPCR cDNA Synthesis kit (Stratagene). Real-time PCR was performed in an Mx3000P QPCR system (Stratagene) using the Brilliant SYBR Green QPCR Master Mix kit (Stratagene), with cDNAs corresponding to 150 ng of total RNA, 12.5 μl of 2 × master mix, 0.375 μl of reference dye, and 0.2 μM of each primer in a 25-μl final reaction volume. All reactions were performed in triplicate. The sequences for PKCδ primers are: forward, 5'-TCTGGGAGTGACATCCTAGACAACAACGGG-3', and reverse, 5'-CAGATGATCTC AGCTGCATAAAACGTAGCC-3'. β-actin was used as internal standard with the primer set purchased from Qiagen (QuantiTect Primers, catalog number QT01136772). The PCR cycling conditions contained an initial denaturation at 95 °C for 10 min, followed by 40 cycles of denaturation at 95 °C for 30 sec, annealing at 60 °C for 30 sec, and extension at 72°C for 30 sec. Fluorescence was detected during the annealing step of each cycle. Dissociation curves were run to verify the singularity of the PCR product. The data were analyzed using the comparative threshold cycle (Ct) method (Livak and Schmittgen, 2001).

Acid extraction of histone

Acid extraction of histones was performed as described previously (Zhu et al., 2001), with modifications. Briefly, fresh cell pellets were suspended with five volumes of lysis buffer (10 mM HEPES, pH 7.9, 1.5 mM MgCl2, 10 mM KCl, 1 × halt protease inhibitor cocktails) and hydrochloride acid at a final concentration of 0.2 M and subsequently lysed on ice for 30 min. After centrifugation at 11,000 × g for 10 min at 4 °C, the histone mixtures were collected from the supernatant.

Immunoblotting

Cell lysates and brain homogenates were prepared as previously described (Zhang et al., 2007c). Immunoblotting was performed as previously described (Kanthasamy et al., 2006). Briefly, the samples containing equal amounts of protein were fractionated through a 7.5% SDS-PAGE and transferred onto a nitrocellulose membrane (Bio-Rad Laboratories, Hercules, CA). Membranes were blotted with the appropriate primary antibody and developed with either IRDye 800 anti-rabbit or Alexa Fluor 680 anti-mouse secondary antibodies. The immunoblot imaging was performed with an Odyssey Infrared Imaging system (Li-cor, Lincoln, NE).

Chromatin immunoprecipitation (ChIP)

ChIP assays were conducted with chromatin isolated from NIE115 cells using the ChIP-IT Express Enzymatic kit from Active Motif according to the manufacturer's instructions with slight modifications. Briefly, after cross-linking, the nuclei were prepared and subjected to enzymatic digestion to generate chromatin fragments between 200 to 1500

bp. The sheared chromatin was collected by centrifugation, and a 10-µl aliquot was removed to serve as a positive input sample. Aliquots of 70-µl sheared chromatin were immunoprecipitated with 3 µg pan-acetyl Histone H4 antibody (Active Motif) and protein-G magnetic beads. Equal aliquots of each chromatin sample were saved for no-antibody controls. The immunoprecipitated DNA was analyzed by PCR to amplify a region (+2 to +289) within the PKCδ promoter. Primers for amplification are: forward, 5'-ATATATCTCGAGTCCTGGGCTCCATTGTGTGTG-3', and reverse, 5'-GTCTATAAG CTTACCTCACCCAGGTGCCGG-3'. Conditions of linear amplification were determined empirically for these primers. PCR conditions are as follows: 94°C 3 min; 94°C 30 sec, 59°C 30 sec, and 68°C 30 sec for 35 cycles. PCR products were resolved by electrophoresis in a 1.2% agarose gel and visualized after ethidium bromide staining.

DNA affinity precipitation assay (DAPA)

Nuclear and cytoplasmic proteins were prepared using the NE-PER nuclear and cytoplasmic extraction kit (Thermo Scientific, Waltham, MA). 5'-biotinylated oligonucleotides corresponding to the sequence between +204 and +238 of the PKCδ promoter were synthesized by Integrated DNA Technologies (Coralville, IA) and annealed. Twenty pmol of oligos was incubated with 100 µg of Dynabeads M-280 (Dynal Biotech, Oslo, Norway) in B&W buffer at room temperature for 10 min. Un-conjugated DNA was washed off with a magnetic particle concentrator (Dynal Biotech). After block by 0.5% BSA in TGED buffer (20 mM HEPES, pH 7.9, 1 mM EDTA, 10% glycerol, 0.01% TritonX-100) at 4 °C for 2 h, the DNA-conjugated beads were incubated with 350 µg of nuclear extracts from NIE115 cells treated with or without 1 mM NaBu for 4 h at 4 °C. After extensive wash

with TGED buffer, the beads were eluted with 50 µl of 2x SDS loading buffer. Complexing proteins were resolved on a 7.5% SDS-PAGE gel and examined by immunoblotting with polyclonal anti-Sp3 and -Sp4 antibodies.

Statistical analysis

Unless otherwise stated, all data were determined from three independent experiments, each done in triplicate, and expressed as average values ± SEM. All statistical analyses were performed using the GraphPad Prism 4.0 software (GraphPad Software, San Diego, CA). One-way analysis of variance (ANOVA test) followed by the Tukey multiple comparison tests was used for statistical comparisons, and differences were considered significant if *P*-values less than 0.05 were obtained.

Results

PKCδ mRNA and protein levels are increased by exposure to HDAC inhibitors *in vivo* and *in vitro*

In the first set of experiments we assessed the effect of HDAC inhibition on the production of PKCδ protein in a variety of primary and cultured cells. As shown in Fig. 1A, treatment with 1 mM NaBu significantly increased the levels of total PKCδ protein in primary mouse nigral (left panel) and striatal (right panel) neurons following 24-48 h drug exposure. Induction of PKCδ levels by NaBu was accompanied by a time-dependent increase in cleaved products of PKCδ. Because butyrate has several effects that may not be due to inhibition of HDAC (Marks et al., 2003), we further examined whether other HDAC

inhibitors had similar effects on PKCδ protein expression. For this, we exposed striatal neurons to increasing concentrations of multiple HDAC inhibitors for 48 h, and PKCδ protein levels were determined by Western blot analysis. As observed with NaBu, a dose-dependent induction of both native and cleaved PKCδ protein was observed in cells treated with VPA, another short-chain fatty acid (Fig. 1B). Scriptaid, which is structurally unrelated to NaBu, also increased total PKCδ levels in the dose range tested (Fig. 1C), whereas induction of PKCδ proteolytic cleavage was only observed at a lower dose (1.23 μM). In addition, PKCδ levels were also significantly up-regulated after treatment of striatal neurons with a lower dose (100 nM) of TSA or apicidin, two other structurally unrelated HDAC inhibitors; however, detectable proteolytic activation of PKCδ was not observed following any of the doses (Fig. 1D-E). Analysis of mouse neuroblastoma NIE115 cells demonstrated that PKCδ protein levels were also elevated up to ~2-fold at 48 h NaBu (1 mM) treatment compared with the untreated cells (Fig. 1F).

We then asked whether the effect of HDAC inhibitors on PKCδ protein expression was exerted at the transcriptional level. Dose-response and time-course studies were performed and PKCδ mRNA levels were analyzed using a real-time RT-PCR approach. As shown in Fig. 2A, exposure of primary nigral (left panel) and striatal (right panel) cultures to 1 mM of NaBu for 24 or 48 h potently increased PKCδ mRNA expression. The magnitude of the inductions varied from 4- to 6-fold relative to untreated cells. Furthermore, when nigral and striatal cells were administered increasing concentrations of NaBu (0.2-5 mM) for 24 h, a dose-dependent induction of PKCδ mRNA, with a maximal effect at 1 mM, was found (Fig. 2B). In addition, similar induction of endogenous PKCδ mRNA by NaBu treatment was also

observed in both NIE115 and mouse dopaminergic MN9D cells (Fig. 2C). The maximal increase of approximately 3-fold was induced by a 48 h sodium butyrate treatment.

To further address whether the effect of HDAC inhibition on PKCδ expression observed above reflects the regulation of PKCδ expression *in vivo*, C57B1/6 mice were administered 1.2 g/kg body weight of NaBu *via* intraperitoneal injection, and the levels of PKCδ in brain at various time points (6-24 h) after injection were determined by Western blot analysis. As shown in Fig. 3A, in the mouse substantia nigra there was a time-dependent upregulation of PKCδ protein, with a maximal 3-fold increase achieved at 24 h after drug injection, whereas TH and actin levels remained unchanged under these conditions. Furthermore, the striatal regions exhibited a similar trend for increased PKCδ protein following NaBu exposure (Fig. 3B). Overall, these data clearly demonstrate a close correlation between HDAC inhibition and PKCδ gene expression *in vivo* and *in vitro*, and suggest that NIE115 and MN9D mouse neuronal cells are relevant model systems to analyze the regulation of PKCδ expression by HDAC inhibition.

Butyrate induces hyperacetylation of histone H4 associated with the PKCδ promoter

Because butyrate inhibits the activity of most HDAC isoforms, we next examined whether the induction of PKCδ expression by NaBu was correlated with a specific change in the histone acetylation of the PKCδ gene promoter. First, the effects of HDAC inhibition by NaBu on global levels of histone acetylation were analyzed. As shown in Fig. 4A, the global levels of histone H3 and H4 acetylation in NIE115 cells were significantly increased after treatment with NaBu, whereas total histone H3 levels were not changed. Next, to further examine whether the change in PKCδ expression occurs directly through chromatin

remodeling, we performed a ChIP assay using chromatin isolated from NIE115 cells and the antibody specific for hyperacetylated histone H4. The results show that exposure of NIE115 cells to 1 mM NaBu resulted in a dramatic enrichment of histone H4 acetylation at the PKCδ promoter. Taken together, these data indicate that chromatin remodeling is at least partly responsible for the transcriptional activation of the PKCδ gene after NaBu treatment.

HDAC inhibition activates PKCδ promoter transcription: delineation of the sodium butyrate responsive elements on PKCδ promoter

To further examine whether the induction of PKCδ transcription by HDAC inhibition was mediated directly by activating the PKCδ promoter, the effects of HDAC inhibitors on PKCδ promoter activity were determined in a luciferase reporter construct-based transient transfection assay. Our previously cloned mouse PKCδ promoter/luciferase reporter construct pGL3-1694/+289, which contains 1694 bp of the 5' flanking sequences and 289 bp of non-coding exon 1 (access number GU182370), or pGL3-Basic empty vector was transfected into NIE115 and MN9D cells. Transfected cells were incubated with increasing concentrations of NaBu (0.2 to 1 mM) for 24 h. As shown in Fig. 5A, the addition of NaBu significantly increased the luciferase activity of pGL3-1694/+289 in a dose-dependent manner up to an average ~5-fold in MN9D (left panel) and NIE115 (right panel) cells, whereas pGL3-Basic control was unchanged, indicating the stimulatory effect of NaBu on the PKCδ promoter is specific. Furthermore, VPA, TSA, scriptaid, or apicidin treatments for 24 h in MN9D cells caused a more robust activation of PKCδ promoter activity than NaBu (Fig. S1). Maximum activation for those HDAC inhibitors ranged from 8- to 14- fold compared to the untreated cells (Fig. S1).

The regulation of PKCδ promoter activity by HDAC inhibition was further confirmed by cotransfection with the pGL3-1694/+289 promoter construct and expression vectors for multiple HDAC isoforms (HDAC 1, 4, 5, and 7) under either basal or butyrate-stimulated conditions. As shown in Fig. 5B, compared to empty vector (EV) transfected cells, ectopic expression of all four HDAC proteins led to a significant inhibition of basal PKCδ promoter activity in both NIE115 and MN9D cells, with HDAC4 and HDAC5 being the most potent repressors (~60% and 80% repression for HDAC4 and HDAC5, respectively). Furthermore, butyrate-induced activation of PKCδ promoter activity was also significantly inhibited by expressing various amounts HDAC1, HDAC4, or HDAC5 in MN9D cells (Fig. 5C, left panel), while butyrate stimulation of the PKCδ promoter after ectopic expression of HDAC7 was minimal. Similar inhibition of butyrate induction of PKCδ promoter activity by overexpressing HDACs was also found in NIE115 cells (Fig. 5C, right panel). Efficient overexpression of these HDACs was verified by Western blot analysis (data not shown). Taken together, these results indicate that NaBu up-regulates PKCδ gene transcription through PKCδ promoter interactions, and suggest that multiple HDACs are involved in regulation of basal PKCδ promoter transcription and in mediating the NaBu response.

To elucidate the mechanism underlying the activation of the PKCδ promoter by NaBu, we first delineated the regions of the PKCδ promoter that respond to butyrate. A series of truncated promoter constructs in -1694/+289 region were analyzed by transient transfection for their response to NaBu treatment in MN9D and NIE115 cells. As shown in Fig. 6A-B, in MN9D cells, luciferase activities from the promoter reporter construct pGL3-147/+289 as well as the pGL3+2/+289 plasmid were strongly stimulated up to 3.9- and

4.2-fold by NaBu, levels comparable to that obtained from the full-size promoter (pGL3-1694/+289). On the other hand, absence of the +2 to +289 sequences led to a significant loss of butyrate responsiveness. Furthermore, similar results were found in NIE115 cells (Fig. 6C). Thus, this preliminary mapping suggests that the major NaBu-responsive elements are located within the +2/+289 region. We therefore focused our follow-up efforts on this region.

Sodium butyrate stimulates PKCδ promoter activity through four GC-box elements

In a previous study, we extensively characterized the mouse PKCδ promoter, and we found that the region between +2 and +289 is GC rich, and contains multiple Sp binding sites, including four consecutive GC boxes designated GC(1) to GC(4) within ~250 bp downstream of the TSS, as well as a CACCC box located at position +35 bp downstream of the TSS (Fig. 7A). Our results also revealed that those Sp sites act as crucial *cis*-elements regulating the basal PKCδ transcription in neuronal cells. To determine whether these Sp sites are involved in the butyrate-induced activation of the PKCδ promoter, we performed site-directed mutagenesis of these sites in the context of pGL3-147/+209 and pGL3+165/+289 constructs. The former possesses the proximal CACCC site, whereas in the latter, only the four GC boxes are present (Fig.7A). Those mutated and wild-type reporter plasmids were used and assayed for luciferase activity following NaBu treatment. As shown in Fig. 7B, exposure to NaBu did not activate luciferase activity of the wild-type pGL3-147/+209, and even reduced its activity in MN9D cells, suggesting that the CACCC site is not involved in the activation by butyrate. Indeed, mutation of the CACCC site (mCACCC) did not diminish the NaBu responsiveness; rather it slightly increased the

responsiveness to NaBu compared to that of wild-type. On the other hand, NaBu significantly activated the luciferase activity of wild-type pGL3+165/+289 up to 3.4- and 4.7-fold in MN9D and NIE115 cells, respectively (Fig. 7C-D). These findings also indicate a minimal 81 bp NaBu-responsive promoter region from +209 to +289. Alteration of the most distal GC(4) or GC(3) site reduced the NaBu responsiveness by 15% and 24%, respectively, compared with that of wild-type pGL3+165/+289 in MN9D cells (Fig. 7C). In contrast, mutation of either the proximal GC(2) box or GC(1) box caused major decrements in response to NaBu, resulting in about 35% and 33% elimination compared to that of wild-type. Furthermore, triple mutants, mGC123, mGC124, mGC134, or mGC134, in which only site GC(4), GC(3), GC(2), or GC(1) is still active, respectively, all resulted in a complete loss of NaBu-induced promoter activity in both cells (Fig. 7D), suggesting that cooperative interactions among the different GC sites are required to mediate the transactivation effect on the PKCδ promoter by NaBu. Taken together, these data suggest that GC(1) and GC(2) sites, and less significantly, GC(3) and GC(4) sites, rather than CACCC site, are the main NaBu-responsive elements, and that, in addition, these GC boxes cooperate in an additive manner in mediating the NaBu response.

To confirm further that Sp sites indeed mediate the transcriptional activation by NaBu, we generated a Sp1 reporter construct (Sp1-luc), composed of SV40 promoter-derived three consensus Sp1 binding elements inserted into the promoter-less luciferase reporter vector (pGL3-Basic). The effects of NaBu on its transcriptional activity were examined in transient transfection studies performed in MN9D and NIE115 cells. As shown in Fig. 7D, the luciferase activities of Sp1-luc were significantly elevated following NaBu exposure (up to ~4.0- and 5.0-fold activation in MN9D and NIE115 cells, respectively), whereas mutations

of all Sp1 consensus binding sites (mSp1-luc) completely abolished the NaBu-induced transcriptional activation. Furthermore, ectopic expression of HDAC isoforms led to dramatic inhibition of both basal and NaBu-induced promoter activity of Sp1-luc (Fig. S2).

Sp family proteins are required for mediating sodium butyrate induction of PKCδ expression

We demonstrated previously that Sp families of transcription factors (Sp1, Sp3, and Sp4) can transactivate PKCδ transcription through specific interaction with the multiple GC-box elements present in the non-coding exon 1 region of PKCδ promoter, with Sp3 being the most robust activator. These findings led to a hypothesis that the NaBu-induced transcriptional activation of PKCδ might be mediated by Sp transcriptional factors. To test this possibility, we analyzed the functional impact of ectopic expression of Sp proteins on the NaBu-induced transcriptional activation in transient transfections. The PKCδ promoter reporter construct pGL3-147/+289, as illustrated in Fig. 6-7, was cotransfected into NIE115 cells along with 4 μg of expression vectors for Sp family proteins (pN3-Sp1, pN3-Sp3, and pN3-Sp4) or a control empty vector (pN3) in the presence or absence of 1 mM NaBu for 24 h. All of these Sp expression vectors have been shown to express stable proteins in both NIE115 and MN9D cells (see Chapter II). In accordance with butyrate induction of PKCδ promoter activity, as shown in Fig. 5-6, exposure of the empty vector-transfected cells to NaBu displayed ~4.5-fold activation of the pGL3-147/+289 reporter, whereas in the absence of NaBu, overexpression of Sp3 alone led to ~2.5-fold activation (Fig. 8A). Importantly, a high level of synergistic transactivation of the promoter activity up to ~11.5-fold was seen

when cells overexpressing Sp3 protein were treated with NaBu. A similar synergistic transactivation effect was also found in Sp1- and Sp4-transfected cells after 24 h of incubation with NaBu (Fig. 8A). These findings clearly indicate that activation of PKCδ promoter by NaBu is mediated by the Sp family of transcription factors. In addition, parallel transfection studies with NIE115 cells with two different amounts of expression vector for wild-type or dominant-negative mutant Sp1/Sp3 were performed to confirm the effects of Sp proteins on NaBu transactivation (Fig. 8B). In these experiments, ectopic expression of wild-type Sp1 or Sp3 caused a dose-dependent increase in the NaBu-induced enhancement of the PKCδ promoter activity. In contrast, expression of a dominant-negative construct pN3-DN-Sp1 or pN3-DN-Sp3, which both have an intact DNA binding domain but lack the complete transactivation domains of Sp1/3, had no effect on the NaBu-mediated induction of PKCδ promoter activity. Interestingly, even the highest dose of these mutant constructs did not affect the basal PKCδ promoter activity.

To corroborate the observed effect of ectopic expression of Sp family proteins on NaBu transactivation of the PKCδ promoter, different types of known Sp specific inhibitors were employed to test whether they can block the induction of PKCδ promoter activity by NaBu. As shown in Fig. 8C, NaBu-induced transactivation of the PKCδ promoter was significantly compromised by pretreatment with mithramycin A, an aureolic antibiotic that is known to bind to the GC-rich motif and selectively inhibit Sp transcription factor binding (Ray et al., 1989; Blume et al., 1991), in a dose-dependent manner. Furthermore, tolfenamic acid, which has been shown to induce Sp protein degradation (Konduri et al., 2009), also inhibited the NaBu transactivation in a dose-dependent manner (Fig. S3).

Sodium butyrate enhances the transactivational activity of Sp proteins

To further investigate the mechanisms underlying the stimulation of PKCδ promoter activity by NaBu, we first determined whether NaBu affects the protein levels of Sp effectors. Previously, we showed that Sp3 and Sp4 are endogenously expressed at appreciable levels in both MN9D and NIE115 cells, but the expression of endogenous Sp1 was not detected in these cells; therefore, in the present study, the effect of NaBu on the expression of Sp3 was examined. As shown in Fig. 9A, the protein levels of Sp3 were not changed following NaBu treatment. We next examined the possibility that NaBu might stimulate PKCδ transcription by elevating the binding of Sp proteins to the PKCδ promoter. DNA affinity protein binding assays (DAPA), using a biotin-labeled oligonucleotide spanning the GC (1) and GC (2) elements between positions +204 and +238 on the PKCδ promoter and nuclear extracts from NIE115 cells, were performed. The association of Sp3 with this oligonucleotide was unaltered after incubation with NaBu (Fig. 9B). These findings indicate that stimulation by NaBu resulted from a mechanism other than alteration of Sp protein levels or DNA binding. We then evaluated whether NaBu could directly increase the transactivating potential of Sp proteins. To test this possibility, we utilized a one-hybrid system, in which Sp1 or Sp3 is fused to the DNA-binding domain of the yeast transcription factor Gal4, and the effects of NaBu on the activity of these chimeric proteins were assayed in MN9D and NIE115 cells using a reporter plasmid pG5-luc containing five Gal4 DNA binding sites. As shown in Fig. 9C, NaBu had a negligible effect on either the pG5-luc reporter alone or pG5-luc cotransfected with the empty control vector Gal4. In contrast, a huge stimulation of transactivation of Gal4-Sp1 or Gal4-Sp3 upon NaBu treatment was observed (12- and 18-fold in MN9D cells; 32- and 31-fold in NIE115 cells for Gal4-Sp3 and

Gal4-Sp1, respectively). However, the transactivation by NaBu was almost abolished when the chimeric proteins Gal4-Sp1DBD or Gal4-Sp3DBD lacking the Sp transactivation domains was used, suggesting the specificity of NaBu on Sp1/3 transactivational ability. It should be noted that under the basal condition, however, Gal4-Sp1 is a stronger activator than Gal4-Sp3. In addition, overexpression of HDAC4 or HDAC5 resulted in a significant reduction in butyrate-induced transactivation of Gal4-Sp1 or Gal4-Sp3, whereas minimal effects on the butyrate induction of Sp1/3 transactivational activity were found when HDAC1 or HDAC7 was overexpressed (Fig. 9D). Overall, these data indicate that NaBu specifically increases the transactivational capacity of Sp1/3 proteins, and that HDAC4 and HDAC5 might be involved in the regulation of Sp transcriptional activity by NaBu.

Characterization of domains of Sp1 and Sp3 for the mediation of responsiveness to sodium butyrate

Sp transcription factors (Sp1, Sp3 and Sp4) contain several conserved regions, which constitute two transactivation domains (A and B boxes) close to the C-terminus with regions rich in serine/threonine and glutamine residues, an extreme N-terminal transactivation domain (D box), an N-terminal DNA binding domain (zinc finger), and a domain of highly charged amino acids (C box) located directly N-terminal to the zinc finger. Additionally, Sp1 and Sp3 each possess an inhibitory domain (ID) located in the extreme N-terminus of Sp1 and near the C-terminus of Sp3, respectively. To identify the regions of Sp1/3 required for NaBu responsiveness, a series of truncated Gal4-Sp1 or Gal4-Sp3 expression constructs were generated and are depicted schematically in Fig. 10A and C. Similar to the above experiments, the ability of these chimeric proteins to transactivate pG5-luc activity in both

the presence and absence of NaBu was assayed in NIE115 cells. As shown in Fig. 10, the chimeras that retained the entire N-terminal part (A+B+C boxes) or A+B boxes of Sp1 or Sp3 displayed comparative capacities to activate transcription in response to NaBu in comparison with Gal4-Sp1 or Gal4-Sp3 full-length fusions. Interestingly, the Gal4-Sp3A+B chimera lacking the inhibitory domain located adjacent to zinc fingers even confers a higher NaBu responsiveness to the G5-luc reporter construct than that obtained following overexpression of Gal4-Sp3 full-length protein, suggesting that the inhibitory domain of Sp3 may have a negative regulatory action in mediating NaBu induction of the PKCδ promoter activity. Further analysis of the N-terminal region revealed that sequences within three subdomains, A^{Q}, $B^{S/T}$, and B^{Q}, which corresponds to amino acids Sp1 (146-494) and Sp3 (81-499), are essential to the transactivation by NaBu, as removal of any one of the three subdomains showed a significant decrease in their capacity to mediate the butyrate-induced transactivation. However, any of these subdomains alone were unable to render the G5-luc reporter construct NaBu responsiveness. Interestingly, the $A^{S/T}$ subdomain of Sp1 (83-145) appeared to have no effect on the ability of NaBu to enhance the transcription activity.

Ectopic expression of p300/CBP stimulates sodium butyrate-mediated transactivation of Sp1 and Sp3

Our previous studies revealed that both p300 and CBP function as coactivators for Sp transcription factors in transactivation of the PKCδ promoter *via* the Sp binding sites under basal conditions (see Chapter II). To investigate whether p300 or CBP are involved in the NaBu induction of PKCδ promoter activity, we performed co-transfection assays with expression vectors for p300 or CBP. As shown in Fig. 11A-B, the coexpression of CBP or

p300 significantly enhanced the NaBu-induced transactivation of Gal4-Sp1 and Gal4-Sp3 in a dose-dependent manner. Interestingly, we found that expression of a p300 mutant lacking HAT activity did not affect the NaBu-stimulated transcriptional activity of Gal4-Sp1 and Gal4-Sp3. These findings indicate a functional role for p300/CBP in the Sp-dependent transcription by NaBu.

Discussion

In this study we present evidence for a new model of mouse PKCδ transcriptional regulation by an epigenetic control mechanism involving HDAC inhibition *in vitro* and *in vivo*. We were particularly interested in these findings because PKCδ is a protein kinase critically involved in apoptotic signaling in various cell types. Indeed, considerable evidence supports the notion that activation of PKCδ *via* caspase-dependent proteolysis plays an essential role in oxidative stress-induced dopaminergic cell death in PD (Anantharam et al., 2002; Kaul et al., 2003). Lines of evidence have also demonstrated that the PKCδ specific inhibitor exhibits a neuroprotective effect in the MPTP mouse model (Zhang et al., 2007a). Given the prominent role of PKCδ in regulating multiple biological events, its expression must therefore be tightly regulated. Although a number of studies have documented the changes in PKCδ levels in response to multiple stimuli, the regulation of PKCδ gene expression at the transcriptional level is poorly understood. The PKCδ promoter lacks a TATA or TATA-like box and contains GC-rich sequences in the proximal promoter region (Kurkinen et al., 2000; Suh et al., 2003). Furthermore, we have extensively characterized the PKCδ promoter (see Chapter II), and we showed that a proximal 400 bp genomic fragment

(-147/+289) surrounding the transcription start site functions as a basal PKCδ promoter to sustain the basal expression of PKCδ in neurons. Further, we identified multiple functional TF binding sites contributing to basal PKCδ expression, including one for NFκB, and five for Sp family transcription factors. Here we designed experiments to determine whether HDAC inhibition has a regulatory role in PKCδ expression in neurons.

We initiated our study by evaluating the possible alterations in PKCδ levels after NaBu exposure in cells maintained *in vitro* and in primary striatal or nigral neurons. The results showed that PKCδ protein levels are dramatically increased in NaBu-exposed cells. Importantly, this induction of PKCδ also occurs in a mouse model following acute NaBu treatment. These novel findings expand the previous observations demonstrating that PKCδ is required for HDAC inhibitors-mediated gene activation (Kim et al., 2003; Kim et al., 2007). We also demonstrated that the up-regulation of PKCδ protein levels by NaBu correlates with an increase in PKCδ mRNA levels. Other structurally unrelated HDAC inhibitors, including apicidin, scriptaid, and TSA, also robustly induce PKCδ mRNA, suggesting that the ability of NaBu to induce PKCδ expression appears not to be due to the structural property of NaBu.

We next investigated the molecular mechanism underlying the NaBu-mediated PKCδ gene activation. Analysis of global histone acetylation levels suggests that NaBu significantly increased the cellular histone acetylation levels. Importantly, an increase in PKCδ promoter histone acetylation was observed after NaBu treatment. Thus, these results suggest that HDAC inhibitors mediate chromatin remolding by enhancing histone acetylation, which plays a role in the NaBu induction of PKCδ. To clarify whether the upregulation of PKCδ mRNA is accompanied by activation of the PKCδ promoter, we analyzed the PKCδ promoter

activity using a promoter region (-1494/+289) that we recently cloned (see Chapter II). Our results indicate that NaBu and other HDAC inhibitors significantly increase the luciferase activity of this reporter. Additional luciferase reporter assays using serial deletion PKCδ reporter constructs revealed that the major NaBu response elements reside in the 289 bp non-coding exon 1 region. The proximal region of the PKCδ promoter that confers the NaBu responsiveness is GC rich and contains multiple Sp binding sites, including one proximal CACCC box and four distal consecutive GC boxes. Previously, we showed that the CACCC box and the GC boxes act differentially in mediating the promoter activation by ectopic expression of Sp transcription factors (see Chapter II). Here, we performed experiments to determine the possible involvement of these Sp sites in the NaBu induction. Unexpectedly, a smaller construct, namely pGL3-147/+209, which possesses the upstream CACCC box but lacks the downstream GC boxes, was not activated by NaBu treatment; moreover, NaBu even caused a strong reduction in promoter activity in this promoter context (-147 to +209) in MN9D cells, suggesting that the CACCC box is not required for NaBu induction. Indeed, mutation of the CACCC box had no effect on NaBu-mediated activation of PKCδ promoter. On the other hand, using another small construct, pGL3+165/+289, we found that all GC boxes are required for full response to NaBu. Moreover, cooperative actions of different GC boxes are also required for mediating the NaBu response, since triple mutation of any three GC boxes completely diminished the NaBu responsiveness. Analysis using a luciferase reporter (Sp1-luc) containing three Sp1 consensus sequences further implicates the cluster of four GC boxes in NaBu-induced transcriptional control of the mouse PKCδ promoter.

The Sp family of transcription factors, Sp1, Sp3, and Sp4, are all structurally similar and bind to GC and GT/CACCC boxes found in a variety of promoter and enhancers through

three characteristic zinc fingers located at the C terminus of the proteins. Sp1 and Sp3 are ubiquitously expressed, whereas the expression of Sp4 is limited to brain (Suske, 1999; Suske et al., 2005). Recent studies have implicated GC-rich Sp1 biding sites in the regulation of a number of HDAC inhibitor regulated genes, including IN4K gene (Yokota et al., 2004), WAF1/Cip gene (Sowa et al., 1999; Han et al., 2001), HMG-CoA synthase gene (Camarero et al., 2003), and HSP70 gene (Marinova et al., 2009). Dissection of the mechanism of NaBu induction of the PKCδ gene revealed a dependence on the Sp proteins. First, the induction of PKCδ promoter activity by NaBu was dramatically enhanced by overexpression of Sp1, Sp3, or Sp4 protein. Exogenous Sp3 had the most potent effect, whereas Sp1 and Sp4 caused weaker activation, which is consistent with our observation that Sp3 is the strongest transactivator of the basal activity of the PKCδ promoter (see Chapter II). Next, we cloned a dominant-negative isoform of the Sp1 or Sp3 protein, which has an intact DNA binding domain but lacks the full transactivation domains. We showed that its ectopic expression did not cause further increase in the NaBu-mediated induction of the PKCδ promoter construct; it had only negligible effects on the basal level of PKCδ promoter activity. Finally, we used pharmacological inhibitors to block the Sp signaling pathways and assessed the effects on NaBu-stimulated PKCδ promoter activity. Fig. 8C shows that mithramycin A, an inhibitor of Sp-mediated transcriptional activation (Ray et al., 1989; Blume et al., 1991), directly blocks the induction of PKCδ promoter activity by NaBu. In addition, another Sp inhibitor, tolfenamic acid, which is known to induce degradation of Sp proteins (Konduri et al., 2009), also significantly diminishes the NaBu responsiveness. We therefore concluded that NaBu activates PKCδ transcription *via* Sp3, Sp1 and Sp4.

Although neither Sp3 level or direct association of Sp3 with the PKCδ promoter was affected by NaBu, NaBu treatment significantly stimulated Sp1- and Sp3-medated luciferase activity of the Gal4-luc reporter construct in one-hybrid assays. Sp1 and Sp3 contain multiple domains, including a zinc finger DNA binding domain and a bipartite transactivation domain composed of glutamine rich- and serine/threonine rich- regions. Using a serial Gal4-Sp1 or Gal4-Sp3 fusion chimeric, we were able to show that the increased transactivational potency of Sp1 and Sp3 by NaBu is specific to the transactivation domains of Sp1 and Sp3. Three subdomains, A^{Q}, $B^{S/T}$, and B^{Q} (amino acids from 146 to 494 in Sp1; amino acids from 81 to 499 for Sp3), are all required for NaBu-induced transcription from the PKCδ promoter. It remains unclear how transcriptional capacities of Sp1 and Sp3 are up-regulated by NaBu. Regulation of Sp1 and Sp3 activity is achieved by protein-protein interactions. Recent studies have revealed that both Sp1 and Sp3 functionally interact with HDAC1 and HDAC2 (Doetzlhofer et al., 1999; Sun et al., 2002; Won et al., 2002). HDACs act as transcriptional repressors and repress gene expression by forming complexes with several co-repressors, including mSin3A, SMRT, and N-CoR (Yang and Seto, 2007). In our experimental conditions, overexpression of HDAC4 and HDAC5 dramatically reduced the NaBu enhancement of transcriptional activity of Gal4-Sp1 and Gal4-Sp3, whereas HDAC1 and HDAC7 displayed much less inhibition. In parallel, multiple HDACs (HDAC1, -4, -5, and -7) overexpression represses PKCδ-specific promoter activity. These data suggest that deacetylases are involved in the transcriptional activation of Sp1/3 by NaBu, possibly through a protein-protein interaction or protein displacement in the PKCδ promoter. At present, we do not know which deacetylase isoform contributes to the NaBu regulation of the PKCδ promoter. In addition to HDACs, Sp1 and Sp3 also bind directly to co-activator p300

and its homolog CBP (Suzuki et al., 2000; Walker et al., 2001). Results from our studies indicate that ectopic expression of p300/CBP stimulated Gal4-Sp1 and Gal4-Sp3 dependent transcription in the presence of NaBu. Interestingly, the p300 stimulation is independent upon the HAT activity. These data suggest that the cooperative, possibly physical, interactions between Sp proteins and p300/CBP may represent a secondary mechanism responsible for the NaBu-stimulated transactivating activity of Sp1/3. The recruitment of p300/CBP into the transcription complex is also supported by our previous observation that transcription from PKCδ promoter is significantly activated by overexpression of p300/CBP (see Chapter II). Taken together, it seems likely that NaBu alters the transcriptional activities of Sp1 and Sp3 by inhibiting HDACs activity, disrupting the repressor complex containing HDACs, and allowing the recruitment of co-activators p300/CBP to the transcription complex bound to the GC-boxes on the PKCδ promoter.

In addition to protein-protein interactions, regulation of the activities of Sp proteins also includes post-translational modifications. For example, the post-translation modification to Sp1/Sp3 by acetylation stimulates their activity (Ammanamanchi et al., 2003; Hung et al., 2006), whereas sumoylation of Sp1/Sp3 causes their inactivation (Spengler and Brattain, 2006). Moreover, phosphorylation of Sp1 also mediates the activation of Sp-dependent transcription (Fojas de Borja et al., 2001). Although our preliminary results suggest that NaBu does not cause gross change in the amount of acetylation of Sp1/3, which is supported by our observation that transcriptional activation by NaBu is HAT independent, it remains to be examined whether HDAC inhibition modulates specific intracellular signaling pathways to affect the amount of phosphorylation or other modification of Sp or Sp-interacting proteins.

In summary, we demonstrate here for the first time that modulation of the HAT/HDAC balance by inhibiting HDAC activity induces pro-apoptotic PKCδ transcription in neurons. Moreover, induction of PKCδ is triggered by acetylation of histone proteins associated with the PKCδ promoter and subsequent enhancement of the transcriptional capacities of Sp transcription factors. We propose that such induction of pro-apoptotic PKCδ by HDAC inhibitors may represent a novel molecular basis for the neurodegenerative action of HDAC inhibitors.

Figure 1: Exposure to HDAC inhibitors increases PKCδ protein expression in primary neurons and in cell lines

A, Primary mouse nigral (*left*) and striatal (*right*) neurons were exposed to 1 mM sodium butyrate (NaBu) for 24 or 48 h, after which whole protein lysates were prepared and subjected to Western blot analysis of PKCδ and actin expression. A representative immunoblot is shown. ***B***-***E***, Primary mouse striatal neurons were exposed to the designated concentrations of HDAC inhibitors VPA (*B*), Scriptaid (*C*), TSA (*D*), or apicidin (*E*) for 48 h, after which protein lysates were prepared and analyzed for PKCδ and actin expression by immunoblot. Representative immunoblots are shown. ***F***, Left: Mouse neuroblastoma NIE115 cells were treated with 1 mM NaBu for 24 or 48 h, lysed, and analyzed by immunoblot for levels of PKCδ and actin. Right: Densitometric analysis. PKCδ bands were quantified and normalized to that of β-actin. Values are shown as mean ± SEM of two independent experiments (*$p<0.05$; between the control and NaBu-treated samples).

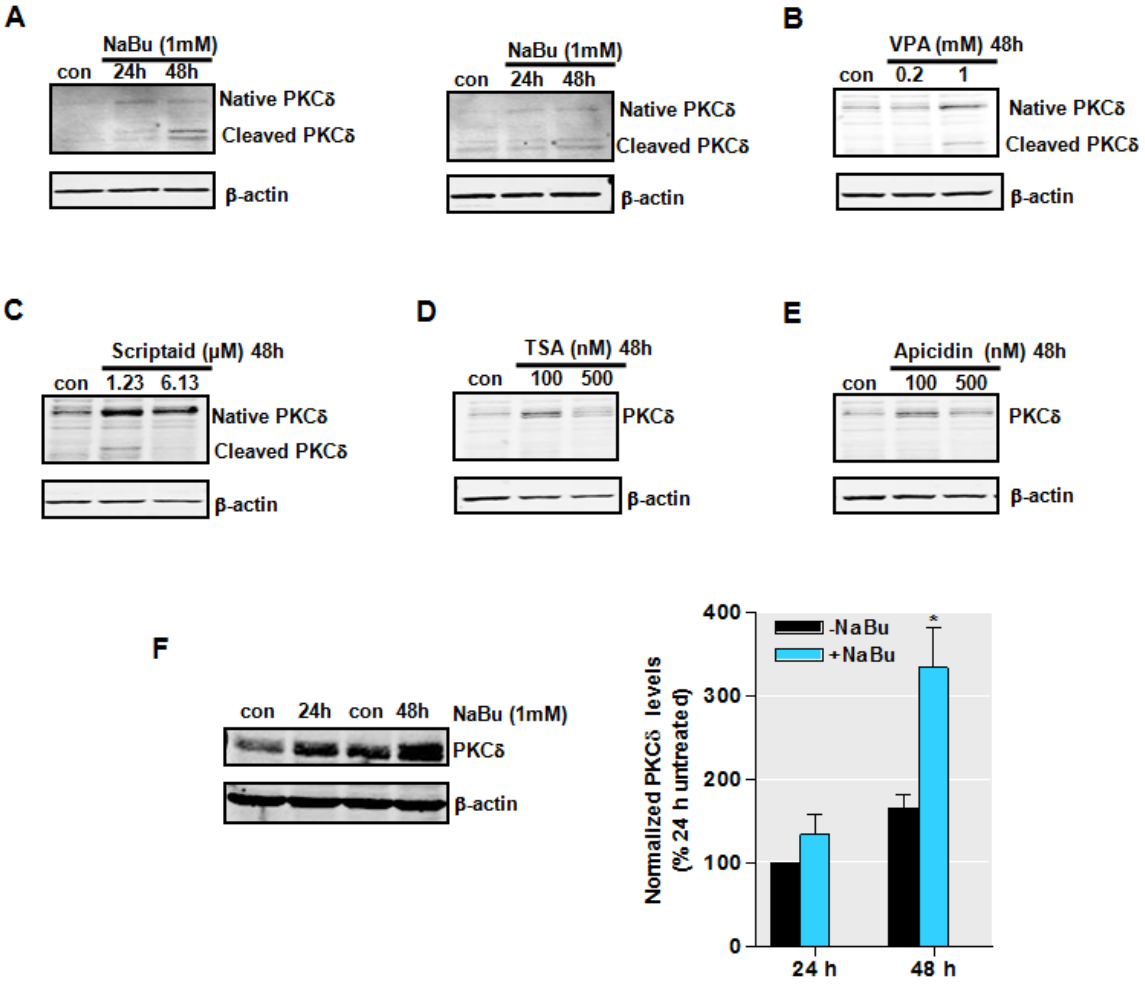

Figure 1

Figure 2: HDAC inhibition increases PKCδ mRNA expression

A*-*B, Primary mouse nigral (*left*) and striatal (*right*) neurons were exposed to 1 mM NaBu for 24 or 48 h (*A*) or to different concentrations of NaBu for 48 h (*B*). Real-time RT-PCR analysis of the PKCδ mRNA level was performed. β-actin mRNA level served as internal control. ***C***, NIE115 (*left*) and MN9D (*right*) cells were exposed to 1 mM NaBu for 24 or 48 h, and PKCδ mRNA expression was evaluated by real-time RT-PCR analysis. β-actin mRNA level served as internal control. All values are expressed as a percentage of the activity of control and represent the mean ± SEM of three independent experiments performed in triplicate (*, $p<0.05$; **, $p<0.01$; ***, $p<0.001$; compared with the control and NaBu-treated samples).

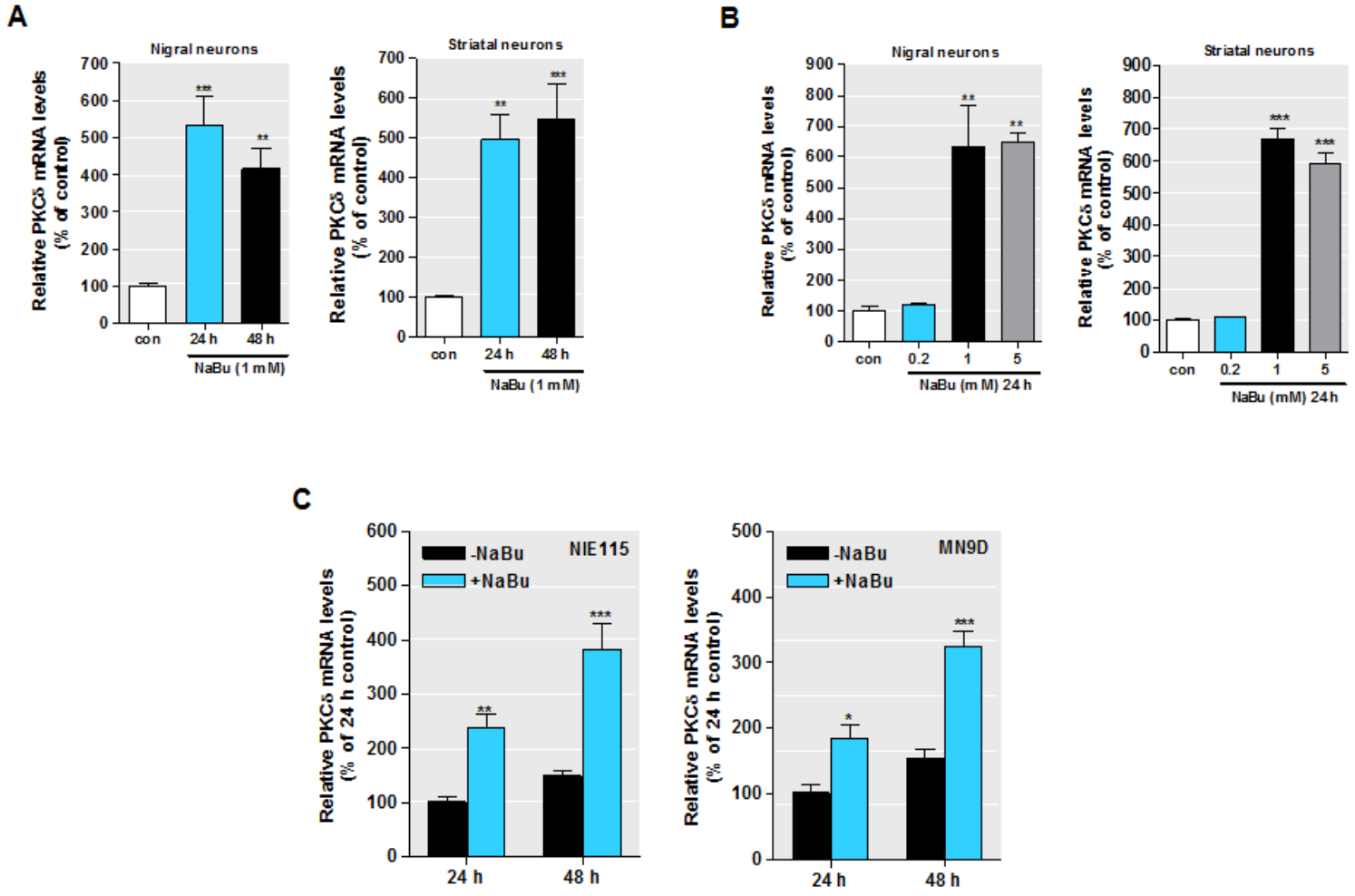

Figure 2

Figure 3: Effects of *in vivo* sodium butyrate injection on PKCδ protein level

A*-*B, C57 black mice were administered 1.2 g/kg NaBu or an equivalent volume of saline via intraperitoneal injection for 6-24 h. Substantia nigral (*A*) and striatum (*B*) tissues from each mouse were harvested and prepared and analyzed for PKCδ, TH, and actin expression by immunoblot. Top: Representative immunoblots are shown. Bottom: Quantitation data. The results are normalized to β-actin and expressed as a percentage of the untreated mice. All data are represented as mean ± SEM from six mice per group.

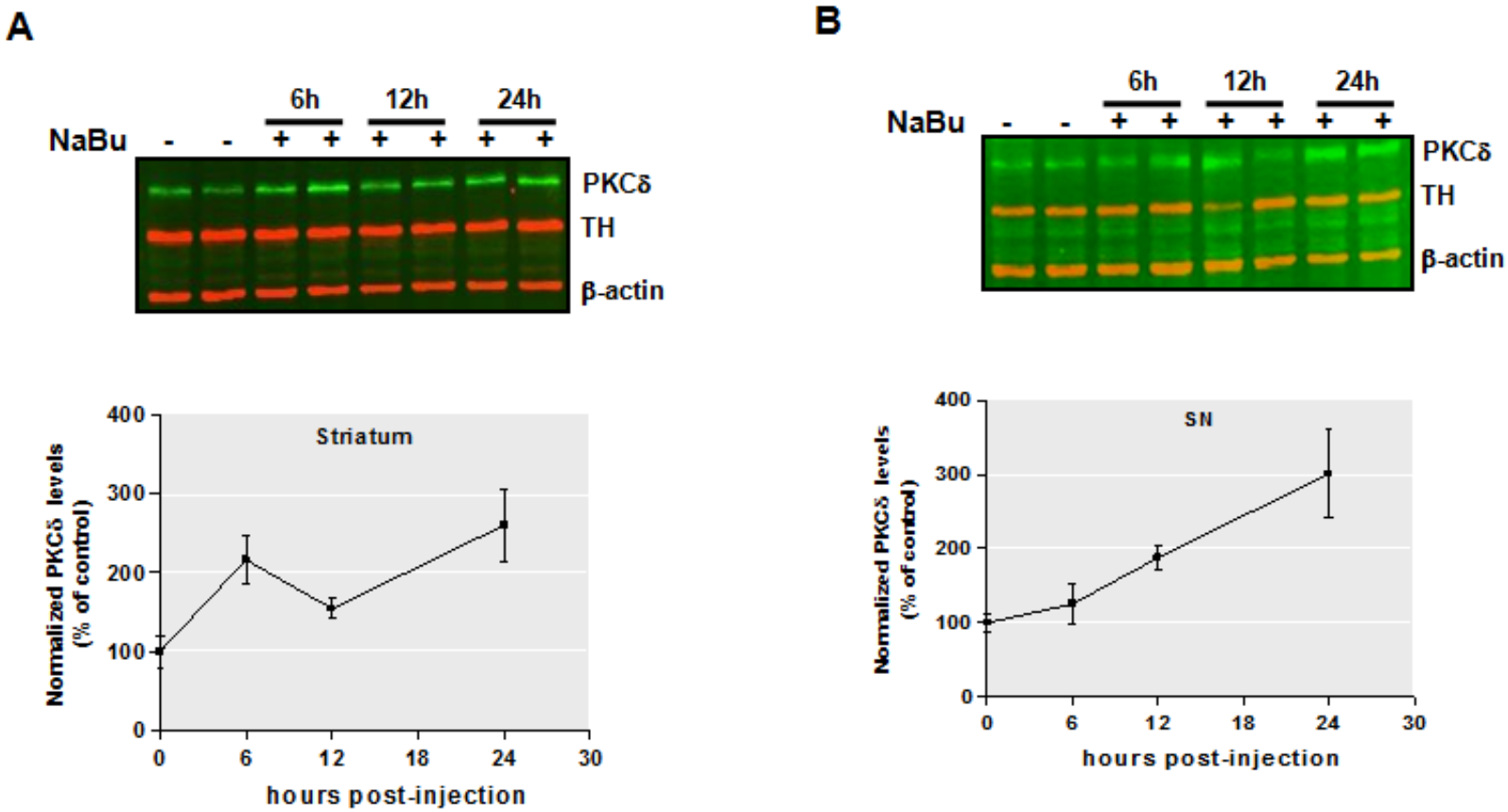

Figure 3

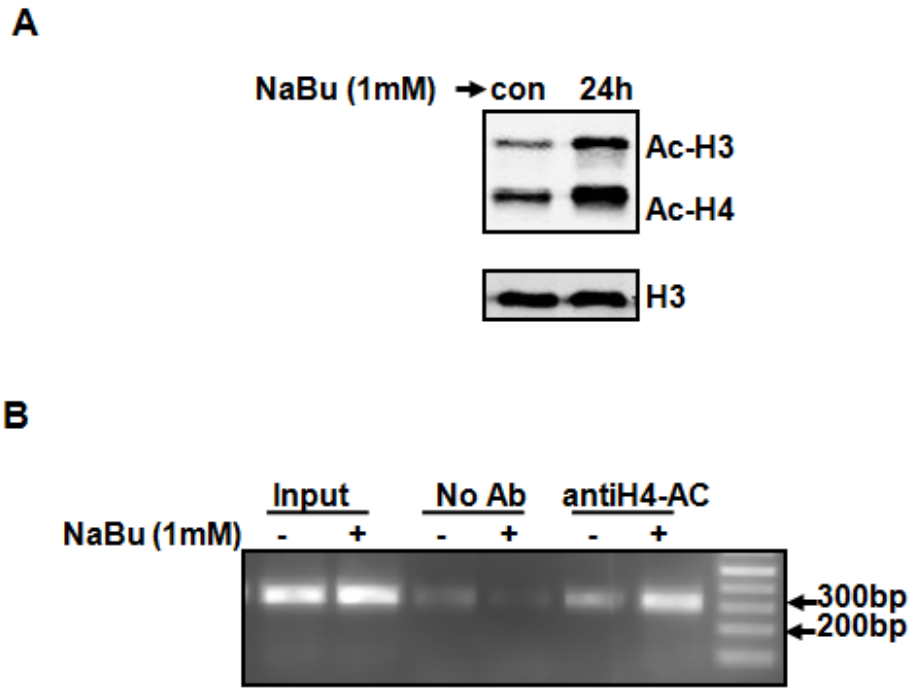

Figure 4: Sodium butyrate increases levels of total histone acetylation and histone acetylation of PKCδ promoter-associated chromatin

A, NIE115 cells were exposed to 1 mM NaBu for 24 h. Total histones were prepared for blotting with specific anti-acetyl-lysine and anti-H3 antibodies. A representative immunoblot is shown. ***B***, ChIP analysis of hyperacetylated histone H4 on PKCδ promoter. NIE115 cells were treated with 1 mM NaBu for 24 h, after which chromatin was prepared and sheared by enzymatic digestion. The sheared DNA was then immunoprecipitated with antibody against acetylated histone H4 or without antibody (No Ab). After reversal of cross-linking, immunoprecipitated DNA fragments were analyzed by PCR amplification with primers specific for the PKCδ promoter region that generates a 312-bp fragment. A representative gel electrophoresis is shown.

Figure 5: Regulation of PKCδ promoter activity by sodium butyrate treatment and ectopic expression of HDACs

A, PKCδ promoter activity is activated after treatment with NaBu. The PKCδ promoter reporter construct, pGL3-1694/+289 or empty vector pGL3-Basic, was transfected into MN9D (*left*) and NIE115 (*right*) cells. After 24 h transfection, the cells were incubated with or without NaBu at concentrations ranging from 0.2 to 1 mM for 24 h. Cells were then harvested and luciferase activities were determined and normalized by total cellular protein. Values are expressed as a percentage of the activity of pGL3-1694/+289-transfected control and represent the mean ± SEM of three independent experiments performed in triplicate (**, $p<0.01$; ***, $p<0.001$; between the control and NaBu-treated samples). ***B***, PKCδ promoter activity is repressed by ectopic expression of HDAC proteins in NIE115 (*black bar*) and MN9D (*blue bar*) cells. Cells were cotransfected with pGL3-1694/+289 and 8 µg of HDAC1, HDAC4, HDAC5, or HDAC7 expression vector or the empty vector control (EV). Luciferase activity was measured after 24 h of transfection and normalized by total cellular protein. Values are expressed as a percentage of the luciferase activity obtained from cells transfected with 8 µg of empty vector (*EV*) and represent the mean ± SEM of three independent experiments performed in triplicate (**, $p<0.01$; ***, $p<0.001$; between the EV- and HDACs-transfected samples). ***C***, Effects of ectopic expression of HDAC proteins on butyrate-induced PKCδ promoter activation. MN9D *(left)* and NIE115 (*right*) cells were cotransfected with pGL3-1694/+289 and increasing concentrations of HDAC1, HDAC4, HDAC5, or HDAC7 expression vector (from 2-8 µg) or the empty vector control (*EV*). After 12 h transfection, the cells were incubated with or without NaBu (1 mM) for 24 h. Cells were then harvested and luciferase activities were determined and normalized by total cellular

protein. Values are expressed as a percentage of the luciferase activity obtained from NaBu-treated cells transfected with 8 µg of empty vector (*EV*) and represent the mean ± SEM of three independent experiments performed in triplicate. Variations in the amount of total DNA were compensated with the corresponding empty vector.

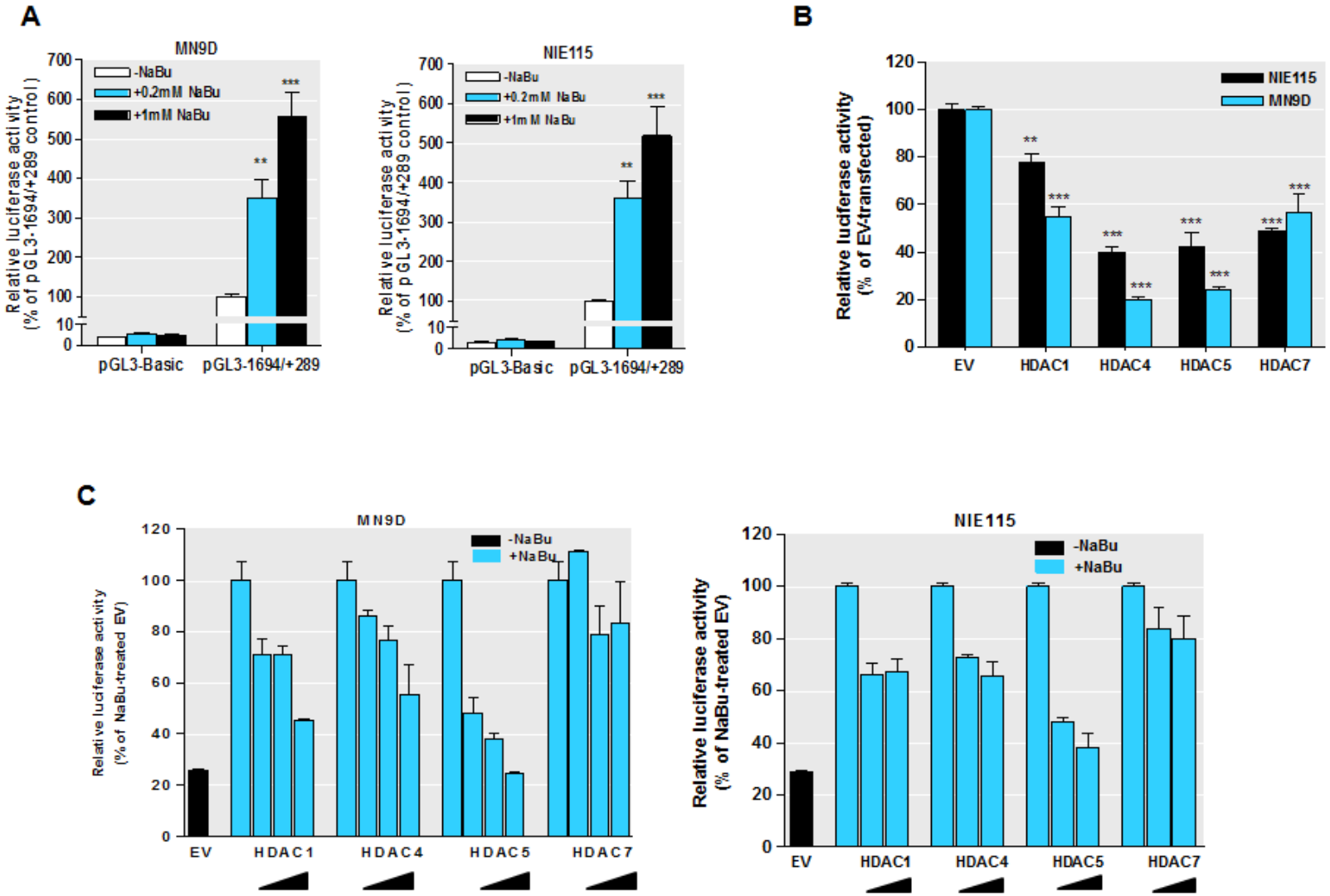

Figure 5

Figure 6: Mapping of sodium butyrate responsive elements on the PKCδ promoter

A, Schematic representation of PKCδ promoter deletion/luciferase reporter constructs. A series of PKCδ promoter deletion derivatives was generated by PCR methods and inserted into the pGL3-Basic luciferase vector. The 5' and 3' positions of the constructs with respect to the transcription start site are depicted. ***B-C***, Each construct as shown in *A* was transiently transfected into MN9D (*B*) and NIE115 (*C*) cells. After 24 h transfection, the cells were incubated with (*black bar*) or without (*blue bar*) 1 mM NaBu for 24 h, and then analyzed for luciferase activities. Values are expressed as a percentage of the activity of pGL3-1694/+289-transfected control and represent the mean ± SEM of three independent experiments performed in triplicate. The number before the times symbol "x" at the top of each blue bar indicates fold activation following NaBu exposure in cells transfected with individual promoter construct.

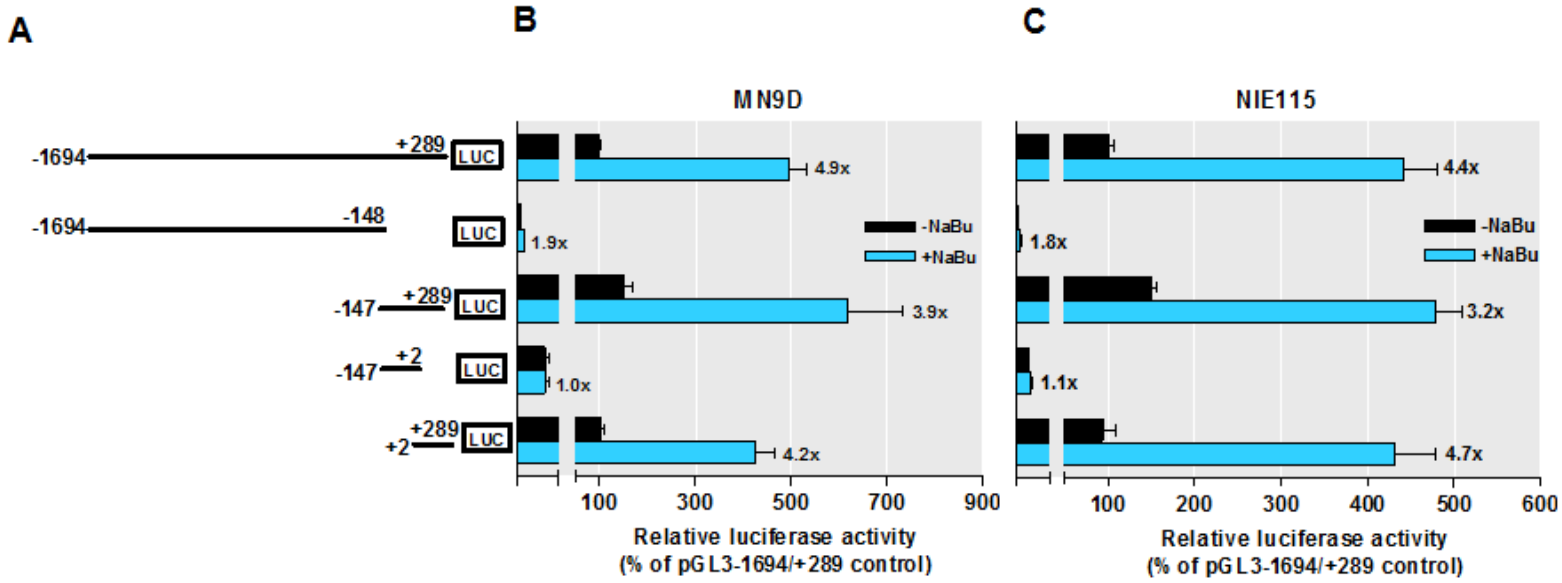

Figure 6

Figure 7: Sodium butyrate activates the PKCδ promoter through the GC-box elements. MN9D and NIE115 cells were transfected with the wild-type or mutated PKCδ promoter and Sp1 site-driven promoter constructs for 24 h. Cells were then incubated with or without NaBu (1 mM) for 24 h, and the luciferase activities were measured and normalized by total cellular protein. The activity measured following transfection of the wild-type construct (pGL3-147/+209, pGL3+165/+289, or Sp1-luc) was arbitrarily set to 100, and all other data are expressed as a percentage thereof. The results represent the mean ±SEM of three independent experiments performed in triplicate. The number before the times symbol "x" at the top of each blue bar indicates fold activation following NaBu exposure in cells transfected with the individual promoter construct. ***A***, Schematic representation of the wild-type PKCδ promoter reporter constructs pGL3-147/+209 and pGL3+165/+289. The potential Sp sites are depicted by either *circle* or *square*. ***B***, MN9D (*left*) and NIE115 (*right*) cells were transfected with 4 μg either wild-type (pGL3-147/+209) or mCACCC mutated luciferase reporter constructs. ***C***, MN9D cells were transfected with the wild-type (pGL3+165/+289) or single mutated luciferase reporter constructs. ***D***, Wild-type (pGL3+165/+289) or triple mutated luciferase reporter constructs, as indicated, were transfected into MN9D (*left*) and NIE115 (*right*) cells. ***E***, Sp1 consensus sites-driven luciferase reporter plasmid (Sp1-luc) or its mutant construct (mSp1-luc) was individually transfected into MN9D (*left*) and NIE115 (*right*) cells.

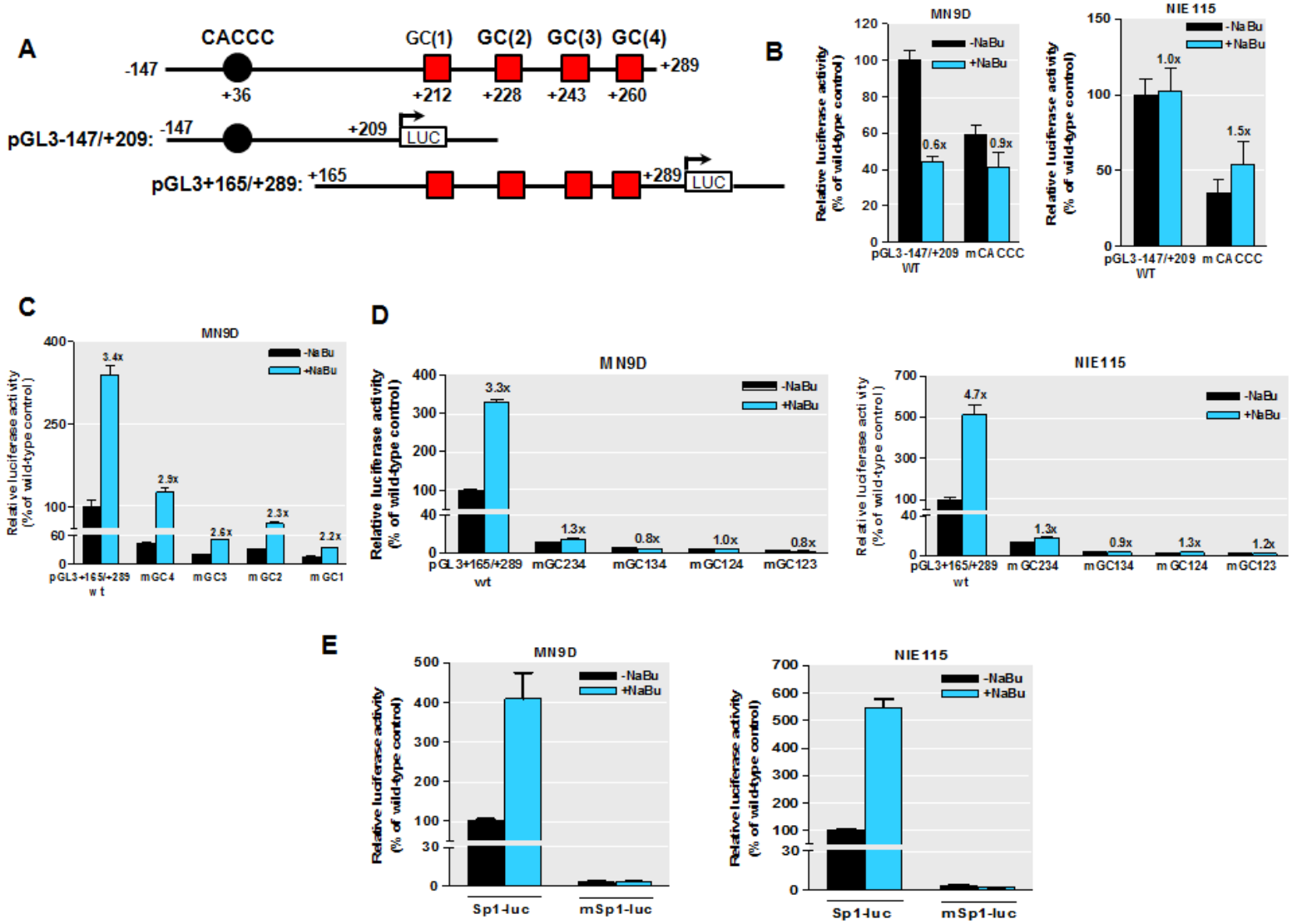

Figure 7

Figure 8: Sp family transcriptional factors mediate responsiveness to sodium butyrate

A, Overexpression of Sp1, Sp3, and Sp4 synergistically activated the NaBu induction of PKCδ promoter activity in NIE115 cells. NIE115 cells were cotransfected with pGL3-147/+289 and 8 μg of pN3-Sp1, pN3-Sp3, pN3-Sp4, or empty vector (EV) pN3. After 24 h transfection, the cells were incubated with or without 1 mM NaBu for 24 h. Luciferase activities were then assayed and normalized by total cellular protein. The activity that was obtained following transfection of empty vector without NaBu treatment was set as 1, and all other data are expressed as a fold induction thereof. The results represent the mean ±SEM of three independent experiments performed in triplicate. ***B***, Overexpression of dominant negative mutant Sp1 or Sp3 protein (Left: pN3-DN-Sp1; Right: pN3-DN-Sp3) lacking the transactivation domains did not enhance the NaBu induction of PKCδ promoter activity in NIE115 cells. NIE115 cells were cotransfected with pGL3-147/+289 and varying concentrations (4 to 8 μg) of pN3-Sp1, pN3-DN-Sp1, pN3-Sp3 or pN3-DN-Sp3 for 24 h. Cells were then exposed to 1 mM NaBu for 24 h, and luciferase activities were determined and normalized. The results represent the mean ±SEM of three independent experiments performed in triplicate. Variations in the amount of total DNA were compensated with the corresponding empty vector pN3. ***C***, Mithramycin A inhibited the NaBu responsiveness. NIE115 cells were transfected with the PKCδ promoter reporter construct pGL3-147/+289 for 24 h. After pretreatment with different doses of mithramycin A for 1 h, the cells were incubated with or without NaBu (1 mM) for 24 h. Cells were then harvested and luciferase activities were determined and normalized by total cellular protein. Values are expressed as a percentage of the activity obtained from control samples without NaBu and mithramycin A

treatment and represent the mean ± SEM of three independent experiments performed in triplicate (***, $p<0.001$; between the samples without and with mithramycin A treatment).

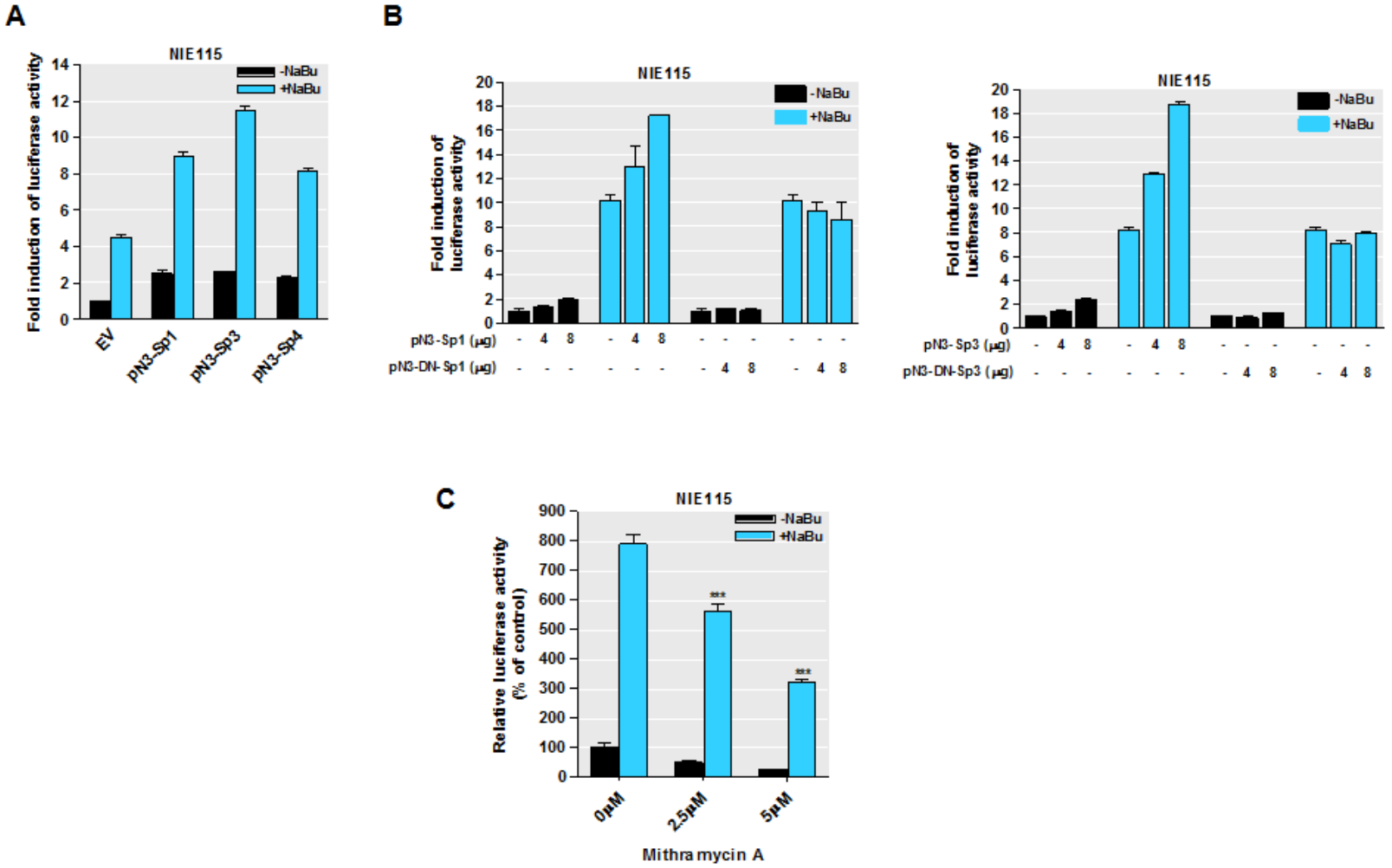

Figure 8

Figure 9: NaBu increases Sp1/3 transcriptional activity

A, Sp3 expression were unaffected by NaBu treatment. NIE115 cells were incubated with or without 1 mM NaBu for 24 h. Whole cell lysates were prepared and immunoblotted for Sp3 or β-actin (loading control). Both short Sp3 (sSp3) and long Sp3 (lSp3) isoforms are shown. ***B***, NaBu treatment did not lead to increased Sp3 DNA binding. NIE115 cells were treated with or without 1 mM NaBu for 24 h, and cells were harvested and nuclear extracts were prepared. Nuclear extracts were incubated with biotinylated PKCδ promoter probe spanning the GC(1) and GC(2) sites. The presence of Sp3 was detected by immunoblotting analysis. A representative immunoblot is shown. ***C***, Stimulation by NaBu of the Sp1/3 transactivational potential. The reporter plasmid pG5-luc, which contains five Gal4 binding sites upstream of a minimal TATA box, and the effector plasmids for Gal4 (pM), Gal4-Sp3 (pM-Sp3), Gal4-Sp3DBD (pM-Sp3DBD), Gal4-Sp1 (pM-Sp1), and Gal4-Sp1DBD (pM-Sp1DBD) were cotransfected into NIE115 (*left*) and MN9D (*right*) cells and incubated with or without 1 mM NaBu for 24 h. Luciferase activities were then determined and normalized by cellular protein. Values are expressed as fold induction of the activity obtained following transfection of the pG5-luc alone without NaBu treatment and represent the mean ± SEM of three independent experiments performed in triplicate. The number before the times symbol "x" at the top of each blue bar indicates fold activation of the activity in the presence of NaBu over that observed in the absence of NaBu. ***D***, Effects of overexpression of HDAC isoforms on the NaBu-induced Gal4-Sp1 (*left*) and Gal4-Sp3 (*right*) transactivation. NIE115 cells were cotransfected with reporter plasmid pG5-luc and 8 μg of Gal4-Sp1 or Gal4-Sp3 in combination with 4 μg of HDAC1, HDAC4, HDAC5, or HDAC7 expression plasmids or empty vector control (pcDNA3.1). The cells were then treated with or without NaBu (1 mM)

for 24 h, and luciferase activities were determined. Values are expressed as fold induction over the activity obtained following transfection of the Gal4 without NaBu treatment and represent the mean ± SEM of three independent experiments performed in triplicate (***, $p<0.001$; between the pCDNA3.1- and HDACs-transfected samples).

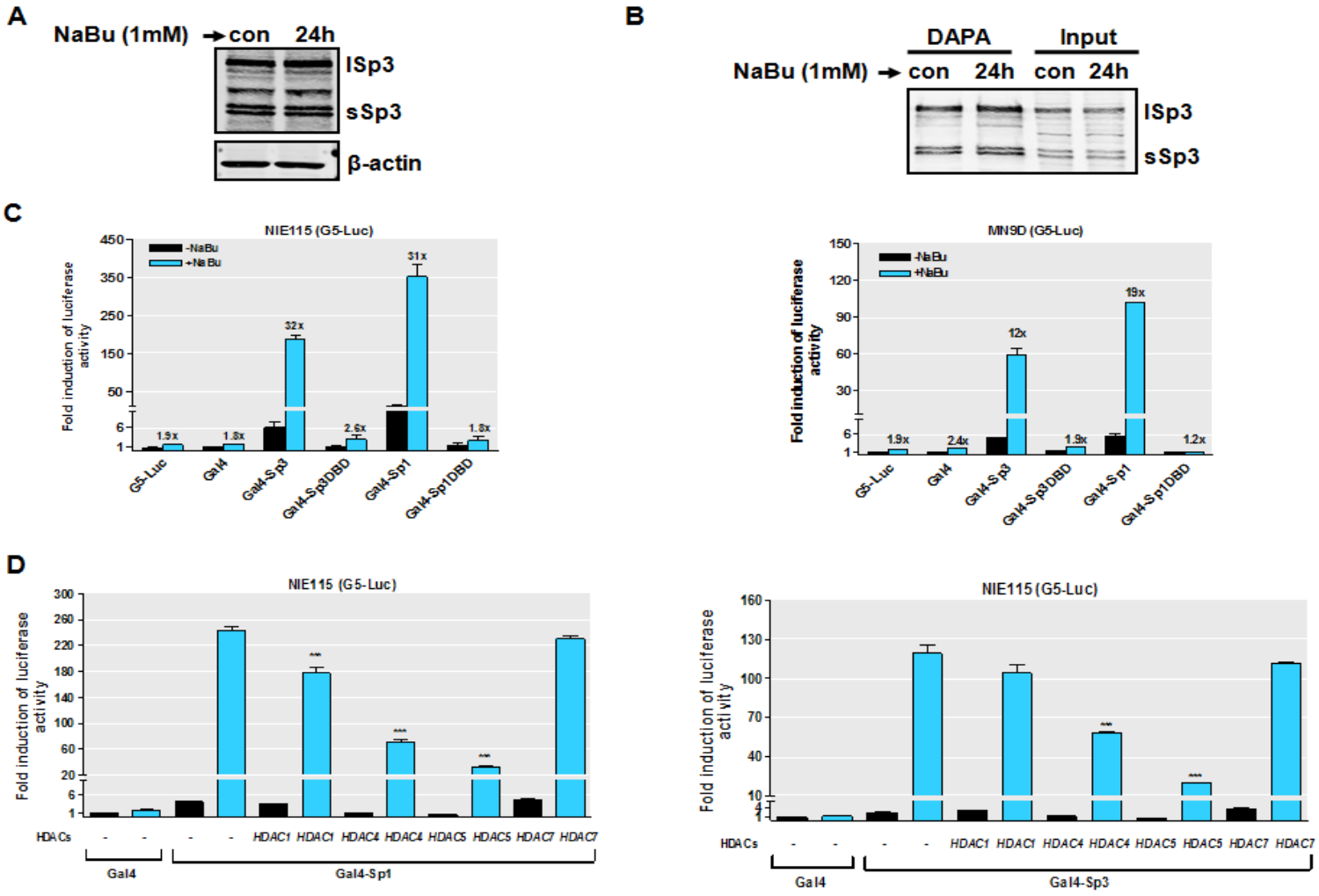

Figure 9

Figure 10: Localization of the domains of Sp1 and Sp3 that are activated in response to NaBu stimulation

A and ***C***, Schematic diagram of the expression constructs carrying Gal4-Sp1 (*A*) and Gal4-Sp3 (*C*) fusion proteins with each of the indicated portions of Sp1 or Sp3. Amino acid positions demarcating each domain are indicated. $A^{S/T}$, serine/threonine-rich subdomain within A box; A^{Q}, glutamine-rich subdomain within A box; $B^{S/T}$, serine/threonine-rich subdomain within B box; B^{Q}, glutamine-rich subdomain within B box; C, C box; Zn, zinc finger domain; D; D box. ***B*** and ***D***, The expression plasmids as shown in *A* and *C*, were cotransfected into NIE115 cells with the pG5-luc reporter plasmid. Gal4 (pM) is the empty vector control plasmid. At 24 h post-transfection, cells were treated with or without NaBu (1 mM) for 24 h. Luciferase activities were then determined and normalized by cellular protein. Values are expressed as fold induction by NaBu for each transfected sample and represent the mean ± SEM of three independent experiments performed in triplicate.

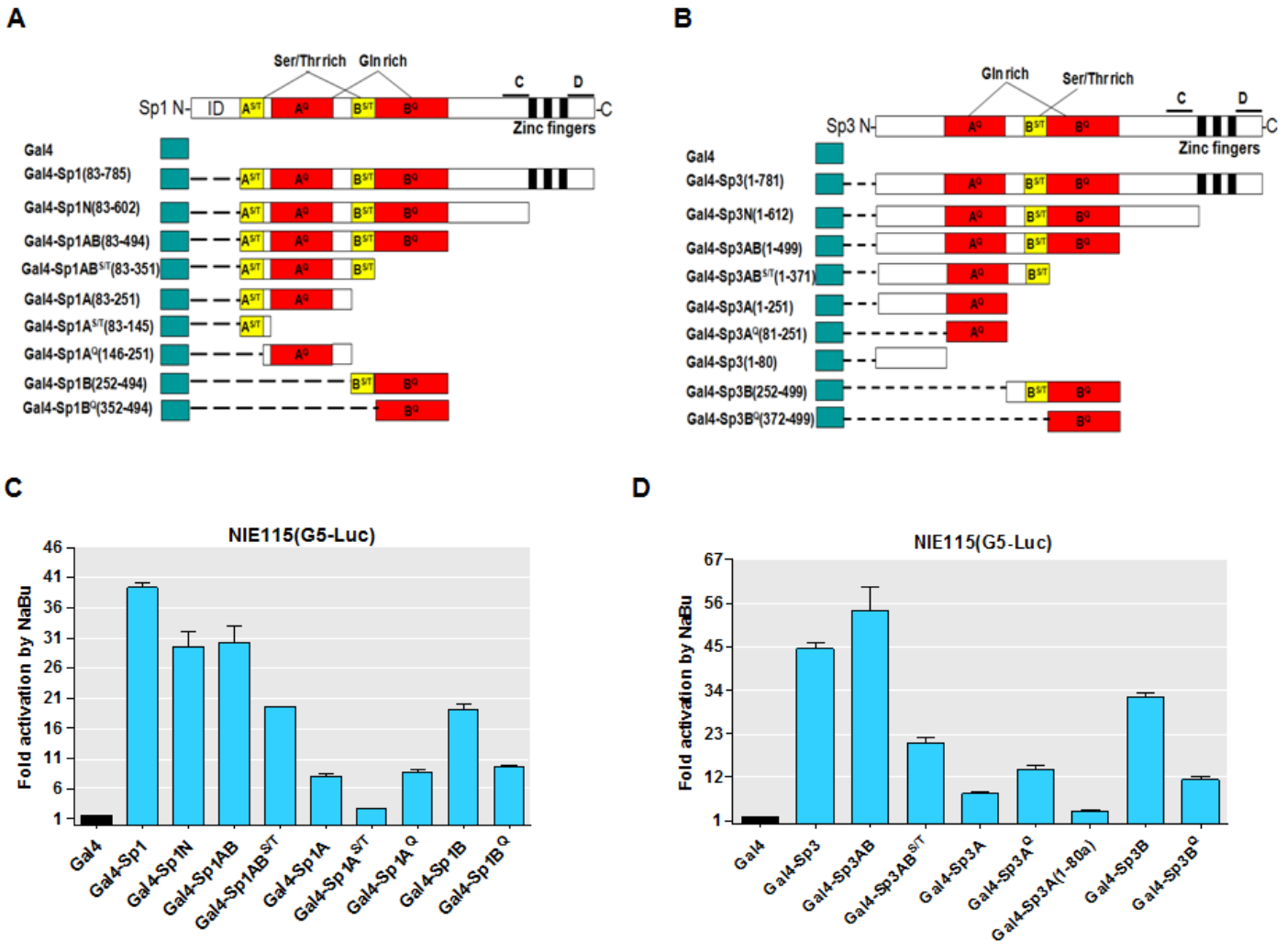

Figure 10

Figure 11. Expression of CBP/p300 stimulates NaBu-induced transactivation of Sp1 and Sp3

A*-*B, NIE115 cells were cotransfected with Gal4-Sp1 or Gal4-Sp3 expression constructs, the luciferase reporter plasmid pG5-luc, and the indicated amounts of CMV-driven expression vectors for p300, p300dHAT (*A*), or CBP (*B*). The cells were then treated with or without NaBu (1 mM) for 24 h, and luciferase activities were determined. Values are expressed as fold induction over the activity obtained following transfection of the Gal4 without NaBu treatment and represent the mean ± SEM of three independent experiments performed in triplicate.

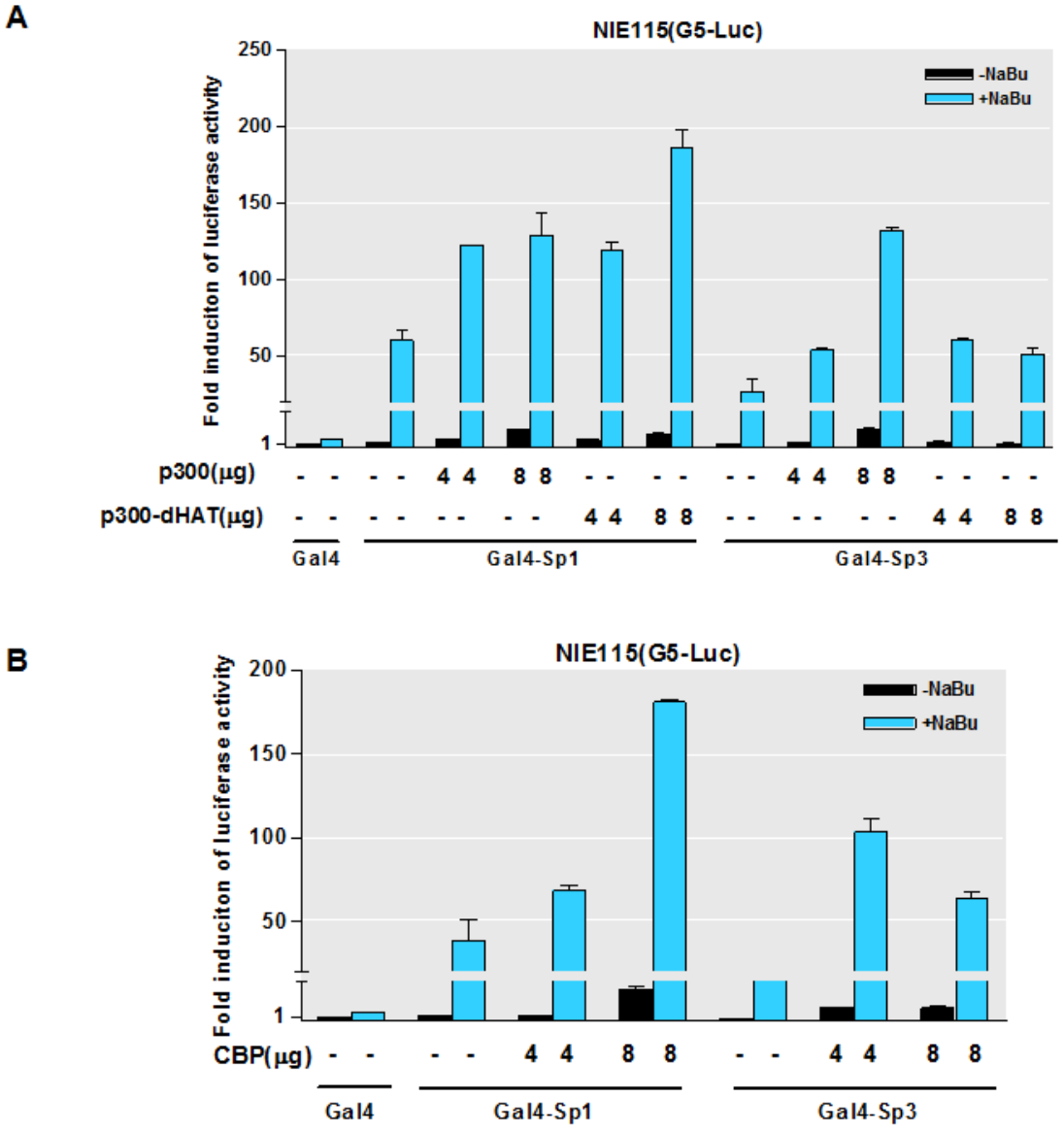

Figure 11

Figure S1: Other HDAC inhibitors stimulate PKCδ promoter activity in MN9D cells

A-D, The PKCδ promoter reporter construct pGL3-1694/+289 was transfected into MN9D cells. After 24 h transfection, the cells were incubated with VPA (*A*), TSA (*B*), apicidin (*C*), or scriptaid (*D*) at the designated concentrations for 24 h. Cells were then harvested and luciferase activities were determined and normalized by total cellular protein. Values are expressed as a percentage of the activity of untreated control and represent the mean ± SEM of three independent experiments performed in triplicate (***, $p<0.001$; between the control and treated samples).

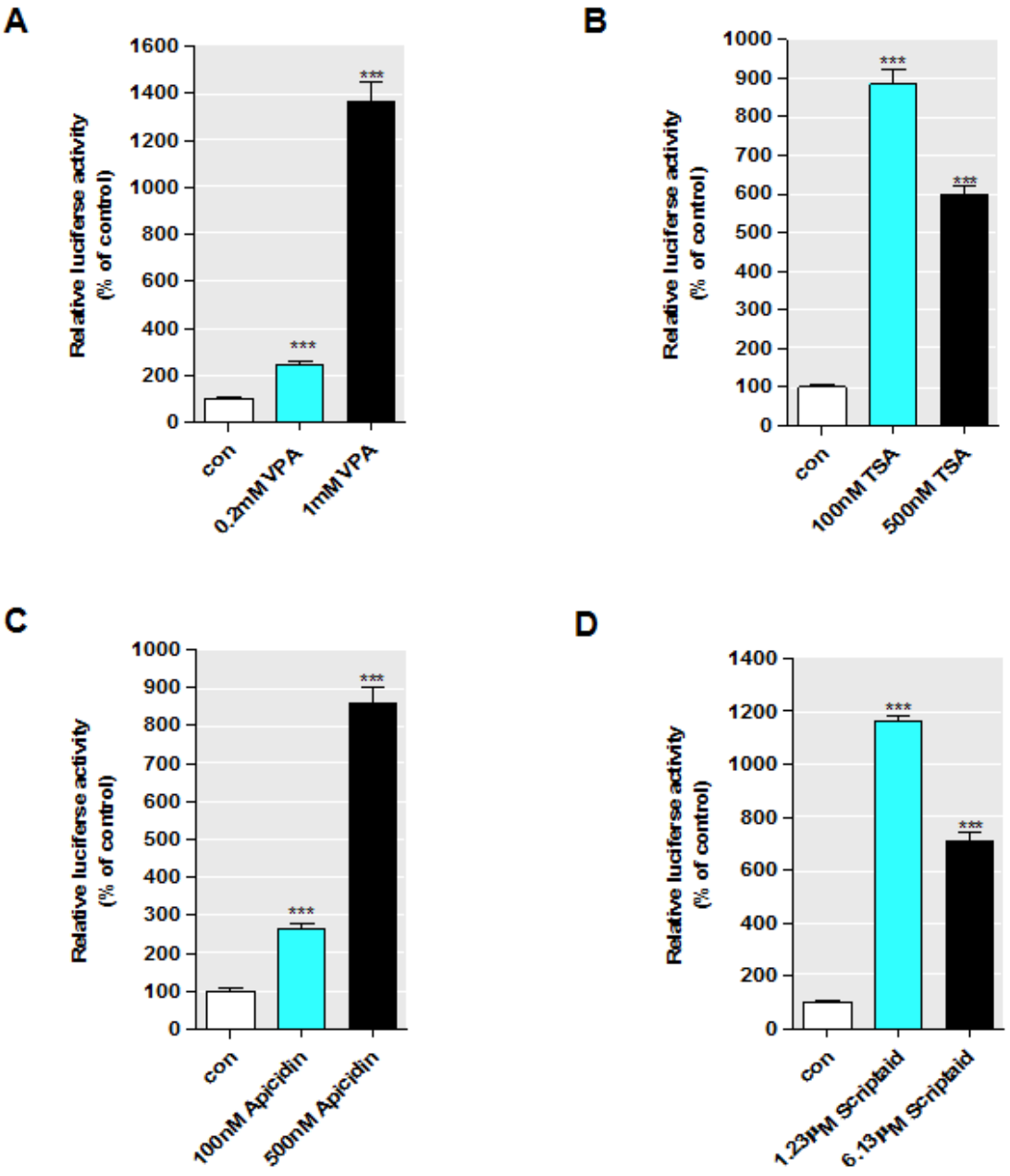

Figure S1

Figure S2: Ectopic expression of HDAC proteins inhibits the promoter activity of Sp1 reporter plasmid (Sp1-luc)

A, Eight µg of HDAC1, HDAC4, HDAC5, or HDAC7 expression vector or the empty vector control (EV), as indicated, were cotransfected with the Sp1 reporter construct Sp1-luc into NIE115 (*black bar*) and MN9D (*blue bar*) cells. Luciferase activity was measured after 24 h of transfection. Values are expressed as a percentage of the luciferase activity obtained from cells transfected with 8 µg of empty vector (*EV*) and represent the mean ± SEM of three independent experiments performed in triplicate (*, $p<0.05$; **, $p<0.01$; ***, $p<0.001$; between the EV- and HDACs-transfected samples). ***B***, NaBu-induced transcriptional activation of Sp1-luc was repressed by ectopic expression HDACs in NIE115 cells. NIE115 cells were cotransfected with Sp1-luc and 8 µg of HDAC1, HDAC4, HDAC5, or HDAC7 expression vector or the empty vector control (EV). After 12 h transfection, the cells were incubated with or without NaBu (1 mM) for 24 h. Cells were then harvested and luciferase activities were determined. Values are expressed as a percentage of the luciferase activity obtained from NaBu-treated cells transfected with 8 µg of empty vector (*EV*) and represent the mean ± SEM of three independent experiments performed in triplicate (*, $p<0.05$; **, $p<0.01$; ***, $p<0.001$; between the EV- and HDACs-transfected samples).

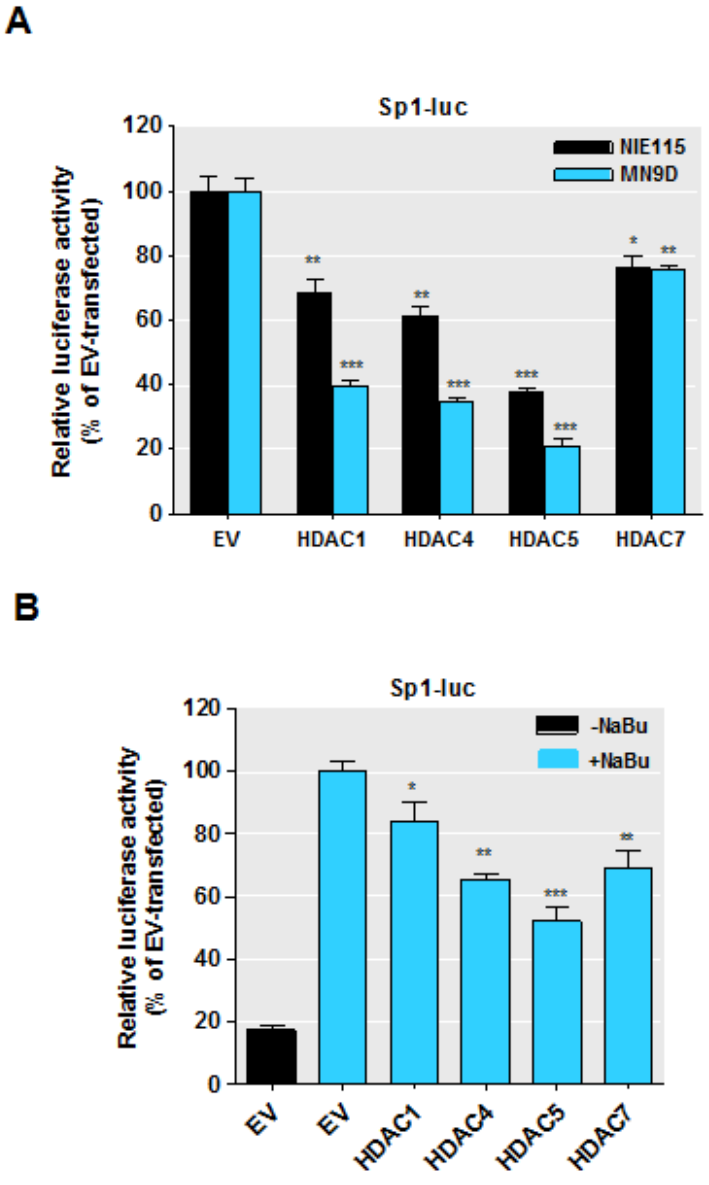

Figure S2

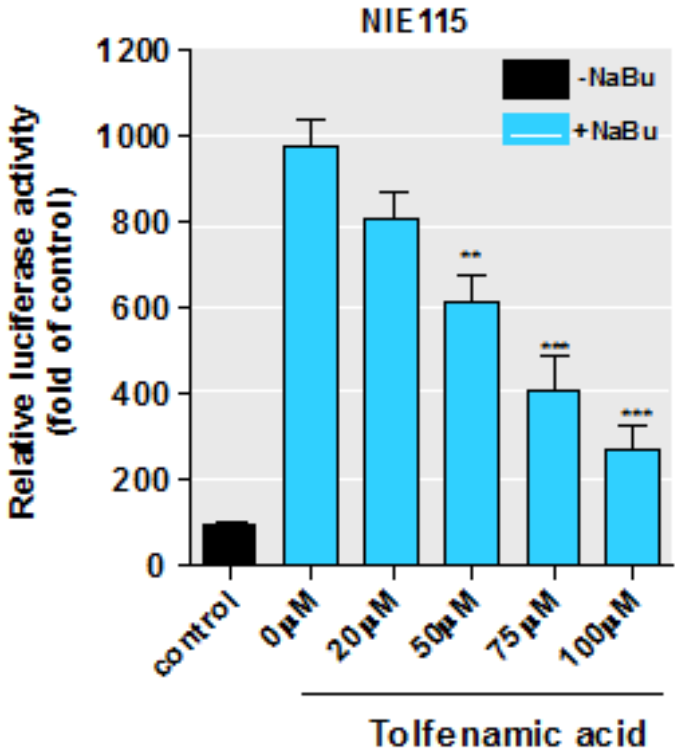

Figure S3: Tolfenamic acid dose-dependently inhibits NaBu responsiveness in NIE115 cells

NIE115 cells were transfected with the PKCδ promoter reporter construct pGL3-147/+289 for 24 h. After pretreatment with different doses of tolfenamic acid for 1 h, the cells were incubated with or without NaBu (1 mM) for 24 h. Cells were then harvested and luciferase activities were determined and normalized by total cellular protein. Values are expressed as a percentage of the activity obtained from control samples without NaBu and tolfenamic acid treatment and represent the mean ± SEM of three independent experiments performed in triplicate (***, $p<0.001$; between the samples without and with tolfenamic acid treatment).

References

Ammanamanchi S, Freeman JW, Brattain MG (2003) Acetylated sp3 is a transcriptional activator. J Biol Chem 278:35775-35780.

Anantharam V, Kitazawa M, Wagner J, Kaul S, Kanthasamy AG (2002) Caspase-3-dependent proteolytic cleavage of protein kinase Cdelta is essential for oxidative stress-mediated dopaminergic cell death after exposure to methylcyclopentadienyl manganese tricarbonyl. J Neurosci 22:1738-1751.

Blume SW, Snyder RC, Ray R, Thomas S, Koller CA, Miller DM (1991) Mithramycin inhibits SP1 binding and selectively inhibits transcriptional activity of the dihydrofolate reductase gene in vitro and in vivo. J Clin Invest 88:1613-1621.

Boutillier AL, Trinh E, Loeffler JP (2003) Selective E2F-dependent gene transcription is controlled by histone deacetylase activity during neuronal apoptosis. J Neurochem 84:814-828.

Boyes J, Byfield P, Nakatani Y, Ogryzko V (1998) Regulation of activity of the transcription factor GATA-1 by acetylation. Nature 396:594-598.

Brodie C, Blumberg PM (2003) Regulation of cell apoptosis by protein kinase c delta. Apoptosis 8:19-27.

Camarero N, Nadal A, Barrero MJ, Haro D, Marrero PF (2003) Histone deacetylase inhibitors stimulate mitochondrial HMG-CoA synthase gene expression via a promoter proximal Sp1 site. Nucleic Acids Res 31:1693-1703.

Chuang DM, Leng Y, Marinova Z, Kim HJ, Chiu CT (2009) Multiple roles of HDAC inhibition in neurodegenerative conditions. Trends Neurosci 32:591-601.

Clarke CE (2007) Parkinson's disease. Bmj 335:441-445.

Dempsey EC, Newton AC, Mochly-Rosen D, Fields AP, Reyland ME, Insel PA, Messing RO (2000) Protein kinase C isozymes and the regulation of diverse cell responses. Am J Physiol Lung Cell Mol Physiol 279:L429-438.

Dietz KC, Casaccia P HDAC inhibitors and neurodegeneration: at the edge between protection and damage. Pharmacol Res 62:11-17.

Doetzlhofer A, Rotheneder H, Lagger G, Koranda M, Kurtev V, Brosch G, Wintersberger E, Seiser C (1999) Histone deacetylase 1 can repress transcription by binding to Sp1. Mol Cell Biol 19:5504-5511.

Dokmanovic M, Clarke C, Marks PA (2007) Histone deacetylase inhibitors: overview and perspectives. Mol Cancer Res 5:981-989.

Fojas de Borja P, Collins NK, Du P, Azizkhan-Clifford J, Mudryj M (2001) Cyclin A-CDK phosphorylates Sp1 and enhances Sp1-mediated transcription. Embo J 20:5737-5747.

Han JW, Ahn SH, Kim YK, Bae GU, Yoon JW, Hong S, Lee HY, Lee YW, Lee HW (2001) Activation of p21(WAF1/Cip1) transcription through Sp1 sites by histone deacetylase inhibitor apicidin: involvement of protein kinase C. J Biol Chem 276:42084-42090.

Hung JJ, Wang YT, Chang WC (2006) Sp1 deacetylation induced by phorbol ester recruits p300 to activate 12(S)-lipoxygenase gene transcription. Mol Cell Biol 26:1770-1785.

Kanthasamy AG, Kitazawa M, Kaul S, Yang Y, Lahiri DK, Anantharam V, Kanthasamy A (2003) Proteolytic activation of proapoptotic kinase PKCdelta is regulated by overexpression of Bcl-2: implications for oxidative stress and environmental factors in Parkinson's disease. Ann N Y Acad Sci 1010:683-686.

Kanthasamy AG, Anantharam V, Zhang D, Latchoumycandane C, Jin H, Kaul S, Kanthasamy A (2006) A novel peptide inhibitor targeted to caspase-3 cleavage site of a proapoptotic kinase protein kinase C delta (PKCdelta) protects against dopaminergic neuronal degeneration in Parkinson's disease models. Free Radic Biol Med 41:1578-1589.

Kaul S, Kanthasamy A, Kitazawa M, Anantharam V, Kanthasamy AG (2003) Caspase-3 dependent proteolytic activation of protein kinase C delta mediates and regulates 1-methyl-4-phenylpyridinium (MPP+)-induced apoptotic cell death in dopaminergic cells: relevance to oxidative stress in dopaminergic degeneration. Eur J Neurosci 18:1387-1401.

Kaul S, Anantharam V, Yang Y, Choi CJ, Kanthasamy A, Kanthasamy AG (2005) Tyrosine phosphorylation regulates the proteolytic activation of protein kinase Cdelta in dopaminergic neuronal cells. J Biol Chem 280:28721-28730.

Kim YH, Lim JH, Lee TJ, Park JW, Kwon TK (2007) Expression of cyclin D3 through Sp1 sites by histone deacetylase inhibitors is mediated with protein kinase C-delta (PKC-delta) signal pathway. J Cell Biochem 101:987-995.

Kim YK, Han JW, Woo YN, Chun JK, Yoo JY, Cho EJ, Hong S, Lee HY, Lee YW, Lee HW (2003) Expression of p21(WAF1/Cip1) through Sp1 sites by histone deacetylase inhibitor apicidin requires PI 3-kinase-PKC epsilon signaling pathway. Oncogene 22:6023-6031.

Kitazawa M, Anantharam V, Kanthasamy AG (2003) Dieldrin induces apoptosis by promoting caspase-3-dependent proteolytic cleavage of protein kinase Cdelta in

dopaminergic cells: relevance to oxidative stress and dopaminergic degeneration. Neuroscience 119:945-964.

Konduri S, Colon J, Baker CH, Safe S, Abbruzzese JL, Abudayyeh A, Basha MR, Abdelrahim M (2009) Tolfenamic acid enhances pancreatic cancer cell and tumor response to radiation therapy by inhibiting survivin protein expression. Mol Cancer Ther 8:533-542.

Kurkinen KM, Keinanen RA, Karhu R, Koistinaho J (2000) Genomic structure and chromosomal localization of the rat protein kinase Cdelta-gene. Gene 242:115-123.

Latchoumycandane C, Anantharam V, Kitazawa M, Yang Y, Kanthasamy A, Kanthasamy AG (2005) Protein kinase Cdelta is a key downstream mediator of manganese-induced apoptosis in dopaminergic neuronal cells. J Pharmacol Exp Ther 313:46-55.

Lemercier C, Brocard MP, Puvion-Dutilleul F, Kao HY, Albagli O, Khochbin S (2002) Class II histone deacetylases are directly recruited by BCL6 transcriptional repressor. J Biol Chem 277:22045-22052.

Livak KJ, Schmittgen TD (2001) Analysis of relative gene expression data using real-time quantitative PCR and the 2(-Delta Delta C(T)) Method. Methods 25:402-408.

Marinova Z, Ren M, Wendland JR, Leng Y, Liang MH, Yasuda S, Leeds P, Chuang DM (2009) Valproic acid induces functional heat-shock protein 70 via Class I histone deacetylase inhibition in cortical neurons: a potential role of Sp1 acetylation. J Neurochem 111:976-987.

Marks PA, Miller T, Richon VM (2003) Histone deacetylases. Curr Opin Pharmacol 3:344-351.

Miettinen S, Roivainen R, Keinanen R, Hokfelt T, Koistinaho J (1996) Specific induction of protein kinase C delta subspecies after transient middle cerebral artery occlusion in the rat brain: inhibition by MK-801. J Neurosci 16:6236-6245.

Miska EA, Karlsson C, Langley E, Nielsen SJ, Pines J, Kouzarides T (1999) HDAC4 deacetylase associates with and represses the MEF2 transcription factor. Embo J 18:5099-5107.

Ray R, Snyder RC, Thomas S, Koller CA, Miller DM (1989) Mithramycin blocks protein binding and function of the SV40 early promoter. J Clin Invest 83:2003-2007.

Reno EM, Haughian JM, Dimitrova IK, Jackson TA, Shroyer KR, Bradford AP (2008) Analysis of protein kinase C delta (PKC delta) expression in endometrial tumors. Hum Pathol 39:21-29.

Saha RN, Pahan K (2006) HATs and HDACs in neurodegeneration: a tale of disconcerted acetylation homeostasis. Cell Death Differ 13:539-550.

Salminen A, Tapiola T, Korhonen P, Suuronen T (1998) Neuronal apoptosis induced by histone deacetylase inhibitors. Brain Res Mol Brain Res 61:203-206.

Sapetschnig A, Koch F, Rischitor G, Mennenga T, Suske G (2004) Complexity of translationally controlled transcription factor Sp3 isoform expression. J Biol Chem 279:42095-42105.

Sowa Y, Orita T, Minamikawa-Hiranabe S, Mizuno T, Nomura H, Sakai T (1999) Sp3, but not Sp1, mediates the transcriptional activation of the p21/WAF1/Cip1 gene promoter by histone deacetylase inhibitor. Cancer Res 59:4266-4270.

Spengler ML, Brattain MG (2006) Sumoylation inhibits cleavage of Sp1 N-terminal negative regulatory domain and inhibits Sp1-dependent transcription. J Biol Chem 281:5567-5574.

Suh KS, Tatunchak TT, Crutchley JM, Edwards LE, Marin KG, Yuspa SH (2003) Genomic structure and promoter analysis of PKC-delta. Genomics 82:57-67.

Sun JM, Chen HY, Moniwa M, Litchfield DW, Seto E, Davie JR (2002) The transcriptional repressor Sp3 is associated with CK2-phosphorylated histone deacetylase 2. J Biol Chem 277:35783-35786.

Suske G (1999) The Sp-family of transcription factors. Gene 238:291-300.

Suske G, Bruford E, Philipsen S (2005) Mammalian SP/KLF transcription factors: bring in the family. Genomics 85:551-556.

Suzuki T, Kimura A, Nagai R, Horikoshi M (2000) Regulation of interaction of the acetyltransferase region of p300 and the DNA-binding domain of Sp1 on and through DNA binding. Genes Cells 5:29-41.

Walker GE, Wilson EM, Powell D, Oh Y (2001) Butyrate, a histone deacetylase inhibitor, activates the human IGF binding protein-3 promoter in breast cancer cells: molecular mechanism involves an Sp1/Sp3 multiprotein complex. Endocrinology 142:3817-3827.

Wang Y, Wang X, Liu L, Wang X (2009) HDAC inhibitor trichostatin A-inhibited survival of dopaminergic neuronal cells. Neurosci Lett 467:212-216.

Won J, Yim J, Kim TK (2002) Sp1 and Sp3 recruit histone deacetylase to repress transcription of human telomerase reverse transcriptase (hTERT) promoter in normal human somatic cells. J Biol Chem 277:38230-38238.

Yang XJ, Seto E (2007) HATs and HDACs: from structure, function and regulation to novel strategies for therapy and prevention. Oncogene 26:5310-5318.

Yang XJ, Ogryzko VV, Nishikawa J, Howard BH, Nakatani Y (1996) A p300/CBP-associated factor that competes with the adenoviral oncoprotein E1A. Nature 382:319-324.

Yang Y, Kaul S, Zhang D, Anantharam V, Kanthasamy AG (2004) Suppression of caspase-3-dependent proteolytic activation of protein kinase C delta by small interfering RNA prevents MPP+-induced dopaminergic degeneration. Mol Cell Neurosci 25:406-421.

Yokota T, Matsuzaki Y, Miyazawa K, Zindy F, Roussel MF, Sakai T (2004) Histone deacetylase inhibitors activate INK4d gene through Sp1 site in its promoter. Oncogene 23:5340-5349.

Zhang D, Anantharam V, Kanthasamy A, Kanthasamy AG (2007a) Neuroprotective effect of protein kinase C delta inhibitor rottlerin in cell culture and animal models of Parkinson's disease. J Pharmacol Exp Ther 322:913-922.

Zhang D, Kanthasamy A, Yang Y, Anantharam V, Kanthasamy A (2007b) Protein kinase C delta negatively regulates tyrosine hydroxylase activity and dopamine synthesis by enhancing protein phosphatase-2A activity in dopaminergic neurons. J Neurosci 27:5349-5362.

Zhu WG, Lakshmanan RR, Beal MD, Otterson GA (2001) DNA methyltransferase inhibition enhances apoptosis induced by histone deacetylase inhibitors. Cancer Res 61:1327-1333.

CHAPTER IV: ALPHA-SYNUCLEIN NEGATIVELY REGULATES PKCδ EXPRESSION TO SUPPRESS APOPTOSIS IN DOPAMINERGIC NEURONS BY REDUCING P300 HAT ACTIVITY

A paper submitted to the *Journal of Neuroscience*

Huajun Jin, Arthi Kanthasamy, Anamitra Ghosh, Yongjie Yang, Vellareddy Anantharam, and Anumantha Kanthasamy

Abstract

We recently demonstrated that PKCδ, an important member of the novel PKC family, is a key oxidative stress-sensitive kinase that can be activated by caspase-3-dependent proteolytic cleavage to induce dopaminergic neuronal cell death. We now report a novel association between α-synuclein (αsyn), a protein associated with the pathogenesis of Parkinson's diseases (PD), and PKCδ, in which αsyn negatively modulates the p300 and NFκB dependent transactivation to down-regulate proapoptotic kinase PKCδ expression and thereby protects against apoptosis in dopaminergic neuronal cells. Stable-expression human wild-type αsyn at physiological levels in dopaminergic neuronal cells resulted in an isoform-dependent transcriptional suppression of PKCδ expression without changes in the stability of mRNA and protein or DNA methylation. The reduction in PKCδ transcription was mediated, in part, through the suppression of constitutive NFκB activity targeted at two proximal PKCδ promoter κB sites. This occurred independently of NFκB/IκBα nuclear

translocation, but was associated with decreased NFκB-p65 acetylation. Also, αsyn reduced p300 levels and its histone acetyl-transferase (HAT) activity, thereby contributing to diminished PKCδ transactivation. Importantly, reduced PKCδ and p300 expression also were observed within nigral dopaminergic neurons in αsyn transgenic mice. These findings expand the role of αsyn in neuroprotection by modulating the expression of the key proapoptotic kinase PKCδ in dopaminergic neurons.

Introduction

Environmental neurotoxic insults and genetic defects in certain genes have been implicated in the etiology of PD (Dauer and Przedborski, 2003; Hatcher et al., 2008). Oxidative stress serves as a central mediator of degenerative processes in PD (Greenamyre and Hastings, 2004; Burke, 2008; Zhou et al., 2008); however, the key cell signaling mechanisms underlying oxidative damage to nigral dopaminergic neurons are not entirely clear. Our laboratory has been studying PKCδ-mediated cell death signaling in the oxidative damage of dopaminergic neurons. PKCδ, a novel PKC isoform, has been recognized as a key proapoptotic effector in various cell types (Brodie and Blumberg, 2003; Kanthasamy et al., 2003). The role of PKCδ in nervous system function is beginning to emerge, and we demonstrated that PKCδ is an oxidative stress-sensitive kinase that is persistently activated by caspase-3-dependent proteolytic cleavage to mediate dopaminergic neurodegeneration in cellular models of PD (Anantharam et al., 2002; Kanthasamy et al., 2003; Kaul et al., 2003). We showed that cytochrome C release and caspase-9 and caspase-3 activation serve as upstream events of the PKCδ-mediated cell pathway during mitochondrial impairment (e.g.,

MPP+) in dopaminergic neuronal cells (Kaul et al., 2003). Importantly, depletion of PKCδ by siRNA or blockage of PKCδ activation by overexpression of a PKCδ kinase-dominant-negative mutant or caspase-cleavage-resistant mutant protects against multiple insults in cultured neurons (Kitazawa et al., 2003; Yang et al., 2004; Latchoumycandane et al., 2005). Furthermore, pharmacological inhibition of PKCδ prevents MPTP-induced degeneration of nigrostriatal dopaminergic neurons in animal models (Zhang et al., 2007a). We also showed that PKCδ inhibits tyrosine hydroxylase (TH) activity and dopamine synthesis in dopaminergic neurons (Zhang et al., 2007b). Despite the known proapoptotic function of PKCδ in dopaminergic neurons, the role of this kinase in cellular stress induced by proteins associated with familial-PD-linked genes is not known.

αSyn is a presynaptic protein predominantly expressed in neurons throughout the mammalian brain. The physiological functions of αsyn are poorly understood, but evidence has suggested a role for it in synaptic plasticity, dopamine synthesis, and membrane trafficking (Clayton and George, 1998; Perez et al., 2002; Outeiro and Lindquist, 2003). The relevance of αsyn to PD pathogenesis is based on case studies of familial PD resulting from mutations or multiplications of αsyn gene, as well as the observation that misfolded αsyn is a major constituent of Lewy bodies in both familial and sporadic PD (Spillantini et al., 1998; Norris et al., 2004). Although altered αsyn processing is thus considered a main determinant of PD, a growing body of evidence suggests a protective role of native αsyn in neurodegeneration (Manning-Bog et al., 2003; Sidhu et al., 2004; Chandra et al., 2005; Leng and Chuang, 2006; Monti et al., 2007).

While studying the PKCδ-dependent cell death mechanisms, we unexpectedly found striking neuroprotection in an αsyn-expressing dopaminergic cell model during exposure to the Parkinsonian neurotoxicant MPP+. This led us to further investigate the molecular mechanisms underlying the neuroprotective function mediated by αsyn in dopaminergic neurons using cell culture and animal models. In the present study, we demonstrate a novel functional association between PKCδ and αsyn in which αsyn represses PKCδ expression by a mechanism involving modulation of both NFκB and p300 signaling pathways in a dopaminergic neuronal cell model and in transgenic αsyn mice. We also show that the deregulation of proapoptotic PKCδ expression protects dopaminergic neurons against MPP+ toxicity. These observations extend the physiological role of native αsyn in protecting against neuronal injury.

Materials and Methods

Reagents

1-methyl-4-phenylpyridinium (MPP+), actinomycin D (ActD), protein A/G beads, sodium butyrate, and mouse β-actin antibody were purchased from Sigma-Aldrich (St. Louis, MO). SN-50 peptide, garcinol, and N-(4-Chloro-3-trifluoromethyl-phenyl)-2-ethoxy-6-pentadecyl-benzamide (CTPB) were obtained from Enzo Life Sciences (Plymouth Meeting, PA). Biotin-16-UTP and the Cell Death Detection ELISA Plus assay kit were purchased from Roche Molecular Biochemicals (Indianapolis, IN). Z-DEVD-FMK was obtained from Alexis Biochemicals (San Diego, CA). Acetyl-DEVD-amino-4-methylcoumarin (Ac-DEVD-AMC) was obtained from Bachem

(King of Prussia, PA). The Bradford protein assay kit was purchased from Bio-Rad Laboratories (Hercules, CA). The DNeasy blood & tissue kit was obtained from Qiagen (Valencia, CA). Hoechst 33342, Lipofectamine Plus reagent, Lipofectamine 2000 reagent, hygromycin B, penicillin, streptomycin, fetal bovine serum, L-glutamine, RPMI 1640 medium, methionine-free RPMI 1640 medium, Neurobasal medium, B27 supplement, and Dulbecco's modified Eagle's medium were purchased from Invitrogen (Carlsbad, CA). Dynabeads M-280 was purchased from Dynal Biotech (Oslo, Norway). [3H]Acetyl-CoA, poly (dI-dC), [35S]-methionine, HRP-linked anti-mouse and anti-rabbit secondary antibodies, and the ECL chemiluminescence kit were obtained from GE Healthcare (Piscataway, NJ). Antibodies to PKCδ, PKCα, PKCβI, PKCζ, p65, p50, IκBα, CBP, p300, and αsyn (#sc-12767, only detecting αsyn of human origin) were purchased from Santa Cruz Biotechnology (Santa Cruz, CA); the rabbit polyclonal antibody for acetyl-lysine, mouse p300, and histone H3 antibodies were obtained from Milipore (Billerica, MA). αSyn monoclonal antibody detecting both human and rat origins was purchased from BD Biosciences (Syn-1, San Diego, CA); the mouse TH antibody was obtained from Chemicon (Temecula, CA); the goat polyclonal antibody for lactate dehydrogenase (LDH) and mouse monoclonal antibody for Lamin B1 were purchased from Abcam (Cambridge, MA). IRDye800 conjugated anti-rabbit secondary antibody was obtained from Rockland Labs (Gilbertsville, PA). Alexa 680-conjugated anti-mouse, Alexa 488-conjugated anti-mouse, Alexa 568-conjugated anti-rabbit secondary antibodies and mouse V5 antibody were obtained from Invitrogen. Anti-goat secondary antibody and normal rabbit IgG were obtained from Santa Cruz Biotechnology.

Plasmids

The plasmid encoding wild-type human αsyn protein (pCEP4-αsyn) was a kind gift from Dr. Eliezer Masliah (University of California, San Diego, CA). A control pCEP4 empty vector was purchased from Invitrogen. To prepare pLenti-V5-PKCδ and pLenti-V5-αsyn lentiviral vectors, full-length mouse PKCδ (gi: 6755081) and human αsyn (gi: 6806897) cDNA were PCR-generated from pGFP-PKCδ (kind gift of Dr. Mary E. Reyland) and pCEP4-αsyn with the following primer pairs, respectively. For PKCδ, forward, 5'-CACCATGGCACCCTTCCTGCGC-3', reverse, 5'-AATGTCCAGGAATTGCTCAAAC -3'; for αsyn, forward, 5'-CACCATGGATGTATTCATGAAAGGAC-3', reverse, 5'-GGCT TCAGGTTCGTAGTCTTG-3'. The PCR products were then subcloned in-frame into the C-terminal V5-tagged expression vector pLenti6/V5-TOPO (Invitrogen) as described (Kitazawa et al., 2005; Latchoumycandane et al., 2005). A control lentiviral construct pLenti-V5-LacZ, encoding β-galactosidase fused to the V5 epitope, was also obtained from Invitrogen. To generate pGL3-PKCδ promoter construct, rat genomic DNA was isolated using the DNeasy blood & tissue kit and used as template to amplify the 1.7 kb DNA fragment (-1700 to +22, +1 denotes the transcription start site) of rat PKCδ gene. PCR conditions used were 94°C for 45 sec; 30 cycles of 94°C for 30 sec, 64.6°C for 30 sec, and 72°C for 2 min; and 72°C for 10 min. Following PCR, the amplified product was cloned into the XhoI/HindIII sites of pGL3-Basic vector (Promega, Madison, WI). All constructs were verified by DNA sequencing.

Primary mesencephalic cultures and treatment

All of the procedures involving animal handling were approved by the Institutional Animal Care Use Committee (IACUC) at the Iowa State University. Primary mesencephalic neuronal cultures were prepared as described in our recent publications (Ghosh et al., 2010; Zhang et al., 2007c). Briefly, 24-well plates containing coverslips were coated overnight with 0.1 mg/ml poly-D-lysine. Mesencephalon tissue was dissected from gestational 14-day-old mouse embryos and kept in ice-cold Ca^{2+}-free Hanks's balanced salt solution. Cells were then dissociated in Hank's balanced salt solution containing trypsin-0.25% EDTA for 30 min at 37 °C. After the incubation, 10% heat-inactivated fetal bovine serum in Dulbecco's modified Eagle's medium was added to inhibit trypsin digestion. The cells were triturated and suspended in Neurobasal medium supplemented with 2% Neurobasal supplement (B27), 500 μM L-glutamine, 100 IU/ml penicillin, and 100 μg/ml streptomycin, plated at 1×10^6 cells in 0.5 ml/well and incubated in a humidified CO_2 incubator (5% CO_2 and 37 °C). Half of the culture medium was replaced every 2 days, and experiments were conducted using between 6 and 7 day cultures. After exposure to the NFκB inhibitor SN50 and the p300 inhibitor garcinol or the activator CTPB for 24 h, the primary cultures were processed for immunocytochemical analysis.

Cell culture and stable expression of α-synuclein

Rat immortalized mesencephalic dopaminergic neuronal cell line (1RB3AN27, referred to as N27 cells) was a kind gift of Dr. Kedar N. Prasad (University of Colorado Health Sciences Center, Denver, CO). Rat striatal GABAergic M213-20 cell line was a generous gift from Dr. William Freed (National Institute on Drug Abuse, National Institutes

of Health, Baltimore, MD). Mouse dopaminergic MN9D cell line was a kind gift from Dr. Syed Ali (National Center for Toxicological Research/FDA, Jefferson, AR). Rat pheochromocytoma PC12 dopaminergic cell line and human dopaminergic neuroblastoma SH-SY5Y cell line were obtained from the American Type Culture Collection (ATCC, Rockville, MD). N27 and PC12 cells were cultured as described (Zhang et al., 2007c). M213-20, MN9D, and SH-SY5Y cells were grown in Dulbecco's modified Eagle's medium supplemented with 10% fetal bovine serum, 2 mM L-glutamine, 50 units penicillin, and 50 units streptomycin.

To generate a stable cell line expressing the human wild-type αsyn, N27 cells were stably transfected with pCEP4-αsyn or pCEP4 empty vector by Lipofectamine Plus reagent according to the procedure recommended by the manufacturer and described (Kaul et al., 2005a). The stable transfectants were selected in 400 µg/ml of hygromycin and further maintained in 200 µg/ml of hygromycin added to N27 growth media.

Animals

Transgenic mice (stock number 008389) that express human wild-type αsyn under the control of the Thy-1 promoter (Andra et al., 1996) and non-carrier littermate control mice were purchased from the Jackson Laboratory (Bar Harbor, Maine). This line of transgenic animals has been characterized previously (Chandra et al., 2005). It expresses high levels of αsyn throughout the brain, but unlike some mutant transgenic lines, it does not display the Parkinson's like phenotype. Six- to eight-week-old male transgenic and non-carrier control mice were housed in standard conditions: constant temperature (22±1°C), humidity (relative, 30%), and a 12 h light/dark cycle with free access to food and water. Animal care procedures

strictly followed the NIH Guide for the Care and Use of Laboratory Animals and were approved by the Iowa State University IACUC.

Immunoblotting and immunoprecipitation

Cell lysates were prepared as described previously (Zhang et al., 2007c). Nuclear and cytoplasmic extracts were isolated using the NE-PER nuclear and cytoplasmic extraction kit (Thermo Scientific, Waltham, MA). The protein concentrations were determined with the Bradford protein assay kit at 595 nm. Immunoblotting and densitometric analysis of immunoblots were performed as described previously (Kanthasamy et al., 2006). Briefly, the indicated protein lysates containing equal amounts of protein were fractionated through a 7.5%-15% SDS-polyacrylamide gel and transferred onto a nitrocellulose membrane (Bio-Rad Laboratories). Membranes were blotted with the appropriate primary antibody and developed with HRP-conjugated secondary antibody followed by ECL detection. IRDye800 anti-rabbit or Alexa 680-conjugated anti-mouse antibodies were also used as secondary antibodies. The immunoblot imaging was performed with either a Kodak image station IS2000MM (Kodak Molecular Imaging System, Rochester, NY) or an Odyssey infrared imaging system (Li-cor, Lincoln, NE), and data were analyzed using one-dimensional image analysis software (Kodak Molecular Imaging System) or Odyssey software 2.0 (Li-cor). Blots were stripped and re-probed with anti-β-actin antibody as an internal control for loading.

For immunoprecipitation studies, briefly, cells were lysed in immunoprecipitation buffer (50 mM Tris-HCl, pH 7.4, 150 mM NaCl, 1 mM EDTA, 10 mM NaF, 1% Trition X-100, 1 × halt protease inhibitor cocktails), and the resultant lysates were incubated on ice for 15 min followed by centrifugation at 16,000 × g for 15 min. The supernatant fractions

were then pre-cleared with protein A or protein G beads for 30 min at 4°C followed by centrifugation at 16,000 × g at 4 °C for 10 min. Five microgram of the indicated antibody along with 50 µl of 50% of protein A or protein G beads was added to the cell lysates and incubated overnight at 4 °C on a rotator. The immunoprecipitates were collected, washed extensively with cold PBS, and prepared for SDS/PAGE gel by addition of 2 × SDS sample buffer and then boiling for 10 min.

Transfections and infections

Transient transfections of αsyn-expressing and vector control N27 cells with promoter reporter were performed using Lipofectamine 2000 reagent in accordance with the manufacture's protocol. Cells were plated in 6-well plates at 4×10^5 cells/well one day before transfection. Four microgram of pGL3-PKCδ construct or pGL3-Basic empty vector was transiently transfected, and 0.5 µg of β-galactosidase vector (pcDNA3.1-βgal, Invitrogen) was added to each well to monitor transfection efficiencies. Twenty-four h post-transfection, the cells were lysed in 200 µl of report lysis buffer (Promega). Luciferase activity was measured on a luminometer (Reporter Microplate, Turner Designs, Sunnyvale, CA) using the Luciferase assay kit (Promega), and β-galactosidase activity was detected using the β-galactosidase assay kit (Promega). The ratio of luciferase activity to β-galactosidase activity was used as a measure of normalized luciferase activity.

Electroporation of small interfering RNAs (siRNAs) was conducted by using a Nucleofector device and the Cell line nucleofector kit (all from Lonza, Walkersville, MD) following the manufacturer's instructions. Specific αsyn siRNA (#16708) and scrambled

negative control siRNA (#4611) were purchased from Ambion (Austin, TX). The p300-specific siRNA (#SI02989693) was purchased from Qiagen. The NFκB-p65-specific siRNA as described (Chen et al., 2006) was synthesized by Integrated DNA Technologies (Coralville, IA). The siRNA sequence for αsyn is 5'-GCAGGAAAGACAAAAGAGGtt-3' and for NFκB-p65 is 5'-GCAGUUCGAUGCUGAUGAAUU-3'. In each electroporation, 2 × 10^6 cells were resuspended in 100 μl of the electroporation buffer supplied with the kit, along with 1.3 μg of gene-specific siRNA or scrambled negative siRNA. The sample was then electroporated using the pre-set nucleofector program #A23 recommended by the manufacture. After electroporation, the cells were immediately transferred to pre-warmed culture medium. The next day media were replaced to normal growth media. Mock transfection with electroporation buffer alone was also included as a transfection control. After 72 h or 96 h from the initial transfection, the cell lysates were collected and analyzed using Western blotting to confirm the extent of αsyn, NFκB-p65, p300, and PKCδ expression. Where indicated, the cell nuclear extracts were prepared and used for EMSA analysis.

Lentiviral constructs (pLenti-V5-PKCδ, pLenti-V5-αsyn, or control construct pLenti-V5-LacZ) were packaged into virus *via* transient transfection of the 293FT packaging cell line (Invitrogen) using Lipofectamine 2000 reagent, as described (Cooper et al., 2006). The lentivirus in the medium was collected by centrifuging at 72 to 96 h post-transfection. All transductions were performed at a multiplicity of infection (MOI) of 1 in the presence of polybrene (6 μg/ml). To assess the effect of transient human αsyn overexpression on PKCδ expression, N27 cells were infected with lentiviral particles encoding V5-αsyn or V5-LacZ for 48 h and collected for immunoblot analysis. To test the effects of restoring PKCδ

expression on MPP^+ neurotoxicity, stable αsyn-expressing and vector control N27 cells were infected with PKCδ or control LacZ lentivirus for 24 h. The cells were then treated with fresh media containing 300 µM MPP^+ for 48 h prior to analysis. In experiments aimed at detecting the expression of pLenti-V5-PKCδ and pLenti-V5-LacZ, the cells were incubated with lentivirus for 48 h and collected for immunoblot analysis.

Caspases-3 activity and DNA fragmentation assays

Caspases-3 activity was measured as previously described (Kaul et al., 2005a). Briefly, after treatment with 300 µM MPP+, cells lysates were prepared and incubated with a specific fluorescent substrate, Ac-DEVD-AMC (50 µM) at 37 °C for 1 h. Caspases-3 activity was then measured using a SpectraMax Gemini XS Microplate Reader (Molecular Devices, Sunnyvale, CA) with excitation at 380 nm and emission at 460 nm. The caspase-3 activity was calculated as fluorescence units per milligram of protein.

DNA fragmentation assay was performed using a Cell Death Detection ELSA plus kit as previously described (Anantharam et al., 2002). Briefly, after treatment with 300 µM MPP+, cells were collected and lysed in 450 µl of lysis buffer supplied with the kit for 30 min at room temperature, and spun down at 2300 × g for 10 min to collect the supernatant. The supernatant was then used to measure DNA fragmentation as per the manufacture's protocol. Measurements were made at 405 and 490 nm using a SpectraMax 190 spectrophotometer (Molecular Devices).

Immunostaining and microscopy

After perfusion with 4% paraformaldehyde, the mice brains were removed,

immersion fixed in 4% paraformaldehyde, and cryoprotected in sucrose. Then the brain was cut on a microtome into 20 μm sections. Sections from substantia nigra were used for dual-labeled immunofluorescence. After washing with PBS, the brain sections were rinsed with blocking buffer containing 2% BSA, 0.05% Tween-20, and 0.5% Triton X-100 in PBS for 45 min and then incubated overnight at 4°C with the following combinations of primary antibodies: anti-PKCδ (1:250, Santa Cruz) and anti-TH (1:1800, Chemicon), or anti-p300 (1:350, Santa Cruz) and anti-TH (1:1800, Chemicon), followed by incubation with anti-rabbit Alexa 568-conjugated (red, 1:1000) and anti-mouse Alexa 488-conjuated secondary antibodies (green, 1:1000) for 1 h at room temperature. After this, Hoechst 33342 (10 μg/ml) was added for 3 min at room temperature to stain the nucleus. The brain sections were mounted and observed with either an oil-immersion 63× PL APO lens with a 1.40 numerical aperture or an oil-immersion 100× PL APO lens with a 1.40 numerical aperture using a Leica SP5 X confocal microscope system (all from Leica, Allendale, NJ) at Confocal Microscopy and Image Analysis Facility at Iowa State University. For final output, images were processed using LAS-AFlite software (Leica). For computer-assisted image analysis, a 0.051 mm^2 area was delineated using this LAS-AFlite software and TH-PKCδ colocalized dopaminergic neurons were counted independently and blindly by two investigators. Data were expressed as either percent of TH-positive cells containing PKCδ immunoreactivity/total TH neurons or number of TH-positive cells containing PKCδ immunoreactivity/area (mm^2).

Immunostaining of PKCδ, TH, and αsyn was performed in primary mesencephalic neurons, αsyn-expressing and vector control N27 cells. Cells grown on coverslips pre-coated with poly-L-lysine or poly-D-lysine were washed with PBS and fixed in 4%

paraformaldehyde for 30 min. After washing, the cells were permeabilized with 0.2% Triton X-100 in PBS, washed with PBS, and blocked with blocking agent (5% bovine serum albumin, 5% goat serum in PBS). Cells were then incubated with the antibody against human αsyn (1:500, Santa Cruz), TH (1:1800, Chemicon), and PKCδ (1:1000, Santa Cruz) overnight. Fluorescently conjugated secondary antibody (Alexa-488-conjugated anti-mouse antibody, green, 1:1500, or Alexa 568-conjugated anti-rabbit antibody red, 1:1500) was used to visualize the protein. Nuclei were counterstained with Hoechst 33342 for 3 min at a final concentration of 10 μg/ml. Finally, images were viewed using an oil-immersion 60 × Plan Apo lens with a 1.45 numerical aperture on a Nikon inverted fluorescence microscope (model TE2000, Nikon, Tokyo, Japan). Images were captured with a SPOT color digital camera (Diagnostic Instruments, Sterling Heights, MI) and processed using Metamorph 5.07 image analysis software (Molecular Devices). For quantitative analysis of immunofluorescence, we measured average pixel intensities from the region of interest (ROI) using the Metamorph 5.07 image analysis software.

Pulse-chase assays

Before pulse-labeling, cells were starved of methionine for 30 min. Cells were subsequently pulse-labeled with methionine-free RPMI 1640 medium containing 125 μCi/ml [35S]-methionine for 2 h. Afterwards, cells were rinsed twice with warm PBS, and chased in complete growth medium for various times up to 48 h. At different chase times, the cells were collected and subsequently subjected to immunoprecipitation using PKCδ antibody as described above. The immunoprecipitates were separated with 10% SDS-PAGE and analyzed by autoradiography at 24-48 h using a PhosphoImager (Personal Molecular Imager

FX, Bio-Rad Laboratories). Band quantifications were processed using Quantity One 4.2.0 software (Bio-Rad Laboratories).

RT-PCR and methylation-specific PCR (MSP)

Total RNA was isolated and converted to cDNA using Absolutely RNA miniprep kit from Stratagene (La Jolla, CA) and High capacity cDNA archive kit from Applied Biosystems (Foster City, CA), respectively. For semiquantitative RT-PCR, 1 μl of the reverse transcriptase reaction mixture served as a template in PCR amplification. PCR amplifications were performed using the following program: 94 °C for 3 min; 35 cycles of 94 °C for 45 sec, 56 °C (PKCδ, η, and λ) or 60 °C (PKCα, ε, ζ, and GAPDH) for 30 sec, 72 °C for 45 sec. PCR products were then separated by electrophoresis in 1-2% agarose gel and visualized by ethidium bromide staining.

Quantitative real-time RT-PCR was performed using Brilliant SYBR Green QPCR Master Mix kit and the Mx3000P QPCR system (all from Stratagene). The p300 primer set was using a QuantiTect Primers assay (Qiagen, #QT01083859). The β-actin was used as an internal control for RNA quantity (sequence is listed in supplemental Table 1). The reaction mixture included 1 μl of cDNA (100 ng RNA used), 12.5 μl of 2 × master mix, 0.375 μl of reference dye, and 0.2 μM of each primer. Cycling conditions contained an initial denaturation at 95 °C for 10 min, followed by 40 cycles of 95 °C for 30 sec, 60 °C for 30 sec, and 72 °C for 30 sec. Fluorescence was detected during the annealing/extension step of each cycle. Dissociation curves were run to verify the singularity of the PCR product. The data were analyzed using the comparative threshold cycle method. Briefly, the relative PKCδ expression (expressed as fold differences) between αsyn-expressing and vector control N27

cells was calculated as 2-(ΔCtSYN - ΔCtVEC), where ΔCt represented the mean Ct value of PKCδ or p300 after normalization to β-actin internal control.

For MSP experiments, genomic DNA was isolated from αsyn-expressing and vector control N27 cells using the DNeasy blood & tissue kit as mentioned earlier. Bisulfite modification was subsequently carried out on 500 ng of genomic DNA by the MethylDetector bisulfite modification kit (Active Motif, Carlsbad, CA) according to the manufacturer's instructions. Two pairs of primers were designed to amplify specifically methylated or unmethylated PKCδ sequence using MethPrimer software (Li and Dahiya, 2002). The cycling condition was: 94 °C for 3 min, after which 35 cycles of 94 °C for 30 sec, 52.5 °C for 30 sec, 68 °C for 30 sec, and finally 72 °C for 5 min. PCR products were loaded onto 2% agarose gels for analysis. Negative control PCRs were performed using water only as template.

Assessments of mRNA stability

The PKCδ mRNA decay experiments were conducted as described (Jing et al., 2005) with some modification. Briefly, cells were treated with 5 μg/ml actinomycin D to block de novo transcription, total RNA were isolated at selected time points thereafter, and the amount of PKCδ mRNA was determined by quantitative real-time RT-PCR. The PKCδ mRNA values were normalized to the amount of β-actin internal control in each sample and expressed as the percentage of mRNA levels present at time 0 (set to 100%) prior to the addition of actinomycin D.

Nuclear run-on assays

The nuclear run-on assays were performed with minor modifications to the method described by (Patrone et al., 2000). Nuclei were prepared from 60 × 106 cells by resuspending in 4 ml of Nonidet P-40 lysis buffer (10 mM Tris-HCl, pH 7.4, 3 mM MgCl2, 10 mM NaCl, 150 mM sucrose and 0.5 % Nonidet P-40), and a 5-min incubation in ice followed. Nuclei were isolated by centrifugation, washed with cell lysis buffer devoid of Nonidet P-40, and the pellets were resuspended in 100 µl of freezing buffer (50 mM Tris-HCl, pH 8.3, 40 % glycerol, 5 mM MgCl2 and 0.1 mM EDTA). One volume of transcription buffer (200 mM KCl, 20 mM Tris-HCl, pH 8.0, 5 mM MgCl2, 4 mM dithiothreitol, 4 mM each of ATP, GTP and CTP, 200 mM sucrose and 20% glycerol) was added to nuclei. Eight µl of biotin-16-UTP was then supplied to the mixture. After incubation for 30 min at 29 °C, the reaction was terminated and total RNA was purified using the Absolutely RNA miniprep kit according to the manufacturer's instructions. RNA was eluted in 60 µl of nuclease-free water and 10 µl was saved as total nuclear RNA. Dynabeads M-280 (50 µl) was subsequently used to capture the run-on RNA. Three µl of run-on RNA or 10 µg total nuclear RNA was subjected to cDNA synthesis and quantitative real-time PCR as described above. To monitor undesired RNA capture by Dynbeads, control reactions were also performed in which conditions were identical except that UTP was added to the transcription system in the place of biotin-16-UTP.

Electrophoretic mobility shift assays (EMSA)

Nuclear and cytoplasmic proteins were prepared using the NE-PER nuclear and cytoplasmic extraction kit as described before. The IRyeTM700-labeled oligos PkcδNFκBs

and NFκB, corresponding to the NFκB-like sequences within the rat PKCδ promoter and the consensus sequence of NFκB respectively, were synthesized by Li-cor and used as labeled probes. The unlabeled competitor oligos were obtained from Integrated DNA Technologies. All oligos sequences are illustrated in supplemental Table 5. Protein-DNA binding reactions were performed with 5-10 μg of nuclear or cytoplasmic proteins, 1 μl of labeled oligonucleotide (50 fmol) in a total volume of 20 μl of mixture containing 10 mM Tris-HCl (pH 7.5), 50 mM NaCl, 0.25% Tween-20, 2.5 mM dithiothreitol (DTT), 0.05 mM EDTA, and 1 μg of poly (dI-dC). After incubation at room temperature for 20 min, the resulting DNA-protein complexes were resolved on a 6.6% non-denaturing polyacrylamide gel at 10 V/cm for about 50 min at 4 °C in 1 × TGE buffer. Gels were analyzed on the Odyssey infrared imaging system (Li-cor). In competition experiments, before the addition of the labeled probe, nuclear extracts were pre-incubated for 30 min at room temperature with a 100-fold molar excess of unlabeled competitor oligos. In super shift experiments, 400 ng of anti-p50, anti-p65, or normal rabbit IgG was incubated with nuclear extracts for 30 min at room temperature prior to the addition of labeled probe.

Histone acetyltransferase activity assays

p300 HAT activity was measured using a p300/CBP immunoprecipitation HAT assay kit from Millipore following the manufacture's protocol with minor modifications as previously described (Nakatani et al., 2003). Briefly, one milligram of nuclear extracts from αsyn-expressing and vector control N27 cells were precipitated with 5 μg of anti-p300 antibody or normal mouse IgG and 50 μl of magnetic protein-G beads (Active Motif) at 4°C overnight. The collected beads were washed with three times cold PBS and incubated with

HAT assay cocktail (50 µl) containing 10 µl of core histones and 100 µM [3H]acetyl-CoA (0.5 µCi/µl) at 30 °C for 30 min. Fifteen µl of the supernatant of eachsample was placed on P81 square papers and [3H]acetyl incorporation into the substrates was measured using a scintillation counter. Data were expressed as mean values of counts, subtracted from background values measured in samples containing normal mouse IgG.

Chromatin immunoprecipitation assays (ChIP)

The ChIP-IT Express enzymatic kit from Active Motif was used to analyze the *in vivo* binding of NFκB p65 and p50 subunits, and p300/CBP co-activators onto the rat PKCδ promoter region. Unless otherwise stated, all reagents, buffers, and supplies were included in the kit. The ChIP assays were performed following the manufacture's instructions with slight modifications. Briefly, ~1.5×10^7 cells were fixed in 1% formaldehyde for 10 min at room temperature. After cross-linking, the nuclei were prepared and chromatin was enzymatic digested to 200-1500 bp fragments (verified through running on a 1% agarose gel) by incubation with the enzymatic shearing cocktail for 12 min at 37 °C. The sheared chromatin was collected by centrifuge, and a 10-µl aliquot was saved as an input sample. Aliquots of 70-µl sheared chromatin were incubated overnight with rotation at 4 °C with protein G magnetic beads and three µg indicated antibody. Equal aliquots of each chromatin sample were saved for no-antibody controls. After extensive washing, reversal of cross-links, and proteinase K digestion, the elute DNA in the immunoprecipitated samples was directly collected on a magnetic stand, and the input DNA was purified by phenol/chloroform extraction and ethanol precipitation. The DNA samples were analyzed by PCR using primer pairs designed to amplify a region (-103 to +60) within PKCδ promoter. Conditions of linear

amplification were determined empirically for the primers. PCR conditions are as follows: 94 °C 3 min; 94 °C 20 sec, 58 °C 30 sec, and 72 °C 30 sec for 35 cycles. The PCR products were resolved by electrophoresis in a 1.0% agarose gel and visualized after ethidium bromide staining.

Bioinformatics

CpG island identification was analyzed with the web-based program CpG Island Searcher (Takai and Jones, 2002). This program defines a CpG island as a region with a G+C content ≥ 50%, longer than 200 bp nucleotides, and an Observation/Expectation CpG ratio > 0.6. The search for the phylogenetic sequence conservation among rat, human, murine, and cow PKCδ promoter was conducted with the DiAlign professional TF Release 3.1.1 (DiAlign TF) (Morgenstern et al., 1996; Morgenstern et al., 1998) (Genomatix Software, Munich, Germany). This program identifies common transcription factor binding sites matches located in aligned regions though a combination of alignment of input sequences using multiple alignment program DiAlign (Morgenstern et al., 1996; Morgenstern et al., 1998) with recognition of potential transcriptional factor binding sites by MatInspector software (Cartharius et al., 2005) (Genomatix Software), which employed matrices library version 8.0. The nucleotide distribution matrix information listed in supplemental Table 4 was obtained through the use of the MatBase program (Genomatix Software).

Data analysis

All statistical analyses were performed using the Prism 4.0 software (GraphPad Software, San Diego, CA). In PKCδ protein and mRNA degradation experiments, a

one-phase exponential decay model was fitted to each data set using the nonlinear regression analysis program of Prism 4.0 software as follows: $Y = Span\ e^{-Kt} + Plateau$, where Y starts at Span + Plateau and decays with a rate constant K. The half-life of the each mRNA or protein was subsequently determined by 0.693/K. The goodness-of-fit was assessed as the square of the correlation coefficient (R^2). Data were analyzed either by Student's t test or one-way ANOVA followed by Tukey's pairwise multiple comparison test. Statistical significance was defined as $p<0.05$.

Results

Expression of human α-synuclein in N27 dopaminergic cells down-regulates PKCδ expression in an isoform-specific manner

We previously reported that PKCδ serves as a key proapoptotic effector in dopaminergic neurons, and caspase-3-mediated proteolytic cleavage of PKCδ is a key mediator in multiple models of dopaminergic neurodegeneration (Anantharam et al., 2002; Kaul et al., 2003; Yang et al., 2004; Kaul et al., 2005b; Kanthasamy et al., 2006; Zhang et al., 2007a). Growing evidence indicates that the neuroprotective mechanism of endogenous αsyn involves deregulation of gene expression of specific stress-signaling molecules linked to neuronal survival (Alves Da Costa et al., 2002; Hashimoto et al., 2002; Manning-Bog et al., 2003; Albani et al., 2004). Analysis in a variety of cell lines, MN9D, N27, PC12, M213-20, and SH-SY5Y, revealed a striking inverse correlation between PKCδ and αsyn protein levels (Supplemental Fig. 1). These observations raised the question of whether αsyn might regulate PKCδ expression and thereby promote cell survival. To address this hypothesis, we

engineered rat-immortalized mesencephalic dopaminergic N27 cell line to express human wild-type αsyn by stably transfecting with plasmid pCEP4-αsyn or pCEP4 control vector. The widely used N27 neuronal cell model represents a homogeneous population of TH-positive dopaminergic cells and is highly useful for studying degenerative mechanisms in PD (Clarkson et al., 1999; Kaul et al., 2005b; Peng et al., 2005a; Zafar et al., 2007; Zhang et al., 2007c; Lee et al., 2009). The stable expression of human αsyn in stable N27 cells was assessed by Western blot assay using the αsyn antibody (Syn-1) that detects both exogenously expressed human αsyn and endogenous rat αsyn. As shown in Fig. 1*A*, the αsyn endogenous level was too low to be detected in vector control N27 cells, whereas exogenously expressed αsyn could readily be detected in the αsyn-expressing N27 cells. Importantly, the level of αsyn achieved in αsyn-expressing N27 cells appears to be within the physiological range, as this level was comparable to that seen in the rat brain substantia nigra (rSN) homogenates (Fig. 1*A*). Further analysis of subcellular localization of αsyn in the stable cells demonstrated that αsyn is exclusively in the cytoplasm but absent in the nucleus (Supplemental Fig. 2). We next determined whether αsyn affects PKCδ expression. Western blot analysis (Fig. 1*B*, left panel) of various PKC isoforms showed a selective suppression of PKCδ in αsyn-expressing N27 cells. Quantitative analysis showed that αsyn caused a ~50% reduction in PKCδ protein levels, whereas PKCα, βI, and ζ were not affected (Fig. 1*B*, right panel). To further determine whether this specific inhibition occurred at the mRNA level, semiquantitative RT-PCR (primer sequences are listed in supplemental Table 1) was carried out (Fig. 1*C*, left panel). Similar to the trend seen in protein levels, only PKCδ mRNA expression was markedly reduced by αsyn. qRT-PCR analysis revealed a dramatic ~80%

reduction in PKCδ mRNA in αsyn-expressing N27 cells (Fig. 1*C*, right panel). To ensure the observed down-regulation of PKCδ gene expression in these two stable cell lines was not an artifact from the selection or maintenance of stable transfectants, we examined the PKCδ expression in transiently transduced N27 cells. As shown in Fig. 1*D*, transient transduction of N27 cells with lentivirus encoding human wild-type αsyn-V5 fusion also resulted in a dramatic decrease in expression of PKCδ gene compared with control lentivirus (lacZ-V5)-infected cells. Taken together, these data demonstrate that αsyn is capable of repressing the PKCδ isoform in N27 dopaminergic cells.

Dysregulation of PKCδ by α-synuclein protects against MPP^+-induced cell death in dopaminergic N27 cells

After we identified that increased αsyn inhibits the steady-state level of PKCδ, we investigated the significance of PKCδ downregulation by αsyn. Previously, we established the proapoptotic function of PKCδ in dopaminergic neurons using siRNA and dominant negative PKCδ mutants (Yang et al., 2004; Kitazawa et al., 2005; Latchoumycandane et al., 2005). In the present study, we employed a lentivirus encoding PKCδ fused to the V5 epitope (PKCδ-V5) to markedly overexpress PKCδ and investigated whether PKCδ gain of function influences the neurotoxicity in N27 cells following MPP^+ treatment. The increased expression of PKCδ after lentiviral infection compared with control lentivirus-infected cells (LacZ) was confirmed by Western blot assay (Supplemental Fig. 3). The extent of MPP^+-induced apoptosis was measured by DNA fragmentation (Fig. 2*A*, left panel) and caspase-3 enzymatic activity (Fig. 2*A*, right panel) analysis. In LacZ control-infected

cultures, αsyn-expressing N27 cells almost completely suppressed MPP^+-induced DNA fragmentation and caspase-3 activity as compared to vector control N27 cells. Importantly, introduction of PKCδ significantly increased MPP^+-induced DNA fragmentation ($p<0.01$) and caspase-3 activity ($p<0.05$) in αsyn-expressing N27 cells. These results suggest that downregulation of PKCδ by αsyn is protective. In further support of these data, MPP^+-induced PKCδ proteolytic cleavage and its nuclear translocation, events associated with apoptosis (Anantharam et al., 2002; DeVries et al., 2002; Kaul et al., 2003; Kaul et al., 2005b), were almost completely diminished in αsyn-expressing N27 cells compared to vector control N27 cells (Fig. 2*B*).

Next, we examined the localization of αsyn in the stable cells following MPP^+ treatment. As shown in Fig. 2*C*, the exclusive localization of αsyn in the cytoplasm was not affected by MPP^+, as determined by Western blot and immunostaining. Interestingly, a recent study demonstrates that subcellular localization of αsyn may contribute to its neurotoxicity: nuclear localization of αsyn promotes apoptosis whereas cytoplasmic localization of αsyn protects cells (Kontopoulos et al., 2006). Taken together, these results support a model in which αsyn acts in the cytoplasm to protect against MPP^+-induced dopaminergic cell death *via* negative regulation of the proapoptotic kinase PKCδ expression.

Increased α-synuclein expression in an animal model is associated with decreased PKCδ levels within nigral dopaminergic neurons

We further extend our findings from a dopaminergic cell culture model to an animal model. Since recent studies conducted in our laboratory demonstrated that PKCδ is expressed

in dopaminergic neurons in nigral regions of the brain (Zhang et al., 2007c), we decided to determine whether an inverse relationship between αsyn and PKCδ expression in nigral dopaminergic neurons existed in vivo. For this purpose, we carried out immunohistological studies in transgenic mice that overexpress wild-type human αsyn (htg) and in non-transgenic control (non-tg) mice. This transgenic line has been characterized previously (Chandra et al., 2005); it expresses high levels of αsyn throughout the brain under the regulatory control of the Thy-1 promoter, and unlike some similar mutant transgenic lines, it does not display the Parkinson's like phenotype upon aging. This mouse line also displayed a dramatic resistance to the neurodegeneration caused by deletion of cysteine-string protein-α (CSPα) (Chandra et al., 2005). The effects of overexpression of αsyn on PKCδ expression within nigral dopaminergic neurons were studied by double-immunostaining nigral tissues for TH (marker of dopaminergic neurons) and PKCδ. As shown in Fig. 3A, a strong PKCδ immunoreactivity (stained in red) was observed in control mice in the cytoplasm of TH-expressing neurons (stained in green). Moreover, the majority of the TH neurons displayed co-localization of TH and PKCδ (yellow color in the merged panel). In contrast, the αsyn transgenic mice exhibited a significant decrease in PKCδ immunoreactivity within TH neurons as well as significant loss of the corresponding co-localization of TH and PKCδ. Quantitative analysis of TH-PKCδ co-localized dopaminergic neurons relative to the number of total TH neurons showed that >70% of TH-positive cells lost their PKCδ expression in αsyn transgenic mice (Fig. 3B) as compared to control mice. Similar results were obtained by quantifying TH-PKCδ co-localized dopaminergic neurons in a delineated area (Supplemental Fig. 4). Western blot analysis confirmed a ~6-fold increase in the levels of

αsyn in the substantia nigra of αsyn transgenic mice (Fig. 3C). Overall, these results establish an in vivo relevance of the relationship between αsyn overexpression and PKCδ expression in dopaminergic neurons.

α-Synuclein attenuates PKCδ promoter activation and transcription efficiency without affecting PKCδ protein turnover or mRNA stability

We next investigated the molecular mechanism underlying the αsyn-induced suppression of PKCδ expression. First, we examined whether αsyn could destabilize PKCδ protein in N27 cells. To this end, we investigated the PKCδ turnover rate by performing a pulse-chase experiment on both αsyn-expressing and vector control N27 cells labeled with [35S]-methionine. αSyn had no effect on PKCδ protein turnover (Fig. 4A). The relative half-life of PKCδ was estimated to be 14.77 h in vector control and 14.07 h in αsyn-expressing N27 cells (Supplemental Table 2), an insignificant difference between the two cells. We also considered the possibility that αsyn might directly alter the PKCδ mRNA instability. To address this possibility, we measured PKCδ mRNA half-life by treating cells with the transcription inhibitor ActD for 0-12 h, and quantified PKCδ mRNA by qRT-PCR (Fig. 4B). The relative half-life of PKCδ mRNA was about 2 h in vector control cells, and the decay continued thereafter. Notably, overexpression of αsyn did not change the relative half-life of PKCδ mRNA (Supplemental Table 3). Taken together, these results demonstrate that αsyn-induced suppression of PKCδ is not due to altered rate of PKCδ protein or mRNA decay, suggesting that there are no post-transcriptional effects of αsyn on PKCδ expression.

We therefore turned our attention to transcriptional steps that could mediate the reduction in PKCδ via αsyn. We first examined whether αsyn caused a decrease in the PKCδ promoter activity. For this, a 1.7 kb (-1700/+22, relative to the transcription start site) region of the rat PKCδ promoter was amplified and cloned into the pGL3-Basic reporter vector. The promoter activity was then studied by transfecting αsyn-expressing and vector control N27 cells with the reporter construct pGL3-PKCδ carrying PKCδ promoter. As shown in Fig. 4C, compared with vector control cells, αsyn resulted in a significant decrease ($p<0.001$) in luciferase activity, suggesting that αsyn-induced suppression of PKCδ is most likely mediated at the level of transcription.

Next, we employed a nuclear run-on assay to investigate the effects of αsyn on PKCδ transcriptional rate. In this assay, nuclei were isolated from either αsyn-expressing or vector control N27 cells and used with the reaction containing biotin-16-UTP. We also prepared nuclei from vector control cells and incubated without biotin-16-UTP as a negative control for the run-on reaction. After the transcriptional reaction, total nuclear RNA was extracted, and then biotinylated RNA was isolated using Streptavidin magnetic beads. qRT-PCR analysis was conducted with the biotinylated RNA and total nuclear RNA pools. Fig. 4D shows the representative amplification plots for PKCδ mRNA (left panel) and β-actin mRNA (right panel). The amount of biotinylated PKCδ mRNA generated in nuclei from αsyn-expressing cells was lower than that obtained from vector control cells, but β-actin mRNA levels were nearly identical, indicating that αsyn specifically inhibits the PKCδ transcriptional rate. Quantitative analysis showed a significant reduction ($p<0.001$) in the PKCδ transcription efficiency in αsyn-expressing cells (Fig. 4E). Collectively, the results of

the run-on experiment, combined with the promoter reporter analysis, strongly suggest the involvement of a transcriptional repression mechanism in the regulation of PKCδ expression. In addition, we also explored the possibility that epigenetic mechanisms such as DNA methylation (Supplemental Fig.5A) may be responsible for the α-syn-induced reduction in PKCδ. Examination of the methylation status of the rat PKCδ promoter by MSP analysis (Supplemental Fig. 5B) revealed an identical methylation pattern in α-syn-expressing and vector cells, suggesting that the hypermethylation mechanism is less likely to be involved in the repression of PKCδ.

Increased α-synuclein expression suppresses PKCδ in part by blocking NFκB activation

To further explore the mechanism of αsyn inhibition of the PKCδ promoter activity, the rat PKCδ proximal promoter (-178 to +22) was aligned for comparison with the homologous sequences from the murine, human, and bovine genome (Supplemental Fig. 6). Murine PKCδ and human PKCδ promoters were well conserved from 89% to 71% compared with rats, although the same region was less conserved in the bovine PKCδ gene (59%). Further analysis revealed six highly conserved transcription factor binding sites (TFBS) in the proximal promoter (Supplemental Fig. 6 and supplemental Table 4). Among these conserved TFBS, the most notable were two potential NFκB binding sites (Supplemental Fig. 6), located at positions -20 to -8 (designated as PkcδNFκB1) and -50 to -38 (designated as PkcδNFκB2). They are in close proximity, providing an enticing platform for NFκB binding and transactivation of the PKCδ gene. Additionally, a previous report indicated that NFκB may be involved in mouse PKCδ expression (Suh et al., 2003). Therefore, we carried out detailed studies on the role of these two κB sites in the regulation of basal PKCδ expression

in N27 cells and also elucidated whether NFκB plays a role in αsyn-mediated downregulation of PKCδ expression. To determine if these sites were able to bind NFκB, we performed EMSA using PKCδ promoter's κB site sequence as a probe and nuclear extracts from vector cells as a source of NFκB (oligonucleotides sequences used in EMSA are listed in supplemental Table 5). As shown in Fig. 5A, in the absence of nuclear extract, the labeled probe is detected as free probe migrating at the gel front (lane 1). In contrast, in the presence of nuclear extract, an intense shifted band is seen in EMSA using PkcδNFκB1 (left panel) or PkcδNFκB2 (right panel) as a probe (Fig. 5A, lane 2). Sequence specificity of the DNA-protein complex was shown by competition with excess of selected unlabeled oligos. The addition of excess unlabeled self oligos, or NFκB consensus oligos, resulted in the ablation of this DNA-protein complex (Fig. 5A, lane 3 and 5). However, an excess of unlabeled mutant PkcδNFκB oligos, or unrelated AP1 consensus oligos, did not interrupt the binding of nuclear proteins (Fig. 5A, lane 4 and 6). In addition, parallel EMSA using NFκB consensus sequence as probe also confirmed that the PKCδ promoter-specific κB sites can compete efficiently against the NFκB consensus sequence for binding NFκB (Supplemental Fig. 7). Thus, these data clearly demonstrate that the PKCδ promoter has two functional NFκB binding sites.

To further characterize NFκB binding to the PKCδ promoter, we performed supershift assay using PkcδNFκB1 as a probe and nuclear extracts from vector cells. As shown in Fig. 5B, in the absence of antibodies, NFκB binding to the PkcδNFκB1 probe was again observed (lane 1), and competition with an excess of self oligos was included as an internal control (lane 2). In the presence of anti-p65 antibody, the protein-DNA complex was interrupted, and a specific supershift band was formed (lane 4). This effect was also observed

with the complete ablation of protein-DNA complex and the formation of an intense supershift band when we added anti-p65 and anti-p50 together (lane 5). In the presence of anti-p50 antibody alone, however, no supershift was formed but the protein-DNA complex was significantly reduced (lane 3). The lack of a clear supershift with p50 antibody may be due to the interruption of the formation of protein-DNA complex by exposure to a specific antibody (Gustin et al., 2004). Normal rabbit IgG antibody displayed no effect on the formation of the protein-DNA complex. Thus, our data demonstrated that NFκB is constitutively activated in N27 cells, and that the activated NFκB bound to the PKCδ promoter comprised of a p50/p65 heterodimer.

If αsyn inhibits the PKCδ promoter activity through the NFκB cis-elements at the PKCδ promoter, we should see a decrease in the NFκB-DNA complex in αsyn-expressing cells. As expected, the nuclear extracts (both 5 μg and 10 μg) from αsyn-expressing cells exhibited reduced DNA binding activity to the PkcδNFκB1 probe as compared with vector control cells (Fig. 5C). A similar result was obtained when the labeled PkcδNFκB2 probe was used (Supplemental Fig. 8). In addition, the binding reaction with cytosolic extracts was also performed as an internal control, in which no NFκB-DNA complex formed because NFκB is sequestered in the cytoplasm in an inactive form by interaction with IκB (Supplemental Fig. 8). Based on these findings, we then carried out a ChIP assay to analyze the effect of αsyn on NFκB activation in vivo. As shown in Fig. 5D, αsyn expression diminished endogenous binding of both p65 and p50 to the PKCδ promoter. No detectable signal was observed in the absence of antibody in the immunoprecipitation process. To further confirm the inhibitory effect of αsyn on NFκB transactivation, parallel studies

employing RNA interference to down-regulate αsyn were performed. For this study, we transfected siRNA-αsyn (si-αsyn) into αsyn-expressing cells and then examined the NFκB binding to the PKCδ promoter's κB element at 72 h post-transfection. EMSA showed that NFκB activity was dramatically increased in αsyn knockdown samples (Fig. 5E). The efficacy of αsyn-siRNA was evaluated by Western blot (Supplemental Fig. 9), and a 90% reduction in the α-syn level was obtained as compared to the negative control siRNA and mock transfected control. Finally, we characterized the requirement of NFκB for constitutive PKCδ expression in N27 cells. To this end, we utilized NFκB-p65 siRNA to directly inhibit the p65 protein. When N27 cells were transfected with siRNA-p65 (si-p65), a ~56% reduction in the p65 level was observed, correlating with a concomitant ~35% decrease in the PKCδ protein level. However, the negative control siRNA and mock transfection control did not show a significant effect on the levels of p65 or PKCδ proteins (Fig. 5F). Collectively, these results indicate that NFκB plays an important role in PKCδ transactivation in N27 cells, and that αsyn-induced down-regulation of PKCδ expression was mediated, at least in part, by reducing the NFκB binding to κB enhancer elements at the PKCδ promoter.

To further confirm the functional role of NFκB in the regulation of PKCδ gene expression in primary dopaminergic neurons, mouse primary mesencephalic cultures were treated with the NFκB inhibitor SN-50, a cell permeable peptide that blocks NFκB nuclear translocation (de Erausquin et al., 2003), and PKCδ immunoreactivity of TH-positive neurons was analyzed immunocytochemically (Fig. 6). Exposure of primary mesencephalic cultures to SN-50 (100 μg/ml) for 24 h induced a significant reduction in PKCδ immunoreactivity in TH-positive neurons (Fig. 6A). Analysis of fluorescent intensity with

Metamorph Image analysis software revealed a ~70% ($p<0.01$) decrease in PKCδ immunoreactivity in SN-50-treated TH-positive neurons (Fig. 6B). Also, the SN-50 (100 μg/ml) treated culture showed reduced p65 level in the nucleus, confirming the inhibitory effect of SN50 on NFκB activation (data not shown). These results confirm that NFκB is an important regulator of PKCδ expression in cultured substantia nigral neurons, and thus, further analyses were carried out to examine the mechanism of action of αsyn in inhibiting NFκB activity to down-regulate PKCδ expression.

α-Synuclein-induced blockade of NFκB activation is associated with decreased acetylation of p65, but does not correlate with alteration of nuclear translocation or protein levels of NFκB/IκBα

Our next objective was to explore the molecular basis of inhibition of NFκB activity by αsyn. Since αsyn is predominantly located in the cytoplasm (Supplemental Fig. 2), the inhibitory effect of αsyn on NFκB activity may be due to its interaction with NFκB in the cytoplasm, preventing NFκB localization to the nucleus. However, in our experimental conditions, we were unable to detect physical interactions between αsyn and NFκB subunits or IκBα by co-immunoprecipitation analysis (data not shown). It may also be possible for αsyn to indirectly modulate NFκB activity by enhancing the cytoplasmic retention of p50/p65 or altering cellular pools of IκBα. To test this possibility, the subcellular distribution of NFκB p50/p65 and IκBα was compared between αsyn-expressing cells and vector control N27 cells. Surprisingly, αsyn did not have any effect on p50/p65 NFκB subunits or IκBα in both cytoplasmic and nuclear fractions (Fig. 7A). To further determine if reduced

NFκB/DNA binding activity by αsyn resulted from alteration of protein levels of NFκB subunits and IκBα, we analyzed p65, p50, and IκBα by Western blot. As shown in Fig. 7B, the total protein levels of p65, p50, and IκBα were not affected by αsyn either.

Studies were then undertaken to determine whether αsyn-mediated downregulation of NFκB activity might be related to NFκB/p65 acetylation, a nuclear event associated with increased transactivation potential of NFκB and regulated by both p300/CBP HAT and HDAC3 (Chen et al., 2001; Chen et al., 2002). In this experiment, whole cell extracts were immunoprecipitated with a p65 antibody, and acetylated p65 (Ac-p65) was detected by Western blot using an antibody specific for acetylated lysine. Total p65 proteins from immunoprecipitates were then re-probed with the p65 antibody. As shown in Fig. 7C, a ~65kDa acetylated p65 showed no overt differences in acetylated p65, but the total p65 levels immunoprecipitated from αsyn-expressing cells were significantly higher than that from vector control cells, which might be due to the different efficiencies achieved during immunoprecipitation steps. Quantification of normalized data (Ac-p65 over total p65) revealed a significant ($p<0.01$) reduction in Ac-p65 in αsyn-expressing cells compared to vector control cells (Fig. 7C, right panel). To further confirm the role of p65 acetylation in the modulation of PKCδ expression, we employed the HDAC inhibitor sodium butyrate, which increased the acetylation of p65 (Duan et al., 2007), possibly by inhibiting HDAC3. We previously reported that certain neurotoxic insults induce PKCδ cleavage via a caspase-3 dependent manner (Kaul et al., 2003; Kaul et al., 2005b). Since we have found that sodium butyrate markedly induced caspase-3-dependent cleavage of PKCδ in N27 cells (data not shown), a caspase-3-specific inhibitor Z-DEVD-FMK was applied to prevent the sodium

butyrate-induced PKCδ cleavage. After co-treatment with sodium butyrate (1 mM) and Z-DEVD-FMK (50 μM) in αsyn-expressing cells, as expected, total cellular acetylation was significantly enhanced. In particular, two most prominent bands were observed at 15 kD and 10 kD, respectively (Fig. 7D, right panel). In correlation with this finding, sodium butyrate treatment resulted in a time-dependent increase in PKCδ protein levels, whereas it had no such effect on the levels of other PKC isoforms (α, βI, ζ), suggesting that increased cellular acetylation can isoform-specifically up-regulate PKCδ (Fig. 7D, left panel). Taken together, these results suggest that αsyn inhibition of NFκB binding to the PKCδ promoter is associated with decreased acetylation of p65, without alteration of NFκB nuclear translocation, IκBα degradation, or NFκB/IκBα protein levels.

α-Synuclein down-regulates p300 proteins, resulting in decreased p300 HAT activity and inhibition of p300-dependent transactivation of PKCδ expression

Because the acetylation of p65 by HATs p300/CBP plays a crucial role in NFκB activation, we hypothesized that p300/CBP may be a target for αsyn to inhibit p65 acetylation. First, to determine what effect, if any, αsyn would exert on these proteins, we measured levels of p300 and CBP by Western blot. As illustrated in Fig. 8A, the amount of nuclear p300 was strikingly reduced (60%) in αsyn-expressing cells, whereas CBP was unaltered, suggesting a selective decrease in p300 proteins by αsyn. Neither p300 nor CBP can be detected in cytoplasmic fractions as they are predominantly nuclear proteins. To further examine whether the decrease in p300 proteins was at the mRNA level, the p300 mRNA was measured by qRT-PCR analysis. However, p300 transcript levels (Supplemental

Fig. 10) were unaffected by αsyn, suggesting that other mechanisms, such as protein degradation, may be required for the decrease in p300 proteins. Next, we assessed the effect of reduced p300 on its HAT activity. In this experiment, p300 HAT activity was determined using an in vitro acetylation of the core histone with endogenous p300 proteins immunoprecipitated from αsyn-expressing and vector control cells. As shown in Fig. 8B, p300 HAT activity decreased by ~70% in αsyn-expressing cells as compared to vector cells, suggesting that the balance between HAT and HDAC activities in αsyn-expressing N27 cells was altered by αsyn. The reduction in p300 HAT activity by αsyn therefore appears to be at least in part a consequence of the depletion of p300 protein in αsyn-expressing cells. In addition to their intrinsic acetyltransferase activity, p300 and CBP are well-known for their roles in bridging multiple sequence-specific transcription factors to general transcriptional machinery to initiate transcription (Chan and La Thangue, 2001). Based on this understanding and our observation of decreased levels of p300 induced by αsyn, we were interested in determining whether αsyn could modulate p300 transactivation potential by disrupting p300 recruitment to the PKCδ promoter. To address this issue, we evaluated p300 binding to the PKCδ promoter by ChIP assay. Chromatin was immunoprecipitated with a p300 antibody and analyzed by PCR amplification of the PKCδ promoter region encompassing the κB binding sites. As shown in Fig. 8C, a small amount of p300 binding onto the PKCδ promoter was detected in vector control cells, whereas in αsyn-expressing cells, it was completely abolished (lane 4 versus 5). This effect was specific to p300, as binding and recruitment of CBP to the PKCδ promoter was not affected by αsyn (Fig. 8C, lane 2 versus 3). While these experiments demonstrated that αsyn blocked p300 association

to the PKCδ promoter, they do not clarify a functional link between loss of p300 and αsyn repression of PKCδ. Therefore, we decided to utilize siRNA-p300 to directly inhibit endogenous p300 function. As shown in Fig. 8D, the transfection of siRNA-p300 (si-p300) into N27 cells resulted in a ~50% reduction in p300 protein, which was correlated with a concomitant ~50% decrease in the PKCδ protein level. Collectively, these results provide direct evidence for a specific loss of p300 protein and a subsequent decrease in HAT activity due to stable expression of αsyn, which could account for decreased p65 acetylation and binding activity, as well as down-regulation of recruitment and binding of p300 to the PKCδ promoter, which is at least partly responsible for the reduction in PKCδ expression.

We further examined the role of p300 HAT in controlling PKCδ expression in primary dopaminergic neurons using the pharmacological modulators of p300. Garcinol, a polyisoprenylated benzophenone derivative isolated from Garcinia indica, has been shown to potently inhibit the activity of p300 and PCAF (Balasubramanyam et al., 2004; Arif et al., 2009). In contrast, CTPB, an anacardic acid-inspired benzamide, has been reported to function as an activator of p300, but not of PCAF (Souto et al., 2010; Balasubramanyam et al., 2003; Mantelingu et al., 2007). We treated mouse primary mesencephalic cultures with either garcinol (5 μM) or CTPB (10 μM), and then PKCδ immunoreactivity of TH-positive neurons was determined. As shown in Fig. 9A, immunocytochemical staining revealed that the level of PKCδ immunoreactivity in TH neurons was dramatically reduced by garcinol exposure, and in contrast, CTPB treatment significantly enhanced PKCδ immunofluorescence. Fluorescent intensity analysis revealed a ~60% ($p<0.01$) decrease and ~170% ($p<0.05$) increase in PKCδ immunoreactivity in garcinol-treated and CTPB-treated TH neurons, respectively (Fig. 9B). These results further demonstrated that p300 can regulate

the PKCδ expression in primary dopamine neurons. Taken together with the reduced p300 levels induced by αsyn (Fig. 8), these results suggest that inhibition of p300-mediated transcriptional events by αsyn could contribute to the down-regulation of PKCδ.

Down-regulation of p300 in α-synuclein transgenic mice

Thus far, the in vitro experiments indicated that p300 is likely to be the major target molecule of αsyn responsible for the ultimate impingement on the PKCδ transcription. The final step in our study was to verify whether αsyn overexpression down-regulates p300 in vivo. To accomplish this, we compared double immunohistochemical labeling of p300 levels within TH positive neurons in the substantia nigra of αsyn transgenic (htg) mice versus control (non-tg) animals. As shown in Fig. 10, p300 (stained in red) is predominantly distributed in the nucleus in TH-positive neurons (stained in green). The majority of TH-positive neurons in control mice exhibited significant p300 expression as shown by the intensive p300 immunoreactivity. In contrast, TH-immunoreactive neurons in αsyn transgenic mice showed weak or no immunoreactivity for p300. Taken together with in vitro results, these findings in an animal model clearly demonstrate that the suppression of p300 by αsyn contributes to the down-regulation of PKCδ.

Discussion

In the present study, we provide evidence that the normal level of human wild-type αsyn is able to attenuate the MPP+-induced dopaminergic degeneration by inhibiting the

proapoptotic PKCδ gene expression. To our knowledge, this is the first evidence that αsyn is implicated in modulation of PKCδ expression via p300. Stable expression of human wild-type αsyn in N27 dopaminergic cells greatly attenuates the MPP+-induced proteolytic cleavage and nuclear translocation of the PKCδ catalytic fragment, leading to a neuroprotective effect. Conversely, restoring PKCδ expression significantly ablates such neuroprotective function. Additionally, we observed that NFκB and p300 are actively involved in the modulation of PKCδ gene expression in primary dopaminergic neurons. NFκB/p300 inhibition remarkably reduces the extent of PKCδ expression in primary dopaminergic neurons, whereas activation of p300 induces a significantly increased level of PKCδ. Furthermore, we show a dramatically decreased expression of both PKCδ and p300 proteins in dopaminergic neurons in αsyn transgenic mice. In addition, we systematically characterized the mechanism by which αsyn represses PKCδ gene expression. We demonstrated that αsyn does not interfere with PKCδ protein and mRNA turnover but acts via direct transcriptional repression. Moreover, we provide evidence linking acetylation events to PKCδ repression mediated by αsyn. First, αsyn inhibits NFκB acetylation, leading to a reduced NFκB transcriptional activity. Second, αsyn disrupts p300 HAT activity. Finally, we show that increasing the cellular acetylation by HDAC inhibitor treatment increases PKCδ expression in an isoform-dependent manner. Collectively, our results support a working model in which αsyn acts to inhibit p300 levels and its HAT activity to repress PKCδ expression and thereby protect against neurotoxicity. These findings might provide mechanistic insights into the physiological role of αsyn in regulating neuronal cell death by suppressing the proapoptotic kinase PKCδ expression. Our proposed model based on the

experimental results is illustrated in Scheme 1, in which the inhibition of PKCδ transcription by cytoplasmic αsyn to prevent cell death occurs by disrupting both NFκB and p300 activation, at least as a consequence of the reduced p300 proteins and subsequent decrease in HAT activity.

αSyn is highly abundant in presynaptic terminals of mammalian brain, making up to 0.1% of total brain proteins (Iwai et al., 1995; Sidhu et al., 2004). Although αsyn may have various roles in dopamine synthesis and homeostasis (Perez et al., 2002; Peng et al., 2005b), membrane trafficking (Outeiro and Lindquist, 2003; Cooper et al., 2006), synaptic plasticity (Clayton and George, 1998; Stephan et al., 2002), and as antioxidant or molecular chaperone (Ostrerova et al., 1999; Zhu et al., 2006), its physiological role is still unclear. Mutations in αsyn gene promote aggregation of αsyn proteins and are linked to PD (Norris et al., 2004). Furthermore, transgenic overexpression of mutant αsyn (A53T) in mice produces neurodegeneration (Giasson et al., 2002; Lee et al., 2002). However, controversy remains about the toxicological properties of wild-type αsyn. Several lines of wild-type αsyn transgenic mice fail to show pathological phenotype (Matsuoka et al., 2001; Rathke-Hartlieb et al., 2001). Furthermore, growing evidence suggests a neuroprotective role for wild-type αsyn. For example, wild-type αsyn, but not its mutant proteins, protects dopaminergic neurons against MPP+ or rotenone toxicity (Jensen et al., 2003). Transgenic mice overexpressing either the wild-type or the A53T mutant αsyn are resistant to paraquat-induced dopaminergic cell death (Manning-Bog et al., 2003). The transgenic model used in the current study that overexpresses wild-type human αsyn exerts neuroprotection against CSPα-induced neurodegeneration (Chandra et al., 2005). Several hypotheses may

explain αsyn-mediated neuroprotection. It is conceivable that αsyn plays a dual role in the nervous system. When expressed at physiological levels, it may function as a normal protein that contributes to cell survival. In contrast, αsyn overexpressed beyond a certain threshold might induce cytotoxicity. A previous study showed that at nanomolar concentrations, αsyn prevented cell death, whereas at both low micromolar and overexpressed levels, αsyn became neurotoxic (Seo et al., 2002). Since the levels of αsyn achieved in our stable N27 cells are within physiological range (Fig. 1A), our results support protective functions of this protein. In addition to the extent of αsyn expression, an alternative possibility is that dysregulation of subcellular αsyn may contribute to PD. αSyn exists either in a membrane-bound state that peripherally attaches to vesicles, or in a soluble form that is freely diffusible in the cytoplasm. The translocation between these two subcellular compartments is crucial for the normal function of αsyn (Bennett, 2005; Wislet-Gendebien et al., 2006). Although αsyn was initially recognized as a cytoplasmic protein (Iwai et al., 1995), several lines of evidence have also documented localization of αsyn in the nucleus (Goers et al., 2003; Zhang et al., 2008). Interestingly, a previous study indicated that nuclear αsyn promoted neurotoxicity, and conversely, cytoplasmic localization of αsyn was neuroprotective (Kontopoulos et al., 2006). In the present study, the cytoplasmic localization of αsyn that prevented MPP+-induced cell death partially confirmed this finding (Fig. 2). Additionally, αsyn has been shown to function as a negative mediator of DA synthesis via interactions with TH and/or PP2A to inhibit TH activity (Perez et al., 2002; Peng et al., 2005b). We also reported that PKCδ negatively regulates TH activity by binding and phosphorylating PP2A (Zhang et al., 2007c). In the present study, we demonstrated that αsyn

represses PKCδ transcription, suggesting that αsyn-mediated repression of PKCδ may alter DA synthesis. Importantly, we found a reduced PKCδ expression in αsyn transgenic mouse models, indicating the αsyn overexpression represses the proapoptotic kinase PKCδ in vivo. These results may explain why αsyn overexpressing mice are resistant to neurodegeneration in dopaminergic neurons despite the high accumulation of the protein in the substantia nigra.

Although our results indicate that p300 pathway is likely the major pathway controlling the down-regulation of PKCδ in transgenic animal, it is possible that other PKCδ downregulation mechanisms come into play, acting alone or in concert, since overexpression of αsyn was found to significantly alter multiple signaling pathways, including stress response, transcription factors, apoptosis-inducing molecules, and membrane-bound proteins (Baptista et al., 2003). Moreover, αsyn has been shown to be able to directly associate with histones and inhibit histone acetylation, suggesting a direct role of the protein in regulation of gene transcription (Goers et al., 2003; Kontopoulos et al., 2006).

We report here for the first time the repression of the PKCδ gene by αsyn in dopaminergic neurons mediated through the transcription factors NFκB and p300. Our results show that αsyn inhibits NFκB transcriptional activity at the level of p65 acetylation, without affecting NFκB/IκBα nuclear translocation, IκBα degradation, or NFκB/IκBα protein levels. It should be noted, however, that acetylation of p65 to mediate NFκB transcriptional activity may be more complex, as acetylation of discrete lysine sites may regulate different nuclear functions (Chen et al., 2002). Independent of regulation of p65 acetylation levels, modulation of p300/CBP-mediated acetylation of p50 has to be considered as one mechanism for the inhibition of p50 binding activity (Fig. 5D) by αsyn, because acetylation of p50 increases its

DNA binding and further induces NFκB transcriptional activity (Deng et al., 2003). Moreover, analysis of the PKCδ promoter has uncovered multiple potential transcription factor sites. Therefore, it is also possible that one or more of those factors may contribute to the attenuation of PKCδ expression by αsyn.

An important finding of this study is that αsyn specifically decreases p300 protein in vivo and in vitro. Our model introduces loss of p300 as an underlying mechanism of its reduced HAT activity. p300 appears to play at least two major roles in αsyn-mediated suppression of PKCδ. First, loss of p300 proteins and its corresponding HAT activity reduces p65 acetylation and binding activity to PKCδ promoter, thereby resulting in downregulation of PKCδ. Second, PKCδ gene expression itself may be dependent on p300. Thus, the depletion of p300 proteins would decrease the recruitment and binding of p300 onto PKCδ promoter, and subsequently may interfere with the interactions between p300 and NFκB or other transcriptional complexes, eventually blocking PKCδ transcription. However, the mechanism by which αsyn disrupts the p300 protein is unclear. Our data indicate that αsyn does not likely regulate p300 protein level at the transcriptional level (Supplemental Fig. 10). Further investigation should reveal whether αsyn inhibits p300 protein by an alternative mechanism, such as degradation mediated by proteasome as reported previously (Poizat et al., 2005).

It is important to note that regulation of acetylation of p65 could not be limited to the acetyltransferase activities of p300 and CBP because deacetylation reactions can also influence the overall acetylation status of NFκB. In fact, it has been reported that p65 is reversibly acetylated by p300 and CBP and subsequently deacetylated by HDACs, most notably, HDAC3 (Kiernan et al., 2003). Therefore, the contribution of HDACs to the

inhibition of p65 acetylation by αsyn remains to be elucidated. In addition to acetylation, p65 is also regulated by the modification of phosphorylation, which can potentiate the transcription by enhancing p65 association with the p300/CBP coactivator (Zhong et al., 2002). The influence of αsyn on NFκB transactivation by alteration of p65 phosphorylation status is yet to be determined.

In summary, our results are based on multiple independent techniques that together elucidate the molecular and cellular mechanisms underlying the down-regulation of PKCδ by αsyn. These findings expand the role of αsyn in neuroprotection and have important implications for the development of novel drug therapies for PD.

Figure 1: α-Synuclein specifically down-regulates PKCδ isoform in N27 dopaminergic cells

A, Whole cell extracts from stably expressing αsyn N27 cells (Syn), vector control N27 cells (Vec), and rat substantia nigra brain (rSN) were prepared. Expression of αsyn and TH were determined by immunoblotting assay with antibodies against αsyn (Syn-1, BD Biosciences) and TH. β-actin was used as a loading control. ***B***, The specific downregulation of PKCδ protein in αsyn-expressing N27 cells. Representative immunoblots (left panel) and quantitation (right panel) of PKC isoforms (δ, α, βI, and ζ) in whole cell lysates in αsyn-expressing (Syn) and vector control (Vec) N27 cells. Data shown are mean ± SEM from three separate experiments (***$p<0.001$). ***C***, Left: semiquantitative RT-PCR analysis of mRNA levels of various PKC isoforms. Amplicon base pairs (bp) are shown at the right sides of the panel. GAPDH was used as loading control. Right: qRT-PCR analysis for PKCδ mRNA expression in αsyn-expressing and vector control N27 cells. Data shown represent mean ± SEM from four separate experiments preformed in triplicate (***$p<0.001$). ***D***, Transient overexpression of human wild-type αsyn in N27 cells by lentiviral infection down-regulates PKCδ protein expression. N27 cells were infected with lentiviruses expressing LacZ-V5 (control lentiviral vector) or αsyn-V5 for 48 h, and whole cell lysates were analyzed for V5 and β-actin (top panel), PKCδ (middle panel), and αsyn (bottom panel). A representative immunoblot is shown.

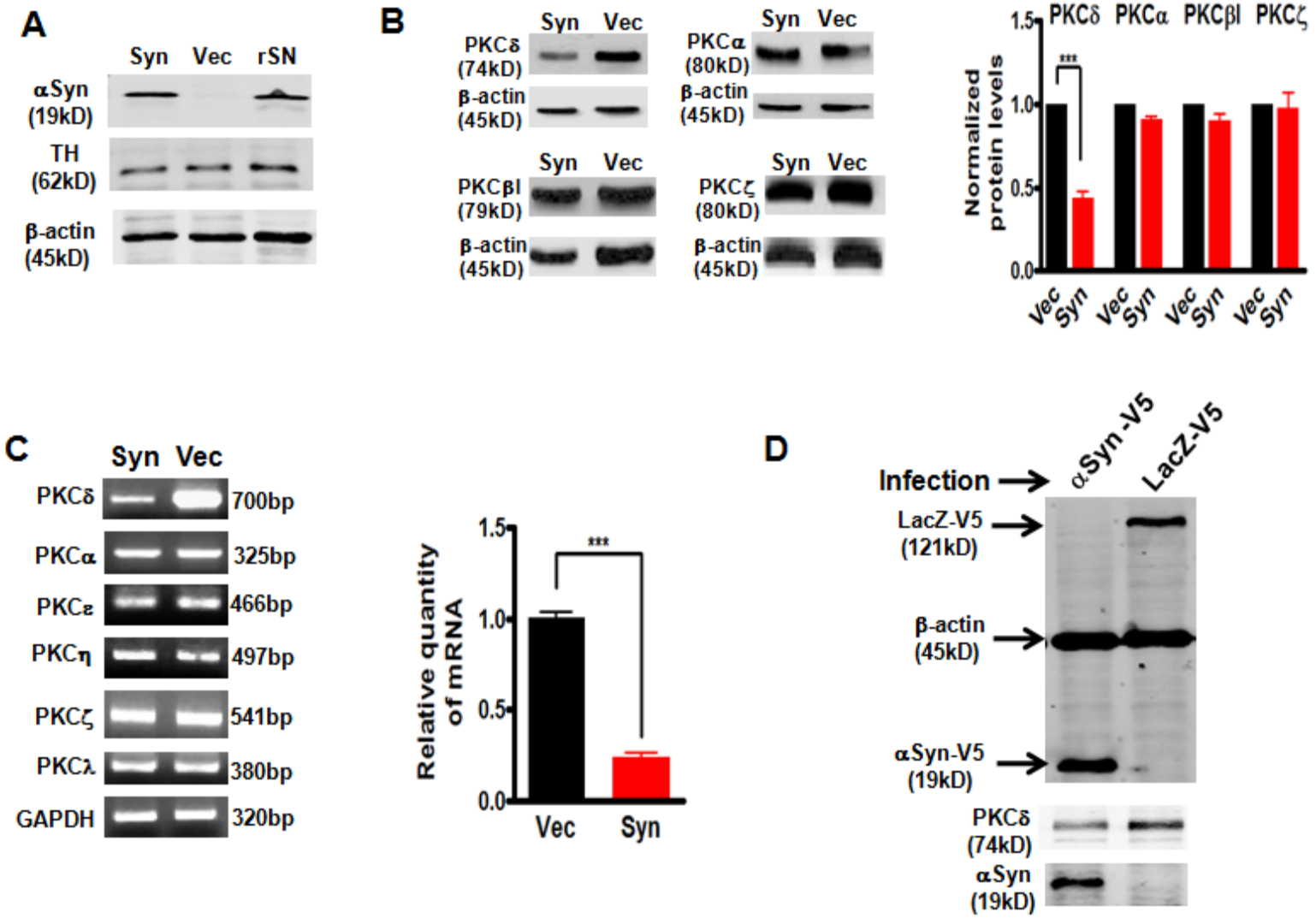

Figure 1

Figure 2: Deregulation of PKCδ by α-synuclein protects against MPP^+-induced cell death in dopaminergic N27 cells

A, Effects of downregulation of PKCδ by αsyn on MPP^+-induced cell death in dopaminergic N27 cells. αSyn-expressing (Syn) and vector control (Vec) N27 cells were infected with lentiviruses expressing LacZ-V5 or PKCδ-V5 for 24 h. The cells were then exposed to MPP^+ (300μM) for 48 h. Cells were collected and assayed for DNA fragmentation (left panel) and caspase-3 activity (right panel). Data shown represent mean ± SEM from two independent experiments performed in quadruplicate (*p<0.05; **p<0.01; and ***p<0.001). ***B***, MPP^+-induced PKCδ proteolytic cleavage and its nuclear translocation were significantly diminished in αsyn-expressing N27 cells. αSyn-expressing (Syn) and vector control (Vec) N27 cells were exposed to MPP^+ (300 μM) for 36 h. Cytoplasmic (C) and nuclear (N) fractions were prepared for immunoblotting analysis of PKCδ. LDH (cytoplasmic fraction) and Lamin B1 (nuclear fraction) were used as loading controls. ***C***, Cytoplasmic localization of αsyn in αsyn-expressing N27 cells was not affected by MPP^+ treatment. αSyn-expressing (Syn) and vector control (Vec) N27 cells were exposed to MPP^+ (300 μM) for 36 h. Cells were either collected for preparation of cytoplasmic and nuclear extracts and immunoblotting analysis of αsyn (left panel) or stained and visualized under a Nikon TE2000 fluorescence microscope (right panel). Scale bar, 10μm. A representative immunoblot and image of αsyn immunostaining (green) and Hoechst staining (blue) are shown.

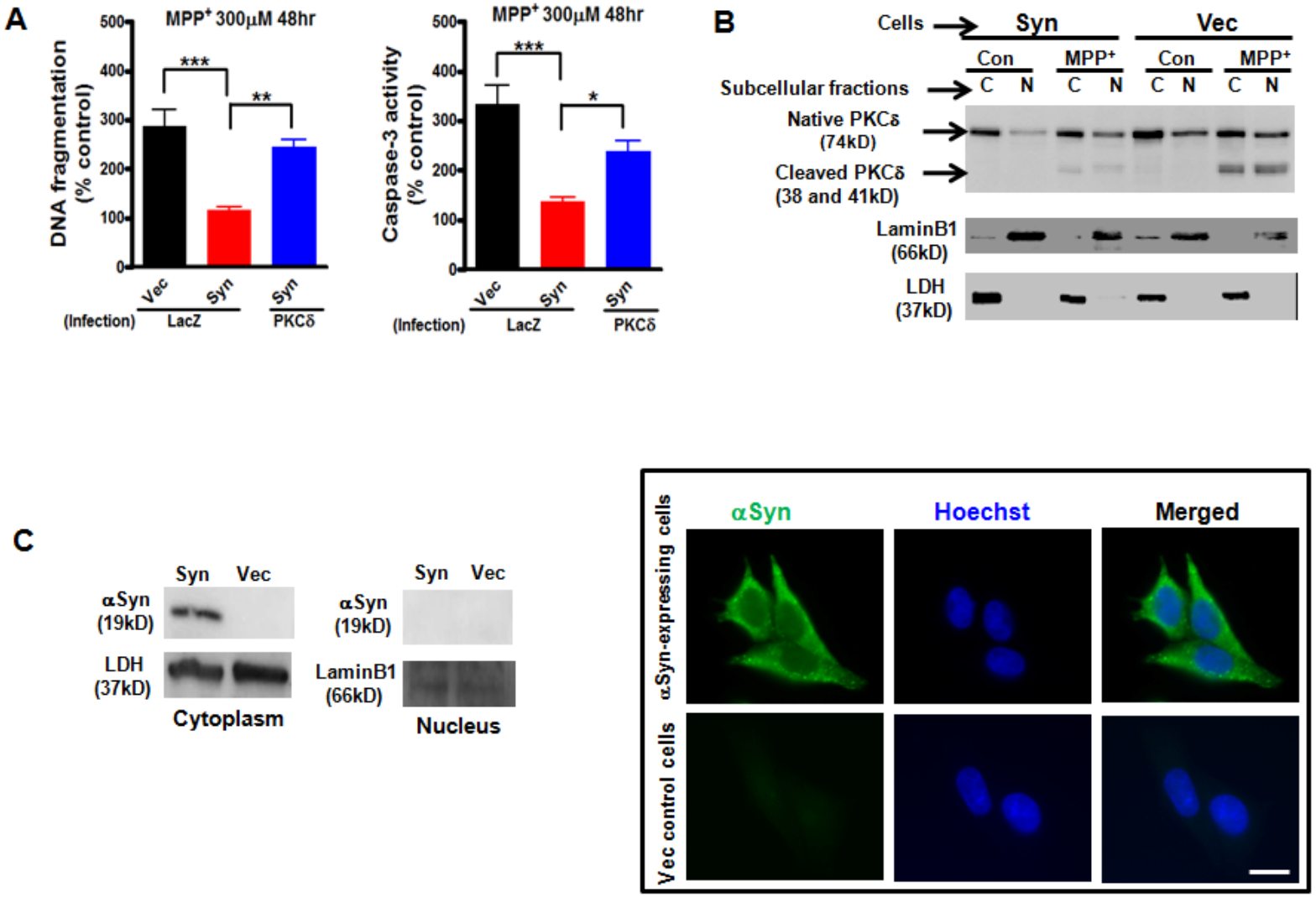

Figure 2

Figure 3: Decreased PKCδ expression in nigral dopaminergic neurons in α-synuclein overexpressing mice

A*,** Representative images of immunohistochemical analysis of PKCδ expression within nigral TH-positive neurons. Substantia nigra sections from non-transgenic control (non-tg) mice and αsyn transgenic mice (htg) were stained with PKCδ polyclonal antibody (1:250 dilution) and TH monoclonal antibody (1:1800 dilution), followed by incubation with Alexa 568-conjugated (red; 1:1000) and Alexa 488-conjuated (green; 1:1000) secondary antibodies. Hoechst 33342 (10 μg/ml) was added to stain the nucleus. Confocal images were obtained using a Leica SP5 X confocal microscope system. Green, TH; red, PKCδ; blue, nucleus. White arrows point to dopaminergic neurons with significant PKCδ staining. Scale bar, 25μm (left panel) and 7.5μm (right panel). Magnifications 63x (left panel) and 430x (right panel). ***B, Quantification of the number of TH neurons containing colocalized PKCδ immunoreactivity was determined by blindly counting 6 fields and averaging. Values expressed as percent of total TH neurons were mean ± SEM and representative for results obtained with three pairs of 6-8-week-old mice (***p<0.001). ***C***, To analyze the levels of αsyn in substantial nigra homogenates from transgenic mice overexpressing human wild-type αsyn and non-transgenic mice**, s**ubstantial nigra homogenates were prepared from transgenic mice (htg) and non-transgenic mice (non-tg) and subjected to immunoblotting analysis of αsyn, and β-actin. Representative immunoblot (left panel) and quantitation (right panel) of αsyn expression were shown. About 6-fold increase in αsyn expression in substantial nigra was found in transgenic mice. Data were shown as mean ± SEM; n=6 (***p<0.001).

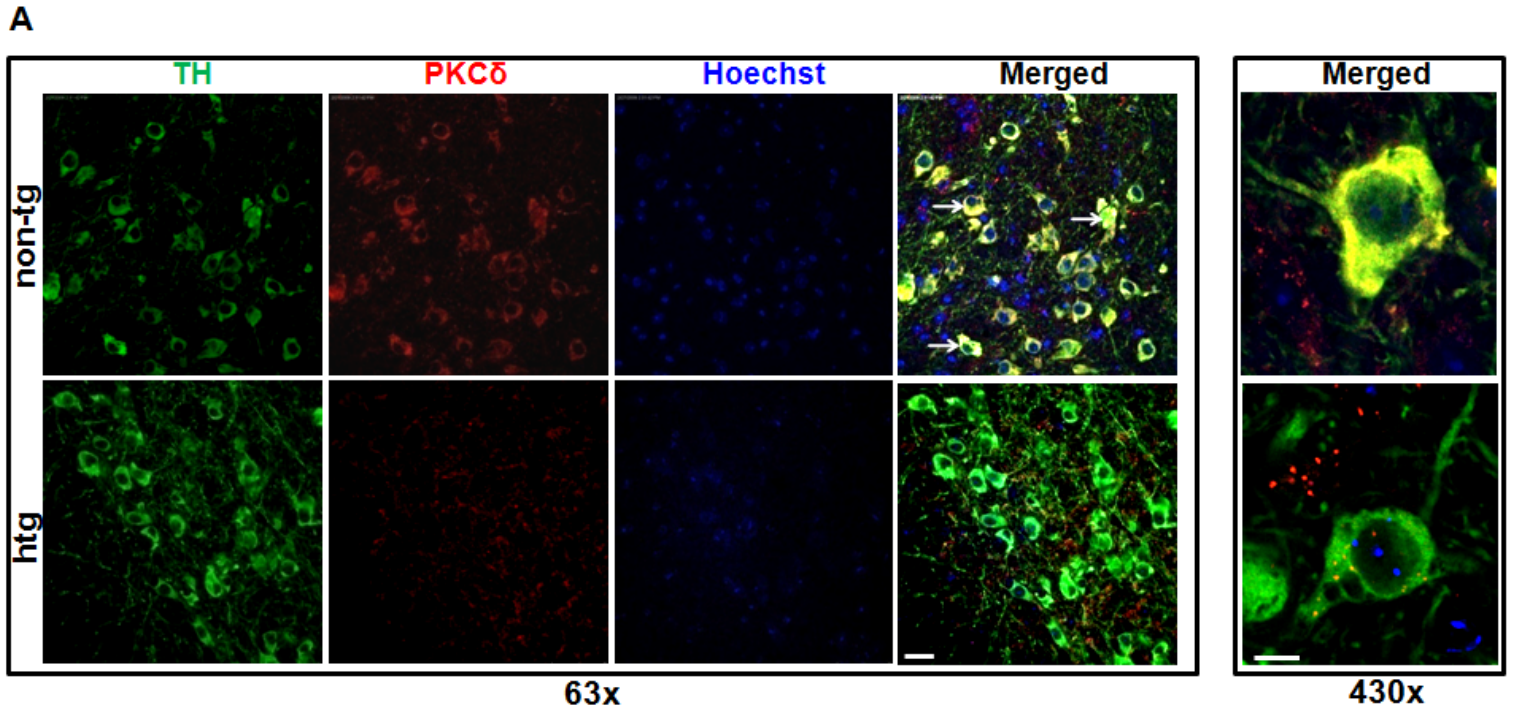

Figure 3

Figure 4: α-Synuclein suppresses PKCδ transcription without affecting PKCδ protein or mRNA stability in N27 dopaminergic cells

A, Left: Pulse-chase analysis of stability of PKCδ protein. αSyn-expressing and vector control N27 cells were labeled with ^{35}S-methionine, and PKCδ protein was analyzed over 48 h as described in Materials and Methods. Right: The bands were quantified and expressed as percentage of amount present at time 0 h. The data plotted were fit to a one-phase exponential decay model using the nonlinear regression analysis program of Prism 4.0 software as follows: $Y = Span\ e^{-Kt} + Plateau$, where Y starts at Span + Plateau and decays with a rate constant K. The half-life of the protein was determined by 0.693/K. The square of the correlation coefficient (R^2) is used as a measure of goodness-of-fit in regression analysis. The results of degradation kinetics of PKCδ protein are shown in supplemental Table 2. Values are mean ± SEM of two independent experiments. ***B***, The stability of PKCδ mRNA was not decreased in αsyn-expressing N27 cells. After treatment with actinomycin D (ActD), total RNA was extracted for qRT-PCR analysis at selected time intervals. The relative abundance of PKCδ mRNA was expressed as a percentage of that present at time 0 h, and data plotted were fit to the one-phase exponential decay model. The results of degradation kinetics of PKCδ mRNA are shown in supplemental Table 3. Values are mean ± SEM of three independent experiments performed in triplicate. ***C***, The PKCδ promoter activation was attenuated in αsyn-expressing cells in reporter assays. Reporter pGL3-PKCδ carrying the PKCδ promoter or pGL3-Basic empty vector was transiently transfected into αsyn-expressing and vector control cells. Cells were collected 24 h post-transfection and assayed for luciferase activity and β-galactosidase activity. Data were normalized and expressed as fold-induction over the pGL3-Basic vector. Values are shown as mean ± SEM

of three independent experiments performed in triplicate (***p<0.001). ***D***, The relative transcription efficiency of PKCδ was examined by quantitative nuclear run-on assay. Representative amplification plots for PKCδ mRNA (left panel) and β-actin mRNA (right panel) are shown. The change in fluorescence intensity (ΔRn) was plotted on the Y axis. The arrow shows the threshold (dashed lines). ***E***, Quantitation of transcription efficiency. Data are expressed as fold-change in the level of nascent run-on PKCδ mRNA in vector control cells, and are shown as mean ± SEM of three independent experiments performed in triplicate (***p<0.001).

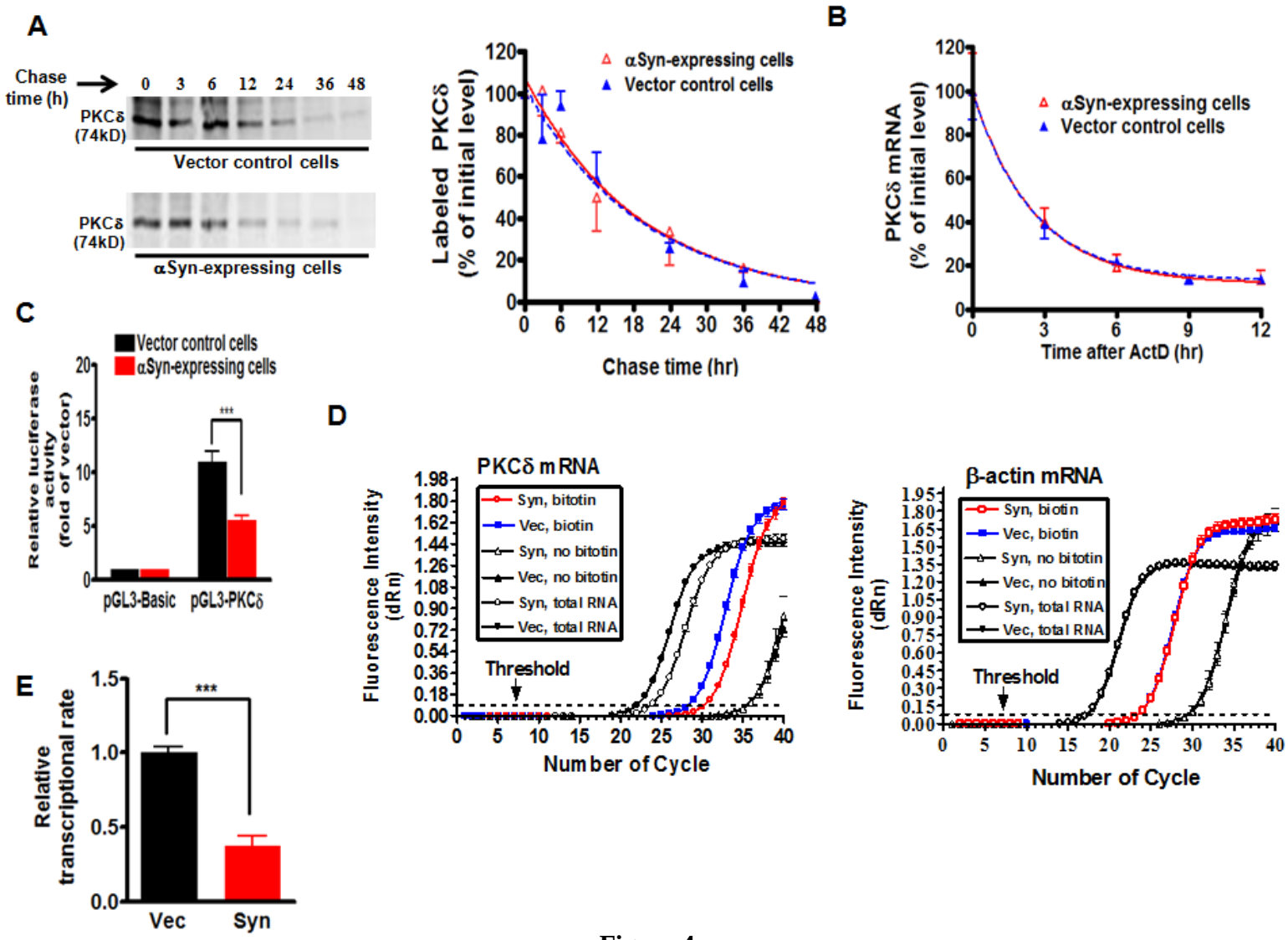

Figure 4

Figure 5: Increased α-Synuclein expression suppresses PKCδ in part by blocking NFκB activation

A, Representative EMSA gel images show the direct binding of NFκB to the putative PKCδ NFκB sites. Competitive EMSA was conducted using labeled probe corresponding to the PKCδ NFκB site 1 (left panel) or the PKCδ NFκB site 2 (right panel) and indicated unlabeled oligos. ***B***, Binding p50 and p65 to the NFκB sites on the PKCδ promoter. The nuclear extracts from vector control cells were incubated with excess of unlabeled self oligos or indicated antibodies prior to adding the labeled probe (PKCδ NFκB site 1). A representative EMSA supershift gel from three independent experiments is shown. ***C***, A representative EMSA gel image indicates the reduced binding of NFκB in vitro to the PKCδ NFκB site 1 in αsyn-expressing N27 cells. ***D***, ChIP analysis of the in vivo binding of NFκB-p65 and p50 on the PKCδ promoter. After reversal of cross-linking, immunoprecipitated genomic DNA fragments were analyzed by PCR using primers designed to amplify the -103 to +60 region of PKCδ promoter. ***E***, Knockdown of αsyn protein increased NFκB activity. αSyn-expressing cells were transient transfected with siRNA-αsyn and scrambled siRNA. 72 h post-transfection, the cells were collected and subjected to EMSA analysis using the labeled probe corresponding to the PKCδ NFκB site 1. Mock transfection was also included as a negative control. ***F***, Transfection of NFκB-p65 siRNA down-regulated PKCδ expression in N27 cells. N27 cells were transfected with p65-siRNA and scrambled siRNA for 96 h, and cells were collected for Western blot analysis. Representative immunoblot (left panel) and quantitation (right panel) of p65 and PKCδ on whole cell lysates in transfected cells. Data are shown as mean ± SEM of two independent experiments (*$p<0.05$, **$p<0.01$).

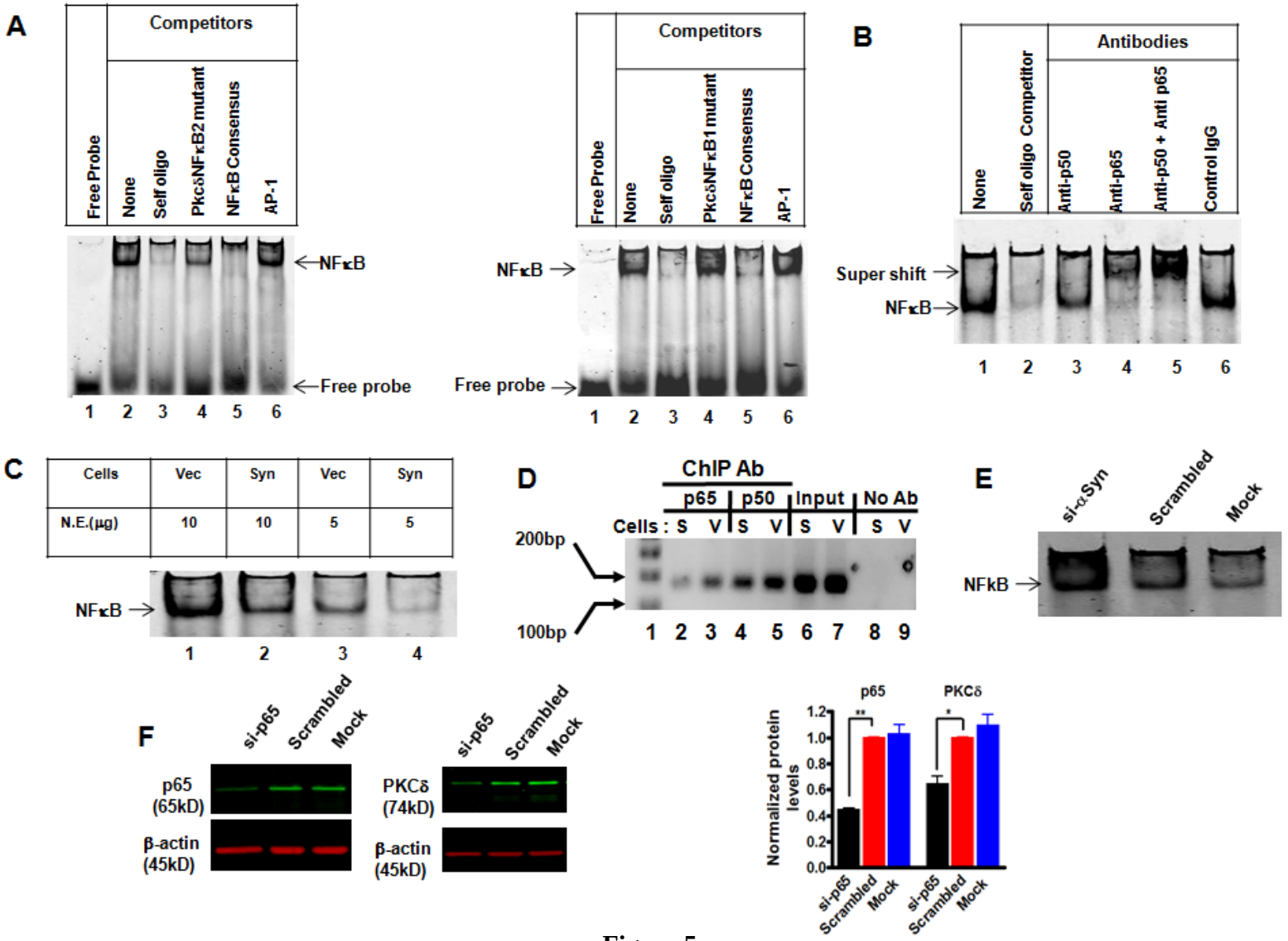

Figure 5

Figure 6: Effect of NFκB inhibition on the PKCδ immunoreactivity in the primary dopaminergic neurons

A, Primary midbrain cultures were treated with or without 100 μg/ml of SN-50 for 24 h. Cultures were immunostained for TH (green) and PKCδ (red). The nuclei were counterstained by Hoechst 33342 (blue). Images were obtained using a Nikon TE2000 fluorescence microscope (magnification 60x). Scale bar, 10μm. Representative immunofluorescence images are shown. The insert shows a higher magnification of the cell body area. ***B***, Immunofluorescence quantification of PKCδ in TH-positive neurons. Fluorescence immunoreactivity of PKCδ was measured from TH-neurons in each group using Metamorph software. Values expressed as percent of control group are mean ± SEM and representative for results obtained from three separate experiments in triplicate (**$p<0.01$).

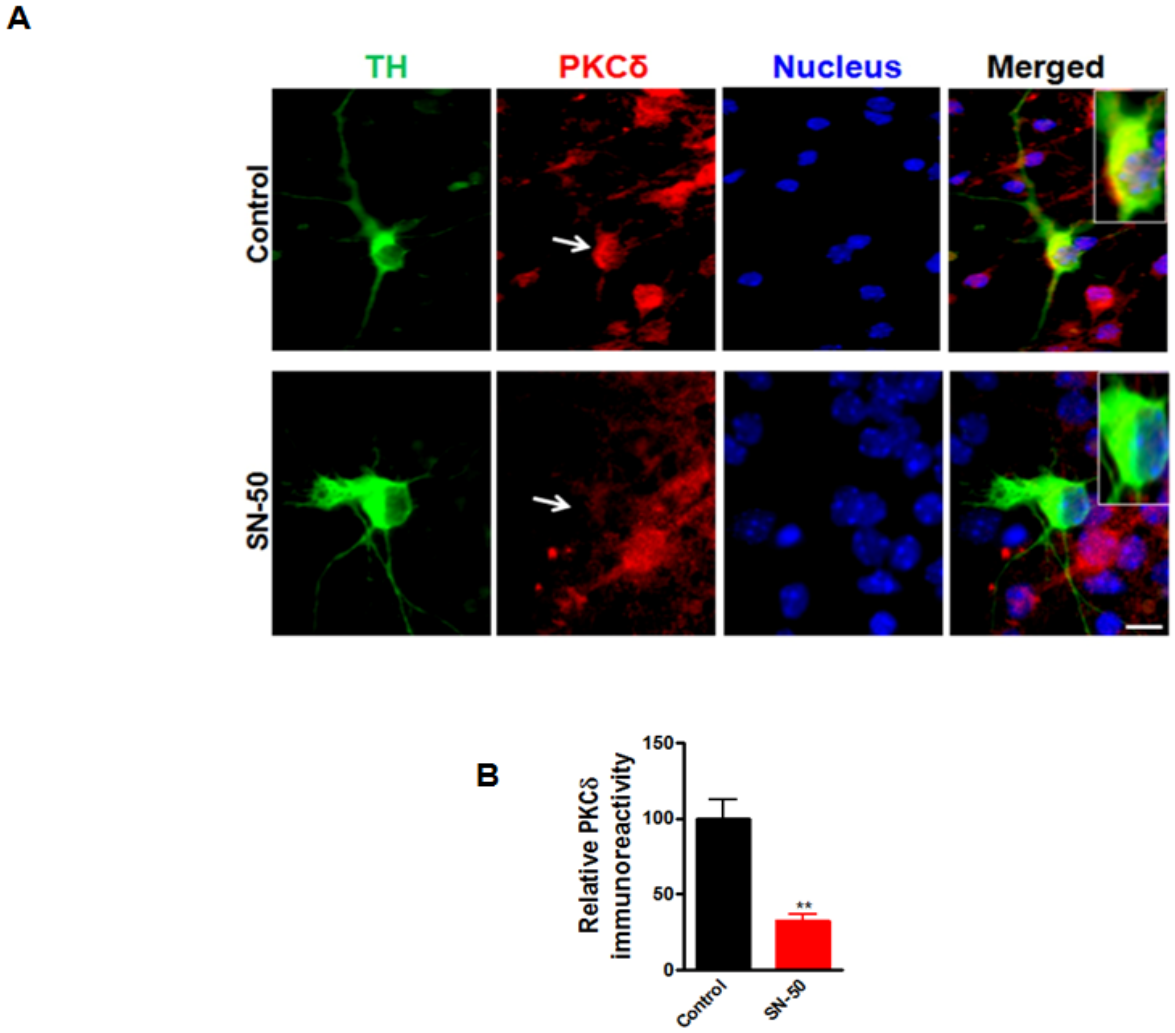

Figure 6

Figure 7: α-Synuclein-induced blockade of NFκB activation is associated with decreased acetylation of p65, but does not correlate with nuclear translocation or protein levels of NFκB/IκBα

A, ***B***, Nuclear translocation and abundance of NFκB/IκBα were not altered by overexpression of αsyn. Representative immunoblot of p65, p50 and IκBα levels on cytoplasmic and nuclear extracts (*A*) or whole cell lysates (*B*) from αsyn (Syn) and vector control (Vec) cells. ***C***, The p65 acetylation levels were reduced in αsyn cells. Whole cell lysates was immunoprecipitated (IP) with p65 antibody. The resulting immunoprecipitates were blotted with anti-acetyl-lysine and anti-p65 antibodies. Densitometric quantitation of the ratio of band intensity of acetylated p65 and total p65 from two independent experiments (means ± SEM; $^{**}p<0.01$) is shown on the right. ***D***, Sodium butyrate (NaBu) specifically enhanced PKCδ isoform expression in αsyn-expressing N27 cells. αSyn-expressing cells were treated with 1 mM NaBu and 50 μM caspase-3 inhibitor Z-DEVD-FMK, and cell lysates were prepared for blotting with specific anti-PKC isoforms (left panel) and anti-acetyl-lysine (right panel) antibodies.

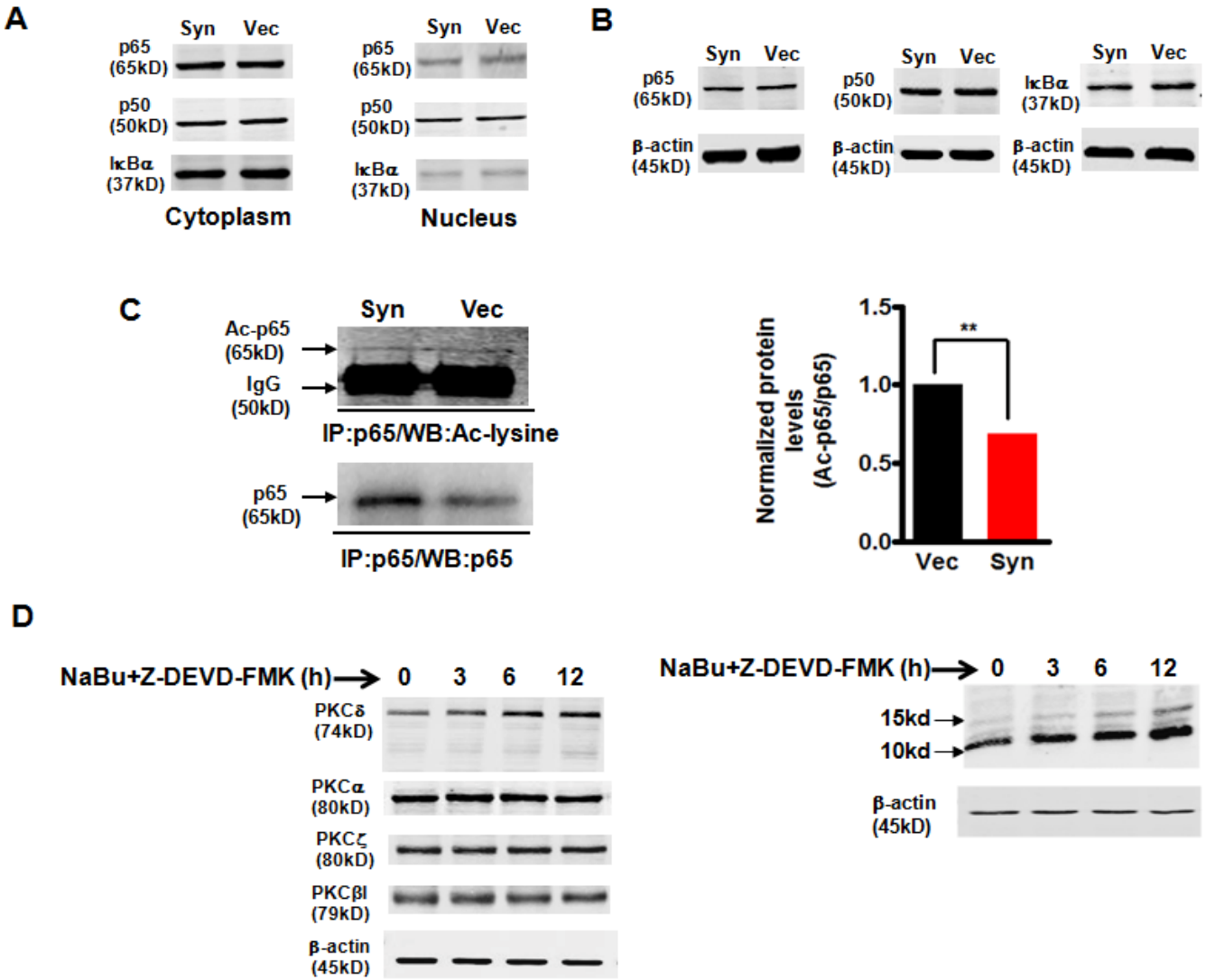

Figure 7

Figure 8: α-Synuclein down-regulates p300 proteins, resulting in decreased p300 HAT activity and inhibition of p300-dependent transactivation of PKCδ gene expression

A, Decreased p300 protein levels in αsyn-expressing cells. Representative immunoblot (left panel) and quantitation (right panel) of p300 and CBP on cytoplasmic and nuclear extracts from αsyn-expressing (Syn) and vector control (Vec) cells. Data are shown as mean ± SEM of two independent experiments (**p<0.01). LDH (cytoplasmic fraction) or histone H3 (nuclear fraction) was used as loading control. ***B***, Decreased p300 HAT activity in αsyn-expressing cells. Data were subtracted from background values that were measured in samples containing normal IgG, and then expressed as the percentage of HAT activity present in vector control cells. Values are shown as mean ± SEM of three independent experiments performed in triplicate (***p<0.001). ***C***, The in vivo binding of p300 on the PKCδ promoter was interrupted by overexpression of αsyn. After reversal of cross-linking, p300-immunoprecipitated genomic DNA fragments were analyzed by PCR using primers designed to amplify the -103 to +60 region of PKCδ promoter. ***D***, Knockdown of p300 by siRNA-p300 decreased PKCδ levels in N27 cells. N27 cells were transfected with p300-siRNA and scrambled siRNA for 96 h, and cells were collected for Western blot analysis. Representative immunoblot (left panel) and quantitation (right panel) of p300 and PKCδ on nuclear extracts or whole cell lysates in transfected cells. Data are shown as mean ± SEM of two independent experiments (*p<0.05, ***p<0.001).

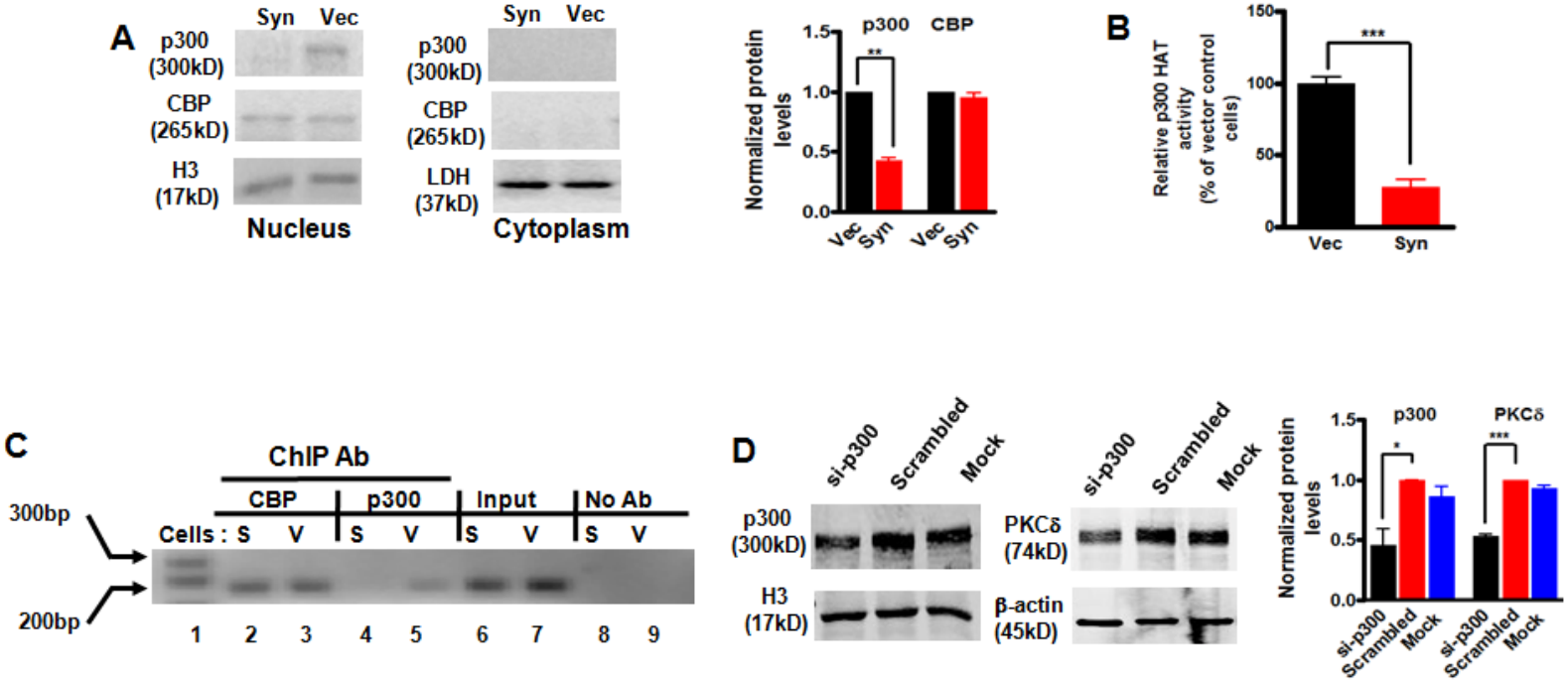

Figure 8

Figure 9: Effect of p300 inhibition or activation on the PKCδ immunoreactivity in the primary dopaminergic neurons

A, Primary midbrain cultures at 7 DIV were treated with or without either 5 μM garcinol or 10 μM CTPB for 24 h. Cultures were immunostained for TH (green) and PKCδ (red). The nuclei were counterstained by Hoechst 33342 (blue). Images were obtained using a Nikon TE2000 fluorescence microscope (magnification 60x). Scale bar, 10μm. Representative immunofluorescence images are shown. The insert shows a higher magnification of the cell body area. ***B***, Immunofluorescence quantification of PKCδ in TH-positive neurons. Fluorescence immunoreactivity of PKCδ was measured from TH-neurons in each group using Metamorph software. Values expressed as percent of control group are mean ± SEM and representative for results obtained from three separate experiments in triplicate (*$p<0.05$, **$p<0.01$).

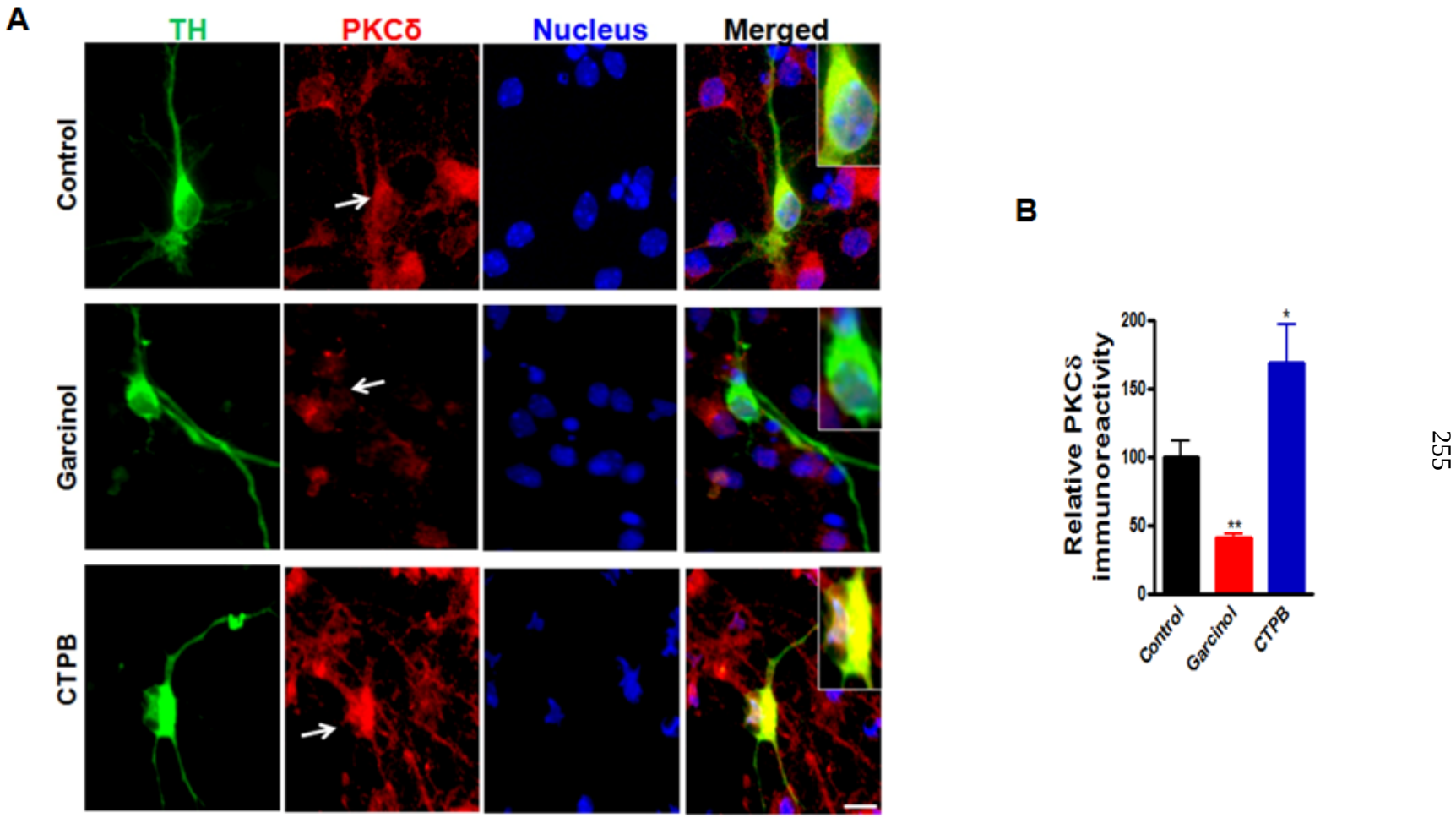

Figure 9

Figure 10: Decreased p300 level within neurons of the substantia nigra in αsyn overexpressing mice

Representative images of immunohistochemical analysis of p300 expression within nigral TH-positive neurons. Substantia nigra sections from non-transgenic control (non-tg) mice and αsyn transgenic mice (htg) were stained with p300 polyclonal antibody (1:350 dilution) and TH monoclonal antibody (1:1800 dilution), followed by incubation with Alexa 568-conjugated (red; 1:1000) and Alexa 488-conjuated (green; 1:1000) secondary antibodies. Hoechst 33342 (10 μg/ml) was added to stain the nucleus. Confocal images were obtained using a Leica SP5 X confocal microscope system. White arrows point to dopaminergic neurons with significant nuclear p300 staining. Green, TH; red, p300; blue, nucleus. Scale bar, 25μm (left panel) and 7.5μm (right panel). Magnifications 63x (left panel) and 250x (right panel).

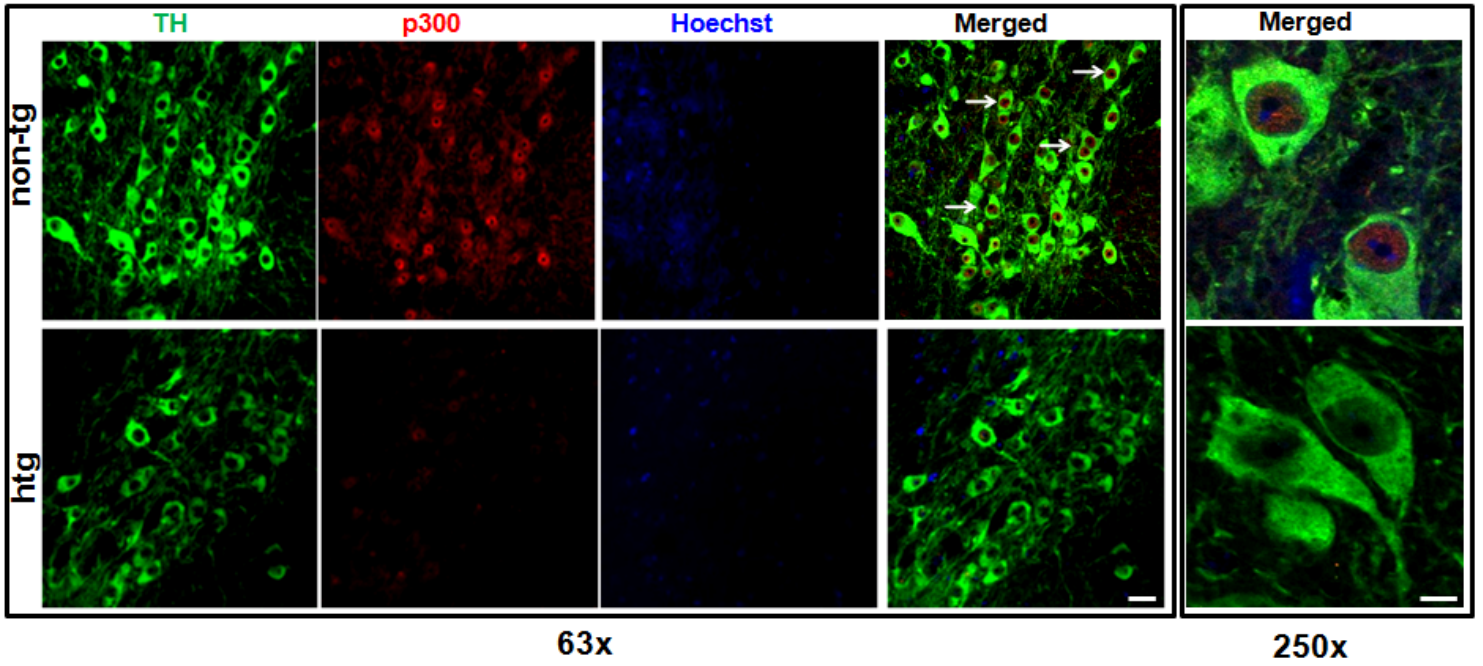

Figure 10

Scheme 1: A proposed model for α-synuclein acting in the cytoplasm to repress PKCδ expression and attenuate dopaminergic neurotoxicity

Constitutively activated NFκB p50/p65 heterodimers and p300/CBP bind to the two proximal promoter κB sites and modulate PKCδ transcription. Expression of αsyn, a cytoplasmic protein, inhibits p300-mediated acetylation of p65, thereby blocking the NFκB biding to PKCδ promoter. In addition, αsyn reduces p300 protein and its HAT activity, resulting in interruption of binding of p300 to the PKCδ promoter and its interaction with general transcription machinery (GTM), causing inhibition of PKCδ transcription. The resulting loss of PKCδ expression confers protection due to reduced proteolytic activation of PKCδ, which is a key proapoptotic function of the kinase during neurotoxic insults.

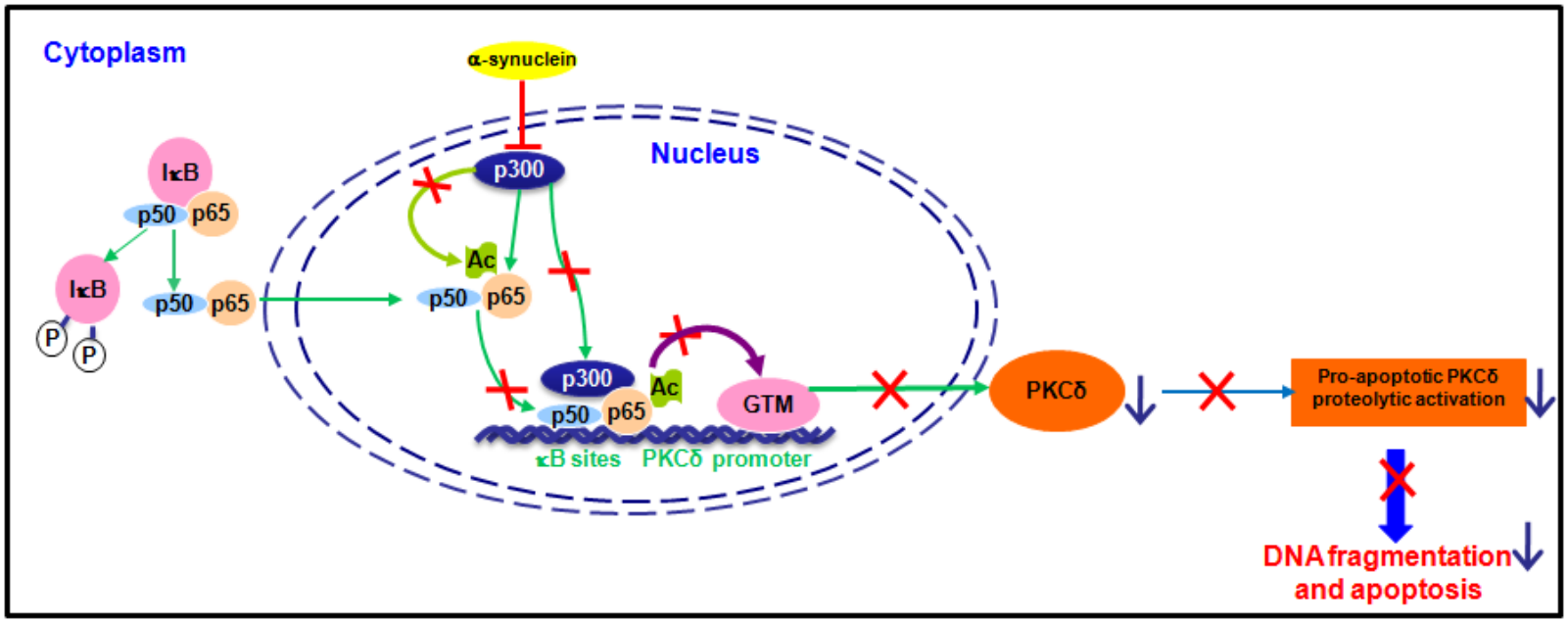

Scheme 1

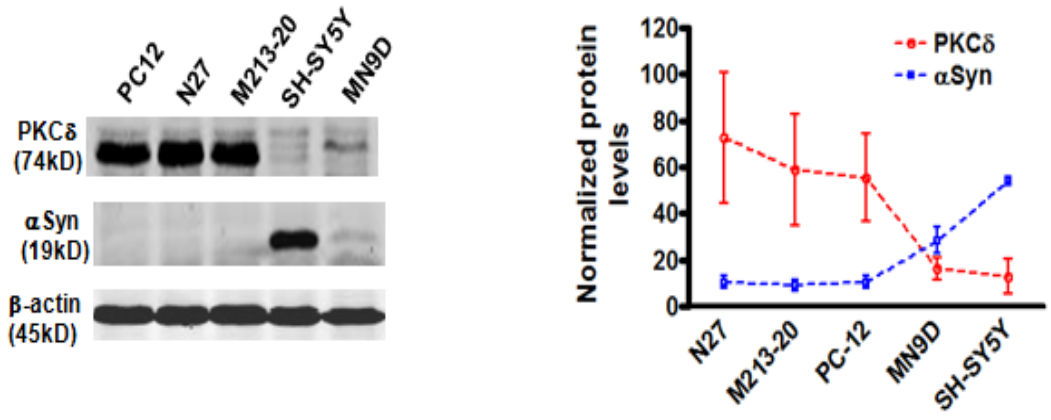

Supplemental Figure 1: Analysis of the relationship between α-synuclein and PKCδ protein levels in a variety of cell lines

Left: representative immunoblot analysis of whole cell lysates from the indicated cell lines for expression of αsyn, PKCδ or β-actin. Right: densitometric analysis. αSyn and PKCδ bands were quantified and normalized to that of β-actin. Values are shown as mean ± SEM of two independent experiments.

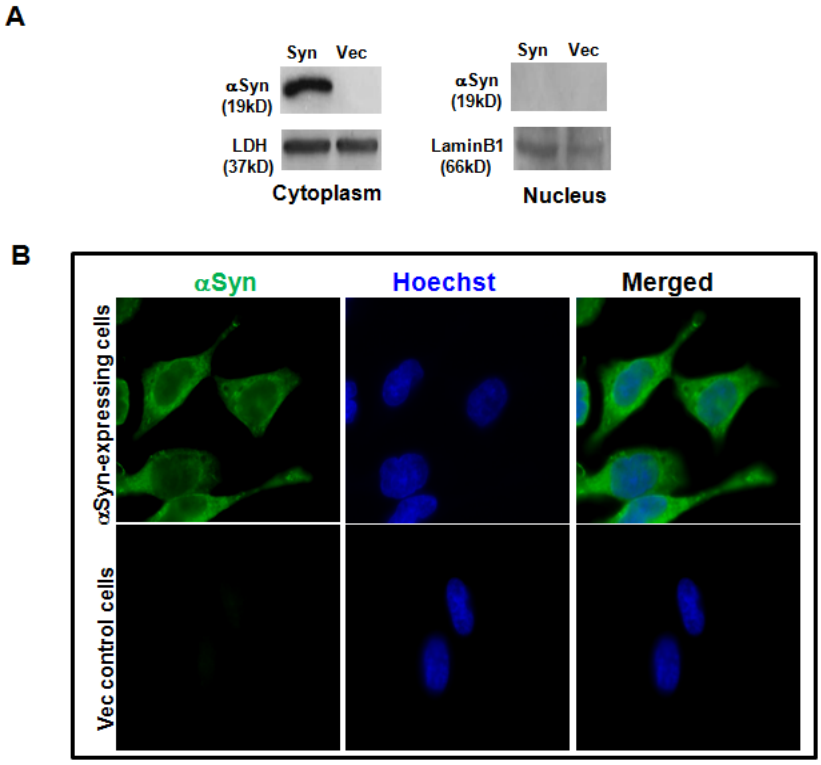

Supplemental Figure 2: α-Synuclein was exclusively located in the cytoplasm in αsyn-expressing N27 cells

A, Cytoplasmic and nuclear extracts from αsyn-expressing (Syn) and vector control (Vec) N27 cells were prepared and subjected to immunoblotting analysis of αsyn. LDH (cytoplasmic fraction) and Lamin B1 (nuclear fraction) were used as loading controls. ***B,*** Stained cells were mounted on slides and visualized under a Nikon TE2000 fluorescence microscope. Images were obtained with a SOPT digital camera. A representative image of αsyn immunostaining (green) and Hoechst staining (blue) is shown. Staining of αsyn-expressing (top panels) and vector control (bottom panels) cells with αsyn reveals immnuoreactivity specificity in the cytoplasm but not in the nucleus of αsyn-expressing cells.

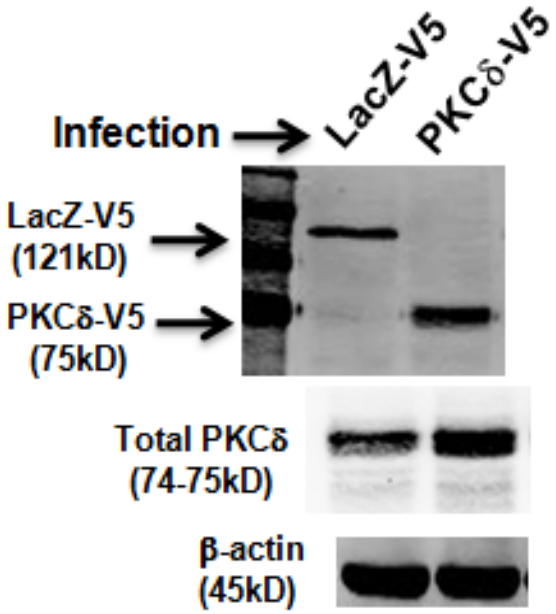

Supplemental Figure 3: Overexpression of PKCδ protein by lentiviral infection

αSyn-expressing N27 cells were infected with lentiviruses expressing LacZ-V5 (control lentiviral vector) or PKCδ-V5 for 48 h, and whole cell lysates were analyzed for V5 (top panel), PKCδ (middle panel), and β-actin (bottom panel). A representative immunoblot is shown.

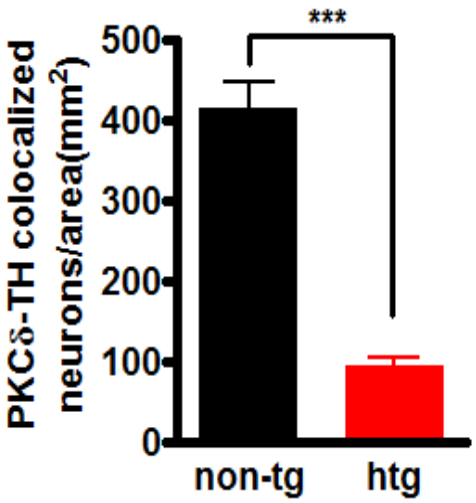

Supplemental Figure 4: Confirmation of the PKCδ-TH double-staining quantification technique

To confirm the validity of quantification data shown in Fig. 3*B*, the quantification was also determined by blindly counting the number of TH neurons containing colocalized PKCδ immunoreactivity per unit of area and averaging. For each experimental condition, at least 6 randomly chosen visual fields were analyzed. Values (expressed as number of TH-PKCδ colocalized neurons per square millimeter) were mean ± SEM and representative for results obtained with three pairs of 6-8-week-old mice (***p<0.001).

A

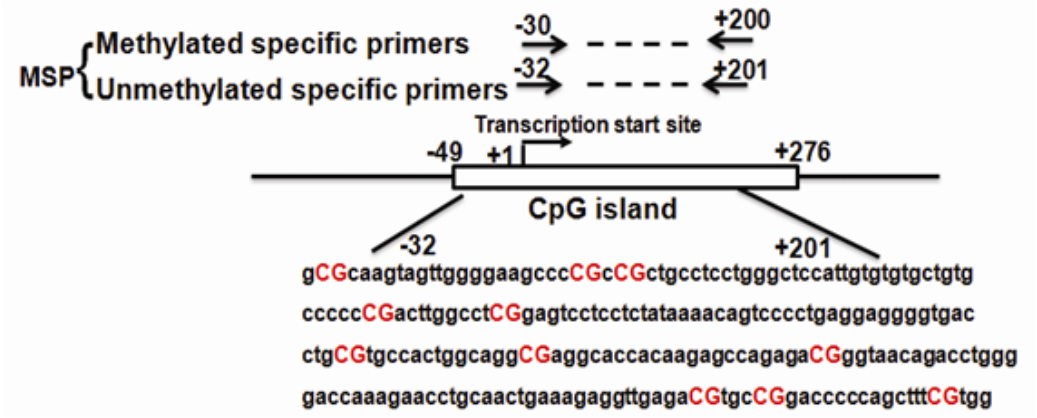

B

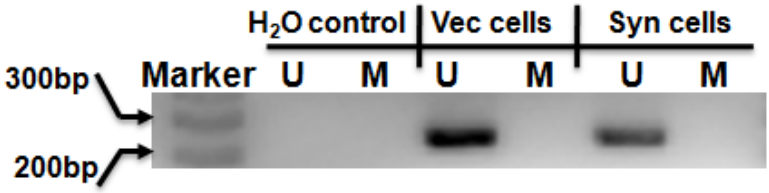

Supplemental Figure 5: α-Synuclein does not affect the methylation status of PKCδ promoter

A, Schematic map of the putative promoter-associated CpG island region showing the location of MSP primers and the sequence of the region studied by MSP. The CpG dinucleotide is shown in red capital letters. ***B***, MSP analysis of methylation status in PKCδ promoter. Bisulfite-modified DNA was used for MSP with primers specific for methylated (M) and unmethylated (U) DNA. Water blank was used as a negative control.

Supplemental Figure 6: Sequence alignment of the proximal PKCδ promoter

The proximal rat PKCδ promoter sequence (-178 to +22, relative to the transcription start site) was aligned with the homologous sequences from the mouse, human, and cow genome using a DiAlign professional program. Sequence differences are indicated and gaps introduced to maximize homology are marked by dashes. The highly conserved TFBSs are labeled, and the NFκB sites are highlighted in red.

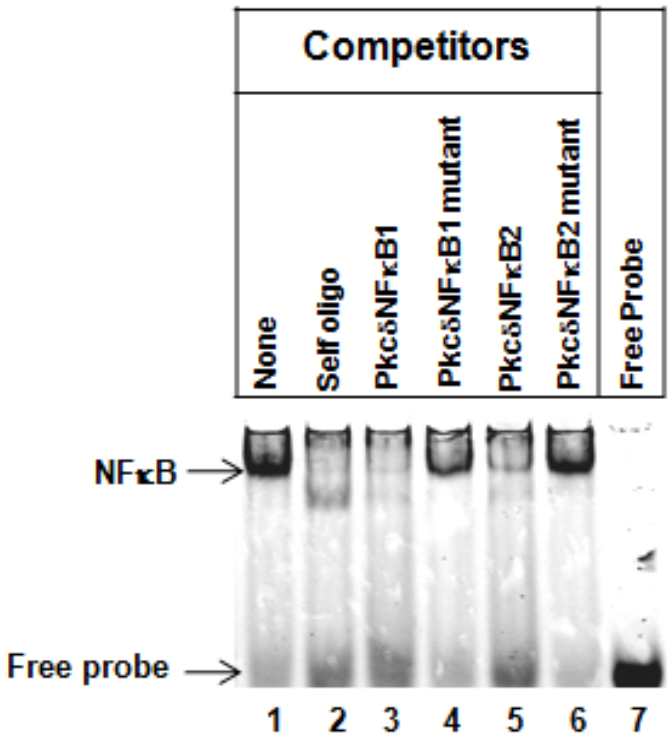

Supplemental Figure 7: The putative NFκB sites on the PKCδ promoter competed with the consensus NFκB probe for NFκB binding

Competitive EMSA was performed with the labeled consensus NFκB probe and indicated unlabeled oligos. A representative EMSA gel image is shown.

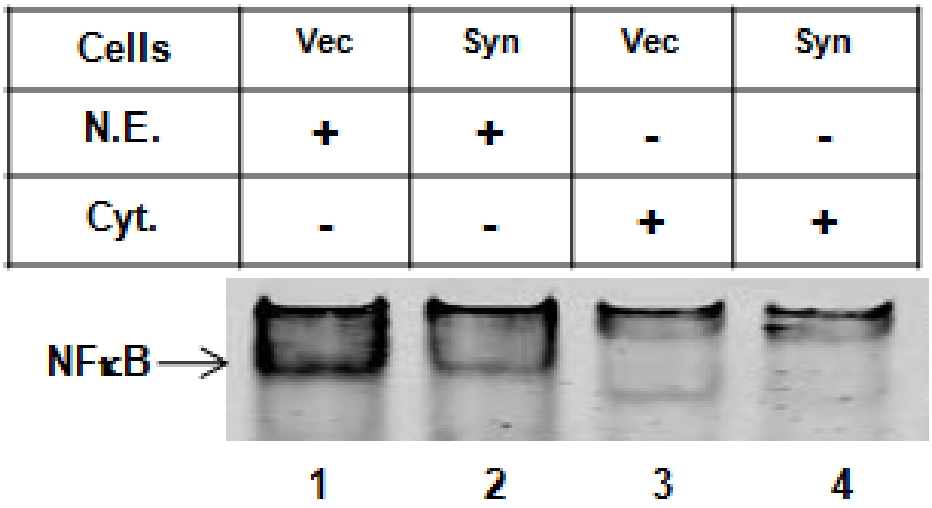

Supplemental Figure 8: Representative EMSA gel images indicate the reduced binding of NFκB *in vitro* to the PKCδ NFκB site 2 in αsyn-expressing N27 cells (Syn) compared to the vector control N27 cells (Vec). N.E., nuclear fractions; Cyt., cytoplasmic fractions.

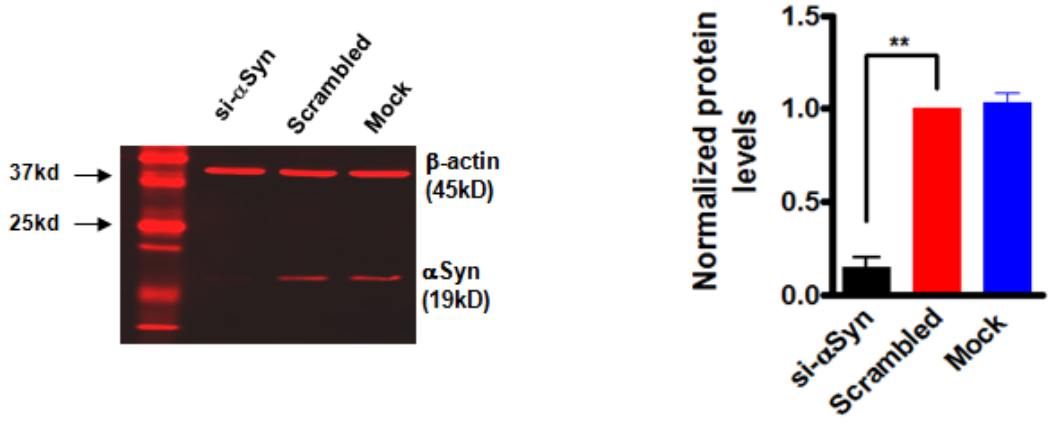

Supplemental Figure 9: Efficient knockdown of α-synuclein by siRNA-αsyn was confirmed by Western blot analysis

Representative immunoblot (left panel) and quantitation (right panel) of αsyn on whole cell lysates in transfected cells. Data are shown as mean ± SEM of two independent experiments (**p<0.01).

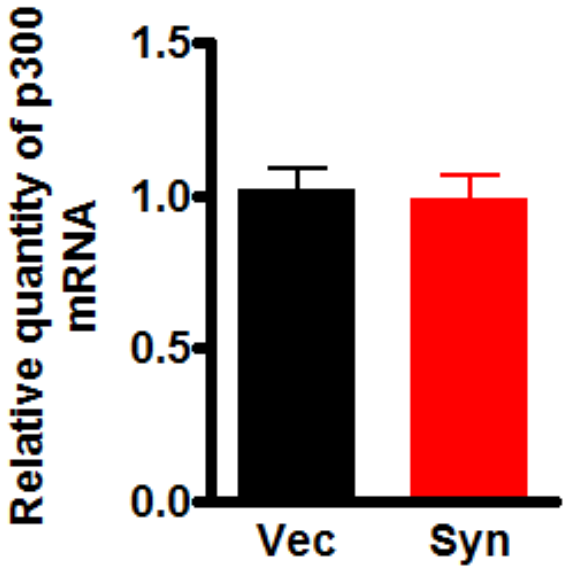

Supplemental Figure 10: Increased α-synuclein expression in N27 cells does not alter the amount of p300 mRNA

Quantitative analysis of p300 mRNA levels in αsyn-expressing (Syn) and vector control (Vec) cells. Data shown represented mean ± SEM of three independent experiments performed in triplicate. Note, p300 transcripts were not altered in αsyn-expressing cells (p>0.05).

Supplemental Table 1: List of primer sequences used in the study

Primer	Sequence (5'-3')	Amplicon
PKCδ Fg	GTCTATCTCGAGCACTCTCCTGAAGCCCACCATG	1901
PKCδ Rg	GTCTATAAGCTTCACACACAATGGAGCCCAGGAG	
PKCδ Fs	GGGCTACGTTTTATGCAGCT	700
PKCδ Rs	AGCAGGTCTGGGAGCTCACT	
PKCα Fs	TGAACCCTCAGTGGAATGAGT	325
PKCα Rs	GGCTGCTTCCTGTCTTCTGAA	
PKCε Fs	CCACCAAGCAGAAGACCAAC	466
PKCε Rs	TTTGTGGACGACGCAGGTAC	
PKCη Fs	GAAGGAGAGTCCATCAAGTC	497
PKCη Rs	TCAGCGTAGACCTGGAAATG	
PKCζ Fs	GGGACGAAGTGCTCATCATC	541
PKCζ Rs	GAGGACCTTGGCATAGCTTC	
PKCλ Fs	GCAGTGAGGTTCGAGATATG	380
PKCλ Rs	CCAGCAGTTTGCAGTTGATG	
GAPDH Fs	CAATGCATCCTGCACCACCAAC	320
GAPDH Rs	CATACTTGGCAGGTTTCTCCAG	
PKCδ Fq	TAAGCCCAAAGTGAAATCCC	138
PKCδ Rq	ACAAAGGAGAAGCCCTTGAA	
β-actin Fq	ATCGCTGACAGGATGCAGAAG	76
β-actin Rq	TCAGGAGGAGCAATGATCTTGA	
Methylated F	CGTAAGTAGTTGGGGAAGTTTC	230
Methylated R	CACGAAAACTAAAAAT CCGAC	
Unmethylated F	GGTGTAAGTAGTTGGGGAAGTTTT	233
Unmethylated R	CCACAAAAACTAAAAATCC AAC	
ChIP F	ACAAGCCAGCAGGAAGAGGA	163
ChIP R	TTATAGAGGAGGACTCCGAGGC	

F, Forward; R, Reverse; g, genomic PCR for cloning the rat PKCδ promoter; s, semiquantitative RT-PCR; q, quantitative RT-PCR.

Supplemental Table 2: Degradation of PKCδ protein in N27 cells

Cells	Half-lives (h)	K	R^2
Vec	14.77 ± 4.54	0.055 ± 0.017	0.971
Syn	14.07 ± 1.89	0.051 ± 0.007	0.845

PKCδ protein degradation data were fit to a one-phase exponential decay model using the nonlinear regression analysis program of Prism 4.0 software as follows: $Y = Span\ e^{-Kt} + Plateau$, where Y starts at Span + Plateau and decays with a rate constant K. The half-life of the each protein was subsequently determined by 0.693/K. The goodness-of-fit was assessed as the square of the correlation coefficient (R^2). Values are expressed as mean ± SEM.

Supplemental Table 3: Stability of PKCδ mRNA in N27 cells

Cells	Half-lives (h)	K	R^2
Vec	1.78 ± 0.17	0.396 ± 0.039	0.734
Syn	1.72 ± 0.24	0.415 ± 0.058	0.816

PKCδ mRNA stability data were fit to a one-phase exponential decay model using the nonlinear regression analysis program of Prism 4.0 software as follows: $Y = Span\ e^{-Kt} + Plateau$, where Y starts at Span + Plateau and decays with a rate constant K. The half-life of the each mRNA was subsequently determined by 0.693/K. The goodness-of-fit was assessed as the square of the correlation coefficient (R^2). Values are expressed as mean ± SEM.

Supplemental Table 4: Phylogenetic conserved putative TF-binding sites locating on rat PKCδ proximal promoter

Family/matri	TF	Position	Strand	Nucleotide Sequence	Binding Profile[a,b,c]
ETSF	NERF1a	-99 to -79	**(+)**	agccagca**GGAAg**aggaatga	nnrnca**GGAAg**nr
HAND	dHand-E12	-68 to -48	**(+)**	ggcagg**ccagcTGGCca**gtgg	**ccagaTGGCcc**cccn
MYOD	Myogenin	-50 to -66	(-)	actggc**CAGCtg**gcctg	rnkynm**CAGCtg**bnsbn
NEUR	Neurogenin 1/ 3	-65 to -53	**(+)**	aggC**CAGct**ggcc	svC**CAT**m**tg**kyn
NFkB	NFkB	-38 to -50	(-)	ccG**GGA**ctcc**cc**a	**GGGA**ntyy**cc**
NFkB	NFkB	-20 to -8	**(+)**	tg**GGGA**agcc**cc**g	**GGGA**ntyy**cc**

a nucleic acid codes used: a-adenine, c-cytosine, g-guanine, t-thymine, r-G or A, y-T or C, k-G or T, m-A or C, s-G or C, w-A or T, v-A or C or G, b-C or G or T, n-A or G or C or T.
b Base pairs written in bold indicate they appear in a position where the matrix exhibits a high conservation profile (consensus index vector > 60).
c Base pairs in capital letters denote the core sequence used by MatInspector (Genomatix Software) for predicting TF-binding sites.

Using the DiAlign TF program (Genomatix Software), six phylogenetic sequences conserved among rat, human, murine, and cow PKCδ promoter were identified. The nucleotide distribution matrix information was obtained from MatBase program (Genomatix Software).

Supplemental Table 5: Sense sequences of the oligonucleotides used in EMSAs

Probe/Competitor	Sense oligonucleotide (5'-3')
PkcδNFkB1	GTAGTTGGGGAAGCCCCGCC (-20 to -8)
PkcδNFkB1 mutant	GTAGTT**agct**AAGCCCCGCC
PkcδNFkB2	GCCAGTGGGGAGTCCCGGGC (-51 to -39)
PkcδNFkB2 mutant	GCCAGT**agct**AGTCCCGGGC
NFkB consensus	AGTTGAGGGGACTTTCCCAGGC
AP-1	CGCTTGATGACTCAGCCGGAA

Nucleotide sequences of the consensus binding motif are underlined. The localizations of the PKCδ NFκB sites, relative to the transcription start site, are shown. Mutated base pairs in mutant oligos are highlighted in bold and in lowercase.

References

Albani D, Peverelli E, Rametta R, Batelli S, Veschini L, Negro A, Forloni G (2004) Protective effect of TAT-delivered alpha-synuclein: relevance of the C-terminal domain and involvement of HSP70. Faseb J 18:1713-1715.

Alves Da Costa C, Paitel E, Vincent B, Checler F (2002) Alpha-synuclein lowers p53-dependent apoptotic response of neuronal cells. Abolishment by 6-hydroxydopamine and implication for Parkinson's disease. J Biol Chem 277:50980-50984.

Anantharam V, Kitazawa M, Wagner J, Kaul S, Kanthasamy AG (2002) Caspase-3-dependent proteolytic cleavage of protein kinase Cdelta is essential for oxidative stress-mediated dopaminergic cell death after exposure to methylcyclopentadienyl manganese tricarbonyl. J Neurosci 22:1738-1751.

Andra K, Abramowski D, Duke M, Probst A, Wiederhold KH, Burki K, Goedert M, Sommer B, Staufenbiel M (1996) Expression of APP in transgenic mice: a comparison of neuron-specific promoters. Neurobiol Aging 17:183-190.

Arif M, Pradhan SK, Thanuja GR, Vedamurthy BM, Agrawal S, Dasgupta D, Kundu TK (2009) Mechanism of p300 specific histone acetyltransferase inhibition by small molecules. J Med Chem 52:267-277.

Balasubramanyam K, Swaminathan V, Ranganathan A, Kundu TK (2003) Small molecule modulators of histone acetyltransferase p300. J Biol Chem 278:19134-19140.

Balasubramanyam K, Altaf M, Varier RA, Swaminathan V, Ravindran A, Sadhale PP, Kundu TK (2004) Polyisoprenylated benzophenone, garcinol, a natural histone

acetyltransferase inhibitor, represses chromatin transcription and alters global gene expression. J Biol Chem 279:33716-33726.

Baptista MJ, O'Farrell C, Daya S, Ahmad R, Miller DW, Hardy J, Farrer MJ, Cookson MR (2003) Co-ordinate transcriptional regulation of dopamine synthesis genes by alpha-synuclein in human neuroblastoma cell lines. J Neurochem 85:957-968.

Bennett MC (2005) The role of alpha-synuclein in neurodegenerative diseases. Pharmacol Ther 105:311-331.

Brodie C, Blumberg PM (2003) Regulation of cell apoptosis by protein kinase c delta. Apoptosis 8:19-27.

Burke RE (2008) Programmed cell death and new discoveries in the genetics of parkinsonism. J Neurochem 104:875-890.

Cartharius K, Frech K, Grote K, Klocke B, Haltmeier M, Klingenhoff A, Frisch M, Bayerlein M, Werner T (2005) MatInspector and beyond: promoter analysis based on transcription factor binding sites. Bioinformatics 21:2933-2942.

Chan HM, La Thangue NB (2001) p300/CBP proteins: HATs for transcriptional bridges and scaffolds. J Cell Sci 114:2363-2373.

Chandra S, Gallardo G, Fernandez-Chacon R, Schluter OM, Sudhof TC (2005) Alpha-synuclein cooperates with CSPalpha in preventing neurodegeneration. Cell 123:383-396.

Chen L, Fischle W, Verdin E, Greene WC (2001) Duration of nuclear NF-kappaB action regulated by reversible acetylation. Science 293:1653-1657.

Chen LF, Mu Y, Greene WC (2002) Acetylation of RelA at discrete sites regulates distinct nuclear functions of NF-kappaB. Embo J 21:6539-6548.

Chen YL, Law PY, Loh HH (2006) Sustained activation of phosphatidylinositol 3-kinase/Akt/nuclear factor kappaB signaling mediates G protein-coupled delta-opioid receptor gene expression. J Biol Chem 281:3067-3074.

Clarkson ED, Edwards-Prasad J, Freed CR, Prasad KN (1999) Immortalized dopamine neurons: A model to study neurotoxicity and neuroprotection. Proc Soc Exp Biol Med 222:157-163.

Clayton DF, George JM (1998) The synucleins: a family of proteins involved in synaptic function, plasticity, neurodegeneration and disease. Trends Neurosci 21:249-254.

Cooper AA, Gitler AD, Cashikar A, Haynes CM, Hill KJ, Bhullar B, Liu K, Xu K, Strathearn KE, Liu F, Cao S, Caldwell KA, Caldwell GA, Marsischky G, Kolodner RD, Labaer J, Rochet JC, Bonini NM, Lindquist S (2006) Alpha-synuclein blocks ER-Golgi traffic and Rab1 rescues neuron loss in Parkinson's models. Science 313:324-328.

Dauer W, Przedborski S (2003) Parkinson's disease: mechanisms and models. Neuron 39:889-909.

de Erausquin GA, Hyrc K, Dorsey DA, Mamah D, Dokucu M, Masco DH, Walton T, Dikranian K, Soriano M, Garcia Verdugo JM, Goldberg MP, Dugan LL (2003) Nuclear translocation of nuclear transcription factor-kappa B by alpha-amino-3-hydroxy-5-methyl-4-isoxazolepropionic acid receptors leads to transcription of p53 and cell death in dopaminergic neurons. Mol Pharmacol 63:784-790.

Deng WG, Zhu Y, Wu KK (2003) Up-regulation of p300 binding and p50 acetylation in tumor necrosis factor-alpha-induced cyclooxygenase-2 promoter activation. J Biol Chem 278:4770-4777.

DeVries TA, Neville MC, Reyland ME (2002) Nuclear import of PKCdelta is required for apoptosis: identification of a novel nuclear import sequence. Embo J 21:6050-6060.

Duan J, Friedman J, Nottingham L, Chen Z, Ara G, Van Waes C (2007) Nuclear factor-kappaB p65 small interfering RNA or proteasome inhibitor bortezomib sensitizes head and neck squamous cell carcinomas to classic histone deacetylase inhibitors and novel histone deacetylase inhibitor PXD101. Mol Cancer Ther 6:37-50.

Ghosh A, Chandran K, Kalivendi SV, Joseph J, Antholine WE, Hillard CJ, Kanthasamy A, Kanthasamy A, Kalyanaraman B (2010) Neuroprotection by a mitochondria-targeted drug in a Parkinson's disease model. Free Radic Biol Med.

Giasson BI, Duda JE, Quinn SM, Zhang B, Trojanowski JQ, Lee VM (2002) Neuronal alpha-synucleinopathy with severe movement disorder in mice expressing A53T human alpha-synuclein. Neuron 34:521-533.

Goers J, Manning-Bog AB, McCormack AL, Millett IS, Doniach S, Di Monte DA, Uversky VN, Fink AL (2003) Nuclear localization of alpha-synuclein and its interaction with histones. Biochemistry 42:8465-8471.

Greenamyre JT, Hastings TG (2004) Biomedicine. Parkinson's--divergent causes, convergent mechanisms. Science 304:1120-1122.

Gustin JA, Ozes ON, Akca H, Pincheira R, Mayo LD, Li Q, Guzman JR, Korgaonkar CK, Donner DB (2004) Cell type-specific expression of the IkappaB kinases determines the significance of phosphatidylinositol 3-kinase/Akt signaling to NF-kappa B activation. J Biol Chem 279:1615-1620.

Hashimoto M, Hsu LJ, Rockenstein E, Takenouchi T, Mallory M, Masliah E (2002) alpha-Synuclein protects against oxidative stress via inactivation of the c-Jun

N-terminal kinase stress-signaling pathway in neuronal cells. J Biol Chem 277:11465-11472.

Hatcher JM, Pennell KD, Miller GW (2008) Parkinson's disease and pesticides: a toxicological perspective. Trends Pharmacol Sci 29:322-329.

Iwai A, Masliah E, Yoshimoto M, Ge N, Flanagan L, de Silva HA, Kittel A, Saitoh T (1995) The precursor protein of non-A beta component of Alzheimer's disease amyloid is a presynaptic protein of the central nervous system. Neuron 14:467-475.

Jensen PJ, Alter BJ, O'Malley KL (2003) Alpha-synuclein protects naive but not dbcAMP-treated dopaminergic cell types from 1-methyl-4-phenylpyridinium toxicity. J Neurochem 86:196-209.

Jing Q, Huang S, Guth S, Zarubin T, Motoyama A, Chen J, Di Padova F, Lin SC, Gram H, Han J (2005) Involvement of microRNA in AU-rich element-mediated mRNA instability. Cell 120:623-634.

Kanthasamy AG, Kitazawa M, Kanthasamy A, Anantharam V (2003) Role of proteolytic activation of protein kinase Cdelta in oxidative stress-induced apoptosis. Antioxid Redox Signal 5:609-620.

Kanthasamy AG, Anantharam V, Zhang D, Latchoumycandane C, Jin H, Kaul S, Kanthasamy A (2006) A novel peptide inhibitor targeted to caspase-3 cleavage site of a proapoptotic kinase protein kinase C delta (PKCdelta) protects against dopaminergic neuronal degeneration in Parkinson's disease models. Free Radic Biol Med 41:1578-1589.

Kaul S, Anantharam V, Kanthasamy A, Kanthasamy AG (2005a) Wild-type alpha-synuclein interacts with pro-apoptotic proteins PKCdelta and BAD to protect dopaminergic

neuronal cells against MPP+-induced apoptotic cell death. Brain Res Mol Brain Res 139:137-152.

Kaul S, Kanthasamy A, Kitazawa M, Anantharam V, Kanthasamy AG (2003) Caspase-3 dependent proteolytic activation of protein kinase C delta mediates and regulates 1-methyl-4-phenylpyridinium (MPP+)-induced apoptotic cell death in dopaminergic cells: relevance to oxidative stress in dopaminergic degeneration. Eur J Neurosci 18:1387-1401.

Kaul S, Anantharam V, Yang Y, Choi CJ, Kanthasamy A, Kanthasamy AG (2005b) Tyrosine phosphorylation regulates the proteolytic activation of protein kinase Cdelta in dopaminergic neuronal cells. J Biol Chem 280:28721-28730.

Kiernan R, Bres V, Ng RW, Coudart MP, El Messaoudi S, Sardet C, Jin DY, Emiliani S, Benkirane M (2003) Post-activation turn-off of NF-kappa B-dependent transcription is regulated by acetylation of p65. J Biol Chem 278:2758-2766.

Kitazawa M, Anantharam V, Kanthasamy AG (2003) Dieldrin induces apoptosis by promoting caspase-3-dependent proteolytic cleavage of protein kinase Cdelta in dopaminergic cells: relevance to oxidative stress and dopaminergic degeneration. Neuroscience 119:945-964.

Kitazawa M, Anantharam V, Yang Y, Hirata Y, Kanthasamy A, Kanthasamy AG (2005) Activation of protein kinase C delta by proteolytic cleavage contributes to manganese-induced apoptosis in dopaminergic cells: protective role of Bcl-2. Biochem Pharmacol 69:133-146.

Kontopoulos E, Parvin JD, Feany MB (2006) Alpha-synuclein acts in the nucleus to inhibit histone acetylation and promote neurotoxicity. Hum Mol Genet 15:3012-3023.

Latchoumycandane C, Anantharam V, Kitazawa M, Yang Y, Kanthasamy A, Kanthasamy AG (2005) Protein kinase Cdelta is a key downstream mediator of manganese-induced apoptosis in dopaminergic neuronal cells. J Pharmacol Exp Ther 313:46-55.

Lee DW, Rajagopalan S, Siddiq A, Gwiazda R, Yang L, Beal MF, Ratan RR, Andersen JK (2009) Inhibition of prolyl hydroxylase protects against 1-methyl-4-phenyl-1,2,3,6-tetrahydropyridine-induced neurotoxicity: model for the potential involvement of the hypoxia-inducible factor pathway in Parkinson disease. J Biol Chem 284:29065-29076.

Lee MK, Stirling W, Xu Y, Xu X, Qui D, Mandir AS, Dawson TM, Copeland NG, Jenkins NA, Price DL (2002) Human alpha-synuclein-harboring familial Parkinson's disease-linked Ala-53 --> Thr mutation causes neurodegenerative disease with alpha-synuclein aggregation in transgenic mice. Proc Natl Acad Sci U S A 99:8968-8973.

Leng Y, Chuang DM (2006) Endogenous alpha-synuclein is induced by valproic acid through histone deacetylase inhibition and participates in neuroprotection against glutamate-induced excitotoxicity. J Neurosci 26:7502-7512.

Li LC, Dahiya R (2002) MethPrimer: designing primers for methylation PCRs. Bioinformatics 18:1427-1431.

Manning-Bog AB, McCormack AL, Purisai MG, Bolin LM, Di Monte DA (2003) Alpha-synuclein overexpression protects against paraquat-induced neurodegeneration. J Neurosci 23:3095-3099.

Mantelingu K, Kishore AH, Balasubramanyam K, Kumar GV, Altaf M, Swamy SN, Selvi R, Das C, Narayana C, Rangappa KS, Kundu TK (2007) Activation of p300 histone acetyltransferase by small molecules altering enzyme structure: probed by surface-enhanced Raman spectroscopy. J Phys Chem B 111:4527-4534.

Matsuoka Y, Vila M, Lincoln S, McCormack A, Picciano M, LaFrancois J, Yu X, Dickson D, Langston WJ, McGowan E, Farrer M, Hardy J, Duff K, Przedborski S, Di Monte DA (2001) Lack of nigral pathology in transgenic mice expressing human alpha-synuclein driven by the tyrosine hydroxylase promoter. Neurobiol Dis 8:535-539.

Monti B, Polazzi E, Batti L, Crochemore C, Virgili M, Contestabile A (2007) Alpha-synuclein protects cerebellar granule neurons against 6-hydroxydopamine-induced death. J Neurochem 103:518-530.

Morgenstern B, Dress A, Werner T (1996) Multiple DNA and protein sequence alignment based on segment-to-segment comparison. Proc Natl Acad Sci U S A 93:12098-12103.

Morgenstern B, Frech K, Dress A, Werner T (1998) DIALIGN: finding local similarities by multiple sequence alignment. Bioinformatics 14:290-294.

Nakatani F, Tanaka K, Sakimura R, Matsumoto Y, Matsunobu T, Li X, Hanada M, Okada T, Iwamoto Y (2003) Identification of p21WAF1/CIP1 as a direct target of EWS-Fli1 oncogenic fusion protein. J Biol Chem 278:15105-15115.

Norris EH, Giasson BI, Lee VM (2004) Alpha-synuclein: normal function and role in neurodegenerative diseases. Curr Top Dev Biol 60:17-54.

Ostrerova N, Petrucelli L, Farrer M, Mehta N, Choi P, Hardy J, Wolozin B (1999) alpha-Synuclein shares physical and functional homology with 14-3-3 proteins. J Neurosci 19:5782-5791.

Outeiro TF, Lindquist S (2003) Yeast cells provide insight into alpha-synuclein biology and pathobiology. Science 302:1772-1775.

Patrone G, Puppo F, Cusano R, Scaranari M, Ceccherini I, Puliti A, Ravazzolo R (2000) Nuclear run-on assay using biotin labeling, magnetic bead capture and analysis by fluorescence-based RT-PCR. Biotechniques 29:1012-1014, 1016-1017.

Peng J, Stevenson FF, Doctrow SR, Andersen JK (2005a) Superoxide dismutase/catalase mimetics are neuroprotective against selective paraquat-mediated dopaminergic neuron death in the substantial nigra: implications for Parkinson disease. J Biol Chem 280:29194-29198.

Peng X, Tehranian R, Dietrich P, Stefanis L, Perez RG (2005b) Alpha-synuclein activation of protein phosphatase 2A reduces tyrosine hydroxylase phosphorylation in dopaminergic cells. J Cell Sci 118:3523-3530.

Perez RG, Waymire JC, Lin E, Liu JJ, Guo F, Zigmond MJ (2002) A role for alpha-synuclein in the regulation of dopamine biosynthesis. J Neurosci 22:3090-3099.

Poizat C, Puri PL, Bai Y, Kedes L (2005) Phosphorylation-dependent degradation of p300 by doxorubicin-activated p38 mitogen-activated protein kinase in cardiac cells. Mol Cell Biol 25:2673-2687.

Rathke-Hartlieb S, Kahle PJ, Neumann M, Ozmen L, Haid S, Okochi M, Haass C, Schulz JB (2001) Sensitivity to MPTP is not increased in Parkinson's disease-associated mutant alpha-synuclein transgenic mice. J Neurochem 77:1181-1184.

Seo JH, Rah JC, Choi SH, Shin JK, Min K, Kim HS, Park CH, Kim S, Kim EM, Lee SH, Lee S, Suh SW, Suh YH (2002) Alpha-synuclein regulates neuronal survival via Bcl-2 family expression and PI3/Akt kinase pathway. Faseb J 16:1826-1828.

Sidhu A, Wersinger C, Moussa CE, Vernier P (2004) The role of alpha-synuclein in both neuroprotection and neurodegeneration. Ann N Y Acad Sci 1035:250-270.

Souto JA, Benedetti R, Otto K, Miceli M, Alvarez R, Altucci L, de Lera AR (2010) New anacardic acid-inspired benzamides: histone lysine acetyltransferase activators. ChemMedChem 5:1530-1540.

Spillantini MG, Crowther RA, Jakes R, Hasegawa M, Goedert M (1998) alpha-Synuclein in filamentous inclusions of Lewy bodies from Parkinson's disease and dementia with lewy bodies. Proc Natl Acad Sci U S A 95:6469-6473.

Stephan A, Davis S, Salin H, Dumas S, Mallet J, Laroche S (2002) Age-dependent differential regulation of genes encoding APP and alpha-synuclein in hippocampal synaptic plasticity. Hippocampus 12:55-62.

Suh KS, Tatunchak TT, Crutchley JM, Edwards LE, Marin KG, Yuspa SH (2003) Genomic structure and promoter analysis of PKC-delta. Genomics 82:57-67.

Takai D, Jones PA (2002) Comprehensive analysis of CpG islands in human chromosomes 21 and 22. Proc Natl Acad Sci U S A 99:3740-3745.

Wislet-Gendebien S, D'Souza C, Kawarai T, St George-Hyslop P, Westaway D, Fraser P, Tandon A (2006) Cytosolic proteins regulate alpha-synuclein dissociation from presynaptic membranes. J Biol Chem 281:32148-32155.

Yang Y, Kaul S, Zhang D, Anantharam V, Kanthasamy AG (2004) Suppression of caspase-3-dependent proteolytic activation of protein kinase C delta by small

interfering RNA prevents MPP+-induced dopaminergic degeneration. Mol Cell Neurosci 25:406-421.

Zafar KS, Inayat-Hussain SH, Ross D (2007) A comparative study of proteasomal inhibition and apoptosis induced in N27 mesencephalic cells by dopamine and MG132. J Neurochem 102:913-921.

Zhang D, Anantharam V, Kanthasamy A, Kanthasamy AG (2007a) Neuroprotective effect of protein kinase C delta inhibitor rottlerin in cell culture and animal models of Parkinson's disease. J Pharmacol Exp Ther 322:913-922.

Zhang D, Kanthasamy A, Yang Y, Anantharam V, Kanthasamy A (2007b) Protein kinase C delta negatively regulates tyrosine hydroxylase activity and dopamine synthesis by enhancing protein phosphatase-2A activity in dopaminergic neurons. J Neurosci 27:5349-5362.

Zhang D, Kanthasamy A, Yang Y, Anantharam V, Kanthasamy A (2007c) Protein kinase Cdelta negatively regulates tyrosine hydroxylase activity and dopamine synthesis by enhancing protein phosphatase-2A activity in dopaminergic neurons. J Neurosci 27:5349-5362.

Zhang L, Zhang C, Zhu Y, Cai Q, Chan P, Ueda K, Yu S, Yang H (2008) Semi-quantitative analysis of alpha-synuclein in subcellular pools of rat brain neurons: an immunogold electron microscopic study using a C-terminal specific monoclonal antibody. Brain Res 1244:40-52.

Zhong H, May MJ, Jimi E, Ghosh S (2002) The phosphorylation status of nuclear NF-kappa B determines its association with CBP/p300 or HDAC-1. Mol Cell 9:625-636.

Zhou C, Huang Y, Przedborski S (2008) Oxidative stress in Parkinson's disease: a mechanism of pathogenic and therapeutic significance. Ann N Y Acad Sci 1147:93-104.

Zhu M, Qin ZJ, Hu D, Munishkina LA, Fink AL (2006) Alpha-synuclein can function as an antioxidant preventing oxidation of unsaturated lipid in vesicles. Biochemistry 45:8135-8142.

CHAPTER V: INCREASED EXPRESSION OF PRO-APOPTOTIC KINASE PKCδ FOLLOWING EXPOSURE TO MANGANESE: IMPLICATIONS FOR GENE-ENVIRONMENT INTERACTIONS IN NEURODEGENERATION

A paper submitted to *Environmental Health Perspectives*

Huajun Jin, Arthi Kanthasamy, Danhui Zhang, Vellareddy Anantharam, and Anumantha Kanthasamy

Abstract

BACKGROUND/OBJECTIVES: Exposure to elevated levels of the essential trace element manganese cause a neurodegenerative disorder, termed manganism, resulting from degeneration of neurons within the basal ganglia. However, the precise mechanisms underlying the known pathological effects of manganese remain elusive. Our previous studies have shown that proteolytic activation of PKCδ, a member of the novel PKC family, plays a key role in manganese-induced neurodegeneration. We are interested in examining whether manganese exposure can result in aberrant expression of PKCδ, which may exert neurodegenerative effects through the consequent potentiation of the activation of PKCδ.

METHODS: As a proof of concept, a mouse model of manganese *via* oral gavage and primary neurons culture, as well as cultured NIE-115 cells was utilized to examine the effects of manganese on PKCδ expression.

RESULTS: Manganese exposure potently induced PKCδ levels in primary striatal neurons and NIE-115 cells. The use of primary neurons from mice lacking PKCδ subsequently demonstrated that the level of PKCδ plays a critical role in manganese-induced neurodegeneration. Experiments on manganese-exposed mice also confirmed the action of manganese in upregulation of PKCδ. Using NIE-115 cells, we further elucidated the mechanisms underlying the manganese-induced up-regulation of PKCδ. We identified that NFκB is essential for both basal and manganese-mediated expression of PKCδ in NIE-115 cells.

CONCLUSIONS: These results demonstrate that the environmental neurotoxicant manganese greatly alters the gene expression of PKCδ, a key oxidative-stress sensitive kinase involved in multiple modes of neurodegeneration.

Introduction

Chronic exposure to elevated levels of manganese, an essential trace metal required for normal brain function, in human and non-human primates is long known to cause manganism, a complex neurodegenerative disorder characterized by symptoms that broadly resembles the dystonic movements associated with Parkinson's disease (PD) (Benedetto et al., 2009). In addition to occupational and industrial settings, such as mining, welding, and steel manufacturing (Keen et al., 2000), chronic liver diseases and parenteral nutrition are also known risk factors for manganese intoxication (Hauser et al., 1994). Manganese accumulates at the highest levels in the striatum, globus pallidus, and substantia nigra in exposed humans and monkeys (Erikson et al., 2004). Pathological changes include neuronal

loss and gliosis within the basal ganglia, principally in globus pallidus and less severe in striatum and substantia nigra pars reticulata (Perl and Olanow, 2007; Aschner et al., 2009a). Current evidence indicates that manganese induces a variety of cellular alterations, including glutathione and dopamine depletion, impairment of iron metabolism and energy metabolism, and increased oxidative stress (Dobson et al., 2004; Olanow, 2004b). While the understanding of the pathogenic mechanisms underlying manganese neurotoxicity remains elusive, a growing number of studies have suggested that apoptosis resulted from oxidative stress and mitochondrial dysfunction plays a pivotal role in manganese toxicity (Liu et al., 2005; Benedetto et al., 2009), Therefore, identification of the molecular targets mediating the manganese-induced apoptotic process is essential in understanding the brain pathologies associated with manganese.

Recently, we discovered that caspase-3-dependent proteolytic activation of proapoptotic PKCδ is a key mediator of manganese-induced neurodegeneration, and that inhibition of PKCδ by employing pharmacological inhibitors or overexpression catalytically inactive PKCδ mutant attenuated the manganese neurotoxicity (Anantharam et al., 2002; Latchoumycandane et al., 2005). These results indicate that PKCδ could represent a valid pharmacological target for development of a neuroprotective strategy against manganese. In the present study, we extend the previous observations by presenting new evidence that chronic manganese exposure markedly increases PKCδ gene expression in the striatum of animals, in primary striatal neuron cultures, and NIE-115 cells. Furthermore, we demonstrated that the potentiation of PKCδ expression is likely through an NFκB signaling pathway. Our results provide a new link between the environmental neurotoxin manganese and PKCδ gene, which plays a key role in manganese-induced neurodegeneration.

Materials and Methods

Reagents

Manganese chloride ($MnCl_2.4H_2O$) was obtained from Fluka (Milwaukee, WI). Poly-D-lysine was purchased from Sigma-Aldrich (St. Louis, MO). Neurobasal medium, Neurobasal supplement (B27), Lipofectamine 2000 reagent, hygromycin B, penicillin, streptomycin, fetal bovine serum, L-glutamine, and Dulbecco's modified Eagle's medium were purchased from Invitrogen (Carlsbad, CA). Antibodies to PKCδ, PKCβI, PKCζ, p65, and p50 were purchased from Santa Cruz Biotechnology (Santa Cruz, CA); the mouse β-actin antibody were purchased from Sigma-Aldrich. IRDye800 conjugated anti-rabbit secondary antibody was obtained from Rockland Labs (Gilbertsville, PA). Alexa 680-conjugated anti-mouse secondary antibody was obtained from Invitrogen.

Animal experiments

Six- to eight-week-old C57B1/6 mice and PKCδ knock-out mice were housed in a temperature-controlled, 12:12 h light/dark room, and were allowed free access to food and water. $MnCl_2.4H_2O$ was dissolved in sterile saline and administered to C57B1/6 mice by a single gavage at a dose of 3 or 10 mg of Mn/kg. An equal volume of saline was given to the control animals. To achieve precise doses of manganese, the amount of manganese delivered was adjusted for the molecular concentration in the tetrahydrate form. These doses were selected based upon previous studies in both human and rodent exhibiting symptoms of manganese intoxication (Mergler et al., 1999; Li et al., 2006; Zhang et al., 2009). Mice were

sacrificed one month after the onset of manganese administration, and the brain areas of interest were immediately and carefully dissected out and stored at -80°C. The PKCδ$^{-/-}$ mice previously have been described (Zhang et al., 2007c). Animal care procedures strictly followed the NIH Guide for the Care and Use of Laboratory Animals and were approved by the Iowa State University IACUC.

Mouse striatal neurons in primary culture and treatment

Plates (6-well) were coated overnight with 0.1 mg/ml poly-D-lysine. Striatal tissue was dissected from gestational 16- to 18-day-old mice embryos from wild-type (C57B1/6) mice or PKCδ knock-out mice (Zhang et al., 2007c), and kept in ice-cold Ca^{2+}-free Hanks's balanced salt solution. Cells were then dissociated in Hank's balanced salt solution containing trypsin-0.25% EDTA for 30 min at 37 °C. After enzyme inhibition with 10% heat-inactivated fetal bovine serum in Dulbecco's modified Eagle's medium, the cells were suspended in Neurobasal medium supplemented with 2% Neurobasal supplement (B27), 500 μM L-glutamine, 100 IU/ml penicillin, and 100 μg/ml streptomycin, plated at 2×10^6 cells in 2 ml/well and incubated in a humidified CO_2 incubator (5% CO_2 and 37 °C). Half of the culture medium was replaced every 2 days, and experiments were conducted between 6 and 7 days cultures. After exposure to doses of $MnCl_2$ ranging from 50 to 150 μM for 24 or 48 h as indicated in figures, the primary striatal cultures were collected for later analysis.

Cell lines

Mouse neuroblastoma NIE-115 cell line was a kind gift from Dr. Debomoy Lahiri (Indiana University School of Medicine, Indianapolis, IN). Mouse dopaminergic MN9D cell

line was a kind gift from Dr. Syed Ali (National Center for Toxicological Research/FDA, Jefferson, AR). Mouse neuroblastoma N2a and mouse BV2 microglia cell lines were obtained from the American Type Culture Collection (ATCC, Rockville, MD). BV2, MN9D, NIE-115 and N2a cells were grown in Dulbecco's modified Eagle's medium supplemented with 10% fetal bovine serum, 2 mM L-glutamine, 50 units penicillin, and 50 units streptomycin.

Plasmid constructs

The PKCδ promoter/luciferase reporter construct pGL3-1448/+1 containing the 1.4-kb upstream region of the transcription start site of the mouse PKCδ gene was constructed by PCR amplification using pGlow-PKCδ-GFP, obtained from Dr. Sanford Sampson (Bar-Ilan University, Ramat-Gan, Israel), as a template as well as the primer sets P-1448/P+1 (see supplemental Table 1 for all primers sequences) and subcloned into the XhoI/HindIII sites of pGL3-Basic luciferase reporter vector (Promega, Madison, WI). Using pGL3-1448/+1 as a template, a series of truncated PKCδ promoter reporter constructs were constructed by PCR with appropriate primers indicated in supplemental Table 1 and cloned into pGL3-Basic vector similar to the preparation of pGL3-1448/+1. All reporter constructs were verified by DNA sequencing. Wild-type NFκB-p65 and NFκB-p50 expression constructs and NFκB-p65 deletion construct p65ΔC, containing p65 amino acids 1 to 337, were obtained from Dr. Vivek Rangnekar (University of Kentucky, Lexington, KY).

Site-directed mutagenesis

Point mutations of potential transcription elements were introduced into the proximal PKCδ promoter reporter plasmid pGL3-147/+1 by using the GeneTailor Site-Directed Mutagenesis System (Invitrogen) with overlapping PCR primers indicated in supplemental Table 1, according to the manufacturer's instructions. To generate double mutants, plasmids carrying a single mutation were used as a template to further introduce the second mutation. The mutated sequences of all mutants were confirmed by DNA sequencing.

Protein isolation and immunoblot analysis

Cell lysates or brain homogenates were prepared as previously described (Zhang et al. 2007). Immunoblotting and densitometric analysis of immunoblots were performed as previously described (Kanthasamy et al. 2006). Briefly, the samples containing equal amounts of protein were fractionated through a 10% SDS-PAGE and transferred onto a nitrocellulose membrane (Bio-Rad, Hercules, CA). Membranes were blotted with the appropriate primary antibody and developed with IRDye800 anti-rabbit or Alexa 680-conjugated anti-mouse secondary antibodies (Invitrogen). The immunosignals were visualized with an Odyssey Infrared Imaging System (Li-cor, Lincoln, NE), and the quantitation of immunoblots was done using Odyssey Software 2.0 (Li-cor).

Sytox green cytotoxicity assays

Cell death was determined after exposing the primary striatal neurons to manganese using the Sytox green cytotoxicity assay. Sytox green is a vital probe of low background fluorescence that is excluded from cells with intact membranes, but labels nucleic acids in

cells that have impaired membrane integrity or that have recently died to produce green fluorescence (Roth et al., 1997; Sherer et al., 2002). The assay was performed as previously described (Kaul et al., 2005b). In brief, the primary striatal neurons were treated with manganese (0-150 μM) and 1 μM Sytox green fluorescent dye for 24 h. The cytotoxic cell death was then quantified by measuring DNA-bound Sytox green using the Synergy 2 Multi-Mode Microplate Reader (excitation 485 nm; emission 538 nm) (BioTek, Winooski, VT). Fluorescent images of Sytox-positive cells were taken with a NIKON TE2000 microscope, and pictures were captured with a SPOT digital camera.

Caspase-3 enzymatic assays

Caspases-3 activity was measured as previously described (Kaul et al., 2005a). Briefly, after treatment with manganese (0-150 μM), cells lysates were prepared and incubated with a specific fluorescent substrate, Ac-DEVD-AMC (50 μM) at 37 °C for 1 h. Caspases-3 activity was then measured using a SpectraMax Gemini XS Microplate Reader (Molecular Devices, Sunnyvale, CA) with excitation at 380 nm and emission at 460 nm. The caspase-3 activity was calculated as fluorescence units per milligram of protein.

Transient transfections and reporter gene assays

Transient transfections of NIE-115 cells were performed using Lipofectamine 2000 reagent (Invitrogen) according to the manufacturer's instructions. Cells were plated at 0.3 × 106 cells/well in six-well plates one day before transfection. Each transfection was performed with 4 μg of reporter constructs along with 0.5 μg of β-galactosidase expression vector pcDNA3.1-βgal (Invitrogen) used to monitor transfection efficiencies. Cells were

harvested at 24 h post-transfection, lysed in 200 μl of Reporter Lysis Buffer (Promega), and assayed for luciferase activity. For cotransfection assays, 8 μg of expression plasmids for p65, p50 or p65 deletion as indicated in figures was added to the reporter plasmids. The total amount of DNA was adjusted by adding empty vector pcDNA-3.1 (Invitrogen). In some experiments, MnCl2 (300 μM) was added 12 h after DNA transfection, and luciferase activity was measured at the indicated times.

Luciferase activity was measured on a Synergy 2 Multi-Mode Microplate Reader (BioTek, Winooski, VT) using the Luciferase assay system (Promega), and β-galactosidase activity was detected using the β-Galactosidase Enzyme assay system (Promega). The ratio of luciferase activity to β-galactosidase activity was used as a measure of normalized luciferase activity. All values were determined from three independent transfection experiments done in triplicate and expressed as average values ± S.E.

Quantitative real-time RT-PCR and methylation specific PCR (MSP)

Total RNA was isolated from fresh cell pellets using the Absolutely RNA Miniprep Kit (Stratagene, La Jolla, CA) according the manufacturer's protocols. Aliquots of 3 μg of total RNA were used for first strand cDNA synthesis by random primer and AffinityScript Multiple Temperature Reverse Transcriptase in a 20 μl reaction volume using an AffinityScript QPCR cDNA Synthesis Kit (Stratagene). Quantitative RT-PCR was performed in an Mx3000P QPCR System (Stratagene) using the Brilliant SYBR Green QPCR Master Mix Kit (Stratagene), with cDNAs corresponding to 150 ng of total RNA, 12.5 μl of 2 × master mix, 0.375 μl of reference dye, and 0.2 μM of each primer in a 25-μl final reaction volume. All reactions were performed in triplicate. Sequences for PKCδ primers used in this

study are shown in supplemental Table 1. β-actin was used as internal standard with the primer set purchased from Qiagen (QuantiTect Primers, catalog number QT01136772). The PCR Cycling conditions contained an initial denaturation at 95 °C for 10 min, followed by 40 cycles of denaturation at 95 °C for 30 sec, annealing at 60 °C for 30 sec, and extension at 72°C for 30 sec. Fluorescence was detected during the annealing step of each cycle. Dissociation curves were run to verify the singularity of the PCR product. The data were analyzed using the comparative threshold cycle (Ct) method (Livak and Schmittgen, 2001) . The PKCδ mRNA values were normalized to the amount of β-actin internal control in each sample and expressed as the fold of mRNA levels of control samples (set to 1).

For MSP experiments, genomic DNA was isolated using the DNeasy blood & tissue kit as mentioned earlier. Bisulfite modification was subsequently carried out on 500 ng of genomic DNA by the MethylDetector bisulfite modification kit (Active Motif, Carlsbad, CA) according to the manufacturer's instructions. Two pairs of primers were designed to amplify specifically methylated or unmethylated PKCδ sequence using MethPrimer software (Li and Dahiya, 2002). The cycling condition was: 94 °C for 3 min, after which 35 cycles of 94 °C for 30 sec, 54 °C for 30 sec, 68 °C for 30 sec, and finally 72 °C for 5 min. PCR products were loaded onto 2% agarose gels for analysis.

Chromatin immunoprecipitation (ChIP)

The ChIP-IT Express enzymatic kit from Active Motif was used to analyze the in vivo binding of NFκB p65 subunit onto the mouse PKCδ promoter region. Unless otherwise stated, all reagents, buffers and supplies were included in the kit. The ChIP assays were performed following the manufacture's instructions with slight modifications. Briefly, ~1.5 ×

107 cells were fixed in 1% formaldehyde for 10 min at room temperature. After cross-linking, the nuclei were prepared and chromatin was enzymatic digested to 200-1500 bp fragments (verified through running on a 1% agarose gel) by incubation with the enzymatic shearing cocktail for 12 min at 37 °C. The sheared chromatin was collected by centrifuge, and a 10-µl aliquot was saved as an input sample. Aliquots of 70-µl sheared chromatin were incubated overnight with rotation at 4 °C with protein G magnetic beads and three µg indicated antibody. Equal aliquots of each chromatin sample were saved for no-antibody controls. After extensive washing, reversal of cross-links, and proteinase K digestion, the elute DNA in the immunoprecipitated samples was directly collected on a magnetic stand, and the input DNA was purified by phenol/chloroform extraction and ethanol precipitation. The DNA samples were analyzed by PCR using primer pairs designed to amplify a region (-103 to +60) within PKCδ promoter. Conditions of linear amplification were determined empirically for the primers. PCR conditions are as follows: 94 °C 3 min; 94 °C 20 sec, 58 °C 30 sec, and 72 °C 30 sec for 35 cycles. The PCR products were resolved by electrophoresis in a 1.0% agarose gel and visualized after ethidium bromide staining.

Bioinformatics

CpG island identification was analyzed with the web-based program CpG Island Searcher (Takai and Jones, 2002). This program defines a CpG island as a region with a G+C content ≥ 50%, longer than 200 bp nucleotides, and an Observation/Expectation CpG ratio > 0.6. The search for the phylogenetic sequence conservation between human and murine PKCδ promoter was conducted with the DiAlign professional TF Release 3.1.1 (DiAlign TF) (Morgenstern et al., 1996; Morgenstern et al., 1998) (Genomatix Software, Munich,

Germany). This program identifies common transcription factor binding site matches located in aligned regions though a combination of alignment of input sequences using multiple alignment program DiAlign (Morgenstern et al., 1996; Morgenstern et al., 1998) with recognition of potential transcriptional factor binding sites by MatInspector software (Cartharius et al., 2005) (Genomatix Software), which employed matrices library version 8.0. The solution parameters for MatInspector program were: core similarity of 0.75 and optimized matrix similarity (default program's settings).

Statistical analysis

Unless otherwise stated, all data were determined from three independent experiments, each done in triplicate, and expressed as average values ± SEM. All statistical analyses were performed using the GraphPad Prism 4.0 software (GraphPad Software, San Diego, CA). One-way analysis of variance followed by the Tukey multiple comparison tests was used for statistical comparisons, and differences were considered significant if *P*-values < 0.05.

Results

Manganese exposure induces PKCδ expression in primary striatal neurons culture

We have previously described that PKCδ functions as an oxidative-stress sensitive kinase and its proteolytic activation plays a critical role in manganese-induced dopaminergic degeneration (Latchoumycandane et al., 2005). Given the importance of PKCδ in modulating manganese-induced apoptotic signaling events, we asked whether manganese nerurotoxicity

involves up-regulation of PKCδ expression as a novel mechanism to promote apoptosis. This possibility is favored by previous studies showing that PKCδ expression is specifically induced in the perifocal cortex and striatum under certain pathologic conditions, such as brain ischemia (Koponen et al., 2000). Furthermore, several lines of evidence linked manganese-induced gene expression changes to manganese intoxication (Gonzalez et al., 2008; Guilarte et al., 2008; Prabhakaran et al., 2009). To test this hypothesis, we first examined the capacity of manganese to potentiate expression of PKCδ in primary striatal cell cultures. Because previous studies on monkeys showed that the levels of manganese in the striatum and globus pallidus can reach to a higher value than 200 μM, we chose the manganese concentrations up to 300 μM to examine its effect in primary striatal neurons. As shown in Figure 1, when the striatal culture was treated with increasing doses of manganese for 24 h or 48 h, both total PKCδ and cleaved PKCδ abundance were time- and dose-dependently increased. These results led us to further evaluate whether increasing PKCδ levels by manganese correlates with neurotoxicity. Accordingly, we examined neurotoxicity following manganese exposure in primary striatal neurons from PKCδ knock-out and wild-type mice. The extent of apoptosis in both primary cultures treated with 50 and 150 μM manganese for 24 h was measured by caspase-3 enzymatic activity (Figure 2A) and Sytox Green cytotoxicity (Figure 2B and 2C) analysis. Manganese induced a dose-dependent increase in the caspase-3 activity and cytotoxicity in striatal neurons from $PKC\delta^{+/+}$ mice, whereas primary striatal neurons from $PKC\delta^{-/-}$ mice showed a significant reduction in the manganese-induced caspase-3 activity ($p<0.01$) and cell death ($p<0.001$). These results clearly suggest that an increase in PKCδ levels is at least partly responsible for

the enhanced susceptibility to manganese toxicity.

Treatment with manganese results in a marked induction of PKCδ protein and mRNA in murine NIE-115 cells

Next, we investigated a potential role of manganese in PKCδ expression by utilizing a cultured neuronal cell line (NIE-115) as an *in vitro* model system. The murine neuroblastoma-derived NIE-115 cells, which express a high level of endogenous tyrosine hydroxylase (Amano et al., 1972), have been well characterized as an *in vitro* model for studying neurodegeneration (Ostlund et al., 2001; Benitez-King et al., 2003; Kranenburg et al., 2005). PKCδ expression at both protein and mRNA levels was determined by using real-time PCR and Western blot analyses, respectively, in NIE-115 cells exposed to manganese. As shown in Figure 3A, exposure of NIE-115 cells to 300 µM $MnCl_2$ at varying intervals revealed a time-dependent induction of PKCδ protein, which was readily apparent at 6 h following addition of manganese and became maximal ~300% increase compared to control at 24 h. At this time point, treated NIE-115 cells with increasing concentrations of manganese also exhibited a dose-dependent induction of PKCδ with optimal response seen at the concentration of 300 µM of manganese (Figure 3B). Essentially equivalent results were obtained when the rat dopaminergic N27 cells were examined (data not shown). Furthermore, similar to the protein levels, the steady-state levels of PKCδ mRNA was also enhanced after incubation with manganese in a time- and dose-dependent fashion (Figure 3C and 3D). Taken together, these results demonstrated that manganese treatment dramatically induces PKCδ expression in NIE-115 cells, and suggested that NIE-115 cells can offer a relevant model system to analyze the regulation of PKCδ expression by manganese.

A 148-bp proximal fragment of the mouse PKCδ promoter is essential for basal PKCδ expression in NIE-115 cells

The aforementioned direct induction of PKCδ mRNA by manganese suggested that the effect of manganese was exerted at the transcriptional level. The mouse PKCδ gene comprises 18 exons, and its genomic structure has been described (Suh et al., 2003). Like other mammalian protein kinase genes, PKCδ promoter lacks a TATA box. Further, it does not contain the so-called initiator element or the downstream promoter element, which are located at various distances downstream of the transcription start site (TSS) and utilized by most TATA-less promoters to initiated transcription. To date, mechanisms responsible for transcriptional regulation of PKCδ, especially in neuronal cells, are largely unknown. Thus, as a first step towards studying the mechanisms of manganese-induced activation of PKCδ transcription, we analyzed PKCδ promoter activity. For this purpose, a reporter construct containing a 1.4 kb fragment upstream of TSS of the mouse PKCδ gene fused to the luciferase gene, pGL3-1448/+1, was transfected into murine neuroblastoma NIE-115 and N-2a, or murine dopaminergic MN9D cells, which express endogenous PKCδ. Luciferase activity of this construct increased nearly 700% when compared with pGL3-Basic control, suggesting that this 1.4-kb sequence possesses functional promoter activity in all three cell lines (Figure 4). To further delineate the region contributing to PKCδ promoter activity, a series of deletion constructs were generated and tested for their relative transcriptional activity in transient transfection studies. As shown in Figure 4, the construct pGL3-147/+1 displayed maximal luciferase activity in all cells. In contrast, the promoter activity was

almost abolished to the level of pGL3-Basic control, when the sequence from -147 to +1 was deleted within the constructs: pGL3-1448/-201, pGL3-1448/-1196, and pGL3-761/-147. Thus, these data suggested that this region between -147 to +1 contains the sequence of nucleotides necessary for basal transcription of mouse PKCδ gene in neuronal cells. Notably, although all three cell lines demonstrated similar profiles of luciferase expression, there were several major differences. For example, the promoter regions -1448/-761 and -761/-147 appear to possess cell-specific repressive elements that negatively regulated transcriptional activity in N2-a and MN9D cells, as the addition of them into the proximal pGL3-147/+1 construct caused a significant reduction in luciferase activity. However, no such effect was observed in NIE-115 cells.

The 148-bp proximal fragment of the mouse PKCδ promoter confers responsiveness to manganese treatment in NIE-115 cells

Having determined that the region between -147 to +1 is required for basal PKCδ promoter expression, we next investigated whether this region mediates the enhancing effect of manganese on PKC expression. NIE-115 cells were transiently transfected with the pGL3-147/+1 or the full-length promoter reporter constructs, and luciferase activity was assayed after incubation with 300 μM manganese for different intervals. As shown in Figure 5A, we observed that manganese promoted a time-dependent activation of the full-length (-1448/+1) promoter activity, with maximal activation seen at 12 h following addition of the drug, ~230% increase over control. Importantly, the proximal -147/+1 promoter sequence exhibited a similar time-dependent response to manganese, albeit to a slightly lesser extent

(Figure 5B). Collectively, these data revealed that the region located between -147 and +1 plays a major role for mediating responsiveness to manganese.

Functional characterization of the 148-bp PKCδ proximal promoter

We further concentrated our following studies on the -147/+1 fragment that mediated the induction by manganese. A comparison of this region with the corresponding region from human PKCδ genes using a DiAlign professional program (Cartharius et al., 2005) revealed that this region is highly conserved between the two species (Figure 6A). Subsequent analysis of this region with the program MatInspector revealed the presence of a number of potentially important transcription factor-binding sites (TFBS) which are conserved between species, suggesting that they may function biologically in the regulation of PKCδ gene expression. Figure 6A depicted the potential regulatory elements that have been identified through the computerized analysis. Because prior studies from us and others have reported that NFκB positively regulate PKCδ expression (Suh et al., 2003), we thought to examine the functions of those two proximal NFκB sites in more detail. Using site-directed mutagenesis, we prepared either single or double mutation of NFκB sites within the context of basal PKCδ reporter construct pGL3-147/+1. Transient transfections of NIE-115 and MN9D cells were carried out with each of these mutant promoter constructs, and the promoter activity of mutated constructs was determined and expressed relative to that of wild-type pGL3-147/+1. As shown in Figure 6B, single mutation of the downstream κB site (κB1, centered at bp -14) dramatically reduced the promoter activity to the levels present in pGL3-Basic groups. In striking contrast, there was no significant reduction in the promoter activity when the

upstream κB site (κB2, centered at bp -44) was mutated, and indeed this even caused a slight increase in the luciferase activity in MN9D cells. When both sites were mutated, the promoter activity was completely abolished. These results suggested that these two binding sites for NFκB were functionally different: the site1 appears to be extremely important for basal PKCδ expression in these cells; however, the site2 appears to be unimportant.

To further determine the potential regulatory role of NFκB for PKCδ in neuronal cells, Wild-type NFκB-p65 and NFκB-p50 expression constructs and NFκB-p65 deletion construct p65ΔC, containing p65 amino acids 1 to 337, were employed to study the effect of overexpressing NFκB on the regulation of the PKCδ promoter activity in NIE-115 and MN9D cells. As shown in Figure 6C, when cells were cotransfected with either p65 or p50 expression vector, luciferase activities were significantly increased, with the extent of transactivation in MN9D cells being more potent than that in NIE-115 cells for each expression vector (3.2- and 2.8-fold stimulation in MN9D cells, and 1.7- and 1.5-fold stimulation in NIE-115 cells for p65 and p50, respectively). By contrast, cotransfection of mutant form of p65 had no discernable effect on the luciferase activity compared to empty vector control, suggesting that transactivation of PKCδ by p65 overexpressing is a specific event. Together, these results suggested that both p65 and p50 are able to potently transactivate the PKCδ promoter in neuronal cells. Overexpression of these NFκB proteins in transfected cells was verified by Western blot analysis (data not shown).

In addition to NFκB binding sites, we also examined the function of other potential binding sites within the 148-bp basal PKCδ promoter region using site-directed mutagenesis analysis. Each mutation PKCδ promoter construct was transiently transfected into NIE-115

cells. As shown in Figure 7, our results showed that mutations of the binding sites for PAX9, KLF3, AP4, KLF12, or Sp2 had no or slight alteration in promoter activity. Surprisingly, when the binding site for NERF1a (-99 to -79) was mutated, the promoter activity was completely abolished, as seen for double NFκB site mutations, suggesting that this site is also essential. In addition, a binding site for PU.1 located at (-141 to -121) appears to have a negative role in control of PKCδ promoter activity as mutation of this site caused a significant induction in the luciferase activity.

Induction of PKCδ expression by manganese depends on NFκB signaling pathways

Recent evidence has suggested a close relationship between manganese and redox-sensitive molecules, including activation protein 1 and NFκB (Liu et al., 2005; Moreno et al., 2008). Based on this understanding and our observation that basal PKCδ promoter activity is regulated by NFκB, we reasoned that NFκB may play a role in the manganese up-regulation of PKCδ gene transcription. To test this hypothesis, transient transfections of NIE-115 cells were performed with the wild-type or NFκB-site-mutated reporter constructs. Luciferase activity was assayed after incubation with 300 μM manganese for 12 h. Again, as shown in Figure 8A, manganese treatment was able to induce a ~230% increase in the promoter activity of the wild-type construct pGL3-147/+1. However, when the reporter containing the mutation of NFκB site 1 was transiently transfected into NIE-115 cells, both basal and manganese-stimulated PKCδ promoter activities were completely abolished, suggesting that this NFκB site is critical for manganese-mediated activation of PKCδ promoter. To further elucidate whether manganese increases expression of PKCδ

through activation of NFκB signaling, we carried out a ChIP assay to examine the effect of manganese on the interactions of NFκB-p65 proteins with PKCδ promoter's κB element *in vivo*. After crosslinking, nuclei were isolated and subjected to enzymatic digestion. The sheared chromatin was immunoprecipitated without or with antibody against NFκB-p65. The ChIP DNA was then served as a template to amplify either the region of bp -122 to +38 spanning these two κB sites at PKCδ promoter (Figure 8B, lane 1-9) or the region of bp -37 to +99 spanning the downstream κB site alone (Figure 8B, lane 10-18). The results demonstrated that exposure to manganese significantly recruited endogenous p65 binding to PKCδ promoter in a time-dependent manner. No detectable signal was observed in the absence of antibody in the immunoprecipitation process. Taken together, these results suggested that manganese can interact with NFκB signaling pathways to induce PKCδ expression.

Manganese-dependent expression of PKC isoforms in the mice brain

Finally, we wanted to test whether manganese exposure also induces elevated PKCδ levels in intact mice. For this purpose, we quantified the proteins of PKC isoforms (α, βI, δ, ζ, and ε) in brain striatal tissue from manganese-exposed and control mice. The striatum was chosen because it is one of the brain regions primarily vulnerable to manganese in human studies on manganese intoxication. C57B1/6 mice were chronically exposed to various doses of $MnCl_2$ for 4 weeks by intragastric gavage, a route mimicking one of the most frequent sources of manganese exposure in humans, and striatal tissues were subjected to Western blot using specific anti-PKC isozyme antibodies. As shown in Figure 9A, oral treatment with

manganese markedly induced the protein level of native PKCδ in the striatum in a dose-dependent manner. Quantification of the immunoblotting signals (Figure 9B) showed that high dose of manganese (10 mg/kg) yielded a ~480% increase in native PKCδ abundance when compared to the control animals. Furthermore, the level of cleaved PKCδ, a catalytically active fragment resulting from proteolytic cleavage, was also significantly enhanced by manganese, with the maximum effect (~220% induction) achieved at 10 mg/kg manganese (Figure 9B). In the olfactory bulb region, which is known to have the largest accumulation of manganese in the brain following inhalation manganese exposure, no significant changes were found in the levels of either native or cleaved PKCδ after treatment with manganese at any dose (Figure 9C). The mechanism behind this effect is unclear, but it may be related to the regional and cellular specificity of manganism pathology (HaMai and Bondy, 2004; Roth, 2009). A similar trend for increased PKCα protein following manganese exposure was also observed, whereas the extent of up-regulation was much less than that observed for PKCδ. Striatal PKCζ protein levels were up-regulated only marginally by manganese. PKCβI showed no measurable change. Interestingly, in contrast to the two up-regulation species: PKCα and PKCδ, manganese exposure potently caused a reduction of PKCε. Maximal reduction (>50%) was achieved at 10 mg/kg manganese (Figure 9B). It should be noted that, unlike PKCδ, PKCε is widely regarded as exhibiting anti-apoptotic properties. Overall, these data demonstrated that striatal protein levels of PKC isozymes are differentially regulated by manganese, and specifically, PKCδ is the most strongly up-regulated PKC isoform in response to manganese exposure, which reinforced our hypothesis that up-regulation of PKCδ expression contributes to the manganese-induced

neurotoxicity.

Discussion

In the present study, we demonstrated for the first time that PKCδ expression is highly induced upon exposure to manganese in both *in vivo* and *in vitro* studies. Importantly, resistance to manganese toxicity is associated with the levels of PKCδ, as primary neurons from PKCδ$^{-/-}$ mice showed a reduced cell death following manganese treatment compared to primary neurons from PKCδ$^{+/+}$ mice, suggesting that the increased PKCδ levels might be responsible, at least in part, for the manganese-induced neuronal degeneration. These data expand our earlier reports that manganese-induced proteolytic activation of PKCδ is a key mediator in manganese neurotoxicity. Furthermore, studies using NIE-115 cell cultures indicated that the induction of PKCδ by manganese is likely mediated through an NFκB-dependent mechanism.

Interestingly, a differential regulation profile of PKC isoforms in response to manganese was revealed in striatum of manganese-exposed animals. Of the five PKC subspecies examined, PKCδ was the most highly up-regulated isoform, implying an involvement of PKCδ up-regulation in the manganese-associated neurotoxicity. The increased PKCδ occurs selectively in the striatum as we could not detect any changes in the olfactory bulb, correlating with the regional and cellular specificity of manganism pathology (HaMai and Bondy, 2004; Roth, 2009). Furthermore, consistent with our previous cell-based reports, manganese exposure also yielded a marked increase in the levels of activated PKCδ, which is at least partly a consequence of PKCδ up-regulation. In addition, we observed a

moderate up-regulation of PKCα as well as a significant down-regulation of PKCε, whereas expression of PKCβI and PKCζ was not, or only marginally, affected (Figure 9). The PKC signaling pathway has been described to be causally involved in the neuronal cell death and survival. Moreover, individual PKC isozymes exert different and sometimes opposing roles in modulating these processes (Gutcher et al., 2003). For example, PKCδ and PKCε have been widely regarded as pro-apoptotic and anti-apoptotic molecules, respectively. Our PKCδ and PKCε data therefore fit with the known roles of these isoforms in cell survival. For PKCα, on the other hand, the majority of published studies support the idea that this kinase is a positive regulator of cell survival (Gutcher et al., 2003). However, there is also literature indicating that PKCα could possibly act as a pro-apoptotic kinase (Nowak, 2002). Our data about up-regulation of PKCα suggests a potential role of this kinase in the molecular events associated with manganese. Nevertheless, further studies are needed to clarify the role of PKCα/PKCε signaling pathways in the pathological action of manganese. In addition to abnormalities of PKC activity and translocation, accruing evidence suggests that aberrant expressions of certain PKC isozymes are associated with pathology of neurodegenerative diseases. For example, decreased PKCβII expression was found in human HD brains (Hashimoto et al., 1992). In a transgenic mice model, loss of PKCγ expression was associated with the neuronal dysfunction in spinocerebellar ataxia type 1 (Skinner et al., 2001). Alterations in PKC levels were also observed in autopsied brains from AD patients (Cole et al., 1988). In the present study, we add to the prior body of knowledge by reporting for the first time on PKC abnormalities in a model of manganese-exposed mice. Of note, the increasing levels of PKCδ proteins are common effects of manganese in primary neurons, NIE-115 cells, and brains.

PKCδ plays a pivotal role in apoptosis in many cell types, and its expression must therefore be tightly regulated. Although it has been reported that PKCδ could be regulated in a number of cell models through either a gnomic or non-genomic mechanism, little information is available on the mechanisms that control PKCδ expression at the transcriptional level, especially in neurons. To our knowledge, only few studies reported the functional elements in the mouse, rat, and human PKCδ promoter, or the characteristics of the factors involved in the control of PKCδ transcription. Therefore, to further investigate the molecular basis of manganese-induced PKCδ gene transcription, we first addressed the regulatory *cis*-acting elements and candidate factors involved in the basal PKCδ gene transcription in neuronal cells. By using deletion studies, we identified a specific proximal PKCδ promoter region present at -147 to +1 that significantly contributes to the basal PKCδ expression in NIE-115, MN9D cells, and N-2a cells. Bioinformatic analysis revealed that this region is highly complex and contains multiple potential TFBS. These include two proximal κB sites located in close proximity, which provides easy access and availability for NFκB to transactivate PKCδ gene. Interestingly, using a site-specific mutagenesis study, a diverse role for these two κB elements was revealed with only the downstream site identified as biologically functional. The mechanisms behind the differential effect are unclear, but sequence and position-specificity might be important. A recent study demonstrated that the functional necessity of the NFκB site could be related to its sequence specificity, as well as its relative position on the promoter (Wang et al., 2005b). Our cotransfection studies using NFκB expression vectors indicated that NFκB proteins act as transactivators of PKCδ gene. This finding is not surprising because previous studies by our laboratory and others have

established a crucial role of NFκB in PKCδ gene expression (Suh et al., 2003). In addition to the NFκB sites, two potential sites for NERF1a and PU.1, which positively and negatively regulate basal PKCδ promoter activity, respectively, were also localized by the mutagenesis analysis. Experiments are in progress to identify the candidate factors that physically interact with these sites, as well as the potential involvement of these cis-elements in manganese-mediated PKCδ gene activation. It also should be noted that epigenetic mechanisms such as DNA methylation may play a role in the manganese induction of PKCδ, since we have shown that the proximal PKCδ promoter region just downstream of TSS is highly methylated (Supplemental Figure 1).

NFκB, a ubiquitously expressed transcription factors in mammalian cells, has been implicated in various physiological processes in nerve system. A variety of stimuli has been shown to activate NFκB in the CNS, such as viral infection and oxidative stress (Meffert and Baltimore, 2005). As a redox-sensitive transcription factor, growing evidence has suggested a role of NFκB in manganese-related toxicity (Liu et al., 2005; Moreno et al., 2008). In the present study, we demonstrated that NFκB is likely to be the major, if not only, contributing factor responsible for manganese-stimulated PKCδ elevation, at least *in vitro*. The role of NFκB in manganese-stimulated upregulation of PKCδ *in vivo*, however, remains to be determined. Loss of NFκB transactivation through mutation of the κB binding site resulted in complete ablation of PKCδ promoter activation in response to manganese. Furthermore, as shown in ChIP assays, manganese caused an increased recruitment of NFκB to the PKCδ promoter in our cell culture model. These data suggest that NFκB is a key transcription factor that regulates PKCδ upregulation in manganese-treated cells.

In summary, our data suggest that manganese exposure positively impacts the PKCδ gene expression in both *in vivo* and *in vitro*. These findings provide further insights into the mechanisms of manganese neurotoxicity.

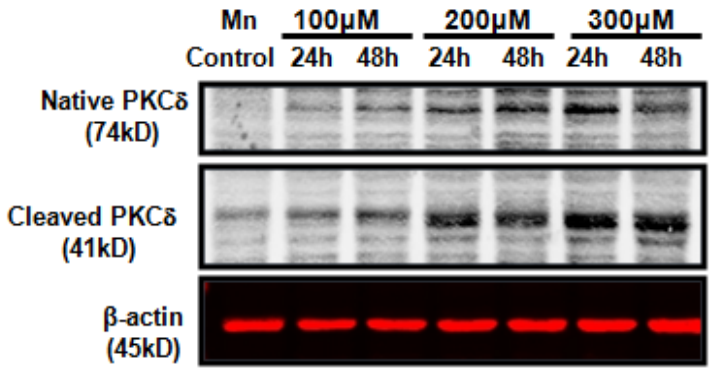

Figure 1: Manganese exposure increases PKCδ protein levels in primary striatal neurons culture.

After incubation with varying doses of manganese for increasing intervals as indicated, the primary striatal neurons were collected, lysed and subjected to Western blot analysis of PKCδ. A representative immunoblot is shown.

Figure 2: PKCδ-deficient primary striatal neurons show resistance to manganese toxicity in culture

PKCδ$^{+/+}$ and PKCδ$^{-/-}$ primary striatal neurons were treated with varying doses of manganese for 24 h and assayed for caspase-3 activity (*A*) and cell death (*B, C*). Cell death was measured using the Sytox Green cytotoxicity assay as described in "Materials and Methods". The caspase-3 activities or cytotoxicities were determined and expressed as a percentage induction relative to unstipulated controls. The results represent the mean ± SEM of two independent experiments performed in pentaplicate. (*C*), Representative phase contrast and Sytox green staining images.

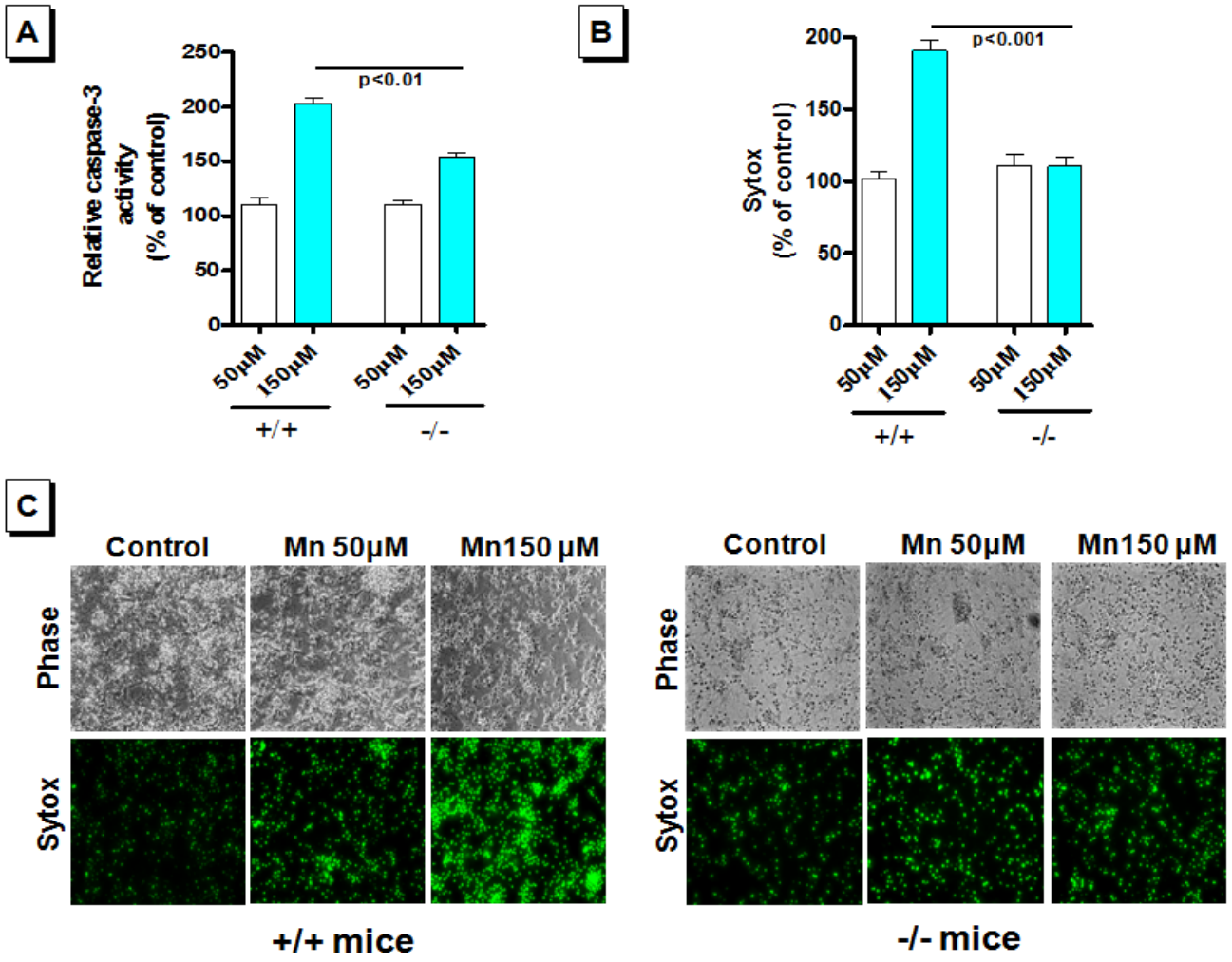

Figure 2

Figure 3. **Treatment with manganese induced PKCδ protein and mRNA in murine NIE-115 cells**

(*A*, *B*) Representative immunoblots of PKCδ in NIE-115 cells after treatment with 300 µM manganese for varying intervals as indicated (*A*), or with increasing doses of manganese for 24 h (*B*). Quantitation data of PKCδ levels are shown on the right. The results are normalized to β-actin and expressed as a percentage of the control cells. Data shown represent as mean ± SEM of three independent experiments (*$p<0.05$; and **$p<0.01$, compared with control). (*C*, *D*) Real-time qRT-PCR analysis demonstrates that the induction of PKCδ mRNA after manganese treatment in a time (*C*)-, and dose (*D*)-dependent fashion. For the time-response, NIE-115 cells were incubated with 300 µM manganese. For the dose-course studies, cells were treated with manganese for 12 h. Results were analyzed as described under Materials and Methods. Data shown represent mean ± SEM of three independent experiments performed in triplicate (*$p<0.05$; **$p<0.01$; and ***$p<0.001$, compared with control).

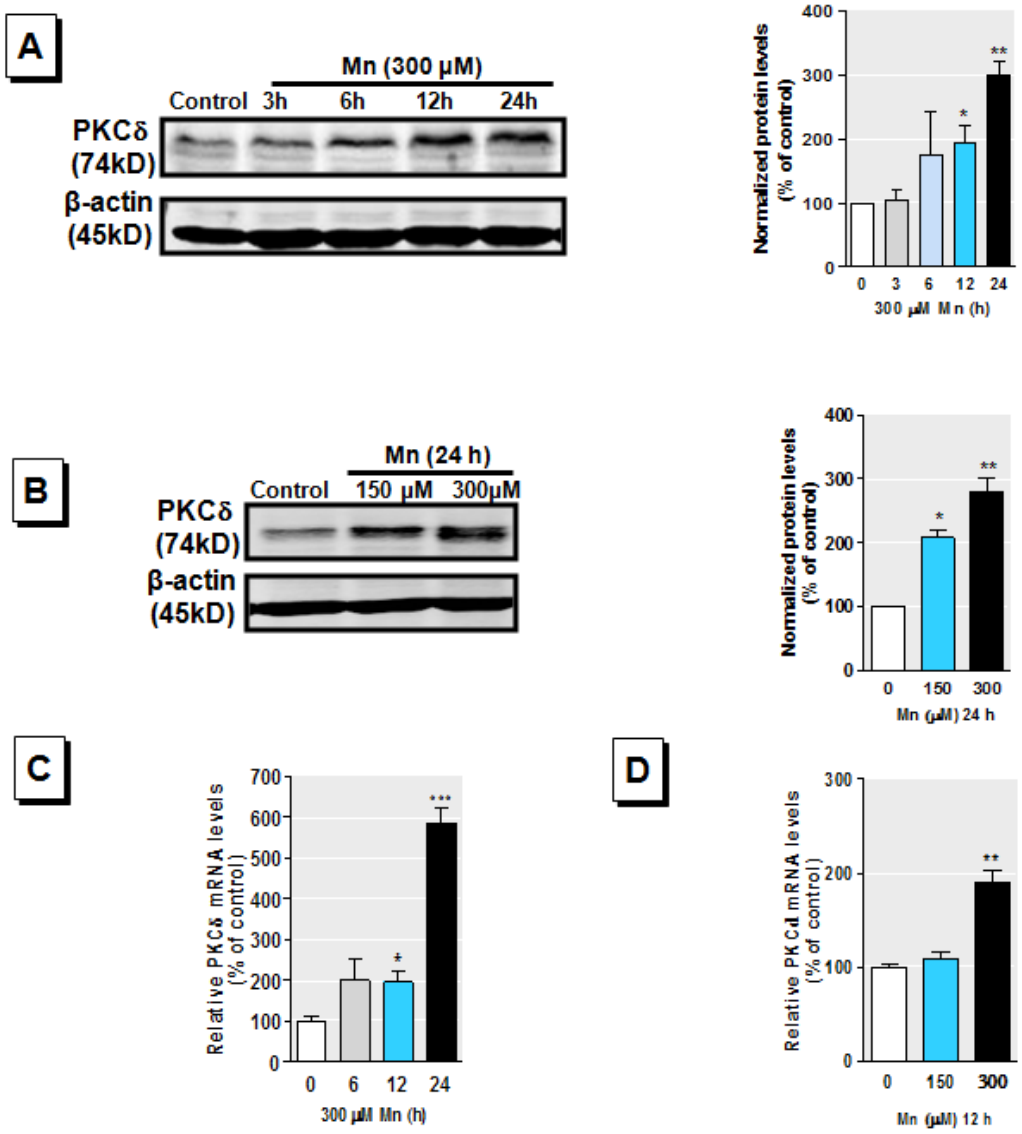

Figure 3

Figure 4: **Deletion analysis of PKCδ promoter activity in NIE-115, N2-a, and MN9D cells**

An extensive series of PKCδ promoter deletion derivatives was generated by PCR methods and inserted into the pGL3-Basic luciferase vector. Each construct was transiently transfected into NIE-115 (*black bar*), N2-a (*open bar*), and MN9D (*blue bar*) cells. Cells were harvested 24 h after transfection and luciferase activities were determined. The plasmid pcDNA3.1-βgal was included in each transfection to correct the differences in transfection efficiencies. The activity of full-length promoter construct (pGL3-1448/+1) was arbitrarily set to 100, and the relative luciferase activity of the other constructs was calculated accordingly. The results represent the mean ± SEM of three independent experiments performed in triplicate. Schematic representation of PKCδ promoter deletion/luciferase reporter constructs is shown on the left. The 5' and 3' positions of the constructs with respect to the transcription start site are depicted.

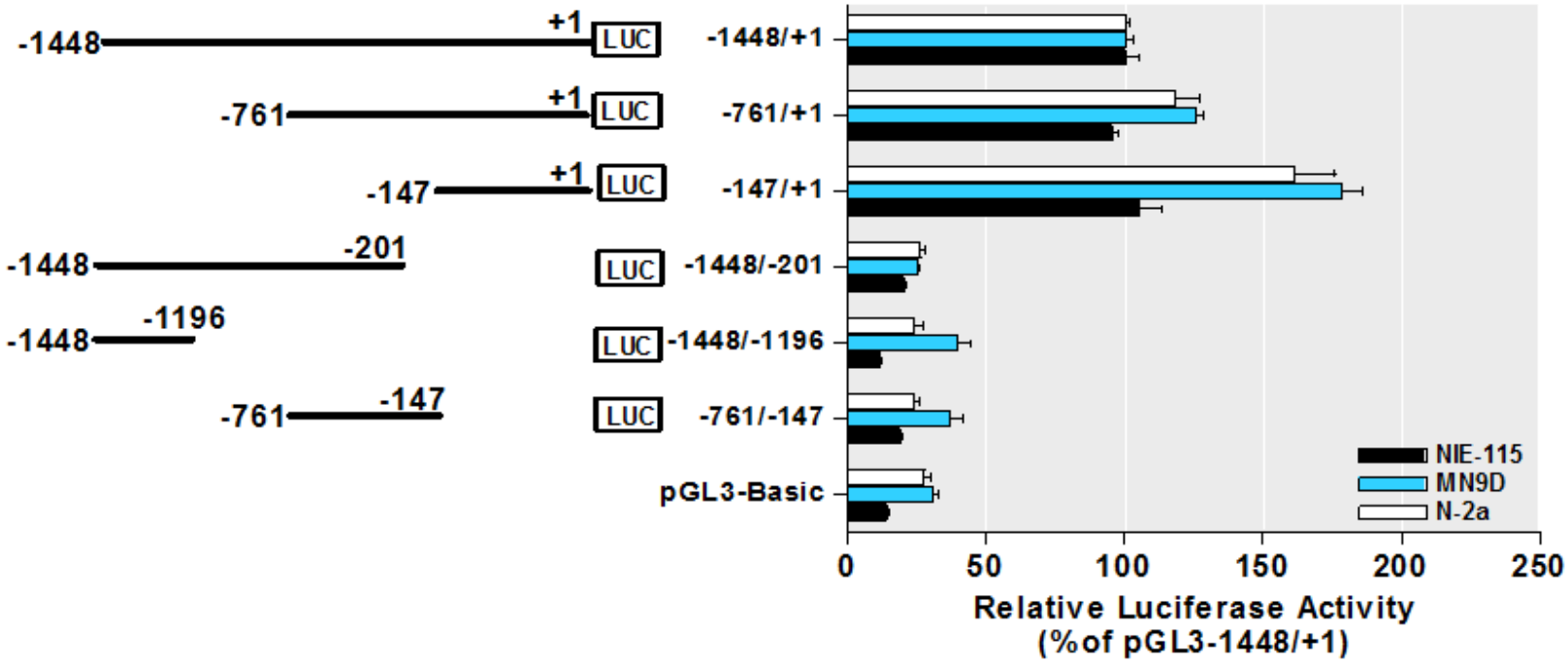

Figure 4

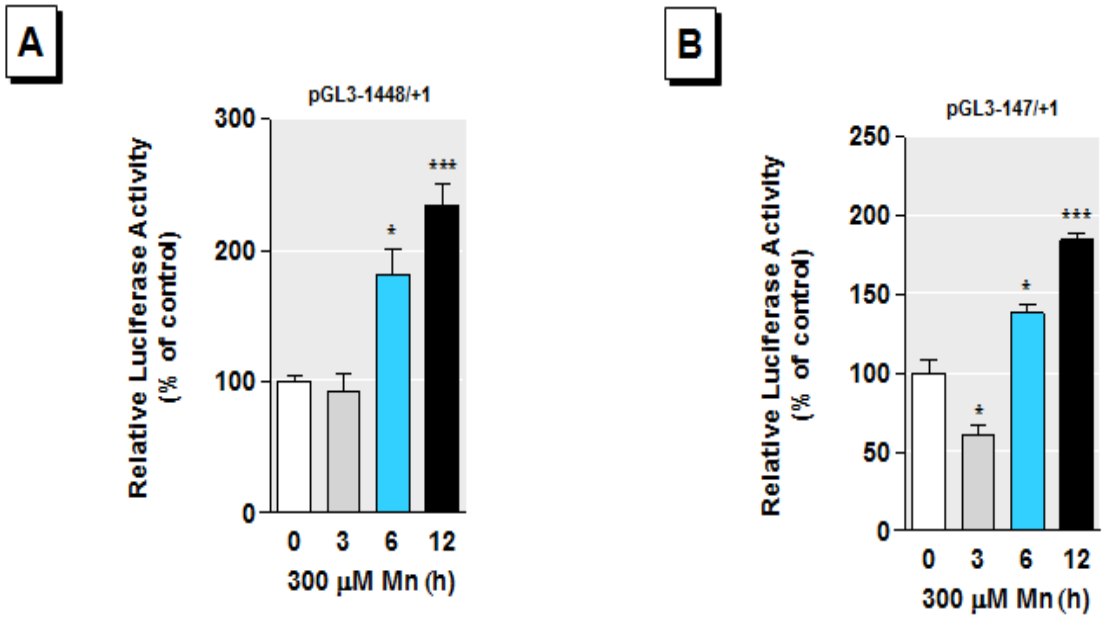

Figure 5: **A sequence located between -147 and +1 confers responsiveness to manganese treatment in NIE-115 cells**

NIE-115 cells transiently transfected with PKCδ promoter constructs pGL3-1448/+1 (*A*) or pGL3-147/+1 (*B*) were incubated with or without 300 µM manganese for increasing intervals as indicated. The plasmid pcDNA3.1-βgal was included in each transfection to correct the differences in transfection efficiencies. Luciferase activities were determined and expressed as a percentage induction relative to unstipulated controls. The results represent the mean ± SEM of three independent experiments performed in triplicate (*p<0.05; and ***p<0.001, compared with untreated cells).

Figure 6: Functional analysis of the 147-bp PKCδ proximal promoter

(*A*) Sequence comparison of the mouse PKCδ promoter region between -147 to +1 with the corresponding regions of the human PKCδ gene. Sequence differences are indicated and gaps introduced to maximize homology are marked by *dashes*. Phylogenetically conserved transcriptional factor-binding sites as well as the potential binding sites present only in the mouse PKCδ promoter are indicated (*overlined*). (*B*) The wild-type or mutated reporter constructs containing targeted substitutions in the NFκB binding sites were individually transfected into NIE-115 and MN9D cells, and luciferase activities were assayed after 24 h. To adjust for transfection efficiency, the plasmid pcDNA3.1-βgal was included in each transfection. The activity of wild-type construct (pGL3-147/+1) was arbitrarily set to 100, and promoter activity of the mutants is expressed as a percentage of the wild-type construct. The results represent the mean ± SEM of three independent experiments performed in triplicate. Schematic representation of the wild-type or mutated PKCδ promoter constructs is shown on the left. The potential transcriptional factor-binding sites are indicated at the *top*. The mutated site is marked with × (*red*). The sequences of wild-type and mutated NFκB site are shown below the bar graph. The substituted nucleotides are shown in **bold**. (*C*) NIE-115 and MN9D cells were cotransfected with the construct pGL3-147/+1 and 8 μg of pcDNA-p65, pcDNA-p65-mutant, pcDNA-p50 or empty vector (EV) pcDNA3.1. Luciferase activities were assayed after 24 h. The plasmid pcDNA3.1-βgal was included in each transfection to adjust for transfection efficiency. The activity that obtained following cotransfection of the construct pGL3-147/+1 with empty vector (EV) was arbitrarily set to 100, and all other data are expressed as a percentage thereof. The results represent the mean

± SEM of three independent experiments performed in triplicate (**p<0.01; and ***p<0.001, compared with EV-transfected cells).

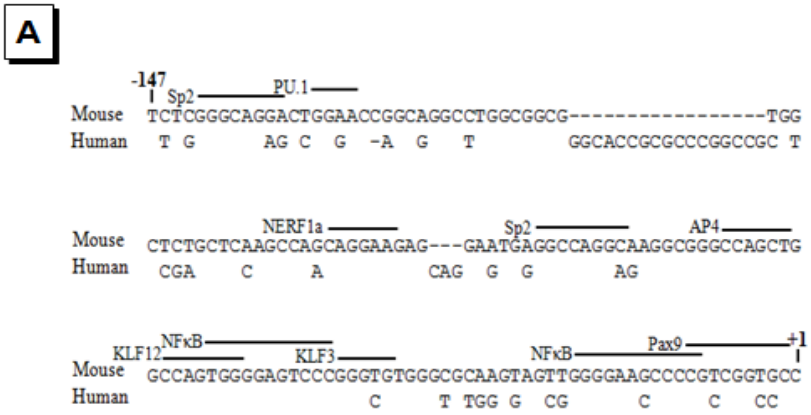

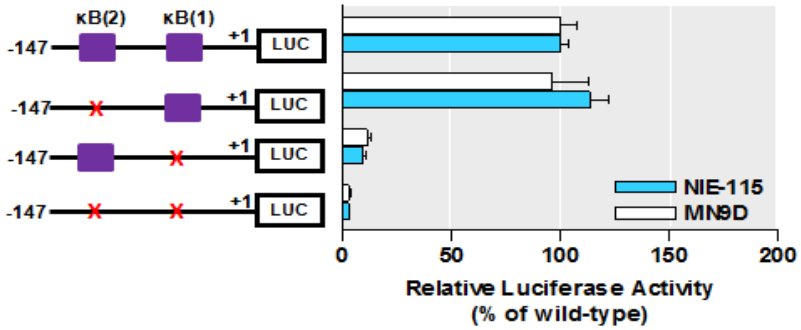

κB site	location	original sequence	substitutions
κB(1)	-20/-8	TGGGGAAGCCCCG	TtGctAAGCCCCG
κB(2)	-38/-50	TGGGGAGTCCCGG	TtGctAGTCCCGG

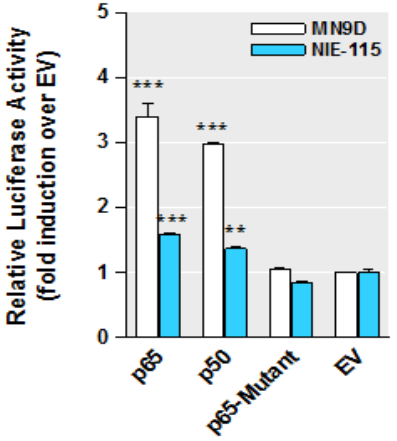

Figure 6

Figure 7: Mutational screening of the putative TFBS in the 147-bp PKCδ proximal promoter in NIE-115 cells

The wild-type or mutated reporter constructs containing targeted substitutions in the other potential transcription factor-binding sites were individually transfected into NIE-115 cells, and luciferase activities were assayed after 24 h. To adjust for transfection efficiency, the plasmid pcDNA3.1-βgal was included in each transfection. The activity of wild-type construct (pGL3-147/+1) was arbitrarily set to 100, and promoter activity of the mutants is expressed as a percentage of the wild-type construct. The results represent the mean ± SEM of three independent experiments performed in triplicate. Schematic representation of the promoter constructs is shown on the left. The potential transcriptional factor-binding sites are indicated at the *top*. The mutated site is marked with × (*red*). The sequences of wild-type and mutated sites are shown below the bar graph. The substituted nucleotides are shown in **bold**.

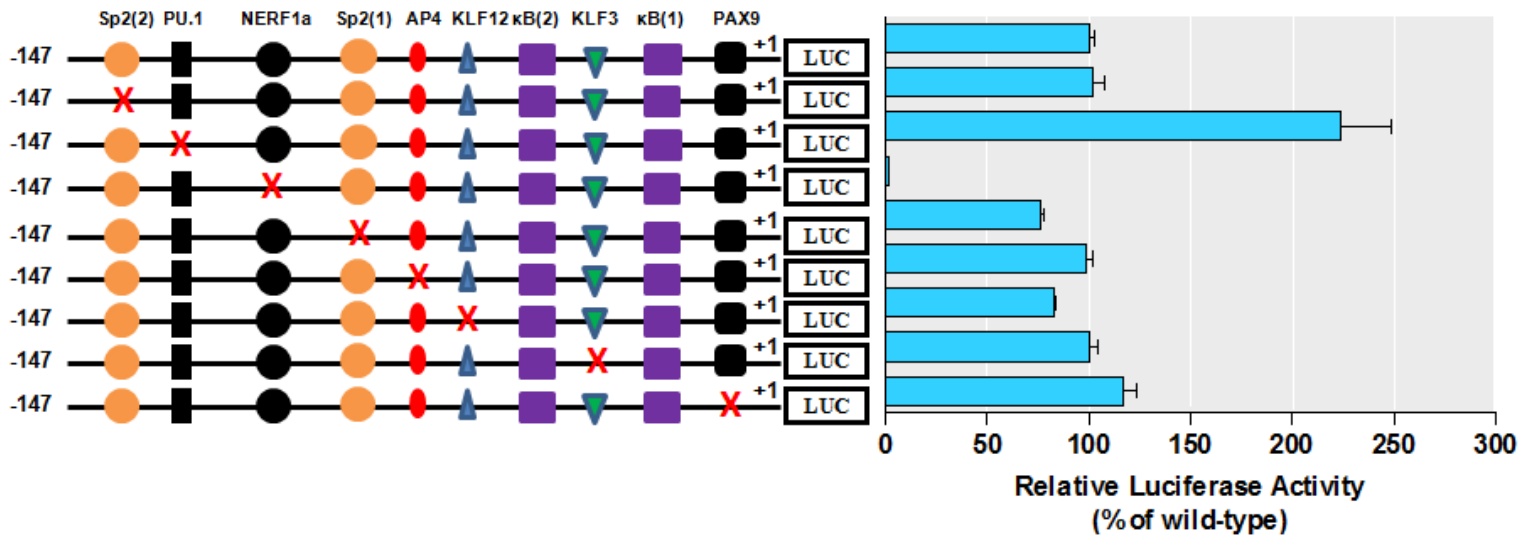

site	location	original sequences	substitutions
PAX9	-20/+1	TGGGGAAGCCCCGTCGGTGCC	TGGGGAAGCCCCGTCG**act**CC
KLF3	-42/-26	CCCGGGTGTGGGCGCAA	CCCG**tccta**GGGCGCAA
KLF12	-58/-44	CTGGCCAGTGGGGAG	CTGGC**tca**TGGGGAG
Ap4	-66/-50	CGGGCCAGCTGGCCAGT	CGGGCC**ga**CTGGCCAGT
Sp2(1)	-72/-58	GCAAGGCGGGCCAGC	GCAAGGC**atta**CAGC
NERF1a	-99/-79	AGCCAGCAGGAAGAGGAATGA	AGCCAGCAG**tcc**GAGGAATGA
PU.1	-141/-121	GCAGGACTGGAACCGGCAGGC	GCAGGACT**agg**ACCGGCAGGC
Sp2(2)	-147/-133	TCTCGGGCAGGACTG	TCTCGGGCA**tagt**TG

Figure 7

Figure 8: Induction of PKCδ expression by manganese depends on NFκB transcription factors

(*A*) NIE-115 cells transiently transfected with PKCδ promoter construct pGL3-147/+1 wild-type or NFκB site 1 mutant of were incubated with or without 300 µM manganese for 12 h. The plasmid pcDNA3.1-βgal was included in each transfection to correct the differences in transfection efficiencies. Luciferase activities were then determined and expressed as a percentage of the unstipulated controls. The results represent the mean ± SEM of three independent experiments performed in triplicate (***p<0.001, compared with untreated cells). (*B*) Assessment of NFκB-p65 binding on the PKCδ promoter by ChIP assays. NIE-115 cells were treated with or without 300 µM manganese for increasing intervals as indicated. Crosslinked chromatin was prepared and sheared by enzymatic digestion. The protein/DNA complex was incubated with or without antibody (No Ab) against p65 for ChIP analysis, and PCR was performed to amplify PKCδ promoter region -122 to +38 (*lane* 1-9) or -37 to +99 (*lane* 10-18), relative to the transcription start site. The ChIP result is representative of two separate experiments with similar results.

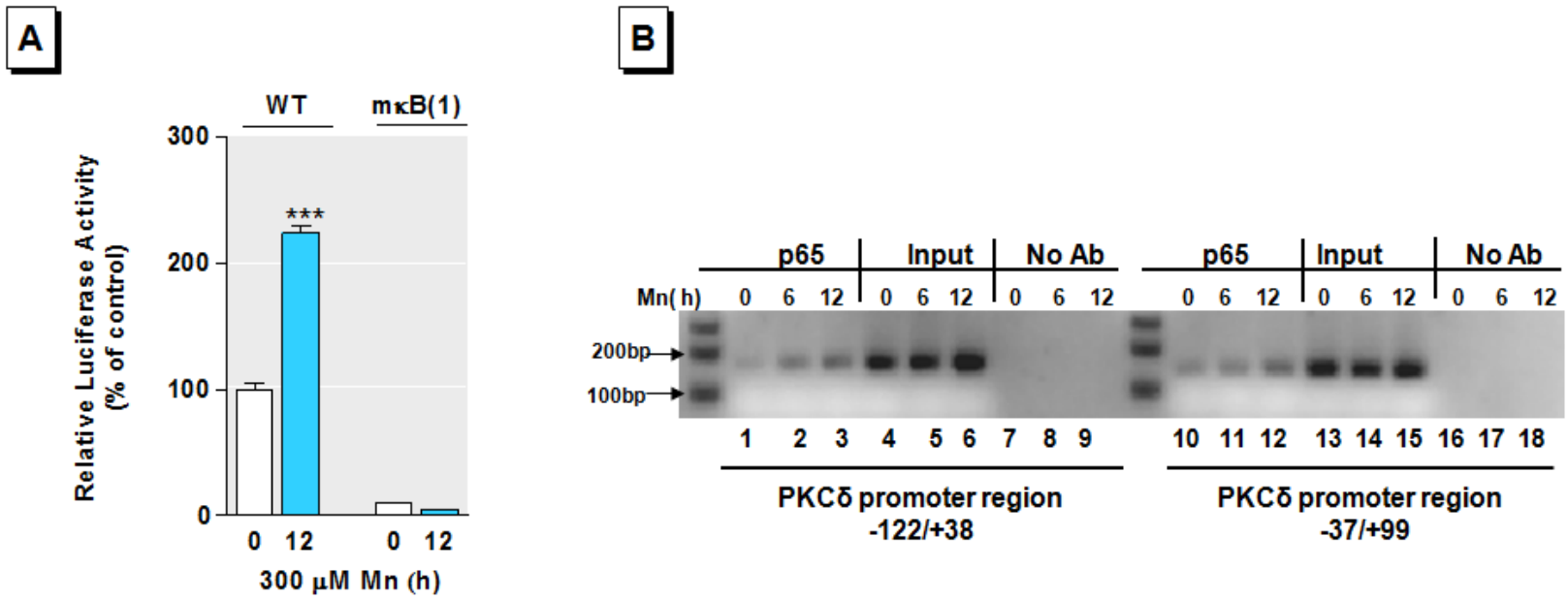

Figure 8

Figure 9: **Effects of *in vivo* chronic manganese exposure on PKCδ protein level**

C57 black mice were administered with 3 mg/kg Mn, 10 mg/kg Mn or an equivalent volume of saline (Vehicle) via oral gavage for 4 weeks. Striatum and olfactory bulb tissues from each mouse were harvested and prepared for immunoblot analyses. (*A*) Representative immunoblots of selected PKC isozymes (*left panel*: PKCδ, α, ε, and ζ; *right panel*: PKCβI) in striatum homogenates. (*B*) Quantitation data. The results are normalized to β-actin and expressed as a percentage of the Vehicle. All data in B represent as mean ± SEM from six to eight mice per group (**p<0.01; and ***p<0.001, compared with Vehicle). (*C*) Representative immunoblots of PKCδ in the olfactory bulb homogenates.

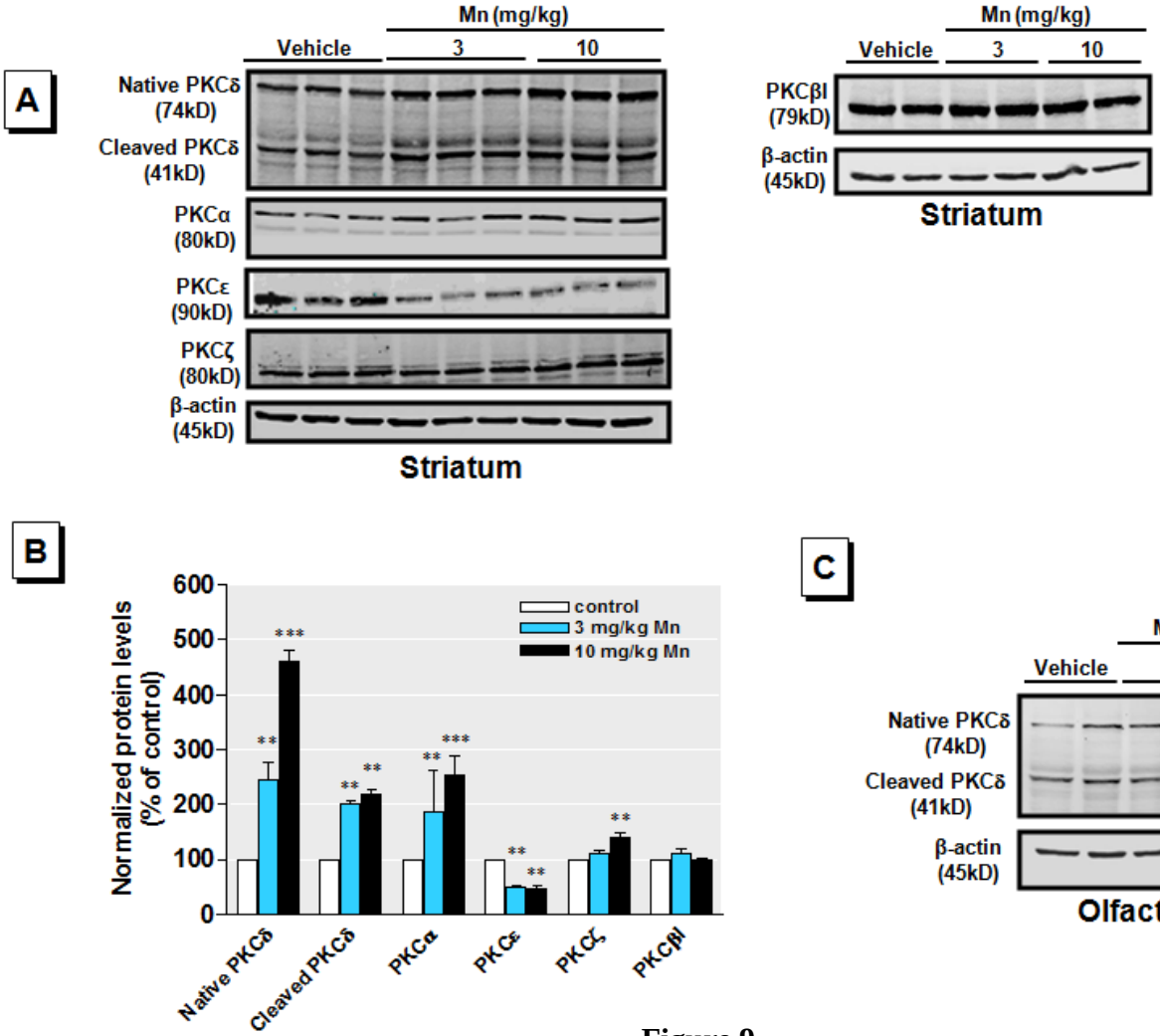

Figure 9

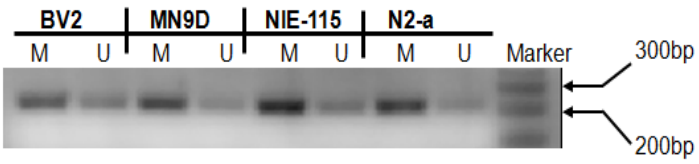

Supplemental Figure 1: MSP analysis of methylation status in PKCδ promoter

Bisulfite-modified DNA from the indicated cell line was used for MSP with primers specific for methylated (M) and unmethylated (U) DNA.

References

Amano T, Richelson E, Nirenberg M (1972) Neurotransmitter synthesis by neuroblastoma clones (neuroblast differentiation-cell culture-choline acetyltransferase-acetylcholinesterase-tyrosine hydroxylase-axons-dendrites). Proc Natl Acad Sci U S A 69:258-263.

Anantharam V, Kitazawa M, Wagner J, Kaul S, Kanthasamy AG (2002) Caspase-3-dependent proteolytic cleavage of protein kinase Cdelta is essential for oxidative stress-mediated dopaminergic cell death after exposure to methylcyclopentadienyl manganese tricarbonyl. J Neurosci 22:1738-1751.

Aschner M, Erikson KM, Hernandez EH, Tjalkens R (2009) Manganese and its Role in Parkinson's Disease: From Transport to Neuropathology. Neuromolecular Med.

Benedetto A, Au C, Aschner M (2009) Manganese-induced dopaminergic neurodegeneration: insights into mechanisms and genetics shared with Parkinson's disease. Chem Rev 109:4862-4884.

Benitez-King G, Tunez I, Bellon A, Ortiz GG, Anton-Tay F (2003) Melatonin prevents cytoskeletal alterations and oxidative stress induced by okadaic acid in N1E-115 cells. Exp Neurol 182:151-159.

Cartharius K, Frech K, Grote K, Klocke B, Haltmeier M, Klingenhoff A, Frisch M, Bayerlein M, Werner T (2005) MatInspector and beyond: promoter analysis based on transcription factor binding sites. Bioinformatics 21:2933-2942.

Cole G, Dobkins KR, Hansen LA, Terry RD, Saitoh T (1988) Decreased levels of protein kinase C in Alzheimer brain. Brain Res 452:165-174.

Dobson AW, Erikson KM, Aschner M (2004) Manganese neurotoxicity. Ann N Y Acad Sci 1012:115-128.

Erikson KM, Dobson AW, Dorman DC, Aschner M (2004) Manganese exposure and induced oxidative stress in the rat brain. Sci Total Environ 334-335:409-416.

Gonzalez LE, Juknat AA, Venosa AJ, Verrengia N, Kotler ML (2008) Manganese activates the mitochondrial apoptotic pathway in rat astrocytes by modulating the expression of proteins of the Bcl-2 family. Neurochem Int 53:408-415.

Guilarte TR, Burton NC, Verina T, Prabhu VV, Becker KG, Syversen T, Schneider JS (2008) Increased APLP1 expression and neurodegeneration in the frontal cortex of manganese-exposed non-human primates. J Neurochem 105:1948-1959.

Gutcher I, Webb PR, Anderson NG (2003) The isoform-specific regulation of apoptosis by protein kinase C. Cell Mol Life Sci 60:1061-1070.

HaMai D, Bondy SC (2004) Oxidative basis of manganese neurotoxicity. Ann N Y Acad Sci 1012:129-141.

Hashimoto T, Kitamura N, Saito N, Komure O, Nishino N, Tanaka C (1992) The loss of beta II-protein kinase C in the striatum from patients with Huntington's disease. Brain Res 585:303-306.

Hauser RA, Zesiewicz TA, Rosemurgy AS, Martinez C, Olanow CW (1994) Manganese intoxication and chronic liver failure. Ann Neurol 36:871-875.

Kaul S, Anantharam V, Kanthasamy A, Kanthasamy AG (2005a) Wild-type alpha-synuclein interacts with pro-apoptotic proteins PKCdelta and BAD to protect dopaminergic neuronal cells against MPP+-induced apoptotic cell death. Brain Res Mol Brain Res 139:137-152.

Kaul S, Anantharam V, Yang Y, Choi CJ, Kanthasamy A, Kanthasamy AG (2005b) Tyrosine phosphorylation regulates the proteolytic activation of protein kinase Cdelta in dopaminergic neuronal cells. J Biol Chem 280:28721-28730.

Keen CL, Ensunsa JL, Clegg MS (2000) Manganese metabolism in animals and humans including the toxicity of manganese. Met Ions Biol Syst 37:89-121.

Koponen S, Goldsteins G, Keinanen R, Koistinaho J (2000) Induction of protein kinase Cdelta subspecies in neurons and microglia after transient global brain ischemia. J Cereb Blood Flow Metab 20:93-102.

Kranenburg O, Bouma B, Gent YY, Aarsman CJ, Kayed R, Posthuma G, Schiks B, Voest EE, Gebbink MF (2005) Beta-amyloid (Abeta) causes detachment of N1E-115 neuroblastoma cells by acting as a scaffold for cell-associated plasminogen activation. Mol Cell Neurosci 28:496-508.

Latchoumycandane C, Anantharam V, Kitazawa M, Yang Y, Kanthasamy A, Kanthasamy AG (2005) Protein kinase Cdelta is a key downstream mediator of manganese-induced apoptosis in dopaminergic neuronal cells. J Pharmacol Exp Ther 313:46-55.

Li GJ, Choi BS, Wang X, Liu J, Waalkes MP, Zheng W (2006) Molecular mechanism of distorted iron regulation in the blood-CSF barrier and regional blood-brain barrier following in vivo subchronic manganese exposure. Neurotoxicology 27:737-744.

Li LC, Dahiya R (2002) MethPrimer: designing primers for methylation PCRs. Bioinformatics 18:1427-1431.

Liu X, Buffington JA, Tjalkens RB (2005) NF-kappaB-dependent production of nitric oxide by astrocytes mediates apoptosis in differentiated PC12 neurons following exposure to manganese and cytokines. Brain Res Mol Brain Res 141:39-47.

Livak KJ, Schmittgen TD (2001) Analysis of relative gene expression data using real-time quantitative PCR and the 2(-Delta Delta C(T)) Method. Methods 25:402-408.

Meffert MK, Baltimore D (2005) Physiological functions for brain NF-kappaB. Trends Neurosci 28:37-43.

Mergler D, Baldwin M, Belanger S, Larribe F, Beuter A, Bowler R, Panisset M, Edwards R, de Geoffroy A, Sassine MP, Hudnell K (1999) Manganese neurotoxicity, a continuum of dysfunction: results from a community based study. Neurotoxicology 20:327-342.

Moreno JA, Sullivan KA, Carbone DL, Hanneman WH, Tjalkens RB (2008) Manganese potentiates nuclear factor-kappaB-dependent expression of nitric oxide synthase 2 in astrocytes by activating soluble guanylate cyclase and extracellular responsive kinase signaling pathways. J Neurosci Res.

Morgenstern B, Dress A, Werner T (1996) Multiple DNA and protein sequence alignment based on segment-to-segment comparison. Proc Natl Acad Sci U S A 93:12098-12103.

Morgenstern B, Frech K, Dress A, Werner T (1998) DIALIGN: finding local similarities by multiple sequence alignment. Bioinformatics 14:290-294.

Nowak G (2002) Protein kinase C-alpha and ERK1/2 mediate mitochondrial dysfunction, decreases in active Na+ transport, and cisplatin-induced apoptosis in renal cells. J Biol Chem 277:43377-43388.

Olanow CW (2004) Manganese-induced parkinsonism and Parkinson's disease. Ann N Y Acad Sci 1012:209-223.

Ostlund P, Lindegren H, Pettersson C, Bedecs K (2001) Up-regulation of functionally impaired insulin-like growth factor-1 receptor in scrapie-infected neuroblastoma cells. J Biol Chem 276:36110-36115.

Perl DP, Olanow CW (2007) The neuropathology of manganese-induced Parkinsonism. J Neuropathol Exp Neurol 66:675-682.

Prabhakaran K, Chapman GD, Gunasekar PG (2009) BNIP3 up-regulation and mitochondrial dysfunction in manganese-induced neurotoxicity. Neurotoxicology 30:414-422.

Roth BL, Poot M, Yue ST, Millard PJ (1997) Bacterial viability and antibiotic susceptibility testing with SYTOX green nucleic acid stain. Appl Environ Microbiol 63:2421-2431.

Roth JA (2009) Are There Common Biochemical and Molecular Mechanisms Controlling Manganism and Parkisonism. Neuromolecular Med.

Sherer TB, Betarbet R, Stout AK, Lund S, Baptista M, Panov AV, Cookson MR, Greenamyre JT (2002) An in vitro model of Parkinson's disease: linking mitochondrial impairment to altered alpha-synuclein metabolism and oxidative damage. J Neurosci 22:7006-7015.

Skinner PJ, Vierra-Green CA, Clark HB, Zoghbi HY, Orr HT (2001) Altered trafficking of membrane proteins in purkinje cells of SCA1 transgenic mice. Am J Pathol 159:905-913.

Suh KS, Tatunchak TT, Crutchley JM, Edwards LE, Marin KG, Yuspa SH (2003) Genomic structure and promoter analysis of PKC-delta. Genomics 82:57-67.

Takai D, Jones PA (2002) Comprehensive analysis of CpG islands in human chromosomes 21 and 22. Proc Natl Acad Sci U S A 99:3740-3745.

Wang N, Ahmed S, Haqqi TM (2005) Genomic structure and functional characterization of the promoter region of human IkappaB kinase-related kinase IKKi/IKKvarepsilon gene. Gene 353:118-133.

Zhang D, Kanthasamy A, Yang Y, Anantharam V, Kanthasamy A (2007) Protein kinase C delta negatively regulates tyrosine hydroxylase activity and dopamine synthesis by enhancing protein phosphatase-2A activity in dopaminergic neurons. J Neurosci 27:5349-5362.

Zhang N, Fitsanakis VA, Erikson KM, Aschner M, Avison MJ, Gore JC (2009) A model for the analysis of competitive relaxation effects of manganese and iron in vivo. NMR Biomed 22:391-404.

CHAPTER VI: GENERAL CONCLUSIONS

The chapters from II to V each shed new light on the functional aspects of the regulation of PKCδ signal transduction in both physiological and pathological conditions. Chapter II characterizes essential *cis*-elements and transcriptional regulators that functionally interact with these sites in the promoter and 5'UTR region of mouse PKCδ gene. Chapter III demonstrates that histone acetylation-mediated changes in chromatin structure are involved in the induction of the PKCδ gene. Chapter IV reveals a functional interaction between PKCδ and the PD-related protein α-synuclein. Chapter V reports an induction of PKCδ gene expression in response to the parkinsonian toxin manganese. The overall conclusions and future perspectives will be discussed in the following sections:

Transcriptional regulation of PKCδ gene expression in neuronal cells involves multiple positive and negative *cis*-elements in the promoter and 5'UTR region

The modulation of PKCδ signal transduction is of particular interest because of its importance in central nervous systems, in both physiological and pathological conditions. Alterations in PKCδ expression could represent an important step in ultimately controlling the PKCδ signaling pathway. In the present investigation we studied how PKCδ gene expression is regulated in neuronal cells. We have identified the mouse PKCδ basal promoter region and characterized a role for two NFκB and one NERF 1a binding sites in the regulation of PKCδ basal transcription. Furthermore, multiple Sp binding sites in the downstream PKCδ promoter segment reside in the 5' UTR region and are also essential *cis*-elements controlling PKCδ expression. Subsequent analysis revealed that only the

proximal NFκB site is functionally active in NIE115 and MN9D cells. The reason for this functional difference between these two κB sites is unknown, but it might be due to a sequence-dependent or position-dependent effect. Further analysis is needed to elucidate if this is also the case in other cell models or *in vivo*. NFκB is a key mediator of a variety of cellular processes. It has long been thought, for example, that activation of NFκB signaling is part of the cellular stress response (see reviews, Mercurio and Manning, 1999; Meffert and Baltimore, 2005). Thus, beside being indispensable for the basal PKCδ expression, the κB element may confer oxidative-stress inducibility to the PKCδ promoter, resulting in an increased production of PKCδ protein and subsequent aberrant activation of PKCδ signaling. The binding of Sp and NFκB factors to their respective sites has been demonstrated by ChIP and EMSA assays. In the basal state, binding of these proteins to a PKCδ promoter potentially facilitates basal expression of PKCδ. The constitutive activation of NFκB in the nucleus of N27 cells is further indicative of NFκB participation in the regulation of PKCδ transcription. Once bound, both the DNA/Sp and DNA/NFκB complexes may recruit transcriptional co-activator or co-repressor complexes to generate additional chromatin structural changes. Such factors may include CBP/p300 and HDAC family proteins. At the present time, it is not clear whether there is any synergistic action between the Sp family factors and NFκB during the process of modulation of PKCδ transactivation, but it is conceivable that these proteins can communicate directly or through other interactions with bridging proteins. In addition to those proximal and downstream regulatory elements, we also delineated an upstream negative/anti-negative cassette, which can oppositely contribute to regulating PKCδ transactivation. However, the precise mechanism underlying their actions and the candidate factors binding to these elements remain to be defined.

An intriguing aspect of PKCδ gene expression is the involvement of epigenetic mechanisms. Our data revealed that the PKCδ non-coding exon1 region is differentially methylated: it was hypermethylated in modest PKCδ-expressing cell lines, including NIE115, MN9D and N2a cells, whereas little or no methylation was observed in the high expressing N27 cells, implicating DNA methylation as a potential mechanism responsible for cell-specific expression of PKCδ. Using an epigenetic approach with HDAC inhibition, we further delineated that histone acetylation leads to enhanced PKCδ expression, which requires Sp protein activity. DNA methylation and histone acetylation oppositely correlate with gene expression. Thus, it will be interesting to determine the functional relevance of these epigenetic PKCδ gene modifications to PD-like neurodegeneration.

Differential regulation of PKCδ gene by manganese and the PD-related gene α-synuclein

In the present study we also investigated the effect of the parkinsonian toxicant manganese and the PD-associated gene α-synuclein on the expression of the PKCδ gene. Our *in vitro* and *in vivo* data clearly demonstrated divergent roles for manganese and α-synuclein in modulating PKCδ signaling. These findings extend the key role for PKCδ kinase signal transduction in parkinsonian neurodegeneration. The mechanism by which α-synuclein down-regulates the PKCδ gene appears to be quite complex, partially involving modulation of p300 and NFκB signaling. The precise mechanism, however, remains to be identified.

In summary, we elucidated the regulatory mechanism of PKCδ transcription in neurons. We also characterized the possible regulation of PKCδ by environmental or genetic factors that are involved in PD pathology. The integrated mechanism of the regulation of

PKCδ expression in neuronal cells and the crosstalk between PKCδ expression and genetic risk factors, as well as environmental risk factors, are outlined in the Figure 11.

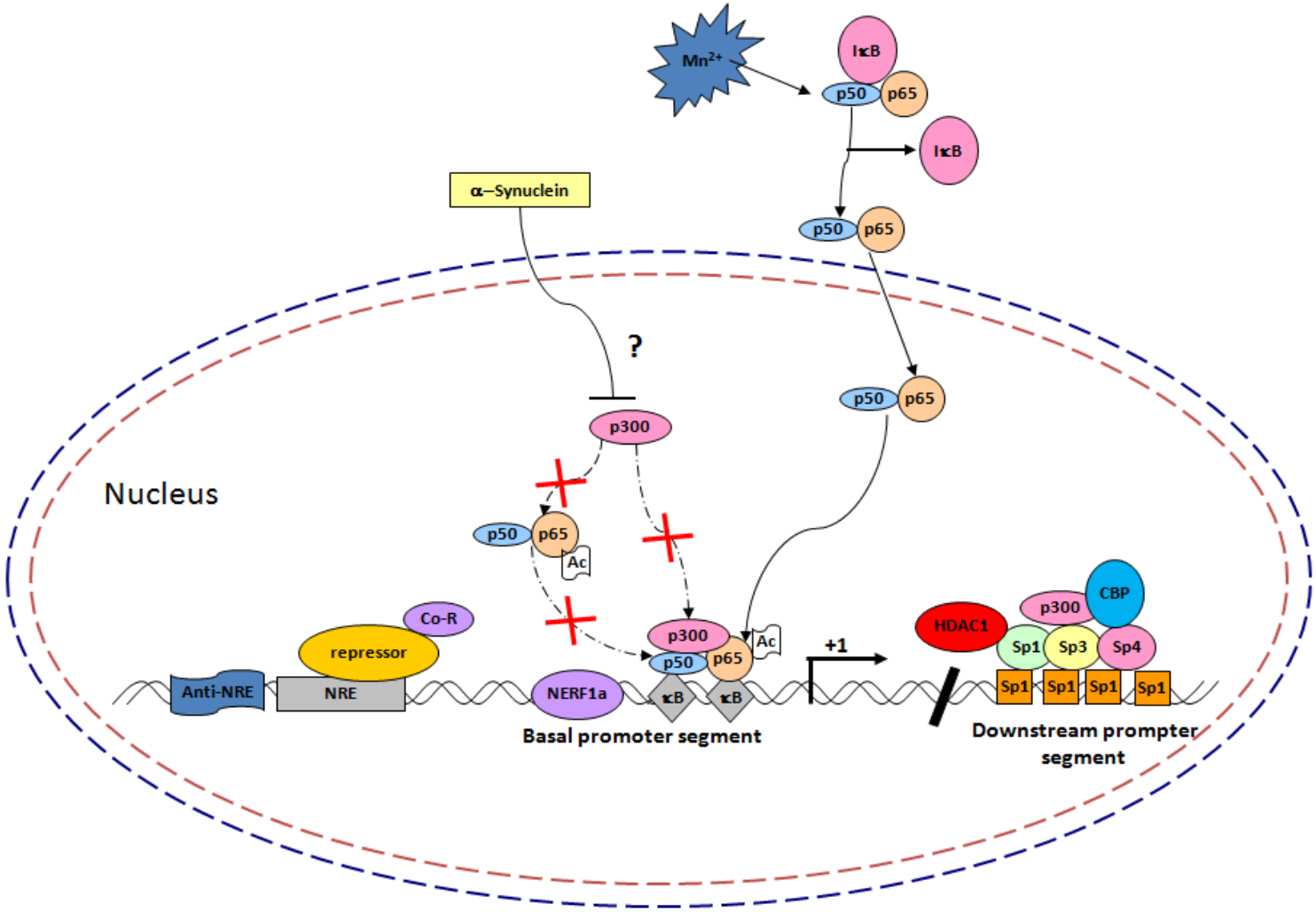

Figure 11. Integrated mechanisms of the regulation of PKCδ expression in neuronal cells, and the crosstalk between PKCδ expression and genetic risk factors, as well as environmental risk factors.

LITERATURE CITED

Abbas N, Lucking CB, Ricard S, Durr A, Bonifati V, De Michele G, Bouley S, Vaughan JR, Gasser T, Marconi R, Broussolle E, Brefel-Courbon C, Harhangi BS, Oostra BA, Fabrizio E, Bohme GA, Pradier L, Wood NW, Filla A, Meco G, Denefle P, Agid Y, Brice A (1999) A wide variety of mutations in the parkin gene are responsible for autosomal recessive parkinsonism in Europe. French Parkinson's Disease Genetics Study Group and the European Consortium on Genetic Susceptibility in Parkinson's Disease. Hum Mol Genet 8:567-574.

Abbott RD, Ross GW, White LR, Tanner CM, Masaki KH, Nelson JS, Curb JD, Petrovitch H (2005) Excessive daytime sleepiness and subsequent development of Parkinson disease. Neurology 65:1442-1446.

Abbott RD, Ross GW, Petrovitch H, Tanner CM, Davis DG, Masaki KH, Launer LJ, Curb JD, White LR (2007) Bowel movement frequency in late-life and incidental Lewy bodies. Mov Disord 22:1581-1586.

Abeliovich A, Schmitz Y, Farinas I, Choi-Lundberg D, Ho WH, Castillo PE, Shinsky N, Verdugo JM, Armanini M, Ryan A, Hynes M, Phillips H, Sulzer D, Rosenthal A (2000) Mice lacking alpha-synuclein display functional deficits in the nigrostriatal dopamine system. Neuron 25:239-252.

Abou-Sleiman PM, Muqit MM, Wood NW (2006) Expanding insights of mitochondrial dysfunction in Parkinson's disease. Nat Rev Neurosci 7:207-219.

Ahn TB, Kim SY, Kim JY, Park SS, Lee DS, Min HJ, Kim YK, Kim SE, Kim JM, Kim HJ, Cho J, Jeon BS (2008) alpha-Synuclein gene duplication is present in sporadic Parkinson disease. Neurology 70:43-49.

Alam ZI, Jenner A, Daniel SE, Lees AJ, Cairns N, Marsden CD, Jenner P, Halliwell B (1997) Oxidative DNA damage in the parkinsonian brain: an apparent selective increase in 8-hydroxyguanine levels in substantia nigra. J Neurochem 69:1196-1203.

Albani D, Peverelli E, Rametta R, Batelli S, Veschini L, Negro A, Forloni G (2004) Protective effect of TAT-delivered alpha-synuclein: relevance of the C-terminal domain and involvement of HSP70. Faseb J 18:1713-1715.

Aleyasin H, Rousseaux MW, Marcogliese PC, Hewitt SJ, Irrcher I, Joselin AP, Parsanejad M, Kim RH, Rizzu P, Callaghan SM, Slack RS, Mak TW, Park DS (2010) DJ-1 protects the nigrostriatal axis from the neurotoxin MPTP by modulation of the AKT pathway. Proc Natl Acad Sci U S A 107:3186-3191.

Allam MF, Campbell MJ, Hofman A, Del Castillo AS, Fernandez-Crehuet Navajas R (2004) Smoking and Parkinson's disease: systematic review of prospective studies. Mov Disord 19:614-621.

Alves Da Costa C, Paitel E, Vincent B, Checler F (2002) Alpha-synuclein lowers p53-dependent apoptotic response of neuronal cells. Abolishment by 6-hydroxydopamine and implication for Parkinson's disease. J Biol Chem 277:50980-50984.

Anantharam V, Kitazawa M, Wagner J, Kaul S, Kanthasamy AG (2002) Caspase-3-dependent proteolytic cleavage of protein kinase Cdelta is essential for

oxidative stress-mediated dopaminergic cell death after exposure to methylcyclopentadienyl manganese tricarbonyl. J Neurosci 22:1738-1751.

Aschner M, Erikson KM, Herrero Hernandez E, Tjalkens R (2009) Manganese and its role in Parkinson's disease: from transport to neuropathology. Neuromolecular Med 11:252-266.

Atsumi M, Li Y, Tomiyama H, Sato K, Hattori N (2006) [A 62-year-old woman with early-onset Parkinson's disease associated with the PINKi gene deletion]. Rinsho Shinkeigaku 46:199-202.

Auluck PK, Chan HY, Trojanowski JQ, Lee VM, Bonini NM (2002) Chaperone suppression of alpha-synuclein toxicity in a Drosophila model for Parkinson's disease. Science 295:865-868.

Banati RB, Daniel SE, Blunt SB (1998) Glial pathology but absence of apoptotic nigral neurons in long-standing Parkinson's disease. Mov Disord 13:221-227.

Bandopadhyay R, Kingsbury AE, Cookson MR, Reid AR, Evans IM, Hope AD, Pittman AM, Lashley T, Canet-Aviles R, Miller DW, McLendon C, Strand C, Leonard AJ, Abou-Sleiman PM, Healy DG, Ariga H, Wood NW, de Silva R, Revesz T, Hardy JA, Lees AJ (2004) The expression of DJ-1 (PARK7) in normal human CNS and idiopathic Parkinson's disease. Brain 127:420-430.

Barghorn S, Davies P, Mandelkow E (2004) Tau paired helical filaments from Alzheimer's disease brain and assembled in vitro are based on beta-structure in the core domain. Biochemistry 43:1694-1703.

Barmack NH, Qian Z, Yoshimura J (2000) Regional and cellular distribution of protein kinase C in rat cerebellar Purkinje cells. J Comp Neurol 427:235-254.

Barroso N, Campos Y, Huertas R, Esteban J, Molina JA, Alonso A, Gutierrez-Rivas E, Arenas J (1993) Respiratory chain enzyme activities in lymphocytes from untreated patients with Parkinson disease. Clin Chem 39:667-669.

Bayer TA, Jakala P, Hartmann T, Havas L, McLean C, Culvenor JG, Li QX, Masters CL, Falkai P, Beyreuther K (1999) Alpha-synuclein accumulates in Lewy bodies in Parkinson's disease and dementia with Lewy bodies but not in Alzheimer's disease beta-amyloid plaque cores. Neurosci Lett 266:213-216.

Beal MF (2001) Experimental models of Parkinson's disease. Nat Rev Neurosci 2:325-334.

Beal MF (2003) Mitochondria, oxidative damage, and inflammation in Parkinson's disease. Ann N Y Acad Sci 991:120-131.

Bender A, Krishnan KJ, Morris CM, Taylor GA, Reeve AK, Perry RH, Jaros E, Hersheson JS, Betts J, Klopstock T, Taylor RW, Turnbull DM (2006) High levels of mitochondrial DNA deletions in substantia nigra neurons in aging and Parkinson disease. Nat Genet 38:515-517.

Benedetti MD, Bower JH, Maraganore DM, McDonnell SK, Peterson BJ, Ahlskog JE, Schaid DJ, Rocca WA (2000) Smoking, alcohol, and coffee consumption preceding Parkinson's disease: a case-control study. Neurology 55:1350-1358.

Berg D, Schweitzer K, Leitner P, Zimprich A, Lichtner P, Belcredi P, Brussel T, Schulte C, Maass S, Nagele T (2005) Type and frequency of mutations in the LRRK2 gene in familial and sporadic Parkinson's disease*. Brain 128:3000-3011.

Berry DM, Antochi R, Bhatia M, Meckling-Gill KA (1996) 1,25-Dihydroxyvitamin D3 stimulates expression and translocation of protein kinase Calpha and Cdelta via a

nongenomic mechanism and rapidly induces phosphorylation of a 33-kDa protein in acute promyelocytic NB4 cells. J Biol Chem 271:16090-16096.

Bertinet DB, Tinivella M, Balzola FA, de Francesco A, Davini O, Rizzo L, Massarenti P, Leonardi MA, Balzola F (2000) Brain manganese deposition and blood levels in patients undergoing home parenteral nutrition. JPEN J Parenter Enteral Nutr 24:223-227.

Betarbet R, Sherer TB, MacKenzie G, Garcia-Osuna M, Panov AV, Greenamyre JT (2000) Chronic systemic pesticide exposure reproduces features of Parkinson's disease. Nat Neurosci 3:1301-1306.

Beyer K (2006) Alpha-synuclein structure, posttranslational modification and alternative splicing as aggregation enhancers. Acta Neuropathol 112:237-251.

Bharti A, Kraeft SK, Gounder M, Pandey P, Jin S, Yuan ZM, Lees-Miller SP, Weichselbaum R, Weaver D, Chen LB, Kufe D, Kharbanda S (1998) Inactivation of DNA-dependent protein kinase by protein kinase Cdelta: implications for apoptosis. Mol Cell Biol 18:6719-6728.

Biere AL, Wood SJ, Wypych J, Steavenson S, Jiang Y, Anafi D, Jacobsen FW, Jarosinski MA, Wu GM, Louis JC, Martin F, Narhi LO, Citron M (2000) Parkinson's disease-associated alpha-synuclein is more fibrillogenic than beta- and gamma-synuclein and cannot cross-seed its homologs. J Biol Chem 275:34574-34579.

Blandini F, Nappi G, Greenamyre JT (1998) Quantitative study of mitochondrial complex I in platelets of parkinsonian patients. Mov Disord 13:11-15.

Bonifati V, Oostra BA, Heutink P (2004) Linking DJ-1 to neurodegeneration offers novel insights for understanding the pathogenesis of Parkinson's disease. J Mol Med 82:163-174.

Bonifati V, Rizzu P, van Baren MJ, Schaap O, Breedveld GJ, Krieger E, Dekker MC, Squitieri F, Ibanez P, Joosse M, van Dongen JW, Vanacore N, van Swieten JC, Brice A, Meco G, van Duijn CM, Oostra BA, Heutink P (2003) Mutations in the DJ-1 gene associated with autosomal recessive early-onset parkinsonism. Science 299:256-259.

Bonuccelli U, Del Dotto P (2006) New pharmacologic horizons in the treatment of Parkinson disease. Neurology 67:S30-38.

Bove J, Prou D, Perier C, Przedborski S (2005) Toxin-induced models of Parkinson's disease. NeuroRx 2:484-494.

Bove J, Zhou C, Jackson-Lewis V, Taylor J, Chu Y, Rideout HJ, Wu DC, Kordower JH, Petrucelli L, Przedborski S (2006) Proteasome inhibition and Parkinson's disease modeling. Ann Neurol 60:260-264.

Braak H, Del Tredici K, Rub U, de Vos RA, Jansen Steur EN, Braak E (2003) Staging of brain pathology related to sporadic Parkinson's disease. Neurobiol Aging 24:197-211.

Brodie C, Blumberg PM (2003) Regulation of cell apoptosis by protein kinase c delta. Apoptosis 8:19-27.

Brooks AI, Chadwick CA, Gelbard HA, Cory-Slechta DA, Federoff HJ (1999) Paraquat elicited neurobehavioral syndrome caused by dopaminergic neuron loss. Brain Res 823:1-10.

Brouillet EP, Shinobu L, McGarvey U, Hochberg F, Beal MF (1993) Manganese injection into the rat striatum produces excitotoxic lesions by impairing energy metabolism. Exp Neurol 120:89-94.

Brown TP, Rumsby PC, Capleton AC, Rushton L, Levy LS (2006) Pesticides and Parkinson's disease--is there a link? Environ Health Perspect 114:156-164.

Burke RE (2008) Programmed cell death and new discoveries in the genetics of parkinsonism. J Neurochem 104:875-890.

Burke RE, Dauer WT, Vonsattel JP (2008) A critical evaluation of the Braak staging scheme for Parkinson's disease. Ann Neurol 64:485-491.

Burn DJ (2007) Sex and Parkinson's disease: a world of difference? J Neurol Neurosurg Psychiatry 78:787.

Cabin DE, Shimazu K, Murphy D, Cole NB, Gottschalk W, McIlwain KL, Orrison B, Chen A, Ellis CE, Paylor R, Lu B, Nussbaum RL (2002) Synaptic vesicle depletion correlates with attenuated synaptic responses to prolonged repetitive stimulation in mice lacking alpha-synuclein. J Neurosci 22:8797-8807.

Cadenas E, Davies KJ (2000) Mitochondrial free radical generation, oxidative stress, and aging. Free Radic Biol Med 29:222-230.

Calne DB, Chu NS, Huang CC, Lu CS, Olanow W (1994) Manganism and idiopathic parkinsonism: similarities and differences. Neurology 44:1583-1586.

Canet-Aviles RM, Wilson MA, Miller DW, Ahmad R, McLendon C, Bandyopadhyay S, Baptista MJ, Ringe D, Petsko GA, Cookson MR (2004) The Parkinson's disease protein DJ-1 is neuroprotective due to cysteine-sulfinic acid-driven mitochondrial localization. Proc Natl Acad Sci U S A 101:9103-9108.

Carbone DL, Popichak KA, Moreno JA, Safe S, Tjalkens RB (2009) Suppression of 1-methyl-4-phenyl-1,2,3,6-tetrahydropyridine-induced nitric-oxide synthase 2 expression in astrocytes by a novel diindolylmethane analog protects striatal neurons against apoptosis. Mol Pharmacol 75:35-43.

Cardoso SM, Pereira C, Oliveira R (1999) Mitochondrial function is differentially affected upon oxidative stress. Free Radic Biol Med 26:3-13.

Casarejos MJ, Menendez J, Solano RM, Rodriguez-Navarro JA, Garcia de Yebenes J, Mena MA (2006) Susceptibility to rotenone is increased in neurons from parkin null mice and is reduced by minocycline. J Neurochem 97:934-946.

Cecarini V, Gee J, Fioretti E, Amici M, Angeletti M, Eleuteri AM, Keller JN (2007) Protein oxidation and cellular homeostasis: Emphasis on metabolism. Biochim Biophys Acta 1773:93-104.

Chandra S, Chen X, Rizo J, Jahn R, Sudhof TC (2003) A broken alpha -helix in folded alpha -Synuclein. J Biol Chem 278:15313-15318.

Chandra S, Gallardo G, Fernandez-Chacon R, Schluter OM, Sudhof TC (2005) Alpha-synuclein cooperates with CSPalpha in preventing neurodegeneration. Cell 123:383-396.

Chartier-Harlin MC, Kachergus J, Roumier C, Mouroux V, Douay X, Lincoln S, Levecque C, Larvor L, Andrieux J, Hulihan M, Waucquier N, Defebvre L, Amouyel P, Farrer M, Destee A (2004) Alpha-synuclein locus duplication as a cause of familial Parkinson's disease. Lancet 364:1167-1169.

Chen CJ, Liao SL (2002) Oxidative stress involves in astrocytic alterations induced by manganese. Exp Neurol 175:216-225.

Chinta SJ, Andersen JK (2008) Redox imbalance in Parkinson's disease. Biochim Biophys Acta 1780:1362-1367.

Choi J, Sullards MC, Olzmann JA, Rees HD, Weintraub ST, Bostwick DE, Gearing M, Levey AI, Chin LS, Li L (2006a) Oxidative damage of DJ-1 is linked to sporadic Parkinson and Alzheimer diseases. J Biol Chem 281:10816-10824.

Choi P, Snyder H, Petrucelli L, Theisler C, Chong M, Zhang Y, Lim K, Chung KK, Kehoe K, D'Adamio L, Lee JM, Cochran E, Bowser R, Dawson TM, Wolozin B (2003) SEPT5_v2 is a parkin-binding protein. Brain Res Mol Brain Res 117:179-189.

Choi SH, Hyman T, Blumberg PM (2006b) Differential effect of bryostatin 1 and phorbol 12-myristate 13-acetate on HOP-92 cell proliferation is mediated by down-regulation of protein kinase Cdelta. Cancer Res 66:7261-7269.

Chung KK, Dawson VL, Dawson TM (2001a) The role of the ubiquitin-proteasomal pathway in Parkinson's disease and other neurodegenerative disorders. Trends Neurosci 24:S7-14.

Chung KK, Thomas B, Li X, Pletnikova O, Troncoso JC, Marsh L, Dawson VL, Dawson TM (2004) S-nitrosylation of parkin regulates ubiquitination and compromises parkin's protective function. Science 304:1328-1331.

Chung KK, Zhang Y, Lim KL, Tanaka Y, Huang H, Gao J, Ross CA, Dawson VL, Dawson TM (2001b) Parkin ubiquitinates the alpha-synuclein-interacting protein, synphilin-1: implications for Lewy-body formation in Parkinson disease. Nat Med 7:1144-1150.

Churchill E, Budas G, Vallentin A, Koyanagi T, Mochly-Rosen D (2008) PKC isozymes in chronic cardiac disease: possible therapeutic targets? Annu Rev Pharmacol Toxicol 48:569-599.

Clark IE, Dodson MW, Jiang C, Cao JH, Huh JR, Seol JH, Yoo SJ, Hay BA, Guo M (2006a) Drosophila pink1 is required for mitochondrial function and interacts genetically with parkin. Nature 441:1162-1166.

Clark LN, Wang Y, Karlins E, Saito L, Mejia-Santana H, Harris J, Louis ED, Cote LJ, Andrews H, Fahn S, Waters C, Ford B, Frucht S, Ottman R, Marder K (2006b) Frequency of LRRK2 mutations in early- and late-onset Parkinson disease. Neurology 67:1786-1791.

Clark LN, Afridi S, Mejia-Santana H, Harris J, Louis ED, Cote LJ, Andrews H, Singleton A, Wavrant De-Vrieze F, Hardy J, Mayeux R, Fahn S, Waters C, Ford B, Frucht S, Ottman R, Marder K (2004) Analysis of an early-onset Parkinson's disease cohort for DJ-1 mutations. Mov Disord 19:796-800.

Clarke CE (2004) Neuroprotection and pharmacotherapy for motor symptoms in Parkinson's disease. Lancet Neurol 3:466-474.

Clayton DF, George JM (1998) The synucleins: a family of proteins involved in synaptic function, plasticity, neurodegeneration and disease. Trends Neurosci 21:249-254.

Cole NB, Dieuliis D, Leo P, Mitchell DC, Nussbaum RL (2008) Mitochondrial translocation of alpha-synuclein is promoted by intracellular acidification. Exp Cell Res 314:2076-2089.

Conway KA, Harper JD, Lansbury PT (1998) Accelerated in vitro fibril formation by a mutant alpha-synuclein linked to early-onset Parkinson disease. Nat Med 4:1318-1320.

Conway KA, Harper JD, Lansbury PT, Jr. (2000a) Fibrils formed in vitro from alpha-synuclein and two mutant forms linked to Parkinson's disease are typical amyloid. Biochemistry 39:2552-2563.

Conway KA, Rochet JC, Bieganski RM, Lansbury PT, Jr. (2001) Kinetic stabilization of the alpha-synuclein protofibril by a dopamine-alpha-synuclein adduct. Science 294:1346-1349.

Conway KA, Lee SJ, Rochet JC, Ding TT, Williamson RE, Lansbury PT, Jr. (2000b) Acceleration of oligomerization, not fibrillization, is a shared property of both alpha-synuclein mutations linked to early-onset Parkinson's disease: implications for pathogenesis and therapy. Proc Natl Acad Sci U S A 97:571-576.

Cook C, Petrucelli L (2009) A critical evaluation of the ubiquitin-proteasome system in Parkinson's disease. Biochim Biophys Acta 1792:664-675.

Cook DG, Fahn S, Brait KA (1974) Chronic manganese intoxication. Arch Neurol 30:59-64.

Cookson MR (2005) The biochemistry of Parkinson's disease. Annu Rev Biochem 74:29-52.

Cookson MR, Dauer W, Dawson T, Fon EA, Guo M, Shen J (2007) The roles of kinases in familial Parkinson's disease. J Neurosci 27:11865-11868.

Corti O, Hampe C, Koutnikova H, Darios F, Jacquier S, Prigent A, Robinson JC, Pradier L, Ruberg M, Mirande M, Hirsch E, Rooney T, Fournier A, Brice A (2003) The p38 subunit of the aminoacyl-tRNA synthetase complex is a Parkin substrate: linking protein biosynthesis and neurodegeneration. Hum Mol Genet 12:1427-1437.

Cross T, Griffiths G, Deacon E, Sallis R, Gough M, Watters D, Lord JM (2000) PKC-delta is an apoptotic lamin kinase. Oncogene 19:2331-2337.

Crossman AR (1989) Neural mechanisms in disorders of movement. Comp Biochem Physiol A 93:141-149.

Crowther RA, Jakes R, Spillantini MG, Goedert M (1998) Synthetic filaments assembled from C-terminally truncated alpha-synuclein. FEBS Lett 436:309-312.

Currie LJ, Harrison MB, Trugman JM, Bennett JP, Wooten GF (2004) Postmenopausal estrogen use affects risk for Parkinson disease. Arch Neurol 61:886-888.

D'Costa AM, Denning MF (2005) A caspase-resistant mutant of PKC-delta protects keratinocytes from UV-induced apoptosis. Cell Death Differ 12:224-232.

da Costa CA, Ancolio K, Checler F (2000) Wild-type but not Parkinson's disease-related ala-53 --> Thr mutant alpha -synuclein protects neuronal cells from apoptotic stimuli. J Biol Chem 275:24065-24069.

Dachsel JC, Taylor JP, Mok SS, Ross OA, Hinkle KM, Bailey RM, Hines JH, Szutu J, Madden B, Petrucelli L, Farrer MJ (2007) Identification of potential protein interactors of Lrrk2. Parkinsonism Relat Disord 13:382-385.

Darios F, Corti O, Lucking CB, Hampe C, Muriel MP, Abbas N, Gu WJ, Hirsch EC, Rooney T, Ruberg M, Brice A (2003) Parkin prevents mitochondrial swelling and cytochrome c release in mitochondria-dependent cell death. Hum Mol Genet 12:517-526.

Dauer W, Przedborski S (2003) Parkinson's disease: mechanisms and models. Neuron 39:889-909.

Davidson WS, Jonas A, Clayton DF, George JM (1998) Stabilization of alpha-synuclein secondary structure upon binding to synthetic membranes. J Biol Chem 273:9443-9449.

Davie CA (2008) A review of Parkinson's disease. Br Med Bull 86:109-127.

Dawson TM, Dawson VL (2003) Molecular pathways of neurodegeneration in Parkinson's disease. Science 302:819-822.

Del Zompo M, Piccardi MP, Ruiu S, Corsini GU, Vaccari A (1991) High-affinity binding of [3H]1-methyl-4-phenyl-2,3-dihydropyridinium ion to mouse striatal membranes: putative vesicular location. Eur J Pharmacol 202:293-294.

Del Zompo M, Piccardi MP, Ruiu S, Corsini GU, Vaccari A (1992) Characterization of a putatively vesicular binding site for [3H]MPP+ in mouse striatal membranes. Brain Res 571:354-357.

Deng H, Dodson MW, Huang H, Guo M (2008) The Parkinson's disease genes pink1 and parkin promote mitochondrial fission and/or inhibit fusion in Drosophila. Proc Natl Acad Sci U S A 105:14503-14508.

Deumens R, Blokland A, Prickaerts J (2002) Modeling Parkinson's disease in rats: an evaluation of 6-OHDA lesions of the nigrostriatal pathway. Exp Neurol 175:303-317.

Devi L, Raghavendran V, Prabhu BM, Avadhani NG, Anandatheerthavarada HK (2008) Mitochondrial import and accumulation of alpha-synuclein impair complex I in human dopaminergic neuronal cultures and Parkinson disease brain. J Biol Chem 283:9089-9100.

Dexter DT, Wells FR, Lees AJ, Agid F, Agid Y, Jenner P, Marsden CD (1989a) Increased nigral iron content and alterations in other metal ions occurring in brain in Parkinson's disease. J Neurochem 52:1830-1836.

Dexter DT, Carter CJ, Wells FR, Javoy-Agid F, Agid Y, Lees A, Jenner P, Marsden CD (1989b) Basal lipid peroxidation in substantia nigra is increased in Parkinson's disease. J Neurochem 52:381-389.

Di Fonzo A, Rohe CF, Ferreira J, Chien HF, Vacca L, Stocchi F, Guedes L, Fabrizio E, Manfredi M, Vanacore N, Goldwurm S, Breedveld G, Sampaio C, Meco G, Barbosa E, Oostra BA, Bonifati V (2005) A frequent LRRK2 gene mutation associated with autosomal dominant Parkinson's disease. Lancet 365:412-415.

Dickson DW (2002) Misfolded, protease-resistant proteins in animal models and human neurodegenerative disease. J Clin Invest 110:1403-1405.

Discalzi G, Pira E, Herrero Hernandez E, Valentini C, Turbiglio M, Meliga F (2000) Occupational Mn parkinsonism: magnetic resonance imaging and clinical patterns following CaNa2-EDTA chelation. Neurotoxicology 21:863-866.

Dong Z, Ferger B, Paterna JC, Vogel D, Furler S, Osinde M, Feldon J, Bueler H (2003) Dopamine-dependent neurodegeneration in rats induced by viral vector-mediated overexpression of the parkin target protein, CDCrel-1. Proc Natl Acad Sci U S A 100:12438-12443.

Dunnett SB, Bjorklund A (1999) Prospects for new restorative and neuroprotective treatments in Parkinson's disease. Nature 399:A32-39.

el-Agnaf OM, Irvine GB (2002) Aggregation and neurotoxicity of alpha-synuclein and related peptides. Biochem Soc Trans 30:559-565.

Eliezer D, Kutluay E, Bussell R, Jr., Browne G (2001) Conformational properties of alpha-synuclein in its free and lipid-associated states. J Mol Biol 307:1061-1073.

Erikson KM, Aschner M (2003) Manganese neurotoxicity and glutamate-GABA interaction. Neurochem Int 43:475-480.

Exner N, Treske B, Paquet D, Holmstrom K, Schiesling C, Gispert S, Carballo-Carbajal I, Berg D, Hoepken HH, Gasser T, Kruger R, Winklhofer KF, Vogel F, Reichert AS,

Auburger G, Kahle PJ, Schmid B, Haass C (2007) Loss-of-function of human PINK1 results in mitochondrial pathology and can be rescued by parkin. J Neurosci 27:12413-12418.

Fallon L, Moreau F, Croft BG, Labib N, Gu WJ, Fon EA (2002) Parkin and CASK/LIN-2 associate via a PDZ-mediated interaction and are co-localized in lipid rafts and postsynaptic densities in brain. J Biol Chem 277:486-491.

Farrer M, Stone J, Mata IF, Lincoln S, Kachergus J, Hulihan M, Strain KJ, Maraganore DM (2005) LRRK2 mutations in Parkinson disease. Neurology 65:738-740.

Farrer MJ (2006) Genetics of Parkinson disease: paradigm shifts and future prospects. Nat Rev Genet 7:306-318.

Finkel T, Holbrook NJ (2000) Oxidants, oxidative stress and the biology of ageing. Nature 408:239-247.

Finkelstein MM, Jerrett M (2007) A study of the relationships between Parkinson's disease and markers of traffic-derived and environmental manganese air pollution in two Canadian cities. Environ Res 104:420-432.

Floor E, Wetzel MG (1998) Increased protein oxidation in human substantia nigra pars compacta in comparison with basal ganglia and prefrontal cortex measured with an improved dinitrophenylhydrazine assay. J Neurochem 70:268-275.

Forno LS (1996) Neuropathology of Parkinson's disease. J Neuropathol Exp Neurol 55:259-272.

Forno LS, Langston JW, DeLanney LE, Irwin I (1988) An electron microscopic study of MPTP-induced inclusion bodies in an old monkey. Brain Res 448:150-157.

Forno LS, DeLanney LE, Irwin I, Langston JW (1993) Similarities and differences between MPTP-induced parkinsonsim and Parkinson's disease. Neuropathologic considerations. Adv Neurol 60:600-608.

Foroud T, Uniacke SK, Liu L, Pankratz N, Rudolph A, Halter C, Shults C, Marder K, Conneally PM, Nichols WC (2003) Heterozygosity for a mutation in the parkin gene leads to later onset Parkinson disease. Neurology 60:796-801.

Fortin DL, Troyer MD, Nakamura K, Kubo S, Anthony MD, Edwards RH (2004) Lipid rafts mediate the synaptic localization of alpha-synuclein. J Neurosci 24:6715-6723.

Fuchs J, Nilsson C, Kachergus J, Munz M, Larsson EM, Schule B, Langston JW, Middleton FA, Ross OA, Hulihan M, Gasser T, Farrer MJ (2007) Phenotypic variation in a large Swedish pedigree due to SNCA duplication and triplication. Neurology 68:916-922.

Fukae J, Sato S, Shiba K, Sato K, Mori H, Sharp PA, Mizuno Y, Hattori N (2009) Programmed cell death-2 isoform1 is ubiquitinated by parkin and increased in the substantia nigra of patients with autosomal recessive Parkinson's disease. FEBS Lett 583:521-525.

Funayama M, Hasegawa K, Kowa H, Saito M, Tsuji S, Obata F (2002) A new locus for Parkinson's disease (PARK8) maps to chromosome 12p11.2-q13.1. Ann Neurol 51:296-301.

Funayama M, Hasegawa K, Ohta E, Kawashima N, Komiyama M, Kowa H, Tsuji S, Obata F (2005) An LRRK2 mutation as a cause for the parkinsonism in the original PARK8 family. Ann Neurol 57:918-921.

Funayama M, Li Y, Tomiyama H, Yoshino H, Imamichi Y, Yamamoto M, Murata M, Toda T, Mizuno Y, Hattori N (2007) Leucine-rich repeat kinase 2 G2385R variant is a risk factor for Parkinson disease in Asian population. Neuroreport 18:273-275.

Gandhi PN, Chen SG, Wilson-Delfosse AL (2009) Leucine-rich repeat kinase 2 (LRRK2): a key player in the pathogenesis of Parkinson's disease. J Neurosci Res 87:1283-1295.

Gandhi PN, Wang X, Zhu X, Chen SG, Wilson-Delfosse AL (2008) The Roc domain of leucine-rich repeat kinase 2 is sufficient for interaction with microtubules. J Neurosci Res 86:1711-1720.

Gandhi S, Muqit MM, Stanyer L, Healy DG, Abou-Sleiman PM, Hargreaves I, Heales S, Ganguly M, Parsons L, Lees AJ, Latchman DS, Holton JL, Wood NW, Revesz T (2006) PINK1 protein in normal human brain and Parkinson's disease. Brain 129:1720-1731.

Gasser T (2007) Update on the genetics of Parkinson's disease. Mov Disord 22 Suppl 17:S343-350.

Geng WD, Boskovic G, Fultz ME, Li C, Niles RM, Ohno S, Wright GL (2001) Regulation of expression and activity of four PKC isozymes in confluent and mechanically stimulated UMR-108 osteoblastic cells. J Cell Physiol 189:216-228.

George JM (2002) The synucleins. Genome Biol 3:REVIEWS3002.

George JM, Jin H, Woods WS, Clayton DF (1995) Characterization of a novel protein regulated during the critical period for song learning in the zebra finch. Neuron 15:361-372.

Giasson BI, Uryu K, Trojanowski JQ, Lee VM (1999) Mutant and wild type human alpha-synucleins assemble into elongated filaments with distinct morphologies in vitro. J Biol Chem 274:7619-7622.

Giasson BI, Murray IV, Trojanowski JQ, Lee VM (2001) A hydrophobic stretch of 12 amino acid residues in the middle of alpha-synuclein is essential for filament assembly. J Biol Chem 276:2380-2386.

Giasson BI, Covy JP, Bonini NM, Hurtig HI, Farrer MJ, Trojanowski JQ, Van Deerlin VM (2006) Biochemical and pathological characterization of Lrrk2. Ann Neurol 59:315-322.

Giasson BI, Duda JE, Murray IV, Chen Q, Souza JM, Hurtig HI, Ischiropoulos H, Trojanowski JQ, Lee VM (2000) Oxidative damage linked to neurodegeneration by selective alpha-synuclein nitration in synucleinopathy lesions. Science 290:985-989.

Gilks WP, Abou-Sleiman PM, Gandhi S, Jain S, Singleton A, Lees AJ, Shaw K, Bhatia KP, Bonifati V, Quinn NP, Lynch J, Healy DG, Holton JL, Revesz T, Wood NW (2005) A common LRRK2 mutation in idiopathic Parkinson's disease. Lancet 365:415-416.

Giordana MT, D'Agostino C, Albani G, Mauro A, Di Fonzo A, Antonini A, Bonifati V (2007) Neuropathology of Parkinson's disease associated with the LRRK2 Ile1371Val mutation. Mov Disord 22:275-278.

Glaser CB, Yamin G, Uversky VN, Fink AL (2005) Methionine oxidation, alpha-synuclein and Parkinson's disease. Biochim Biophys Acta 1703:157-169.

Glickman MH, Ciechanover A (2002) The ubiquitin-proteasome proteolytic pathway: destruction for the sake of construction. Physiol Rev 82:373-428.

Gloeckner CJ, Kinkl N, Schumacher A, Braun RJ, O'Neill E, Meitinger T, Kolch W, Prokisch H, Ueffing M (2006) The Parkinson disease causing LRRK2 mutation I2020T is associated with increased kinase activity. Hum Mol Genet 15:223-232.

Gluck MR, Youngster SK, Ramsay RR, Singer TP, Nicklas WJ (1994) Studies on the characterization of the inhibitory mechanism of 4'-alkylated 1-methyl-4-phenylpyridinium and phenylpyridine analogues in mitochondria and electron transport particles. J Neurochem 63:655-661.

Goldberg AL (2003) Protein degradation and protection against misfolded or damaged proteins. Nature 426:895-899.

Goldwurm S, Zini M, Mariani L, Tesei S, Miceli R, Sironi F, Clementi M, Bonifati V, Pezzoli G (2007) Evaluation of LRRK2 G2019S penetrance: relevance for genetic counseling in Parkinson disease. Neurology 68:1141-1143.

Gorell JM, Johnson CC, Rybicki BA, Peterson EL, Kortsha GX, Brown GG, Richardson RJ (1999) Occupational exposure to manganese, copper, lead, iron, mercury and zinc and the risk of Parkinson's disease. Neurotoxicology 20:239-247.

Greene JC, Whitworth AJ, Kuo I, Andrews LA, Feany MB, Pallanck LJ (2003) Mitochondrial pathology and apoptotic muscle degeneration in Drosophila parkin mutants. Proc Natl Acad Sci U S A 100:4078-4083.

Greggio E, Jain S, Kingsbury A, Bandopadhyay R, Lewis P, Kaganovich A, van der Brug MP, Beilina A, Blackinton J, Thomas KJ, Ahmad R, Miller DW, Kesavapany S, Singleton A, Lees A, Harvey RJ, Harvey K, Cookson MR (2006) Kinase activity is required for the toxic effects of mutant LRRK2/dardarin. Neurobiol Dis 23:329-341.

Gschwendt M (1999) Protein kinase C delta. Eur J Biochem 259:555-564.

Gschwendt M, Kittstein W, Marks F (1986) A novel type of phorbol ester-dependent protein phosphorylation in the particulate fraction of mouse epidermis. Biochem Biophys Res Commun 137:766-774.

Haas RH, Nasirian F, Nakano K, Ward D, Pay M, Hill R, Shults CW (1995) Low platelet mitochondrial complex I and complex II/III activity in early untreated Parkinson's disease. Ann Neurol 37:714-722.

Haehner A, Hummel T, Hummel C, Sommer U, Junghanns S, Reichmann H (2007) Olfactory loss may be a first sign of idiopathic Parkinson's disease. Mov Disord 22:839-842.

Hancock DB, Martin ER, Mayhew GM, Stajich JM, Jewett R, Stacy MA, Scott BL, Vance JM, Scott WK (2008) Pesticide exposure and risk of Parkinson's disease: a family-based case-control study. BMC Neurol 8:6.

Haque ME, Thomas KJ, D'Souza C, Callaghan S, Kitada T, Slack RS, Fraser P, Cookson MR, Tandon A, Park DS (2008) Cytoplasmic Pink1 activity protects neurons from dopaminergic neurotoxin MPTP. Proc Natl Acad Sci U S A 105:1716-1721.

Hardy J (2006) No definitive evidence for a role for the environment in the etiology of Parkinson's disease. Mov Disord 21:1790-1791.

Hardy J, Lewis P, Revesz T, Lees A, Paisan-Ruiz C (2009) The genetics of Parkinson's syndromes: a critical review. Curr Opin Genet Dev 19:254-265.

Harper SJ, Wilkie N (2003) MAPKs: new targets for neurodegeneration. Expert Opin Ther Targets 7:187-200.

Hartmann A, Michel PP, Troadec JD, Mouatt-Prigent A, Faucheux BA, Ruberg M, Agid Y, Hirsch EC (2001a) Is Bax a mitochondrial mediator in apoptotic death of dopaminergic neurons in Parkinson's disease? J Neurochem 76:1785-1793.

Hartmann A, Troadec JD, Hunot S, Kikly K, Faucheux BA, Mouatt-Prigent A, Ruberg M, Agid Y, Hirsch EC (2001b) Caspase-8 is an effector in apoptotic death of dopaminergic neurons in Parkinson's disease, but pathway inhibition results in neuronal necrosis. J Neurosci 21:2247-2255.

Hartmann A, Hunot S, Michel PP, Muriel MP, Vyas S, Faucheux BA, Mouatt-Prigent A, Turmel H, Srinivasan A, Ruberg M, Evan GI, Agid Y, Hirsch EC (2000) Caspase-3: A vulnerability factor and final effector in apoptotic death of dopaminergic neurons in Parkinson's disease. Proc Natl Acad Sci U S A 97:2875-2880.

Hasegawa K, Stoessl AJ, Yokoyama T, Kowa H, Wszolek ZK, Yagishita S (2009) Familial parkinsonism: study of original Sagamihara PARK8 (I2020T) kindred with variable clinicopathologic outcomes. Parkinsonism Relat Disord 15:300-306.

Hashimoto M, Hsu LJ, Rockenstein E, Takenouchi T, Mallory M, Masliah E (2002) alpha-Synuclein protects against oxidative stress via inactivation of the c-Jun N-terminal kinase stress-signaling pathway in neuronal cells. J Biol Chem 277:11465-11472.

Hastings TG (2009) The role of dopamine oxidation in mitochondrial dysfunction: implications for Parkinson's disease. J Bioenerg Biomembr 41:469-472.

Hatano T, Kubo S, Sato S, Hattori N (2009) Pathogenesis of familial Parkinson's disease: new insights based on monogenic forms of Parkinson's disease. J Neurochem 111:1075-1093.

Hatano T, Kubo S, Imai S, Maeda M, Ishikawa K, Mizuno Y, Hattori N (2007) Leucine-rich repeat kinase 2 associates with lipid rafts. Hum Mol Genet 16:678-690.

Hatano Y, Li Y, Sato K, Asakawa S, Yamamura Y, Tomiyama H, Yoshino H, Asahina M, Kobayashi S, Hassin-Baer S, Lu CS, Ng AR, Rosales RL, Shimizu N, Toda T, Mizuno Y, Hattori N (2004a) Novel PINK1 mutations in early-onset parkinsonism. Ann Neurol 56:424-427.

Hatano Y, Sato K, Elibol B, Yoshino H, Yamamura Y, Bonifati V, Shinotoh H, Asahina M, Kobayashi S, Ng AR, Rosales RL, Hassin-Baer S, Shinar Y, Lu CS, Chang HC, Wu-Chou YH, Atac FB, Kobayashi T, Toda T, Mizuno Y, Hattori N (2004b) PARK6-linked autosomal recessive early-onset parkinsonism in Asian populations. Neurology 63:1482-1485.

Haugarvoll K, Wszolek ZK (2009) Clinical features of LRRK2 parkinsonism. Parkinsonism Relat Disord 15 Suppl 3:S205-208.

Hauser RA, Zesiewicz TA, Rosemurgy AS, Martinez C, Olanow CW (1994) Manganese intoxication and chronic liver failure. Ann Neurol 36:871-875.

Hazell AS, Norenberg MD (1997) Manganese decreases glutamate uptake in cultured astrocytes. Neurochem Res 22:1443-1447.

Hazell AS, Desjardins P, Butterworth RF (1999) Chronic exposure of rat primary astrocyte cultures to manganese results in increased binding sites for the 'peripheral-type' benzodiazepine receptor ligand 3H-PK 11195. Neurosci Lett 271:5-8.

Hering R, Strauss KM, Tao X, Bauer A, Woitalla D, Mietz EM, Petrovic S, Bauer P, Schaible W, Muller T, Schols L, Klein C, Berg D, Meyer PT, Schulz JB, Wollnik B,

Tong L, Kruger R, Riess O (2004) Novel homozygous p.E64D mutation in DJ1 in early onset Parkinson disease (PARK7). Hum Mutat 24:321-329.

Hernan MA, Takkouche B, Caamano-Isorna F, Gestal-Otero JJ (2002) A meta-analysis of coffee drinking, cigarette smoking, and the risk of Parkinson's disease. Ann Neurol 52:276-284.

Herrero Hernandez E, Discalzi G, Valentini C, Venturi F, Chio A, Carmellino C, Rossi L, Sacchetti A, Pira E (2006) Follow-up of patients affected by manganese-induced Parkinsonism after treatment with CaNa2EDTA. Neurotoxicology 27:333-339.

Hershko A, Ciechanover A (1998) The ubiquitin system. Annu Rev Biochem 67:425-479.

Ho CC, Rideout HJ, Ribe E, Troy CM, Dauer WT (2009) The Parkinson disease protein leucine-rich repeat kinase 2 transduces death signals via Fas-associated protein with death domain and caspase-8 in a cellular model of neurodegeneration. J Neurosci 29:1011-1016.

Hodara R, Norris EH, Giasson BI, Mishizen-Eberz AJ, Lynch DR, Lee VM, Ischiropoulos H (2004) Functional consequences of alpha-synuclein tyrosine nitration: diminished binding to lipid vesicles and increased fibril formation. J Biol Chem 279:47746-47753.

Horovitz-Fried M, Jacob AI, Cooper DR, Sampson SR (2007) Activation of the nuclear transcription factor SP-1 by insulin rapidly increases the expression of protein kinase C delta in skeletal muscle. Cell Signal 19:556-562.

Horovitz-Fried M, Cooper DR, Patel NA, Cipok M, Brand C, Bak A, Inbar A, Jacob AI, Sampson SR (2006) Insulin rapidly upregulates protein kinase Cdelta gene expression in skeletal muscle. Cell Signal 18:183-193.

Hsu LJ, Sagara Y, Arroyo A, Rockenstein E, Sisk A, Mallory M, Wong J, Takenouchi T, Hashimoto M, Masliah E (2000) alpha-synuclein promotes mitochondrial deficit and oxidative stress. Am J Pathol 157:401-410.

Huang CC, Chu NS, Lu CS, Wang JD, Tsai JL, Tzeng JL, Wolters EC, Calne DB (1989) Chronic manganese intoxication. Arch Neurol 46:1104-1106.

Huynh DP, Scoles DR, Nguyen D, Pulst SM (2003) The autosomal recessive juvenile Parkinson disease gene product, parkin, interacts with and ubiquitinates synaptotagmin XI. Hum Mol Genet 12:2587-2597.

Iaccarino C, Crosio C, Vitale C, Sanna G, Carri MT, Barone P (2007) Apoptotic mechanisms in mutant LRRK2-mediated cell death. Hum Mol Genet 16:1319-1326.

Ibanez P, Bonnet AM, Debarges B, Lohmann E, Tison F, Pollak P, Agid Y, Durr A, Brice A (2004) Causal relation between alpha-synuclein gene duplication and familial Parkinson's disease. Lancet 364:1169-1171.

Ii K, Ito H, Tanaka K, Hirano A (1997) Immunocytochemical co-localization of the proteasome in ubiquitinated structures in neurodegenerative diseases and the elderly. J Neuropathol Exp Neurol 56:125-131.

Imai Y, Soda M, Inoue H, Hattori N, Mizuno Y, Takahashi R (2001) An unfolded putative transmembrane polypeptide, which can lead to endoplasmic reticulum stress, is a substrate of Parkin. Cell 105:891-902.

Inglis KJ, Chereau D, Brigham EF, Chiou SS, Schobel S, Frigon NL, Yu M, Caccavello RJ, Nelson S, Motter R, Wright S, Chian D, Santiago P, Soriano F, Ramos C, Powell K, Goldstein JM, Babcock M, Yednock T, Bard F, Basi GS, Sham H, Chilcote TJ, McConlogue L, Griswold-Prenner I, Anderson JP (2009) Polo-like kinase 2 (PLK2)

phosphorylates alpha-synuclein at serine 129 in central nervous system. J Biol Chem 284:2598-2602.

Inoue M, Kishimoto A, Takai Y, Nishizuka Y (1977) Studies on a cyclic nucleotide-independent protein kinase and its proenzyme in mammalian tissues. II. Proenzyme and its activation by calcium-dependent protease from rat brain. J Biol Chem 252:7610-7616.

Ischiropoulos H, Beckman JS (2003) Oxidative stress and nitration in neurodegeneration: cause, effect, or association? J Clin Invest 111:163-169.

Ishikawa A, Tsuji S (1996) Clinical analysis of 17 patients in 12 Japanese families with autosomal-recessive type juvenile parkinsonism. Neurology 47:160-166.

Jackson-Lewis V, Jakowec M, Burke RE, Przedborski S (1995) Time course and morphology of dopaminergic neuronal death caused by the neurotoxin 1-methyl-4-phenyl-1,2,3,6-tetrahydropyridine. Neurodegeneration 4:257-269.

Jaleel M, Nichols RJ, Deak M, Campbell DG, Gillardon F, Knebel A, Alessi DR (2007) LRRK2 phosphorylates moesin at threonine-558: characterization of how Parkinson's disease mutants affect kinase activity. Biochem J 405:307-317.

Jankovic J (1988) Parkinson's disease: recent advances in therapy. South Med J 81:1021-1027.

Jankovic J (2005) Searching for a relationship between manganese and welding and Parkinson's disease. Neurology 64:2021-2028.

Jankovic J (2008) Parkinson's disease: clinical features and diagnosis. J Neurol Neurosurg Psychiatry 79:368-376.

Jao CC, Der-Sarkissian A, Chen J, Langen R (2004) Structure of membrane-bound alpha-synuclein studied by site-directed spin labeling. Proc Natl Acad Sci U S A 101:8331-8336.

Javitch JA, D'Amato RJ, Strittmatter SM, Snyder SH (1985) Parkinsonism-inducing neurotoxin, N-methyl-4-phenyl-1,2,3,6 -tetrahydropyridine: uptake of the metabolite N-methyl-4-phenylpyridine by dopamine neurons explains selective toxicity. Proc Natl Acad Sci U S A 82:2173-2177.

Jellinger K (1990) New developments in the pathology of Parkinson's disease. Adv Neurol 53:1-16.

Jellinger KA (2000) Cell death mechanisms in Parkinson's disease. J Neural Transm 107:1-29.

Jellinger KA (2009) A critical evaluation of current staging of alpha-synuclein pathology in Lewy body disorders. Biochim Biophys Acta 1792:730-740.

Jenco JM, Rawlingson A, Daniels B, Morris AJ (1998) Regulation of phospholipase D2: selective inhibition of mammalian phospholipase D isoenzymes by alpha- and beta-synucleins. Biochemistry 37:4901-4909.

Jenner P (2003) Oxidative stress in Parkinson's disease. Ann Neurol 53 Suppl 3:S26-36; discussion S36-28.

Jenner P, Olanow CW (1996) Oxidative stress and the pathogenesis of Parkinson's disease. Neurology 47:S161-170.

Jensen PH, Nielsen MS, Jakes R, Dotti CG, Goedert M (1998) Binding of alpha-synuclein to brain vesicles is abolished by familial Parkinson's disease mutation. J Biol Chem 273:26292-26294.

Jensen PJ, Alter BJ, O'Malley KL (2003) Alpha-synuclein protects naive but not dbcAMP-treated dopaminergic cell types from 1-methyl-4-phenylpyridinium toxicity. J Neurochem 86:196-209.

Jiang H, Ren Y, Zhao J, Feng J (2004) Parkin protects human dopaminergic neuroblastoma cells against dopamine-induced apoptosis. Hum Mol Genet 13:1745-1754.

Jo E, McLaurin J, Yip CM, St George-Hyslop P, Fraser PE (2000) alpha-Synuclein membrane interactions and lipid specificity. J Biol Chem 275:34328-34334.

Junn E, Taniguchi H, Jeong BS, Zhao X, Ichijo H, Mouradian MM (2005) Interaction of DJ-1 with Daxx inhibits apoptosis signal-regulating kinase 1 activity and cell death. Proc Natl Acad Sci U S A 102:9691-9696.

Kachergus J, Mata IF, Hulihan M, Taylor JP, Lincoln S, Aasly J, Gibson JM, Ross OA, Lynch T, Wiley J, Payami H, Nutt J, Maraganore DM, Czyzewski K, Styczynska M, Wszolek ZK, Farrer MJ, Toft M (2005) Identification of a novel LRRK2 mutation linked to autosomal dominant parkinsonism: evidence of a common founder across European populations. Am J Hum Genet 76:672-680.

Kahle PJ, Haass C, Kretzschmar HA, Neumann M (2002) Structure/function of alpha-synuclein in health and disease: rational development of animal models for Parkinson's and related diseases. J Neurochem 82:449-457.

Kanthasamy AG, Kitazawa M, Kanthasamy A, Anantharam V (2003) Role of proteolytic activation of protein kinase Cdelta in oxidative stress-induced apoptosis. Antioxid Redox Signal 5:609-620.

Kanthasamy AG, Anantharam V, Zhang D, Latchoumycandane C, Jin H, Kaul S, Kanthasamy A (2006) A novel peptide inhibitor targeted to caspase-3 cleavage site of

a proapoptotic kinase protein kinase C delta (PKCdelta) protects against dopaminergic neuronal degeneration in Parkinson's disease models. Free Radic Biol Med 41:1578-1589.

Kaul S, Kanthasamy A, Kitazawa M, Anantharam V, Kanthasamy AG (2003) Caspase-3 dependent proteolytic activation of protein kinase C delta mediates and regulates 1-methyl-4-phenylpyridinium (MPP+)-induced apoptotic cell death in dopaminergic cells: relevance to oxidative stress in dopaminergic degeneration. Eur J Neurosci 18:1387-1401.

Kaul S, Anantharam V, Yang Y, Choi CJ, Kanthasamy A, Kanthasamy AG (2005) Tyrosine phosphorylation regulates the proteolytic activation of protein kinase Cdelta in dopaminergic neuronal cells. J Biol Chem 280:28721-28730.

Keen CL, Ensunsa JL, Clegg MS (2000) Manganese metabolism in animals and humans including the toxicity of manganese. Met Ions Biol Syst 37:89-121.

Keeney PM, Xie J, Capaldi RA, Bennett JP, Jr. (2006) Parkinson's disease brain mitochondrial complex I has oxidatively damaged subunits and is functionally impaired and misassembled. J Neurosci 26:5256-5264.

Khan NL, Jain S, Lynch JM, Pavese N, Abou-Sleiman P, Holton JL, Healy DG, Gilks WP, Sweeney MG, Ganguly M, Gibbons V, Gandhi S, Vaughan J, Eunson LH, Katzenschlager R, Gayton J, Lennox G, Revesz T, Nicholl D, Bhatia KP, Quinn N, Brooks D, Lees AJ, Davis MB, Piccini P, Singleton AB, Wood NW (2005) Mutations in the gene LRRK2 encoding dardarin (PARK8) cause familial Parkinson's disease: clinical, pathological, olfactory and functional imaging and genetic data. Brain 128:2786-2796.

Kikkawa U, Matsuzaki H, Yamamoto T (2002a) Protein kinase C delta (PKC delta): activation mechanisms and functions. J Biochem 132:831-839.

Kikkawa U, Matsuzaki H, Yamamoto T (2002b) Protein kinase C delta (PKC delta): activation mechanisms and functions. In: J Biochem, pp 831-839.

Kim RH, Smith PD, Aleyasin H, Hayley S, Mount MP, Pownall S, Wakeham A, You-Ten AJ, Kalia SK, Horne P, Westaway D, Lozano AM, Anisman H, Park DS, Mak TW (2005) Hypersensitivity of DJ-1-deficient mice to 1-methyl-4-phenyl-1,2,3,6-tetrahydropyrindine (MPTP) and oxidative stress. Proc Natl Acad Sci U S A 102:5215-5220.

Kirik D, Rosenblad C, Bjorklund A (1998) Characterization of behavioral and neurodegenerative changes following partial lesions of the nigrostriatal dopamine system induced by intrastriatal 6-hydroxydopamine in the rat. Exp Neurol 152:259-277.

Kitada T, Asakawa S, Hattori N, Matsumine H, Yamamura Y, Minoshima S, Yokochi M, Mizuno Y, Shimizu N (1998) Mutations in the parkin gene cause autosomal recessive juvenile parkinsonism. Nature 392:605-608.

Kitazawa M, Anantharam V, Kanthasamy AG (2003) Dieldrin induces apoptosis by promoting caspase-3-dependent proteolytic cleavage of protein kinase Cdelta in dopaminergic cells: relevance to oxidative stress and dopaminergic degeneration. Neuroscience 119:945-964.

Klein C, Schlossmacher MG (2006) The genetics of Parkinson disease: Implications for neurological care. Nat Clin Pract Neurol 2:136-146.

Klein C, Schlossmacher MG (2007) Parkinson disease, 10 years after its genetic revolution: multiple clues to a complex disorder. Neurology 69:2093-2104.

Klein C, Pramstaller PP, Kis B, Page CC, Kann M, Leung J, Woodward H, Castellan CC, Scherer M, Vieregge P, Breakefield XO, Kramer PL, Ozelius LJ (2000) Parkin deletions in a family with adult-onset, tremor-dominant parkinsonism: expanding the phenotype. Ann Neurol 48:65-71.

Konishi H, Yamauchi E, Taniguchi H, Yamamoto T, Matsuzaki H, Takemura Y, Ohmae K, Kikkawa U, Nishizuka Y (2001) Phosphorylation sites of protein kinase C delta in H2O2-treated cells and its activation by tyrosine kinase in vitro. Proc Natl Acad Sci U S A 98:6587-6592.

Kopito RR (2000) Aggresomes, inclusion bodies and protein aggregation. Trends Cell Biol 10:524-530.

Kordower JH, Kanaan NM, Chu Y, Suresh Babu R, Stansell J, 3rd, Terpstra BT, Sortwell CE, Steece-Collier K, Collier TJ (2006) Failure of proteasome inhibitor administration to provide a model of Parkinson's disease in rats and monkeys. Ann Neurol 60:264-268.

Kotake Y, Ohta S (2003) MPP+ analogs acting on mitochondria and inducing neuro-degeneration. Curr Med Chem 10:2507-2516.

Krachler M, Rossipal E (2000) Concentrations of trace elements in extensively hydrolysed infant formulae and their estimated daily intakes. Ann Nutr Metab 44:68-74.

Krieger D, Krieger S, Jansen O, Gass P, Theilmann L, Lichtnecker H (1995) Manganese and chronic hepatic encephalopathy. Lancet 346:270-274.

Kruger R, Kuhn W, Muller T, Woitalla D, Graeber M, Kosel S, Przuntek H, Epplen JT, Schols L, Riess O (1998) Ala30Pro mutation in the gene encoding alpha-synuclein in Parkinson's disease. Nat Genet 18:106-108.

Kubo S, Nemani VM, Chalkley RJ, Anthony MD, Hattori N, Mizuno Y, Edwards RH, Fortin DL (2005) A combinatorial code for the interaction of alpha-synuclein with membranes. J Biol Chem 280:31664-31672.

Kurkinen KM, Keinanen RA, Karhu R, Koistinaho J (2000) Genomic structure and chromosomal localization of the rat protein kinase Cdelta-gene. Gene 242:115-123.

Kuroda Y, Mitsui T, Kunishige M, Shono M, Akaike M, Azuma H, Matsumoto T (2006) Parkin enhances mitochondrial biogenesis in proliferating cells. Hum Mol Genet 15:883-895.

Langston JW, Ballard P, Tetrud JW, Irwin I (1983) Chronic Parkinsonism in humans due to a product of meperidine-analog synthesis. Science 219:979-980.

Langston JW, Irwin I, Langston EB, Forno LS (1984) 1-Methyl-4-phenylpyridinium ion (MPP+): identification of a metabolite of MPTP, a toxin selective to the substantia nigra. Neurosci Lett 48:87-92.

Larsen CN, Price JS, Wilkinson KD (1996) Substrate binding and catalysis by ubiquitin C-terminal hydrolases: identification of two active site residues. Biochemistry 35:6735-6744.

Larsen CN, Krantz BA, Wilkinson KD (1998) Substrate specificity of deubiquitinating enzymes: ubiquitin C-terminal hydrolases. Biochemistry 37:3358-3368.

Latchoumycandane C, Anantharam V, Kitazawa M, Yang Y, Kanthasamy A, Kanthasamy AG (2005) Protein kinase Cdelta is a key downstream mediator of

manganese-induced apoptosis in dopaminergic neuronal cells. J Pharmacol Exp Ther 313:46-55.

LaVoie MJ, Hastings TG (1999) Dopamine quinone formation and protein modification associated with the striatal neurotoxicity of methamphetamine: evidence against a role for extracellular dopamine. J Neurosci 19:1484-1491.

LaVoie MJ, Ostaszewski BL, Weihofen A, Schlossmacher MG, Selkoe DJ (2005) Dopamine covalently modifies and functionally inactivates parkin. Nat Med 11:1214-1221.

Lee HJ, Choi C, Lee SJ (2002a) Membrane-bound alpha-synuclein has a high aggregation propensity and the ability to seed the aggregation of the cytosolic form. J Biol Chem 277:671-678.

Lee MK, Stirling W, Xu Y, Xu X, Qui D, Mandir AS, Dawson TM, Copeland NG, Jenkins NA, Price DL (2002b) Human alpha-synuclein-harboring familial Parkinson's disease-linked Ala-53 --> Thr mutation causes neurodegenerative disease with alpha-synuclein aggregation in transgenic mice. Proc Natl Acad Sci U S A 99:8968-8973.

Lee SJ, Kim SJ, Kim IK, Ko J, Jeong CS, Kim GH, Park C, Kang SO, Suh PG, Lee HS, Cha SS (2003) Crystal structures of human DJ-1 and Escherichia coli Hsp31, which share an evolutionarily conserved domain. J Biol Chem 278:44552-44559.

Lee VM, Trojanowski JQ (2006) Mechanisms of Parkinson's disease linked to pathological alpha-synuclein: new targets for drug discovery. Neuron 52:33-38.

Lees AJ (2009) The Parkinson chimera. Neurology 72:S2-11.

Leibersperger H, Gschwendt M, Gernold M, Marks F (1991) Immunological demonstration of a calcium-unresponsive protein kinase C of the delta-type in different species and murine tissues. Predominance in epidermis. J Biol Chem 266:14778-14784.

Leng Y, Chuang DM (2006) Endogenous alpha-synuclein is induced by valproic acid through histone deacetylase inhibition and participates in neuroprotection against glutamate-induced excitotoxicity. J Neurosci 26:7502-7512.

Leong SL, Cappai R, Barnham KJ, Pham CL (2009) Modulation of alpha-synuclein aggregation by dopamine: a review. Neurochem Res 34:1838-1846.

Leroy E, Boyer R, Polymeropoulos MH (1998a) Intron-exon structure of ubiquitin c-terminal hydrolase-L1. DNA Res 5:397-400.

Leroy E, Boyer R, Auburger G, Leube B, Ulm G, Mezey E, Harta G, Brownstein MJ, Jonnalagada S, Chernova T, Dehejia A, Lavedan C, Gasser T, Steinbach PJ, Wilkinson KD, Polymeropoulos MH (1998b) The ubiquitin pathway in Parkinson's disease. Nature 395:451-452.

Lesage S, Brice A (2009) Parkinson's disease: from monogenic forms to genetic susceptibility factors. Hum Mol Genet 18:R48-59.

Lesage S, Durr A, Tazir M, Lohmann E, Leutenegger AL, Janin S, Pollak P, Brice A (2006) LRRK2 G2019S as a cause of Parkinson's disease in North African Arabs. N Engl J Med 354:422-423.

Lesage S, Ibanez P, Lohmann E, Pollak P, Tison F, Tazir M, Leutenegger AL, Guimaraes J, Bonnet AM, Agid Y, Durr A, Brice A (2005) G2019S LRRK2 mutation in French and North African families with Parkinson's disease. Ann Neurol 58:784-787.

Lewitt PA (2008) Levodopa for the treatment of Parkinson's disease. N Engl J Med 359:2468-2476.

Li HT, Lin DH, Luo XY, Zhang F, Ji LN, Du HN, Song GQ, Hu J, Zhou JW, Hu HY (2005) Inhibition of alpha-synuclein fibrillization by dopamine analogs via reaction with the amino groups of alpha-synuclein. Implication for dopaminergic neurodegeneration. Febs J 272:3661-3672.

Li WW, Yang R, Guo JC, Ren HM, Zha XL, Cheng JS, Cai DF (2007) Localization of alpha-synuclein to mitochondria within midbrain of mice. Neuroreport 18:1543-1546.

Liou HH, Tsai MC, Chen CJ, Jeng JS, Chang YC, Chen SY, Chen RC (1997) Environmental risk factors and Parkinson's disease: a case-control study in Taiwan. Neurology 48:1583-1588.

Liu J, Yang D, Minemoto Y, Leitges M, Rosner MR, Lin A (2006a) NF-kappaB is required for UV-induced JNK activation via induction of PKCdelta. Mol Cell 21:467-480.

Liu WS, Heckman CA (1998) The sevenfold way of PKC regulation. Cell Signal 10:529-542.

Liu X, Sullivan KA, Madl JE, Legare M, Tjalkens RB (2006b) Manganese-induced neurotoxicity: the role of astroglial-derived nitric oxide in striatal interneuron degeneration. Toxicol Sci 91:521-531.

Liu Y, Fallon L, Lashuel HA, Liu Z, Lansbury PT, Jr. (2002) The UCH-L1 gene encodes two opposing enzymatic activities that affect alpha-synuclein degradation and Parkinson's disease susceptibility. Cell 111:209-218.

Lockhart PJ, Lincoln S, Hulihan M, Kachergus J, Wilkes K, Bisceglio G, Mash DC, Farrer MJ (2004) DJ-1 mutations are a rare cause of recessively inherited early onset parkinsonism mediated by loss of protein function. J Med Genet 41:e22.

Loh KP, Huang SH, De Silva R, Tan BK, Zhu YZ (2006) Oxidative stress: apoptosis in neuronal injury. Curr Alzheimer Res 3:327-337.

Lohmann E, Periquet M, Bonifati V, Wood NW, De Michele G, Bonnet AM, Fraix V, Broussolle E, Horstink MW, Vidailhet M, Verpillat P, Gasser T, Nicholl D, Teive H, Raskin S, Rascol O, Destee A, Ruberg M, Gasparini F, Meco G, Agid Y, Durr A, Brice A (2003) How much phenotypic variation can be attributed to parkin genotype? Ann Neurol 54:176-185.

Lonnerdal B (1994) Nutritional aspects of soy formula. Acta Paediatr Suppl 402:105-108.

Lotharius J, Brundin P (2002) Pathogenesis of Parkinson's disease: dopamine, vesicles and alpha-synuclein. Nat Rev Neurosci 3:932-942.

Lowe J, McDermott H, Landon M, Mayer RJ, Wilkinson KD (1990) Ubiquitin carboxyl-terminal hydrolase (PGP 9.5) is selectively present in ubiquitinated inclusion bodies characteristic of human neurodegenerative diseases. J Pathol 161:153-160.

Lu CS, Huang CC, Chu NS, Calne DB (1994) Levodopa failure in chronic manganism. Neurology 44:1600-1602.

Lu YW, Tan EK (2008) Molecular biology changes associated with LRRK2 mutations in Parkinson's disease. J Neurosci Res 86:1895-1901.

Lucking CB, Bonifati V, Periquet M, Vanacore N, Brice A, Meco G (2001) Pseudo-dominant inheritance and exon 2 triplication in a family with parkin gene mutations. Neurology 57:924-927.

Lucking CB, Durr A, Bonifati V, Vaughan J, De Michele G, Gasser T, Harhangi BS, Meco G, Denefle P, Wood NW, Agid Y, Brice A (2000) Association between early-onset Parkinson's disease and mutations in the parkin gene. N Engl J Med 342:1560-1567.

Lydeard JR, Harper JW (2010) Inhibitors for E3 ubiquitin ligases. Nat Biotechnol 28:682-684.

Macedo MG, Anar B, Bronner IF, Cannella M, Squitieri F, Bonifati V, Hoogeveen A, Heutink P, Rizzu P (2003) The DJ-1L166P mutant protein associated with early onset Parkinson's disease is unstable and forms higher-order protein complexes. Hum Mol Genet 12:2807-2816.

Machida Y, Chiba T, Takayanagi A, Tanaka Y, Asanuma M, Ogawa N, Koyama A, Iwatsubo T, Ito S, Jansen PH, Shimizu N, Tanaka K, Mizuno Y, Hattori N (2005) Common anti-apoptotic roles of parkin and alpha-synuclein in human dopaminergic cells. Biochem Biophys Res Commun 332:233-240.

Maher P (2008) Proteasome inhibitors prevent oxidative stress-induced nerve cell death by a novel mechanism. Biochem Pharmacol 75:1994-2006.

Mann VM, Cooper JM, Daniel SE, Srai K, Jenner P, Marsden CD, Schapira AH (1994) Complex I, iron, and ferritin in Parkinson's disease substantia nigra. Ann Neurol 36:876-881.

Manning-Bog AB, McCormack AL, Purisai MG, Bolin LM, Di Monte DA (2003) Alpha-synuclein overexpression protects against paraquat-induced neurodegeneration. J Neurosci 23:3095-3099.

Manning-Bog AB, McCormack AL, Li J, Uversky VN, Fink AL, Di Monte DA (2002) The herbicide paraquat causes up-regulation and aggregation of alpha-synuclein in mice: paraquat and alpha-synuclein. J Biol Chem 277:1641-1644.

Maraganore DM, de Andrade M, Elbaz A, Farrer MJ, Ioannidis JP, Kruger R, Rocca WA, Schneider NK, Lesnick TG, Lincoln SJ, Hulihan MM, Aasly JO, Ashizawa T, Chartier-Harlin MC, Checkoway H, Ferrarese C, Hadjigeorgiou G, Hattori N, Kawakami H, Lambert JC, Lynch T, Mellick GD, Papapetropoulos S, Parsian A, Quattrone A, Riess O, Tan EK, Van Broeckhoven C (2006) Collaborative analysis of alpha-synuclein gene promoter variability and Parkinson disease. Jama 296:661-670.

Maries E, Dass B, Collier TJ, Kordower JH, Steece-Collier K (2003) The role of alpha-synuclein in Parkinson's disease: insights from animal models. Nat Rev Neurosci 4:727-738.

Markey SP, Johannessen JN, Chiueh CC, Burns RS, Herkenham MA (1984) Intraneuronal generation of a pyridinium metabolite may cause drug-induced parkinsonism. Nature 311:464-467.

Maroteaux L, Scheller RH (1991) The rat brain synucleins; family of proteins transiently associated with neuronal membrane. Brain Res Mol Brain Res 11:335-343.

Mata IF, Lockhart PJ, Farrer MJ (2004) Parkin genetics: one model for Parkinson's disease. Hum Mol Genet 13 Spec No 1:R127-133.

Mata IF, Wedemeyer WJ, Farrer MJ, Taylor JP, Gallo KA (2006a) LRRK2 in Parkinson's disease: protein domains and functional insights. Trends Neurosci 29:286-293.

Mata IF, Ross OA, Kachergus J, Huerta C, Ribacoba R, Moris G, Blazquez M, Guisasola LM, Salvador C, Martinez C, Farrer M, Alvarez V (2006b) LRRK2 mutations are a common cause of Parkinson's disease in Spain. Eur J Neurol 13:391-394.

Mattson MP (2000) Apoptosis in neurodegenerative disorders. Nat Rev Mol Cell Biol 1:120-129.

Mattson MP (2006) Neuronal life-and-death signaling, apoptosis, and neurodegenerative disorders. Antioxid Redox Signal 8:1997-2006.

McCormack AL, Thiruchelvam M, Manning-Bog AB, Thiffault C, Langston JW, Cory-Slechta DA, Di Monte DA (2002) Environmental risk factors and Parkinson's disease: selective degeneration of nigral dopaminergic neurons caused by the herbicide paraquat. Neurobiol Dis 10:119-127.

McGeer PL, McGeer EG (2008) Glial reactions in Parkinson's disease. Mov Disord 23:474-483.

McNaught KS, Jenner P (2001) Proteasomal function is impaired in substantia nigra in Parkinson's disease. Neurosci Lett 297:191-194.

McNaught KS, Olanow CW (2006) Proteasome inhibitor-induced model of Parkinson's disease. Ann Neurol 60:243-247.

McNaught KS, Perl DP, Brownell AL, Olanow CW (2004) Systemic exposure to proteasome inhibitors causes a progressive model of Parkinson's disease. Ann Neurol 56:149-162.

McNaught KS, Belizaire R, Jenner P, Olanow CW, Isacson O (2002) Selective loss of 20S proteasome alpha-subunits in the substantia nigra pars compacta in Parkinson's disease. Neurosci Lett 326:155-158.

McNaught KS, Belizaire R, Isacson O, Jenner P, Olanow CW (2003) Altered proteasomal function in sporadic Parkinson's disease. Exp Neurol 179:38-46.

Meffert MK, Baltimore D (2005) Physiological functions for brain NF-kappaB. Trends Neurosci 28:37-43.

Menzies FM, Yenisetti SC, Min KT (2005) Roles of Drosophila DJ-1 in survival of dopaminergic neurons and oxidative stress. Curr Biol 15:1578-1582.

Mercurio F, Manning AM (1999) NF-kappaB as a primary regulator of the stress response. Oncogene 18:6163-6171.

Mergler D, Huel G, Bowler R, Iregren A, Belanger S, Baldwin M, Tardif R, Smargiassi A, Martin L (1994) Nervous system dysfunction among workers with long-term exposure to manganese. Environ Res 64:151-180.

Migliore L, Coppede F (2009) Environmental-induced oxidative stress in neurodegenerative disorders and aging. Mutat Res 674:73-84.

Miller DW, Ahmad R, Hague S, Baptista MJ, Canet-Aviles R, McLendon C, Carter DM, Zhu PP, Stadler J, Chandran J, Klinefelter GR, Blackstone C, Cookson MR (2003) L166P mutant DJ-1, causative for recessive Parkinson's disease, is degraded through the ubiquitin-proteasome system. J Biol Chem 278:36588-36595.

Miller RL, James-Kracke M, Sun GY, Sun AY (2009) Oxidative and inflammatory pathways in Parkinson's disease. Neurochem Res 34:55-65.

Miwa H, Kubo T, Suzuki A, Nishi K, Kondo T (2005) Retrograde dopaminergic neuron degeneration following intrastriatal proteasome inhibition. Neurosci Lett 380:93-98.

Mizuno Y, Hattori N, Mori H, Suzuki T, Tanaka K (2001a) Parkin and Parkinson's disease. Curr Opin Neurol 14:477-482.

Mizuno Y, Ohta S, Tanaka M, Takamiya S, Suzuki K, Sato T, Oya H, Ozawa T, Kagawa Y (1989) Deficiencies in complex I subunits of the respiratory chain in Parkinson's disease. Biochem Biophys Res Commun 163:1450-1455.

Mizuno Y, Hattori N, Kubo S, Sato S, Nishioka K, Hatano T, Tomiyama H, Funayama M, Machida Y, Mochizuki H (2008) Progress in the pathogenesis and genetics of Parkinson's disease. Philos Trans R Soc Lond B Biol Sci 363:2215-2227.

Mizuno Y, Hattori N, Kitada T, Matsumine H, Mori H, Shimura H, Kubo S, Kobayashi H, Asakawa S, Minoshima S, Shimizu N (2001b) Familial Parkinson's disease. Alpha-synuclein and parkin. Adv Neurol 86:13-21.

Mizuta I, Satake W, Nakabayashi Y, Ito C, Suzuki S, Momose Y, Nagai Y, Oka A, Inoko H, Fukae J, Saito Y, Sawabe M, Murayama S, Yamamoto M, Hattori N, Murata M, Toda T (2006) Multiple candidate gene analysis identifies alpha-synuclein as a susceptibility gene for sporadic Parkinson's disease. Hum Mol Genet 15:1151-1158.

Mochizuki H, Goto K, Mori H, Mizuno Y (1996) Histochemical detection of apoptosis in Parkinson's disease. J Neurol Sci 137:120-123.

Monti B, Polazzi E, Batti L, Crochemore C, Virgili M, Contestabile A (2007) Alpha-synuclein protects cerebellar granule neurons against 6-hydroxydopamine-induced death. J Neurochem 103:518-530.

Moore DJ (2006) Parkin: a multifaceted ubiquitin ligase. Biochem Soc Trans 34:749-753.

Moore DJ, Zhang L, Dawson TM, Dawson VL (2003) A missense mutation (L166P) in DJ-1, linked to familial Parkinson's disease, confers reduced protein stability and impairs homo-oligomerization. J Neurochem 87:1558-1567.

Moore DJ, West AB, Dawson VL, Dawson TM (2005) Molecular pathophysiology of Parkinson's disease. Annu Rev Neurosci 28:57-87.

Mori H, Kondo T, Yokochi M, Matsumine H, Nakagawa-Hattori Y, Miyake T, Suda K, Mizuno Y (1998) Pathologic and biochemical studies of juvenile parkinsonism linked to chromosome 6q. Neurology 51:890-892.

Mortiboys H, Thomas KJ, Koopman WJ, Klaffke S, Abou-Sleiman P, Olpin S, Wood NW, Willems PH, Smeitink JA, Cookson MR, Bandmann O (2008) Mitochondrial function and morphology are impaired in parkin-mutant fibroblasts. Ann Neurol 64:555-565.

Mouradian MM (2002) Recent advances in the genetics and pathogenesis of Parkinson disease. Neurology 58:179-185.

Mueller JC, Fuchs J, Hofer A, Zimprich A, Lichtner P, Illig T, Berg D, Wullner U, Meitinger T, Gasser T (2005) Multiple regions of alpha-synuclein are associated with Parkinson's disease. Ann Neurol 57:535-541.

Muftuoglu M, Elibol B, Dalmizrak O, Ercan A, Kulaksiz G, Ogus H, Dalkara T, Ozer N (2004) Mitochondrial complex I and IV activities in leukocytes from patients with parkin mutations. Mov Disord 19:544-548.

Mukhopadhyay D, Riezman H (2007) Proteasome-independent functions of ubiquitin in endocytosis and signaling. Science 315:201-205.

Murphy DD, Rueter SM, Trojanowski JQ, Lee VM (2000) Synucleins are developmentally expressed, and alpha-synuclein regulates the size of the presynaptic vesicular pool in primary hippocampal neurons. J Neurosci 20:3214-3220.

Murray IV, Giasson BI, Quinn SM, Koppaka V, Axelsen PH, Ischiropoulos H, Trojanowski JQ, Lee VM (2003) Role of alpha-synuclein carboxy-terminus on fibril formation in vitro. Biochemistry 42:8530-8540.

Naik MU, Benedikz E, Hernandez I, Libien J, Hrabe J, Valsamis M, Dow-Edwards D, Osman M, Sacktor TC (2000) Distribution of protein kinase Mzeta and the complete protein kinase C isoform family in rat brain. J Comp Neurol 426:243-258.

Nakamura K, Nemani VM, Wallender EK, Kaehlcke K, Ott M, Edwards RH (2008) Optical reporters for the conformation of alpha-synuclein reveal a specific interaction with mitochondria. J Neurosci 28:12305-12317.

Navarro A, Boveris A (2009) Brain mitochondrial dysfunction and oxidative damage in Parkinson's disease. J Bioenerg Biomembr 41:517-521.

Neumann M, Muller V, Gorner K, Kretzschmar HA, Haass C, Kahle PJ (2004) Pathological properties of the Parkinson's disease-associated protein DJ-1 in alpha-synucleinopathies and tauopathies: relevance for multiple system atrophy and Pick's disease. Acta Neuropathol 107:489-496.

Newton AC (1995a) Protein kinase C. Seeing two domains. Curr Biol 5:973-976.

Newton AC (1995b) Protein kinase C: structure, function, and regulation. J Biol Chem 270:28495-28498.

Newton AC (2003) Regulation of the ABC kinases by phosphorylation: protein kinase C as a paradigm. Biochem J 370:361-371.

Newton AC, Johnson JE (1998) Protein kinase C: a paradigm for regulation of protein function by two membrane-targeting modules. Biochim Biophys Acta 1376:155-172.

Nichols WC, Pankratz N, Hernandez D, Paisan-Ruiz C, Jain S, Halter CA, Michaels VE, Reed T, Rudolph A, Shults CW, Singleton A, Foroud T (2005) Genetic screening for a single common LRRK2 mutation in familial Parkinson's disease. Lancet 365:410-412.

Nicklas WJ, Vyas I, Heikkila RE (1985) Inhibition of NADH-linked oxidation in brain mitochondria by 1-methyl-4-phenyl-pyridine, a metabolite of the neurotoxin, 1-methyl-4-phenyl-1,2,5,6-tetrahydropyridine. Life Sci 36:2503-2508.

Nishioka K, Hayashi S, Farrer MJ, Singleton AB, Yoshino H, Imai H, Kitami T, Sato K, Kuroda R, Tomiyama H, Mizoguchi K, Murata M, Toda T, Imoto I, Inazawa J, Mizuno Y, Hattori N (2006) Clinical heterogeneity of alpha-synuclein gene duplication in Parkinson's disease. Ann Neurol 59:298-309.

Norris EH, Giasson BI, Hodara R, Xu S, Trojanowski JQ, Ischiropoulos H, Lee VM (2005) Reversible inhibition of alpha-synuclein fibrillization by dopaminochrome-mediated conformational alterations. J Biol Chem 280:21212-21219.

Nussbaum RL, Polymeropoulos MH (1997) Genetics of Parkinson's disease. Hum Mol Genet 6:1687-1691.

Obeso JA, Rodriguez-Oroz MC, Goetz CG, Marin C, Kordower JH, Rodriguez M, Hirsch EC, Farrer M, Schapira AH, Halliday G (2010) Missing pieces in the Parkinson's disease puzzle. Nat Med 16:653-661.

Okubadejo N, Britton A, Crews C, Akinyemi R, Hardy J, Singleton A, Bras J (2008) Analysis of Nigerians with apparently sporadic Parkinson disease for mutations in LRRK2, PRKN and ATXN3. PLoS One 3:e3421.

Olanow CW (2004a) Manganese-induced parkinsonism and Parkinson's disease. Ann N Y Acad Sci 1012:209-223.

Olanow CW (2004b) The scientific basis for the current treatment of Parkinson's disease. Annu Rev Med 55:41-60.

Olanow CW (2007) The pathogenesis of cell death in Parkinson's disease--2007. Mov Disord 22 Suppl 17:S335-342.

Olanow CW, Tatton WG (1999) Etiology and pathogenesis of Parkinson's disease. Annu Rev Neurosci 22:123-144.

Oliveira SA, Scott WK, Martin ER, Nance MA, Watts RL, Hubble JP, Koller WC, Pahwa R, Stern MB, Hiner BC, Ondo WG, Allen FH, Jr., Scott BL, Goetz CG, Small GW, Mastaglia F, Stajich JM, Zhang F, Booze MW, Winn MP, Middleton LT, Haines JL, Pericak-Vance MA, Vance JM (2003) Parkin mutations and susceptibility alleles in late-onset Parkinson's disease. Ann Neurol 53:624-629.

Olzmann JA, Brown K, Wilkinson KD, Rees HD, Huai Q, Ke H, Levey AI, Li L, Chin LS (2004) Familial Parkinson's disease-associated L166P mutation disrupts DJ-1 protein folding and function. J Biol Chem 279:8506-8515.

Ono Y, Fujii T, Ogita K, Kikkawa U, Igarashi K, Nishizuka Y (1988) The structure, expression, and properties of additional members of the protein kinase C family. J Biol Chem 263:6927-6932.

Oshikawa T, Kuroiwa H, Yano R, Yokoyama H, Kadoguchi N, Kato H, Araki T (2009) Systemic administration of proteasome inhibitor protects against MPTP neurotoxicity in mice. Cell Mol Neurobiol 29:769-777.

Ostrerova N, Petrucelli L, Farrer M, Mehta N, Choi P, Hardy J, Wolozin B (1999) alpha-Synuclein shares physical and functional homology with 14-3-3 proteins. J Neurosci 19:5782-5791.

Ozelius LJ, Senthil G, Saunders-Pullman R, Ohmann E, Deligtisch A, Tagliati M, Hunt AL, Klein C, Henick B, Hailpern SM, Lipton RB, Soto-Valencia J, Risch N, Bressman SB (2006) LRRK2 G2019S as a cause of Parkinson's disease in Ashkenazi Jews. N Engl J Med 354:424-425.

Paisan-Ruiz C, Jain S, Evans EW, Gilks WP, Simon J, van der Brug M, Lopez de Munain A, Aparicio S, Gil AM, Khan N, Johnson J, Martinez JR, Nicholl D, Carrera IM, Pena AS, de Silva R, Lees A, Marti-Masso JF, Perez-Tur J, Wood NW, Singleton AB (2004) Cloning of the gene containing mutations that cause PARK8-linked Parkinson's disease. Neuron 44:595-600.

Pal PK, Samii A, Calne DB (1999) Manganese neurotoxicity: a review of clinical features, imaging and pathology. Neurotoxicology 20:227-238.

Palacino JJ, Sagi D, Goldberg MS, Krauss S, Motz C, Wacker M, Klose J, Shen J (2004) Mitochondrial dysfunction and oxidative damage in parkin-deficient mice. J Biol Chem 279:18614-18622.

Pankratz N, Nichols WC, Elsaesser VE, Pauciulo MW, Marek DK, Halter CA, Wojcieszek J, Rudolph A, Pfeiffer RF, Foroud T (2009) Alpha-synuclein and familial Parkinson's disease. Mov Disord 24:1125-1131.

Parihar MS, Parihar A, Fujita M, Hashimoto M, Ghafourifar P (2009) Alpha-synuclein overexpression and aggregation exacerbates impairment of mitochondrial functions by augmenting oxidative stress in human neuroblastoma cells. Int J Biochem Cell Biol 41:2015-2024.

Park J, Lee SB, Lee S, Kim Y, Song S, Kim S, Bae E, Kim J, Shong M, Kim JM, Chung J (2006) Mitochondrial dysfunction in Drosophila PINK1 mutants is complemented by parkin. Nature 441:1157-1161.

Parker WD, Jr., Boyson SJ, Parks JK (1989) Abnormalities of the electron transport chain in idiopathic Parkinson's disease. Ann Neurol 26:719-723.

Parker WD, Jr., Parks JK, Swerdlow RH (2008) Complex I deficiency in Parkinson's disease frontal cortex. Brain Res 1189:215-218.

Paterna JC, Leng A, Weber E, Feldon J, Bueler H (2007) DJ-1 and Parkin modulate dopamine-dependent behavior and inhibit MPTP-induced nigral dopamine neuron loss in mice. Mol Ther 15:698-704.

Pearn J, Gardner-Thorpe C (2001) James Parkinson (1755-1824): a pioneer of child care. J Paediatr Child Health 37:9-13.

Peng J, Andersen JK (2003) The role of c-Jun N-terminal kinase (JNK) in Parkinson's disease. IUBMB Life 55:267-271.

Penn AM, Roberts T, Hodder J, Allen PS, Zhu G, Martin WR (1995) Generalized mitochondrial dysfunction in Parkinson's disease detected by magnetic resonance spectroscopy of muscle. Neurology 45:2097-2099.

Perier C, Tieu K, Guegan C, Caspersen C, Jackson-Lewis V, Carelli V, Martinuzzi A, Hirano M, Przedborski S, Vila M (2005) Complex I deficiency primes Bax-dependent

neuronal apoptosis through mitochondrial oxidative damage. Proc Natl Acad Sci U S A 102:19126-19131.

Perier C, Bove J, Wu DC, Dehay B, Choi DK, Jackson-Lewis V, Rathke-Hartlieb S, Bouillet P, Strasser A, Schulz JB, Przedborski S, Vila M (2007) Two molecular pathways initiate mitochondria-dependent dopaminergic neurodegeneration in experimental Parkinson's disease. Proc Natl Acad Sci U S A 104:8161-8166.

Periquet M, Fulga T, Myllykangas L, Schlossmacher MG, Feany MB (2007) Aggregated alpha-synuclein mediates dopaminergic neurotoxicity in vivo. J Neurosci 27:3338-3346.

Perrin RJ, Woods WS, Clayton DF, George JM (2000) Interaction of human alpha-Synuclein and Parkinson's disease variants with phospholipids. Structural analysis using site-directed mutagenesis. J Biol Chem 275:34393-34398.

Peter D, Jimenez J, Liu Y, Kim J, Edwards RH (1994) The chromaffin granule and synaptic vesicle amine transporters differ in substrate recognition and sensitivity to inhibitors. J Biol Chem 269:7231-7237.

Peters CA, Cutler RE, Maizels ET, Robertson MC, Shiu RP, Fields P, Hunzicker-Dunn M (2000) Regulation of PKC delta expression by estrogen and rat placental lactogen-1 in luteinized rat ovarian granulosa cells. Mol Cell Endocrinol 162:181-191.

Petit A, Kawarai T, Paitel E, Sanjo N, Maj M, Scheid M, Chen F, Gu Y, Hasegawa H, Salehi-Rad S, Wang L, Rogaeva E, Fraser P, Robinson B, St George-Hyslop P, Tandon A (2005) Wild-type PINK1 prevents basal and induced neuronal apoptosis, a protective effect abrogated by Parkinson disease-related mutations. J Biol Chem 280:34025-34032.

Phillips JB, Williams AJ, Adams J, Elliott PJ, Tortella FC (2000) Proteasome inhibitor PS519 reduces infarction and attenuates leukocyte infiltration in a rat model of focal cerebral ischemia. Stroke 31:1686-1693.

Pickart CM, Cohen RE (2004) Proteasomes and their kin: proteases in the machine age. Nat Rev Mol Cell Biol 5:177-187.

Plun-Favreau H, Klupsch K, Moisoi N, Gandhi S, Kjaer S, Frith D, Harvey K, Deas E, Harvey RJ, McDonald N, Wood NW, Martins LM, Downward J (2007) The mitochondrial protease HtrA2 is regulated by Parkinson's disease-associated kinase PINK1. Nat Cell Biol 9:1243-1252.

Pollanen MS, Dickson DW, Bergeron C (1993) Pathology and biology of the Lewy body. J Neuropathol Exp Neurol 52:183-191.

Polymeropoulos MH, Higgins JJ, Golbe LI, Johnson WG, Ide SE, Di Iorio G, Sanges G, Stenroos ES, Pho LT, Schaffer AA, Lazzarini AM, Nussbaum RL, Duvoisin RC (1996) Mapping of a gene for Parkinson's disease to chromosome 4q21-q23. Science 274:1197-1199.

Polymeropoulos MH, Lavedan C, Leroy E, Ide SE, Dehejia A, Dutra A, Pike B, Root H, Rubenstein J, Boyer R, Stenroos ES, Chandrasekharappa S, Athanassiadou A, Papapetropoulos T, Johnson WG, Lazzarini AM, Duvoisin RC, Di Iorio G, Golbe LI, Nussbaum RL (1997) Mutation in the alpha-synuclein gene identified in families with Parkinson's disease. Science 276:2045-2047.

Ponassi R, Terrinoni A, Chikh A, Rufini A, Lena AM, Sayan BS, Melino G, Candi E (2006) p63 and p73, members of the p53 gene family, transactivate PKCdelta. Biochem Pharmacol 72:1417-1422.

Poole AC, Thomas RE, Andrews LA, McBride HM, Whitworth AJ, Pallanck LJ (2008) The PINK1/Parkin pathway regulates mitochondrial morphology. Proc Natl Acad Sci U S A 105:1638-1643.

Poon HF, Frasier M, Shreve N, Calabrese V, Wolozin B, Butterfield DA (2005) Mitochondrial associated metabolic proteins are selectively oxidized in A30P alpha-synuclein transgenic mice--a model of familial Parkinson's disease. Neurobiol Dis 18:492-498.

Popat RA, Van Den Eeden SK, Tanner CM, McGuire V, Bernstein AL, Bloch DA, Leimpeter A, Nelson LM (2005) Effect of reproductive factors and postmenopausal hormone use on the risk of Parkinson disease. Neurology 65:383-390.

Power JH, Blumbergs PC (2009) Cellular glutathione peroxidase in human brain: cellular distribution, and its potential role in the degradation of Lewy bodies in Parkinson's disease and dementia with Lewy bodies. Acta Neuropathol 117:63-73.

Przedborski S, Vila M (2003) The 1-methyl-4-phenyl-1,2,3,6-tetrahydropyridine mouse model: a tool to explore the pathogenesis of Parkinson's disease. Ann N Y Acad Sci 991:189-198.

Przedborski S, Jackson-Lewis V, Naini AB, Jakowec M, Petzinger G, Miller R, Akram M (2001) The parkinsonian toxin 1-methyl-4-phenyl-1,2,3,6-tetrahydropyridine (MPTP): a technical review of its utility and safety. J Neurochem 76:1265-1274.

Quilty MC, King AE, Gai WP, Pountney DL, West AK, Vickers JC, Dickson TC (2006) Alpha-synuclein is upregulated in neurones in response to chronic oxidative stress and is associated with neuroprotection. Exp Neurol 199:249-256.

Quinn N (1995) Parkinsonism--recognition and differential diagnosis. Bmj 310:447-452.

Rajput AH (2001) Environmental toxins accelerate Parkinson's disease onset. Neurology 56:4-5.

Ramirez A, Heimbach A, Grundemann J, Stiller B, Hampshire D, Cid LP, Goebel I, Mubaidin AF, Wriekat AL, Roeper J, Al-Din A, Hillmer AM, Karsak M, Liss B, Woods CG, Behrens MI, Kubisch C (2006) Hereditary parkinsonism with dementia is caused by mutations in ATP13A2, encoding a lysosomal type 5 P-type ATPase. Nat Genet 38:1184-1191.

Ramsay RR, Salach JI, Dadgar J, Singer TP (1986) Inhibition of mitochondrial NADH dehydrogenase by pyridine derivatives and its possible relation to experimental and idiopathic parkinsonism. Biochem Biophys Res Commun 135:269-275.

Recchia A, Debetto P, Negro A, Guidolin D, Skaper SD, Giusti P (2004) Alpha-synuclein and Parkinson's disease. Faseb J 18:617-626.

Ren J, Datta R, Shioya H, Li Y, Oki E, Biedermann V, Bharti A, Kufe D (2002) p73beta is regulated by protein kinase Cdelta catalytic fragment generated in the apoptotic response to DNA damage. J Biol Chem 277:33758-33765.

Ren Y, Zhao J, Feng J (2003) Parkin binds to alpha/beta tubulin and increases their ubiquitination and degradation. J Neurosci 23:3316-3324.

Reyland ME, Anderson SM, Matassa AA, Barzen KA, Quissell DO (1999) Protein kinase C delta is essential for etoposide-induced apoptosis in salivary gland acinar cells. J Biol Chem 274:19115-19123.

Riederer P, Sofic E, Rausch WD, Schmidt B, Reynolds GP, Jellinger K, Youdim MB (1989) Transition metals, ferritin, glutathione, and ascorbic acid in parkinsonian brains. J Neurochem 52:515-520.

Riparbelli MG, Callaini G (2007) The Drosophila parkin homologue is required for normal mitochondrial dynamics during spermiogenesis. Dev Biol 303:108-120.

Rosenstock HA, Simons DG, Meyer JS (1971) Chronic manganism. Neurologic and laboratory studies during treatment with levodopa. Jama 217:1354-1358.

Ross CA, Poirier MA (2004) Protein aggregation and neurodegenerative disease. Nat Med 10 Suppl:S10-17.

Ross OA, Wu YR, Lee MC, Funayama M, Chen ML, Soto AI, Mata IF, Lee-Chen GJ, Chen CM, Tang M, Zhao Y, Hattori N, Farrer MJ, Tan EK, Wu RM (2008) Analysis of Lrrk2 R1628P as a risk factor for Parkinson's disease. Ann Neurol 64:88-92.

Roth JA (2006) Homeostatic and toxic mechanisms regulating manganese uptake, retention, and elimination. Biol Res 39:45-57.

Rybicki BA, Johnson CC, Uman J, Gorell JM (1993) Parkinson's disease mortality and the industrial use of heavy metals in Michigan. Mov Disord 8:87-92.

Ryer EJ, Sakakibara K, Wang C, Sarkar D, Fisher PB, Faries PL, Kent KC, Liu B (2005) Protein kinase C delta induces apoptosis of vascular smooth muscle cells through induction of the tumor suppressor p53 by both p38-dependent and p38-independent mechanisms. J Biol Chem 280:35310-35317.

Santamaria AB (2008) Manganese exposure, essentiality & toxicity. Indian J Med Res 128:484-500.

Santpere G, Ferrer I (2009) LRRK2 and neurodegeneration. Acta Neuropathol 117:227-246.

Saporito MS, Brown EM, Miller MS, Carswell S (1999) CEP-1347/KT-7515, an inhibitor of c-jun N-terminal kinase activation, attenuates the 1-methyl-4-phenyl

tetrahydropyridine-mediated loss of nigrostriatal dopaminergic neurons In vivo. J Pharmacol Exp Ther 288:421-427.

Schapira AH, Cooper JM, Dexter D, Jenner P, Clark JB, Marsden CD (1989) Mitochondrial complex I deficiency in Parkinson's disease. Lancet 1:1269.

Schiesling C, Kieper N, Seidel K, Kruger R (2008) Review: Familial Parkinson's disease--genetics, clinical phenotype and neuropathology in relation to the common sporadic form of the disease. Neuropathol Appl Neurobiol 34:255-271.

Schober A (2004) Classic toxin-induced animal models of Parkinson's disease: 6-OHDA and MPTP. Cell Tissue Res 318:215-224.

Schulz-Schaeffer WJ (2010) The synaptic pathology of alpha-synuclein aggregation in dementia with Lewy bodies, Parkinson's disease and Parkinson's disease dementia. Acta Neuropathol 120:131-143.

Seo JH, Rah JC, Choi SH, Shin JK, Min K, Kim HS, Park CH, Kim S, Kim EM, Lee SH, Lee S, Suh SW, Suh YH (2002) Alpha-synuclein regulates neuronal survival via Bcl-2 family expression and PI3/Akt kinase pathway. Faseb J 16:1826-1828.

Serpell LC, Berriman J, Jakes R, Goedert M, Crowther RA (2000) Fiber diffraction of synthetic alpha-synuclein filaments shows amyloid-like cross-beta conformation. Proc Natl Acad Sci U S A 97:4897-4902.

Shanmugam M, Krett NL, Maizels ET, Cutler RE, Jr., Peters CA, Smith LM, O'Brien ML, Park-Sarge OK, Rosen ST, Hunzicker-Dunn M (1999) Regulation of protein kinase C delta by estrogen in the MCF-7 human breast cancer cell line. Mol Cell Endocrinol 148:109-118.

Sharon R, Bar-Joseph I, Frosch MP, Walsh DM, Hamilton JA, Selkoe DJ (2003) The formation of highly soluble oligomers of alpha-synuclein is regulated by fatty acids and enhanced in Parkinson's disease. Neuron 37:583-595.

Shashidharan P, Good PF, Hsu A, Perl DP, Brin MF, Olanow CW (2000) TorsinA accumulation in Lewy bodies in sporadic Parkinson's disease. Brain Res 877:379-381.

Shavali S, Brown-Borg HM, Ebadi M, Porter J (2008) Mitochondrial localization of alpha-synuclein protein in alpha-synuclein overexpressing cells. Neurosci Lett 439:125-128.

Shimura H, Schlossmacher MG, Hattori N, Frosch MP, Trockenbacher A, Schneider R, Mizuno Y, Kosik KS, Selkoe DJ (2001) Ubiquitination of a new form of alpha-synuclein by parkin from human brain: implications for Parkinson's disease. Science 293:263-269.

Shimura H, Hattori N, Kubo S, Yoshikawa M, Kitada T, Matsumine H, Asakawa S, Minoshima S, Yamamura Y, Shimizu N, Mizuno Y (1999) Immunohistochemical and subcellular localization of Parkin protein: absence of protein in autosomal recessive juvenile parkinsonism patients. Ann Neurol 45:668-672.

Shimura H, Hattori N, Kubo S, Mizuno Y, Asakawa S, Minoshima S, Shimizu N, Iwai K, Chiba T, Tanaka K, Suzuki T (2000) Familial Parkinson disease gene product, parkin, is a ubiquitin-protein ligase. Nat Genet 25:302-305.

Shin SY, Kim CG, Ko J, Min DS, Chang JS, Ohba M, Kuroki T, Choi YB, Kim YH, Na DS, Kim JW, Lee YH (2004) Transcriptional and post-transcriptional regulation of the

PKC delta gene by etoposide in L1210 murine leukemia cells: implication of PKC delta autoregulation. J Mol Biol 340:681-693.

Sian J, Dexter DT, Lees AJ, Daniel S, Agid Y, Javoy-Agid F, Jenner P, Marsden CD (1994) Alterations in glutathione levels in Parkinson's disease and other neurodegenerative disorders affecting basal ganglia. Ann Neurol 36:348-355.

Sidhu A, Wersinger C, Moussa CE, Vernier P (2004) The role of alpha-synuclein in both neuroprotection and neurodegeneration. Ann N Y Acad Sci 1035:250-270.

Silvestri L, Caputo V, Bellacchio E, Atorino L, Dallapiccola B, Valente EM, Casari G (2005) Mitochondrial import and enzymatic activity of PINK1 mutants associated to recessive parkinsonism. Hum Mol Genet 14:3477-3492.

Singleton AB, Farrer M, Johnson J, Singleton A, Hague S, Kachergus J, Hulihan M, Peuralinna T, Dutra A, Nussbaum R, Lincoln S, Crawley A, Hanson M, Maraganore D, Adler C, Cookson MR, Muenter M, Baptista M, Miller D, Blancato J, Hardy J, Gwinn-Hardy K (2003) alpha-Synuclein locus triplication causes Parkinson's disease. Science 302:841.

Smythies J, Galzigna L (1998) The oxidative metabolism of catecholamines in the brain: a review. Biochim Biophys Acta 1380:159-162.

Soderling TR (1990) Protein kinases. Regulation by autoinhibitory domains. J Biol Chem 265:1823-1826.

Sofic E, Riederer P, Heinsen H, Beckmann H, Reynolds GP, Hebenstreit G, Youdim MB (1988) Increased iron (III) and total iron content in post mortem substantia nigra of parkinsonian brain. J Neural Transm 74:199-205.

Song DD, Shults CW, Sisk A, Rockenstein E, Masliah E (2004) Enhanced substantia nigra mitochondrial pathology in human alpha-synuclein transgenic mice after treatment with MPTP. Exp Neurol 186:158-172.

Spillantini MG, Crowther RA, Jakes R, Hasegawa M, Goedert M (1998) alpha-Synuclein in filamentous inclusions of Lewy bodies from Parkinson's disease and dementia with lewy bodies. Proc Natl Acad Sci U S A 95:6469-6473.

Spillantini MG, Schmidt ML, Lee VM, Trojanowski JQ, Jakes R, Goedert M (1997) Alpha-synuclein in Lewy bodies. Nature 388:839-840.

Spira PJ, Sharpe DM, Halliday G, Cavanagh J, Nicholson GA (2001) Clinical and pathological features of a Parkinsonian syndrome in a family with an Ala53Thr alpha-synuclein mutation. Ann Neurol 49:313-319.

Staropoli JF, McDermott C, Martinat C, Schulman B, Demireva E, Abeliovich A (2003) Parkin is a component of an SCF-like ubiquitin ligase complex and protects postmitotic neurons from kainate excitotoxicity. Neuron 37:735-749.

Steinberg SF (2008) Structural basis of protein kinase C isoform function. Physiol Rev 88:1341-1378.

Steinlechner S, Stahlberg J, Volkel B, Djarmati A, Hagenah J, Hiller A, Hedrich K, Konig I, Klein C, Lencer R (2007) Co-occurrence of affective and schizophrenia spectrum disorders with PINK1 mutations. J Neurol Neurosurg Psychiatry 78:532-535.

Stichel CC, Zhu XR, Bader V, Linnartz B, Schmidt S, Lubbert H (2007) Mono- and double-mutant mouse models of Parkinson's disease display severe mitochondrial damage. Hum Mol Genet 16:2377-2393.

Stokes AH, Hastings TG, Vrana KE (1999) Cytotoxic and genotoxic potential of dopamine. J Neurosci Res 55:659-665.

Suh KS, Tatunchak TT, Crutchley JM, Edwards LE, Marin KG, Yuspa SH (2003) Genomic structure and promoter analysis of PKC-delta. Genomics 82:57-67.

Sulzer D (2007) Multiple hit hypotheses for dopamine neuron loss in Parkinson's disease. Trends Neurosci 30:244-250.

Sun F, Kanthasamy A, Song C, Yang Y, Anantharam V, Kanthasamy AG (2008) Proteasome inhibitor-induced apoptosis is mediated by positive feedback amplification of PKCdelta proteolytic activation and mitochondrial translocation. J Cell Mol Med 12:2467-2481.

Suntres ZE (2002) Role of antioxidants in paraquat toxicity. Toxicology 180:65-77.

Tabrizi SJ, Orth M, Wilkinson JM, Taanman JW, Warner TT, Cooper JM, Schapira AH (2000) Expression of mutant alpha-synuclein causes increased susceptibility to dopamine toxicity. Hum Mol Genet 9:2683-2689.

Taira T, Saito Y, Niki T, Iguchi-Ariga SM, Takahashi K, Ariga H (2004) DJ-1 has a role in antioxidative stress to prevent cell death. EMBO Rep 5:213-218.

Takeda A, Mallory M, Sundsmo M, Honer W, Hansen L, Masliah E (1998) Abnormal accumulation of NACP/alpha-synuclein in neurodegenerative disorders. Am J Pathol 152:367-372.

Tan EK, Skipper LM (2007) Pathogenic mutations in Parkinson disease. Hum Mutat 28:641-653.

Tan EK, Shen H, Tan LC, Farrer M, Yew K, Chua E, Jamora RD, Puvan K, Puong KY, Zhao Y, Pavanni R, Wong MC, Yih Y, Skipper L, Liu JJ (2005) The G2019S LRRK2

mutation is uncommon in an Asian cohort of Parkinson's disease patients. Neurosci Lett 384:327-329.

Tanaka M, Kim YM, Lee G, Junn E, Iwatsubo T, Mouradian MM (2004) Aggresomes formed by alpha-synuclein and synphilin-1 are cytoprotective. J Biol Chem 279:4625-4631.

Tanner CM (1992a) Epidemiology of Parkinson's disease. Neurol Clin 10:317-329.

Tanner CM (1992b) Occupational and environmental causes of parkinsonism. Occup Med 7:503-513.

Tanner CM, Ottman R, Goldman SM, Ellenberg J, Chan P, Mayeux R, Langston JW (1999) Parkinson disease in twins: an etiologic study. Jama 281:341-346.

Tansey MG, McCoy MK, Frank-Cannon TC (2007) Neuroinflammatory mechanisms in Parkinson's disease: potential environmental triggers, pathways, and targets for early therapeutic intervention. Exp Neurol 208:1-25.

Taylor KS, Cook JA, Counsell CE (2007) Heterogeneity in male to female risk for Parkinson's disease. J Neurol Neurosurg Psychiatry 78:905-906.

Taymans JM, Cookson MR (2010) Mechanisms in dominant parkinsonism: The toxic triangle of LRRK2, alpha-synuclein, and tau. Bioessays 32:227-235.

Toker A (1998) Signaling through protein kinase C. Front Biosci 3:D1134-1147.

Tomiyama H, Li Y, Funayama M, Hasegawa K, Yoshino H, Kubo S, Sato K, Hattori T, Lu CS, Inzelberg R, Djaldetti R, Melamed E, Amouri R, Gouider-Khouja N, Hentati F, Hatano Y, Wang M, Imamichi Y, Mizoguchi K, Miyajima H, Obata F, Toda T, Farrer MJ, Mizuno Y, Hattori N (2006) Clinicogenetic study of mutations in LRRK2 exon 41 in Parkinson's disease patients from 18 countries. Mov Disord 21:1102-1108.

Tsang AH, Chung KK (2009) Oxidative and nitrosative stress in Parkinson's disease. Biochim Biophys Acta 1792:643-650.

Twelves D, Perkins KS, Counsell C (2003) Systematic review of incidence studies of Parkinson's disease. Mov Disord 18:19-31.

Uversky VN (2004) Neurotoxicant-induced animal models of Parkinson's disease: understanding the role of rotenone, maneb and paraquat in neurodegeneration. Cell Tissue Res 318:225-241.

Uversky VN, Yamin G, Munishkina LA, Karymov MA, Millett IS, Doniach S, Lyubchenko YL, Fink AL (2005) Effects of nitration on the structure and aggregation of alpha-synuclein. Brain Res Mol Brain Res 134:84-102.

Valente EM, Bentivoglio AR, Dixon PH, Ferraris A, Ialongo T, Frontali M, Albanese A, Wood NW (2001) Localization of a novel locus for autosomal recessive early-onset parkinsonism, PARK6, on human chromosome 1p35-p36. Am J Hum Genet 68:895-900.

Valente EM, Salvi S, Ialongo T, Marongiu R, Elia AE, Caputo V, Romito L, Albanese A, Dallapiccola B, Bentivoglio AR (2004a) PINK1 mutations are associated with sporadic early-onset parkinsonism. Ann Neurol 56:336-341.

Valente EM, Abou-Sleiman PM, Caputo V, Muqit MM, Harvey K, Gispert S, Ali Z, Del Turco D, Bentivoglio AR, Healy DG, Albanese A, Nussbaum R, Gonzalez-Maldonado R, Deller T, Salvi S, Cortelli P, Gilks WP, Latchman DS, Harvey RJ, Dallapiccola B, Auburger G, Wood NW (2004b) Hereditary early-onset Parkinson's disease caused by mutations in PINK1. Science 304:1158-1160.

Van Den Eeden SK, Tanner CM, Bernstein AL, Fross RD, Leimpeter A, Bloch DA, Nelson LM (2003) Incidence of Parkinson's disease: variation by age, gender, and race/ethnicity. Am J Epidemiol 157:1015-1022.

van der Walt JM, Nicodemus KK, Martin ER, Scott WK, Nance MA, Watts RL, Hubble JP, Haines JL, Koller WC, Lyons K, Pahwa R, Stern MB, Colcher A, Hiner BC, Jankovic J, Ondo WG, Allen FH, Jr., Goetz CG, Small GW, Mastaglia F, Stajich JM, McLaurin AC, Middleton LT, Scott BL, Schmechel DE, Pericak-Vance MA, Vance JM (2003) Mitochondrial polymorphisms significantly reduce the risk of Parkinson disease. Am J Hum Genet 72:804-811.

van Duijn CM, Dekker MC, Bonifati V, Galjaard RJ, Houwing-Duistermaat JJ, Snijders PJ, Testers L, Breedveld GJ, Horstink M, Sandkuijl LA, van Swieten JC, Oostra BA, Heutink P (2001) Park7, a novel locus for autosomal recessive early-onset parkinsonism, on chromosome 1p36. Am J Hum Genet 69:629-634.

van Leyen K, Siddiq A, Ratan RR, Lo EH (2005) Proteasome inhibition protects HT22 neuronal cells from oxidative glutamate toxicity. J Neurochem 92:824-830.

Varastet M, Riche D, Maziere M, Hantraye P (1994) Chronic MPTP treatment reproduces in baboons the differential vulnerability of mesencephalic dopaminergic neurons observed in Parkinson's disease. Neuroscience 63:47-56.

Vekrellis K, Rideout HJ, Stefanis L (2004) Neurobiology of alpha-synuclein. Mol Neurobiol 30:1-21.

Vercammen L, Van der Perren A, Vaudano E, Gijsbers R, Debyser Z, Van den Haute C, Baekelandt V (2006) Parkin protects against neurotoxicity in the 6-hydroxydopamine rat model for Parkinson's disease. Mol Ther 14:716-723.

Vila M, Przedborski S (2003) Targeting programmed cell death in neurodegenerative diseases. Nat Rev Neurosci 4:365-375.

Vila M, Jackson-Lewis V, Vukosavic S, Djaldetti R, Liberatore G, Offen D, Korsmeyer SJ, Przedborski S (2001) Bax ablation prevents dopaminergic neurodegeneration in the 1-methyl- 4-phenyl-1,2,3,6-tetrahydropyridine mouse model of Parkinson's disease. Proc Natl Acad Sci U S A 98:2837-2842.

Viswanath V, Wu Y, Boonplueang R, Chen S, Stevenson FF, Yantiri F, Yang L, Beal MF, Andersen JK (2001) Caspase-9 activation results in downstream caspase-8 activation and bid cleavage in 1-methyl-4-phenyl-1,2,3,6-tetrahydropyridine-induced Parkinson's disease. J Neurosci 21:9519-9528.

von Coelln R, Dawson VL, Dawson TM (2004) Parkin-associated Parkinson's disease. Cell Tissue Res 318:175-184.

Wakabayashi K, Engelender S, Yoshimoto M, Tsuji S, Ross CA, Takahashi H (2000) Synphilin-1 is present in Lewy bodies in Parkinson's disease. Ann Neurol 47:521-523.

Wakabayashi K, Hayashi S, Kakita A, Yamada M, Toyoshima Y, Yoshimoto M, Takahashi H (1998) Accumulation of alpha-synuclein/NACP is a cytopathological feature common to Lewy body disease and multiple system atrophy. Acta Neuropathol 96:445-452.

Walsh MP (2007) The global experience with lead in gasoline and the lessons we should apply to the use of MMT. Am J Ind Med 50:853-860.

Wang C, Lu R, Ouyang X, Ho MW, Chia W, Yu F, Lim KL (2007) Drosophila overexpressing parkin R275W mutant exhibits dopaminergic neuron degeneration and mitochondrial abnormalities. J Neurosci 27:8563-8570.

Wang C, Ko HS, Thomas B, Tsang F, Chew KC, Tay SP, Ho MW, Lim TM, Soong TW, Pletnikova O, Troncoso J, Dawson VL, Dawson TM, Lim KL (2005) Stress-induced alterations in parkin solubility promote parkin aggregation and compromise parkin's protective function. Hum Mol Genet 14:3885-3897.

Waragai M, Wei J, Fujita M, Nakai M, Ho GJ, Masliah E, Akatsu H, Yamada T, Hashimoto M (2006) Increased level of DJ-1 in the cerebrospinal fluids of sporadic Parkinson's disease. Biochem Biophys Res Commun 345:967-972.

Wasserman GA, Liu X, Parvez F, Ahsan H, Levy D, Factor-Litvak P, Kline J, van Geen A, Slavkovich V, LoIacono NJ, Cheng Z, Zheng Y, Graziano JH (2006) Water manganese exposure and children's intellectual function in Araihazar, Bangladesh. Environ Health Perspect 114:124-129.

Werner CJ, Heyny-von Haussen R, Mall G, Wolf S (2008) Proteome analysis of human substantia nigra in Parkinson's disease. Proteome Sci 6:8.

Whitehouse PJ, Hedreen JC, White CL, 3rd, Price DL (1983) Basal forebrain neurons in the dementia of Parkinson disease. Ann Neurol 13:243-248.

Wilkinson KD (1997) Regulation of ubiquitin-dependent processes by deubiquitinating enzymes. Faseb J 11:1245-1256.

Wilkinson KD, Lee KM, Deshpande S, Duerksen-Hughes P, Boss JM, Pohl J (1989) The neuron-specific protein PGP 9.5 is a ubiquitin carboxyl-terminal hydrolase. Science 246:670-673.

Winkler S, Hagenah J, Lincoln S, Heckman M, Haugarvoll K, Lohmann-Hedrich K, Kostic V, Farrer M, Klein C (2007) alpha-Synuclein and Parkinson disease susceptibility. Neurology 69:1745-1750.

Winklhofer KF (2007) The parkin protein as a therapeutic target in Parkinson's disease. Expert Opin Ther Targets 11:1543-1552.

Winterbourn CC (2008) Reconciling the chemistry and biology of reactive oxygen species. Nat Chem Biol 4:278-286.

Wood-Kaczmar A, Gandhi S, Yao Z, Abramov AY, Miljan EA, Keen G, Stanyer L, Hargreaves I, Klupsch K, Deas E, Downward J, Mansfield L, Jat P, Taylor J, Heales S, Duchen MR, Latchman D, Tabrizi SJ, Wood NW (2008) PINK1 is necessary for long term survival and mitochondrial function in human dopaminergic neurons. PLoS One 3:e2455.

Wooten GF, Currie LJ, Bovbjerg VE, Lee JK, Patrie J (2004) Are men at greater risk for Parkinson's disease than women? J Neurol Neurosurg Psychiatry 75:637-639.

Xiromerisiou G, Hadjigeorgiou GM, Gourbali V, Johnson J, Papakonstantinou I, Papadimitriou A, Singleton AB (2007) Screening for SNCA and LRRK2 mutations in Greek sporadic and autosomal dominant Parkinson's disease: identification of two novel LRRK2 variants. Eur J Neurol 14:7-11.

Xu J, Zhong N, Wang H, Elias JE, Kim CY, Woldman I, Pifl C, Gygi SP, Geula C, Yankner BA (2005) The Parkinson's disease-associated DJ-1 protein is a transcriptional co-activator that protects against neuronal apoptosis. Hum Mol Genet 14:1231-1241.

Yamada M, Ohno S, Okayasu I, Okeda R, Hatakeyama S, Watanabe H, Ushio K, Tsukagoshi H (1986) Chronic manganese poisoning: a neuropathological study with determination of manganese distribution in the brain. Acta Neuropathol 70:273-278.

Yamamoto N, Sawada H, Izumi Y, Kume T, Katsuki H, Shimohama S, Akaike A (2007) Proteasome inhibition induces glutathione synthesis and protects cells from oxidative stress: relevance to Parkinson disease. J Biol Chem 282:4364-4372.

Yamin G, Uversky VN, Fink AL (2003) Nitration inhibits fibrillation of human alpha-synuclein in vitro by formation of soluble oligomers. FEBS Lett 542:147-152.

Yang Y, Nishimura I, Imai Y, Takahashi R, Lu B (2003) Parkin suppresses dopaminergic neuron-selective neurotoxicity induced by Pael-R in Drosophila. Neuron 37:911-924.

Yang Y, Kaul S, Zhang D, Anantharam V, Kanthasamy AG (2004) Suppression of caspase-3-dependent proteolytic activation of protein kinase C delta by small interfering RNA prevents MPP+-induced dopaminergic degeneration. Mol Cell Neurosci 25:406-421.

Yang Y, Gehrke S, Imai Y, Huang Z, Ouyang Y, Wang JW, Yang L, Beal MF, Vogel H, Lu B (2006) Mitochondrial pathology and muscle and dopaminergic neuron degeneration caused by inactivation of Drosophila Pink1 is rescued by Parkin. Proc Natl Acad Sci U S A 103:10793-10798.

Yao D, Gu Z, Nakamura T, Shi ZQ, Ma Y, Gaston B, Palmer LA, Rockenstein EM, Zhang Z, Masliah E, Uehara T, Lipton SA (2004) Nitrosative stress linked to sporadic Parkinson's disease: S-nitrosylation of parkin regulates its E3 ubiquitin ligase activity. Proc Natl Acad Sci U S A 101:10810-10814.

Yoritaka A, Hattori N, Uchida K, Tanaka M, Stadtman ER, Mizuno Y (1996) Immunohistochemical detection of 4-hydroxynonenal protein adducts in Parkinson disease. Proc Natl Acad Sci U S A 93:2696-2701.

Yoshino H, Nakagawa-Hattori Y, Kondo T, Mizuno Y (1992) Mitochondrial complex I and II activities of lymphocytes and platelets in Parkinson's disease. J Neural Transm Park Dis Dement Sect 4:27-34.

Yu Z, Xu X, Xiang Z, Zhou J, Zhang Z, Hu C, He C (2010) Nitrated alpha-synuclein induces the loss of dopaminergic neurons in the substantia nigra of rats. PLoS One 5:e9956.

Zarranz JJ, Alegre J, Gomez-Esteban JC, Lezcano E, Ros R, Ampuero I, Vidal L, Hoenicka J, Rodriguez O, Atares B, Llorens V, Gomez Tortosa E, del Ser T, Munoz DG, de Yebenes JG (2004) The new mutation, E46K, of alpha-synuclein causes Parkinson and Lewy body dementia. Ann Neurol 55:164-173.

Zhang D, Anantharam V, Kanthasamy A, Kanthasamy AG (2007a) Neuroprotective effect of protein kinase C delta inhibitor rottlerin in cell culture and animal models of Parkinson's disease. J Pharmacol Exp Ther 322:913-922.

Zhang D, Kanthasamy A, Yang Y, Anantharam V, Kanthasamy A (2007b) Protein kinase C delta negatively regulates tyrosine hydroxylase activity and dopamine synthesis by enhancing protein phosphatase-2A activity in dopaminergic neurons. J Neurosci 27:5349-5362.

Zhang L, Zhang C, Zhu Y, Cai Q, Chan P, Ueda K, Yu S, Yang H (2008) Semi-quantitative analysis of alpha-synuclein in subcellular pools of rat brain neurons: an immunogold electron microscopic study using a C-terminal specific monoclonal antibody. Brain Res 1244:40-52.

Zhang L, Shimoji M, Thomas B, Moore DJ, Yu SW, Marupudi NI, Torp R, Torgner IA, Ottersen OP, Dawson TM, Dawson VL (2005) Mitochondrial localization of the Parkinson's disease related protein DJ-1: implications for pathogenesis. Hum Mol Genet 14:2063-2073.

Zhang Y, Dawson VL, Dawson TM (2000a) Oxidative stress and genetics in the pathogenesis of Parkinson's disease. Neurobiol Dis 7:240-250.

Zhang Y, Gao J, Chung KK, Huang H, Dawson VL, Dawson TM (2000b) Parkin functions as an E2-dependent ubiquitin- protein ligase and promotes the degradation of the synaptic vesicle-associated protein, CDCrel-1. Proc Natl Acad Sci U S A 97:13354-13359.

Zimprich A, Biskup S, Leitner P, Lichtner P, Farrer M, Lincoln S, Kachergus J, Hulihan M, Uitti RJ, Calne DB, Stoessl AJ, Pfeiffer RF, Patenge N, Carbajal IC, Vieregge P, Asmus F, Muller-Myhsok B, Dickson DW, Meitinger T, Strom TM, Wszolek ZK, Gasser T (2004) Mutations in LRRK2 cause autosomal-dominant parkinsonism with pleomorphic pathology. Neuron 44:601-607.

ACKNOWLEDGEMENTS

I would like to convey my deepest gratitude to my principle supervisor, Dr. Anumantha G. Kanthasamy, for his excellent guidance, support, encouragement, understanding, and for providing me with the great opportunity to undertake research at the Iowa State University. His expertise and invaluable comments greatly helped me and were critical to the completion of this dissertation. I would also like to thank my committee members, Dr. Drena Dobbs, Dr. Michael Shogren-Knaak, Dr. Arthi Kanthasamy, and Dr. Qijing Zhang during their comments and guidance for the past several years.

I would like to thank Dr. Vellareddy Anantharam and Ms. Mary Ann deVries for their enthusiastic help over the years. I am also grateful to Dr. Yongjie Yang for teaching me some experimental techniques when I joined the lab. I would also like to thank all my previous and current lab colleagues at the Iowa Center for Advanced Neurotoxicology, Drs. Faneng Sun, Calivarathan Latchoumycandane, Danhui Zhang, Siddarth Kaul, and Prashanth Chandramani, Qi Xu, Meng-Hsien Lin, Anamitra Ghosh, Hariharan Swaminathan, Arunkumar Asaithambi, Richard Gordon, Chunjuan Song, Hilary Afeseh-Ngwa, Daqing Huang, Dustin Martin, Dongsuk Kim, Muhammet Ay, Colleen Hogan, and Mattew Neal.

Thanks are also given to all BMS staffs, Kim M. Adams, Linda Erickson, Nada Pavlovic, and William B. Robertson, and program coordinator of MCDB, Katie Blair for all their help.

Finally, this dissertation is dedicated with love to my parents and my wife, Ying Zheng, who are the constant source of great love and inspiration to me.